# UPGRADING HYDROTHERMAL LIQUEFACTION BIOCRUDE OIL FROM WET BIOWASTE INTO TRANSPORTATION FUEL

BY

WAN-TING CHEN

DISSERTATION

Submitted in partial fulfillment of the requirements
for the degree of Doctor of Philosophy in Agricultural and Biological Engineering
in the Graduate College of the
University of Illinois at Urbana-Champaign, 2017

Urbana, Illinois

Doctoral Committee:

Professor Yuanhui Zhang, Chair
Professor Hong Yang
Professor Chia-Fon Lee
Dr. B.K. Sharma

# ABSTRACT

The objective of this study is to develop viable technologies to upgrade biocrude oil converted from wet biowaste via hydrothermal liquefaction (HTL). Three types of feedstocks (algae, swine manure, and food processing waste) were converted into biocrude oil via HTL for upgradation processes, which includes pretreating feedstocks, separation, esterification and neutralization of biocrude oil.

Previous studies have revealed that excessive ash content in mixed-culture algal biomass (AW) appeared to reduce the higher heating value (HHV) and hydrocarbon compositions in the biocrude oil. To resolve this issue, physical pretreatments on AW biomass were carried out to decrease the ash content and improve the biocrude oil quality. AW biomass with different ash content was converted into biocrude oil via HTL at 300°C for 1 h reaction time, which is the previously determined optimum condition for producing biocrude oil. As the ash content of AW biomass was decreased from 53.3 wt.% to 39.0-43.5 wt.% after screen pretreatments, the HHV of the biocrude oil was substantially improved from 27.5 MJ/kg to 32.3 MJ/kg and the amounts of the light oil (boiling point of 100-300°C) were increased from 31wt.% to 49 wt.%. In contrast, GC-MS analyses of pretreated algal biocrude oil and aqueous products demonstrate that the ash content promoted denitrogenation, catalyzed the formation of hydrocarbons, and mitigated the recalcitrant compounds in aqueous products under the HTL processes. In order to elucidate the role of the ash content under the HTL processes, model algae, *Chlorella*, with different amounts of representative ash content (egg shells in this study) were converted into biocrude oil at the same reaction condition (*i.e.*, 300°C for 1 hr reaction time). Elemental and thermogravimetric analyses of the biocrude oil both show that when the ash content in the algal feedstock was below 40 wt.%, the HHV and boiling point distribution of the algal biocrude oil could be hardly changed. This result signifies the feasibility of using ash-rich biomass as an HTL feedstock and diminishes the necessity of multi-step pretreatments of ash-rich biomass for biofuel applications.

This study also demonstrates a proof-of-concept in the production of high quality renewable biofuel from wet biowaste via hydrothermal liquefaction (HTL). Distillation was employed to effectively separate the biocrude oil converted from swine manure (SW), food processing waste (FPW), and *Spirulina platensis* (SP) via HTL into different fractions.

Distillation curves of different types of HTL biocrude oil were reported. Physicochemical characterizations, including density, viscosity, elemental test, chemical compositions, and acidity, were conducted on distillates separated from different feedstocks. SW-, FPW-, and SP-derived biocrude respectively contains 15 wt.% , 56 wt.%,  and 15 wt.% distillates with heating values of 43-46 MJ/kg and alkanes with carbon numbers ranging from C8 to C18. Compared to the distillates from SW- and SP-derived biocrude oil, the distillates from FPW-derived biocrude demonstrate the closest density and energy content to petroleum diesel, though this type of distillates contained an excessively high acidity that needs to be reduced from 35.3 mg KOH/g to ≤ 3 mg/g (the requirements suggested by the ASTM standard for a 10 vol.% biodiesel). Therefore, an orthogonal array design of esterification experiment was performed to optimize the reaction temperature (50-70°C), reaction time (0.5 h-6 h), catalysts concentration (0.5 wt.%-2 wt.%), and the molar ratio of FPW-distillates to methanol (1:5-1:15), for achieving the lowest acidity. Compared to other available methods to upgrade HTL biocrude oil, the integrative upgrading approach proposed by this study (distillation plus esterification/neutralization) demonstrates a competitive energy consumption ratio (0.03-0.06) to zeolite cracking (0.07), supercritical fluid (SCF) treatment (0.17), and hydrotreating (0.24) (assuming 50% heat is recovered from upgrading processes). Moreover, the reaction severity of the upgrading approach used in this study (with log $R_o$ of 5.9-9.5) is much lower than those of zeolite cracking (with log $R_o$ of 11.0), SCF treatment (with log $R_o$ of 10.6), and hydrotreating (with log $R_o$ of 11.3), without the consumption of high pressure hydrogen gas. Finally, the fuel specification analysis and engine test were conducted with the drop-in biodiesel, which was prepared with 10 vol.% (HTL10) and 20 vol.% (HTL20) upgraded distillates and 80-90 vol.% petroleum diesel. According to the fuel specification analysis, HTL10 and HTL20 exhibited a qualified Cetane number (>40 min), lubricity (<520 μm), and oxidation stability (>6 hr), as well as a comparable viscosity (0.2%-19% lower) and net heat of combustion (3%-4% lower) to those of petroleum diesel. Further, diesel engine tests demonstrated that HTL10 can lead to a superior power output (8% higher) and lower emissions of $NO_x$ (3-7%), CO (1-44%), $CO_2$ (1-4%), and unburned hydrocarbons (10-21%). The present study showcases an energy-efficient and technically cohesive approach to produce renewable high-quality drop-in biofuels for demanding transport applications.

# ACKNOWLEDGEMENTS

First and foremost, I would like to appreciate sincerely to my advisor, Professor Yuanhui Zhang, for his always-passionate discussion, positive encouragement, and generous support during my PhD study. Without his advice and guidance, I cannot complete this dissertation smoothly. Working with him, I have improved and learned tremendously in research, mentoring, teaching, and engineering skills. His enthusiasm for research, teaching, and engineering work in the field of bioenvironmental engineering, hydrothermal liquefaction, and biowaste treatment inspired me to be a better researcher and educator. I feel extremely fortunate to be part of his research group.

The appreciation also goes to Prof. Chia-Fon Lee, Prof. Hong Yang, and Dr. B.K. Sharma. Thanks for their kind help on improving my PhD dissertation, serving as my committee members, and giving me valuable and constructive feedbacks. Without their help and advice, this work cannot be accomplished in a good manner.

Also, I would like to deeply thank Prof. K.C. Ting, Prof. Rohit Bhargava, Prof. Jesse Thompson, Prof. Giovana Tommaso, Prof. Richard Gates, Prof. Alan Hansen, Prof. Kenneth Suslick, Prof. Tony Graft, and Prof. Prasanta Kalita's encouragement and generous help. Without their support, mentoring, and guidance, I cannot be on the right track of my research program. My heartfelt thanks also deeply go to Mr. Tom Burton and Mr. Steve Ford's assistance on maintaining the HTL lab when we worked in 1032 and 780/790 buildings.

In addition, I want to thank all my co-workers, especially Dr. Yigang Sun, Dr. Shihan Zhang, Dr. Yongqi Lu, and Dr. Lance Schideman. Thanks for their kind assistance and patient discussion on my experimental design. My sincere gratitude also goes to fellow graduate students and researchers, Peng Zhang, Chih-Ting Kuo, Bidhya Kunwar, Timothy Lee, Karthik Nithyanandan, Ming-Hsu Chen, Kai-Chieh Tsao, Yurun Miao, Sun Min Kim, Young Hwan Shin, Marcio Aredes, Haifeng Liu, Mingxia Zheng, Chao Gai, Mitch Minarick, Ana Martin, Rowena Carpio, Jakob Breinl, Hao Li, Jamison Watson, Buchun Si, Michael Stablein, Aersi Aierzhati, Zach Mazur, Matthew Ong, Libin Yang, Megan Swoboda, Mengzi Wang, and Shaochen Guan. I benefited significantly from their valuable discussion and share of know-how. Besides, I want to express my thanks to all of my undergraduate and high-school assistants, Liyin Tang, Junchao Ma, Ferisca Chobi, Brian Lai, Wanyi Qian, Ken Nair, Karalyn Scheppe, Karina Barrios, Morgan Fuehne, Nikou Pishevar, Nate Wells, Zhenwei Wu, Alice Lin, Bianca Chan, Tarik Hunt, Sergej

Radovanovic, Patrick Dziura, Ahmed Abbas, Erinn Thomas, Ashley Arroyo, and Briana Green. Thanks for their kind assistance and accompany when I worked in lab 232.

At last but not least, I would like to sincerely appreciate all my family in Taiwan, especially my parents, Hsiu-Hua Tian and Ming-Shan Chen. I want to express my deep gratitude to my Mother and Father. Thanks for your selfless support, love and encouragement. I love you and miss the days living closer to you. My appreciation also goes to my friends and colleagues here in UIUC, especially my best friend and partner, Mei-Hsiu Lai. Further, I want to thank Shi-Fang Chen, Haibo Huang, Liangcheng Yang, Ravi Challa, Kejia Chen, Ji Sun Choi, Danielle Mai, Elizabeth Horstman, Yanfen Li, Nicole Jackson, Kaitlin Tyler, Chaoyang Liu, Robert Reis, Lauren Logan, Lucas Trevisan, and Yijie Xiong. Thanks for their always-patient discussion and generous support.

# TABLE OF CONTENTS

# CHAPTER 1. INTRODUCTION

Conversion of wet biowaste into biofuel needs a comprehensive understanding in science and engineering. As Figure 1-1 shows, biological digestions such as anaerobic digestions (AD), biochemical processes such as oil extraction and thermochemical decomposition such as pyrolysis all are possible conversion technologies for wet biowaste such as manure or mixed-culture algae from wastewater treatment plants (AW). However, wet biowaste typically contains high moisture contents (more than 50%) and thus they are not suitable for conventional oilseed extraction processes (2012; Zhou et al., 2013). Traditionally, anaerobic digestion (AD) is the dominant conversion technology used for wet biowaste. Despite the long history of applications, AD generally suffers from poor conversion efficiencies (< 50%), slow reaction rates (> 1 month), and high capital costs, all of which typically make it not economically viable without a subsidy or regulatory imperative. Therefore, seeking an energetically feasible approach to convert wet biowaste into biofuel and other valuable products remains as a critical issue. Among the current available conversions for wet biowaste, hydrothermal liquefaction (HTL), involving direct liquefaction of biomass with water, has been demonstrated as an energetically favorable approach (Vardon et al., 2012; Yu, 2012). Previous studies have also proven that HTL can effectively convert wet biowaste into biocrude oil, which contains closer higher heating values (HHV) to heavy crude (Table 1-1) (Chen et al., 2014c; Zhou et al., 2013).

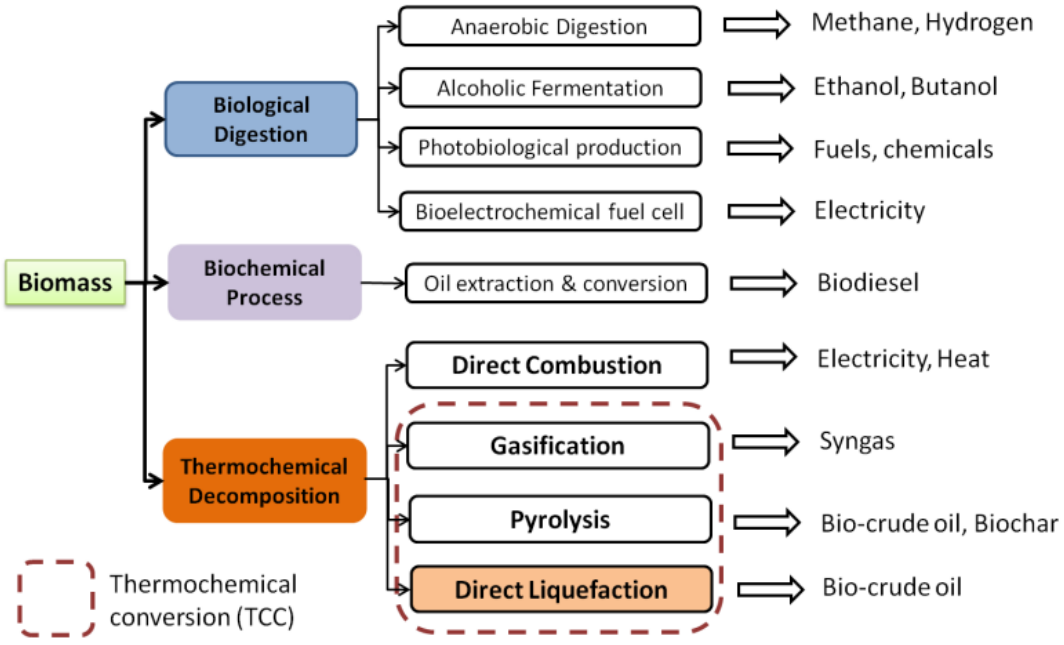


**Figure 1-1. Biomass conversion technologies and products (Yu, 2012)**

**Table 1-1. Properties of bio-crude oil from liquefaction, fast pyrolysis and heavy fuel oil from petroleum (Adapted from (Huber et al., 2006a; Peterson et al., 2008; Yu, 2012))**

| Property | Liquefaction oil | Pyrolysis oil [a,b] | Heavy fuel oil [a] |
|---|---|---|---|
| Moisture (wt%) | 5-10 | 15-30 | 0.1 |
| pH | n.a. | 2.5 | n.a. |
| Specific gravity | 1.1 | 1.2 | 0.94 |
| Elemental composition (wt%) | | | |
| C | 70-77 | 54-58 | 85 |
| H | 8-10 | 5-7 | 11 |
| O | 10-16 | 35-40 | 1.0 |
| N | 5-7 | 0-0.2 | 0.3 |
| Ash | 5 | 0-0.2 | 0.1 |
| Higher heating value (MJ/kg) | 34-38 | 16-23 | 40-49 |
| Viscosity (cps) [a] | 15000 @ 61°C | 40-100@ 50°C | 180 |
| Distillation residue (wt%) [a] | n.a. | Up to 50 | 1 |

n.a.: not available; [a] (Huber et al., 2006); [b] (Peterson et al., 2008)

Researchers have proven that HTL can convert up to 70% volatile solids (dry mass basis) of wet biowaste (*e.g.*, swine manure) into biocrude oil with heating values between 32-38 MJ/kg, which is 75-90% of petroleum crude heating value (He et al., 2000a; He et al., 2001a; He et al., 2001b; He et al., 2000b). This conversion of swine manure to biocrude oil has been accomplished at temperatures (< 305°C), retention times (30-60 min), water contents (80%), and pressures of 10.5 MPa. In addition to biocrude oil, byproducts such as gas (~95-99% $CO_2$), aqueous products and solid residue are also generated simultaneously during the HTL process. An example illustrating a typical HTL process and its associated products is listed in Figure 1-2.

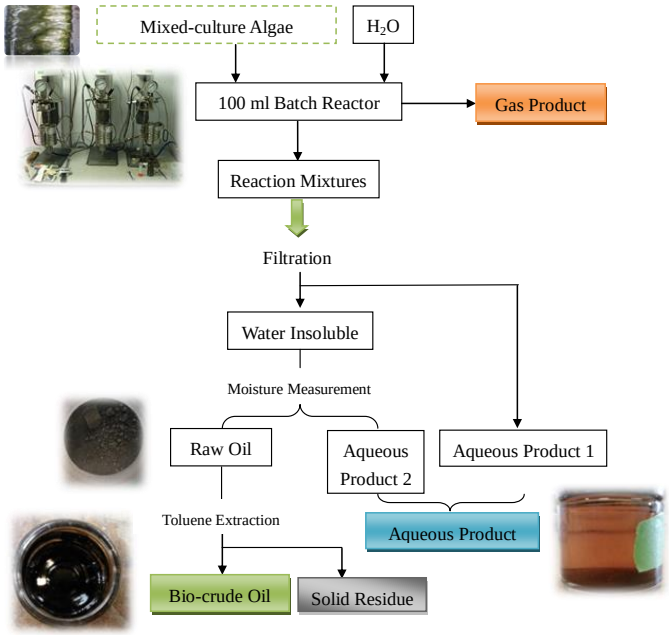


**Figure 1-2. HTL of wet biowaste feedstock into biocrude oil and other byproducts (Chen et al., 2014c)**

Although HTL appears to serve as a promising integrated tool to treat the wet biowaste and produce biofuel products at the same time, the practical application of biocrude oil and other byproducts remains as a critical bottleneck to further promote this technique. Previous studies have revealed that the HTL biocrude oil could be used as transportation fuel with proper refine processes, such as hydrogenation or catalytic hydrocracking (Chen et al., 2014c; Duan & Savage, 2011c; Peterson et al., 2008). Duan and Savage has reported that HHV of algal biocrude oil can be upgraded to closer to petroleum crude (42-43 MJ/kg) by catalytic treatment with 20% HZSM-5 at 430°C for 6 hours reaction time under supercritical water (Duan & Savage, 2011c). Hydrogenation and deoxygenation of biocrude oil were successfully carried out in this study. Nevertheless, the nitrogen content of biocrude oil after catalytic treatment (~2.6%) was still higher than that of petroleum crude oil (~0.5%). Denitrogenation appears to be a critical issue for using biocrude oil as transportation fuel. Moreover, multiple previous studies have demonstrates that catalysts (*e.g.*, zeolites, Pt/C, Raney-Ni, Rh *etc*.) have little impact on upgrading the quality of biocrude oil (*e.g.*, deoxygenation) in one-step HTL reaction (Anastasakis & Ross, 2011; Savage, 2009; Yu, 2012; Zhang et al., 2013a; Zhou et al., 2010; Zhou et al., 2012). In fact, it was found that the deoxygenation and denitrogenation would be more effective when catalytic hydroprocessing reacted directly to biocrude oil products (Cheng et al., 2014a; Duan & Savage, 2011c).

In addition to catalytic hydrprocessing, emulsification has been proposed as a milder method to upgrade HTL biocrude oil, since emulsification can simply mix diesel and bio-oil converted from pyrolysis, which is a thermochemical process similar to HTL (Chiaramonti et al., 2003a; Chiaramonti et al., 2003b; Xiu & Shahbazi, 2012).

Pretreatment of the HTL feedstock has also been suggested for upgrading the quality of HTL biocrude oil. It was reported that screening of mixed-culture algal biomass from wastewater can improve the biocrude oil quality (Chen, 2013). Moreover, it has been proven that ultrasonication of cellulose, rice husk, and corn stalk can greatly improve the corresponding biocrude oil yields and energy recovery by 10-20% under HTL (Shi et al., 2013b). Strong alkaline, such as NaOH or KOH, was also commonly used to decompose lignocelluloses or proteins in the feedstocks to improve the quantity and quality of HTL biocrude oil (Anastasakis & Ross, 2011; Yu et al., 2014). Figure 1-3 summarizes possible approaches to upgrade HTL biocrude oil.

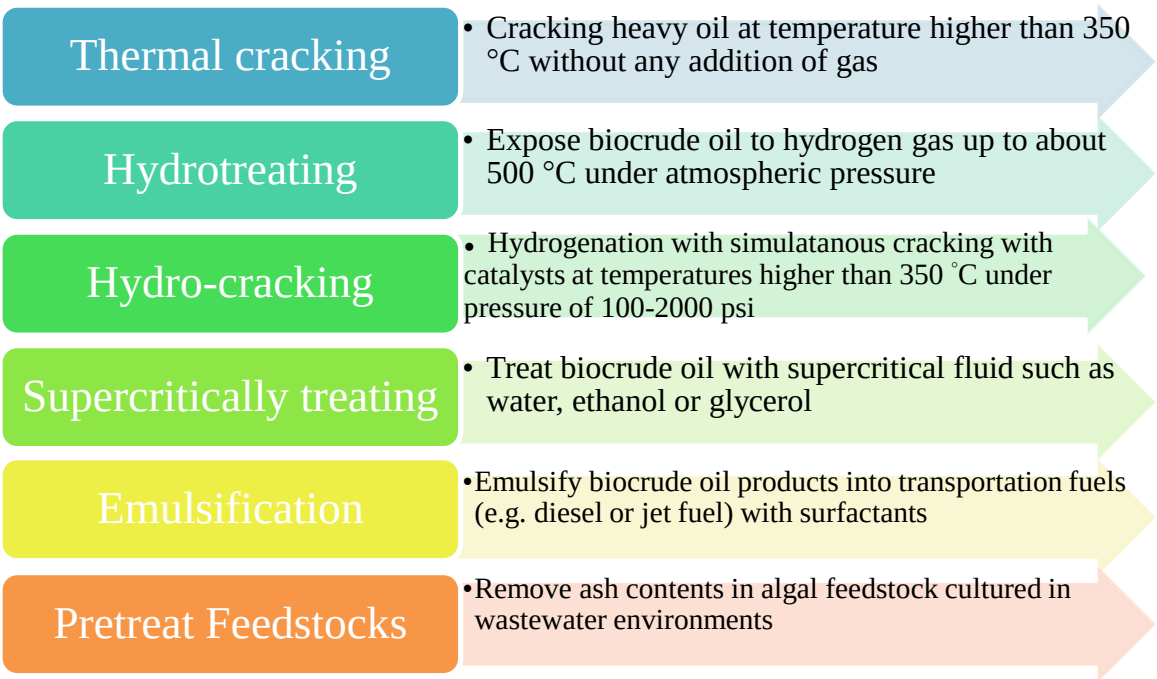


**Figure 1-3. Possible approaches to upgrade HTL biocrude oil into transportation fuels**

# CHAPTER 2. LITERATURE REVIEW

In order to upgrade biocrude oil converted from wet biowaste via hydrothermal liquefaction (HTL), a thorough review of HTL processes and HTL products characteristics must be conducted so that effective upgrading mechanisms can be proposed. HTL, also refers to as hydrous pyrolysis, is a thermochemical depolymerization process in an enclosed reactor to convert wet biomass into biocude oil and chemicals at moderate temperature (typically 200–400$^{o}$C) and high pressure (typically 10-25 MPa). Wet biowaste such as food processing waste, manure, and municipal sludge typically have high moisture content and thus make HTL an appropriate process. In HTL processes, water serves as an important reactant. As the reaction condition approaches to the critical point of water, several properties of water are drastically changed and able to bring about fast, homogeneous, and efficient reactions (Calvo & Vallejo, 2002; Narayan et al., 2005; Savage, 2009). Because sub-critical water has a leading role as a heat transfer and extracting medium, HTL is relatively independent of the size of biomass particles or heating rates. The product yield and their chemical properties are primarily affected by the types of feedstock, processing conditions, and existence of catalyst. HTL biocrude oil from wet biowaste typically contains high nitrogen content and many types of aromatics. Upgrading of the HTL biocrude is necessary for transportation grade fuel. Post hydrothermal wastewater (PHWW) typically has a very high chemical oxygen demand (COD) and various nutrients (primarily nitrogen) that need to be treated before discharge to waterways. Gaseous products of HTL contain malodors thus must be treated before emit to atmosphere. In this chapter, important factors influencing HTL, HTL products characteristics, and potential methods to upgrade HTL biocrude oil are described.

## 2.1 Pretreatment of Feedstocks

Wet biowaste often require pretreatment prior to entering an HTL reactor. There are three general pretreatment principles: physical (Biller et al., 2013; Chakraborty et al., 2013; Chakraborty et al., 2012; Chen et al., 2014a; Cheng et al., 2014c; Costanzo et al., 2015; Eboibi et al., 2015; Jazrawi et al., 2015; Miao et al., 2012; Miao et al., 2014; Minarick et al., 2011), chemical (Barreiro et al., 2014; Jazrawi et al., 2015; Leng et al., 2016; Vardon et al., 2012) and biological (Barreiro et al., 2014; Kaushik et al., 2014), and a combination of the three. Pretreating HTL feedstocks has three general purposes: 1) extracting value-added products such

as polysaccharides and crude lipids (Barreiro et al., 2014; Biller et al., 2013; Chakraborty et al., 2013; Chakraborty et al., 2012; Cheng et al., 2014c; Costanzo et al., 2015; Eboibi et al., 2015; Jazrawi et al., 2015; Kaushik et al., 2014; Miao et al., 2012; Miao et al., 2014; Vardon et al., 2012); 2) removing non-volatile components such as ash and metals (Chen et al., 2014a; Leng et al., 2016); and 3) achieving reasonable properties such as solid contents suitable for an energy-efficient HTL conversion (Minarick et al., 2011). Table 2-1 summarizes different pretreatment methods for HTL of wet biowaste.

**Table 2-1. Comparison of different pretreatment methods for HTL feedstocks that contains protein contents**

| Category | Feedstock | Pretreatment Mechanism | Value-added Products during Pretreatment | Pros | Cons |
|---|---|---|---|---|---|
| **Physical Pretreatment** | | | | | |
| Maio et al., 2014 (Miao et al., 2014) | Yeast (C. curvatus) | Low-temperature liquefaction (160-300°C) | Polysaccharides and proteins derivatives | Produce value-added chemical and biocrude oil with lower nitrogen | Multi-step processes; potential loss of organic matter |
| Eboibi et al., 2015 (Eboibi et al., 2015) | Microalgae (Tetraselmis sp.) | Low-temperature liquefaction (130-200°C) | Protein derivatives | Produce biocrude oil with improved yields and lower nitrogen | Multi-step processes; Organic carbon lost to the pretreatment process water; high energy input |
| W. Costanzo et al., 2015 (Costanzo et al., 2015) | Microalgae (Spirulina, Nannochloropsis, Chlorella, & Scenedesmus) | Low-temperature liquefaction (125-225°C) | Nitrogen-rich nutrient streams | Produce nutrient streams and biocrude oil with lower nitrogen | Multi-step processes; Organic matter lost to the pretreatment process |
| Chen et al., 2014 (Chen et al., 2014a) | Mixed-culture algal biomass | Centrifugation & ultrasonication | N/A | Produce biocrude oil with improved yields and heating value | Multi-step processes; require additional energy for pretreatment |
| Cheng et al., 2014 (Cheng et al., 2014c) | Microalgae (Nannochloropsis) | Microwave irradiation | Biodiesel | Produce biodiesel and biocrude oil simultaneously | Multi-step processes; biocrude oil with lower HHV |
| Biller et al., 2013 (Biller et al., 2013) | Microalgae (Nannochloropsis, Chlorogloeopsis, Pseudochoricystis) | Microwave irradiation | Lipids and phytochemicals | Produce biocrude oil with lower nitrogen | Multi-step processes; Organic matter lost to the pretreatment process water. |
| Chakraborty et al., 2012; Miao et al., 2012 (Chakraborty et al., 2012; Miao et al., 2012) | Microalgae (Chlorella) | Low-temperature liquefaction (140-200°C) | Polysaccharides | Lower solid residue yield; produce biocrude oil with lower nitrogen | Multi-step processes; lost of organic matters |
| Minarick et al., 2011 (Minarick et al., 2011) | Swine Manure | Filtration & centrifugation | N/A | Achieve a higher solid content of feedstock; improve the energy recovery of HTL | Require additional energy for pretreatment |

**Table 2-1. Comparison of different pretreatment methods for HTL feedstocks that contains protein contents (cont.)**

| Category | Feedstock | Pretreatment Mechanism | Value-added Products during Pretreatment | Pros | Cons |
|---|---|---|---|---|---|
| **Chemical Pretreatment** | | | | | |
| C. Jazrawi et al., 2015 (Jazrawi et al., 2015) | Microalgae (Chlorella) | Extraction with sulphuric or formic acids | Protein derivatives | Produce biocrude oil with lower nitrogen | Unselective removal of nitrogen-containing compounds. |
| D. Barreiro et al., 2014 (Barreiro et al., 2014) | Microalgae (Nannochloropsis & Scenedesmus) | Soxhlet extraction with hexane | Crude lipids | Produce lipids and biocrude oil simultaneously | Produce biocrude oil with higher N; lower yield of biocrude oil |
| Vardon et al., 2012 (Vardon et al., 2012) | Microalgae (Scenedesmus) | Soxhlet extraction with hexane | Crude lipids | Produce lipids and biocrude oil simultaneously | Produce biocrude oil with higher N; lower yield of biocrude oil |
| Leng et al., 2016 (Leng et al., 2016) | Sewage sludge | Extraction with organic solvents (e.g., acetic acid, hydrogen peroxide, *etc.*) | Solid residue or biochar containing metals | Produce biocrude oil and biochar with lower metal concentrations | Require hazardous chemicals for demetalization; lower biocrude oil yield |
| **Biological pretreatment** | | | | | |
| R. Kaushik et al., 2014 (Kaushik et al., 2014) | Food Waste | Enzymatic hydrolysis | Hydrochar | Produce hydrochar with higher heating values | Require expensive enzymes; difficult to recycle enzymes |
| D. Barreiro et al., 2014 (Barreiro et al., 2014) | Microalgae (Nannochloropsis & Scenedesmus) | Enzymatic hydrolysis | Amino acid concentrates | Produce biocrude oil with lower N & higher heating values | Loss of algal biomass; unselective extraction of amino acids |

Extraction of value-added co-products from wet biowaste prior to HTL conversion has been extensively studied for augmenting the overall economics of the process (Chakraborty et al., 2013; Chakraborty et al., 2012; Miao et al., 2012; Miao et al., 2014). For example, polysaccharides can be extracted at low liquefaction temperature (140-200°C), and produce biocrude oil at medium liquefaction temperature (220-300°C) from microalgae (Chakraborty et al., 2013; Chakraborty et al., 2012; Miao et al., 2012; Miao et al., 2014). Extraction of crude lipids has also been investigated through microwave and Soxhlet extraction with hexane (Barreiro et al., 2014; Biller et al., 2013; Cheng et al., 2014c; Vardon et al., 2012), while the protein derivatives (*e.g.,* amino acids and nitrogen-rich nutrient streams) have been extracted with sulphuric or formic acids, enzymatic hydrolysis, at mild liquefaction (125-225°C) (Costanzo et al., 2015; Eboibi et al., 2015; Jazrawi et al., 2015; Kaushik et al., 2014). Pretreatment methods are often unselective for extracting polysaccharides and proteins. Ionic liquid extraction could be used for extracting proteins from wet biowaste with 75-100% selectivity of proteins in a single-step extraction and reuse of the ionic liquid (Pei et al., 2009). Pretreatment generally requires multi-step processes to extract different type of value-added products, and the residual can be then subjected to HTL to produce biocrude oil. Such multi-step processes often require multi-reactors thus complicating the overall process. A continuous HTL reactor is critically needed for simultaneously obtaining value-added chemicals (at lower liquefaction temperature) and biocrude oil (at higher liquefaction temperature). In such a continuous reactor, the loss of organic matter during the pretreatment processes could be prevented. Further biochemical characterizations of value-added products are also significantly needed for different application potentials. For instance, the protein derivatives from algal biomass could be used as pigments (Leema et al., 2010), building blocks for polymer synthesis (Kumar et al., 2014), and food additives (Spolaore et al., 2006).

Removing non-volatile components from wet biowaste, such as ash content and metals, is another focus in the feedstock pretreatment. Excessive ash content in mixed-culture algal biomass would reduce the higher heating value (HHV) and hydrocarbon compositions in the HTL biocrude oil (Chen et al., 2014a; Chen et al., 2014c). To resolve this issue, physical pretreatments were carried out to reduce the ash content (from 28.6% to 18.6%) by centrifugation and improve the HTL biocrude oil yield (from 30 wt.% to 55 wt.%) and quality by centrifugation plus ultrasonication (Chen et al., 2014a). However, how the ash content interacts

with volatile components in the feedstock under HTL processes still remains unclear and requires further investigation to elucidate the role of the ash content in HTL processes. Chemical pretreatments on wet biowaste to remove the ash content have also been investigated. Leng et al. (Leng et al., 2016) extracted metals from sewage sludge with acetic acid, hydroxylammonium chloride, and hydrogen peroxide, and then converted the chemically pretreated sewage sludge via HTL. Although the biochar and biocrude oil with lower metal concentrations were produced, the chemical pretreatment led to a relatively lower biocrude oil yield, largely due to the loss of organic matter during multi-step pretreatment processes. More selective method for extracting metallic compounds has to be investigated. Adsorbents, such as resins, zeolites, and activated carbon were used to extract ash content since these absorbents can be further modified to mitigate specific metallic and mineral elements and recycled through phase separation (Chen & Huang, 2007; Chen et al., 2012; Sprynskyy, 2009).

Achieving reasonable total solid contents for more efficient energy recovery in HTL conversion is another driving force to pretreat wet biowaste. Oftentimes, the solid content in the wet biowaste is less than 10 wt.% in reality. HTL process requires elevating the total feedstock and water to desirable reaction temperature. Manure slurry from typical swine confinement facilities contain 1-2 wt.% solids (Minarick et al., 2011), but HTL process requires a solid content higher than 10 wt.% in order to obtain a positive energy balance (Chen et al., 2014b; He et al., 2000a; He et al., 2001a; He et al., 2001b; He et al., 2000b). In order to produce biocrude oil with reasonable quality and quantity (He et al., 2001b; Minarick et al., 2011; Zhang et al., 2013b), the removal of moisture content is essential (Vardon et al., 2012). Minarick et al. (Minarick et al., 2011) has dewatered swine manure using coarse filtration and centrifugation, and thereby improve the energy recovery of HTL processes by 2-2.5 times. Additional costs and energy consumptions for the dewatering pretreatment processes should be incorporated for further up-scaled techno-economic analyses of the HTL process.

### 2.2 HTL Process

Key parameters affecting HTL processes include feedstock types, process modes (such as batch and continuous), process conditions (such as temperature, retention time and pressure), and catalysts. This section summarizes the HTL process of different feedstocks in terms of conversion efficiency and product characteristics.

### 2.2.1 Feedstock Type

Wet biowaste includes animal manure, municipal sludge, food processing waste and algal biomass grown in wastewater environments. Their biochemical compositions are summarized in Table 2-2 in terms of compounds (crude fat or lipid, protein, carbohydrate and ash) and major elements (C, H, N, and O). These are the wet biowaste have been hydrothermally liquefied in the past twenty years with some promising results in terms of biocrude yields and high-heating values (HHV). Compositions of food processing wastes can vary widely among different plants such as a slaughterhouse and a cheese plant. Typically, the higher the amounts of crude fat in the feedstocks, the higher the biocrude oil yields (Biller & Ross, 2011a; Pavlovič et al., 2013; Vardon et al., 2011), while the presence of lignin generally leads to char formation under HTL (Demirbaş, 2000a; Zhong & Wei, 2004). The highest HTL biocrude oil yield occurred with feedstocks containing high crude fat and non-fibrous carbohydrates at relatively lower temperatures (250-300°C) and shorter retention time (5-30 min) due to the fast decompositions of crude fat and non-fibrous carbohydrates (Pavlovič et al., 2013; Peterson et al., 2008). Kabyemela et al. observed a 55% conversion of glucose after 2 sec at 300°C (Kabyemela et al., 1999). Triacylglycerides (TAGs) were readily hydrolyzed in hot compressed water without catalysts (Peterson et al., 2008; Toor et al., 2011). Feedstocks containing more proteins or fibrous carbohydrates require a higher reaction temperatures (300-350°C) and longer retention time (30-120 min). Sasaki et al. reported that the reaction rate of cellulose begin to accelerate at about 350°C at 25 MPa (Peterson et al., 2008). Rogalinski et al. (Rogalinski et al., 2005; Toor et al., 2011) observed the decomposition of amino acids from bovine serum albumin in subcritical water hydrolysis at 250-330°C and 4-180 s retention time, with an almost complete degradation of all amino acids at 330°C and 200 s reaction time.

In addition to biocrude oil, other value-added chemicals can also be produced from HTL of food processing waste. Yoshida et al. converted fish meat at 240-350°C with a 5-30 min reaction time to produce biocrude oil and aqueous products containing value-added chemicals such as amino acids, lactic acids, and phosphoric acids (Yoshida et al., 1999). Quitain et al. hydrothermally treated shrimp shells at 250-400°C for a 5-60 min reaction time to produce amino acids and glucosamine (Quitain et al., 2001). Changing World Technologies applied hydrothermal process to convert turkey offal into biocrude oil and fertilizer (Adams et al., 2004).

**Table 2-2. Compositions of different feedstocks containing protein contents for HTL conversion (wt.%)**

| Category | Crude Fat | Crude Protein | Carbohy-drates[b] | Ash Content | C | H | N | Optimum Conditions for Biocrude Oil Production | Optimum Biocrude Oil Yields[f] | Optimum HHV of Biocrude Oil |
|---|---|---|---|---|---|---|---|---|---|---|
| **Food Processing Waste** | | | | | | | | | | |
| Shrimp shells (Quitain et al., 2001) | N/A[c] | N/A | N/A | N/A | N/A | N/A | N/A | 250°C/60 min | N/A | N/A |
| Fish meat (Yoshida et al., 1999) | N/A | N/A | N/A | N/A | 58.7 | 11.1 | 8.66 | 300°C/5 min | 16 | N/A |
| Swine slaughtering house waste[a] | 44.0 | 24.8 | 27.0 | 4.20 | 50.4 | 7.18 | 2.93 | 280°C/30 min | 58 | 39 |
| Cheese processing waste[a] | 52.3 | 14.8 | 31.5 | 1.45 | 60.7 | 8.49 | 3.33 | 260°C/30 min | 69 | 40 |
| Salad dressing processing waste[a] | 40.8 | 2.76 | 48.9 | 7.53 | 54.0 | 7.93 | 0.57 | 260°C/30 min | 55 | 40 |
| **Animal Manure** | | | | | | | | | | |
| Swine Manure[d] (Chen et al., 2014b; Dong et al., 2009; He et al., 2000a; He et al., 2001a; Wang, 2011b; Zhang, 2010) | 20.3 | 24.5 | 38.9 | 16.3 | 41.1 | 5.42 | 3.36 | 295-305°C/15-30 min | 40 | 39 |

**Table 2-2. Compositions of different feedstocks containing protein contents for HTL conversion (wt.%) (cont.)**

| Category | Crude Fat | Crude Protein | Carbohy-drates[b] | Ash Content | C | H | N | Optimum Conditions for Biocrude Oil Production | Optimum Biocrude Oil Yields[f] | Optimum HHV of Biocrude Oil |
|---|---|---|---|---|---|---|---|---|---|---|
| **Animal Manure (cont.)** | | | | | | | | | | |
| Swine Manure-14 day (G-F)[e] (Wang, 2011b) | 16.7 | 37.9 | 27.1 | 18.3 | N/A | N/A | N/A | 305°C/30 min | 40 | N/A |
| Swine Manure-21 day (G-F)[e] (Wang, 2011b) | 17.9 | 43.3 | 20.5 | 18.3 | N/A | N/A | N/A | 305°C/30 min | 38 | N/A |
| Swine Manure (Xiu et al., 2010; Xiu et al., 2011b) | 4.86 | 17.1 | 55.7 | 22.3 | 33.5 | 6.16 | 2.81 | 340°C/15min | 24 | 36 |
| Cattle Manure (Yin et al., 2010) | N/A | N/A | N/A | 7.16 | 35.4 | 4.73 | 2.38 | 310°C/15 min | 49 | 36 |
| Separated Dairy Manure (Theegala & Midgett, 2012) | N/A | N/A | N/A | 16.8 | N/A | N/A | N/A | 350°C/15 min | N/A | 33 |
| Human Feces[a] | 24.4 | 34.5 | 25.0 | 16.0 | 45.5 | 6.5 | 5.7 | 340°C/10-30min | 34 | 41 |

**Table 2-2. Compositions of different feedstocks containing protein contents for HTL conversion (wt.%) (cont.)**

| Category | Crude Fat | Crude Protein | Carbohy-drates[b] | Ash Content | C | H | N | Optimum Conditions for Biocrude Oil Production | Optimum Biocrude Oil Yields[f] | Optimum HHV of Biocrude Oil |
|---|---|---|---|---|---|---|---|---|---|---|
| **Algae** | | | | | | | | | | |
| | | | | | Microalgae | | | | | |
| Tetraselmis (Eboibi et al., 2014a) | 14 | 58 | 22 | 6 | 42.0 | 6.8 | 8.0 | 350°C/5 min | 65[g] | 35-39 |
| Nannochlor-opsis (Brown et al., 2010) | 28 | 52 | 12 | 8 | 43.3 | 6.0 | 6.4 | 350°C/60 min | 43 | 39 |
| Dunaliella (Zou et al., 2010) | 22.2 | 32.1 | 33.5 | 12.2 | 40.3 | 5.41 | 9.22 | 360°C/30 min | 37 | 27 |
| Chlorella (Gai et al., 2014a; Yu et al., 2011a) | 0.10 | 71.3 | 23.0 | 5.6 | 51.4 | 6.6 | 11.1 | 280-300°C/60-120 min | 39-43 | 37-39 |
| Spirulina (Yu, 2012) | 5.10 | 64.4 | 21.0 | 9.5 | 49.3 | 6.4 | 11.0 | 280°C /120 min | 45-50 | 33-37 |
| Diatom (Yu, 2012; Zhang, 2014) | 5.57 | 40.0 | 10.0 | 32.6 | 33.7 | 4.90 | 5.51 | 320°C/45 min | 33 | 33 |
| | | | | | Macroalgae | | | | | |
| Laminaria (Anastasakis & Ross, 2011) | N/A[c] | N/A[c] | N/A[c] | 24.2 | 31.3 | 3.7 | 2.4 | 350°C/15 min | 19.3 | 37 |
| Alaria (López Barreiro et al., 2015) | <0.7 | 15.0 | <50.7 | 33.6 | 33.0 | 4.4 | 2.5 | 360°C/15 min | 29.4 | 35 |
| Enteromor-pha (Zhou | N/A[c] | N/A[c] | N/A[c] | 30.1 | 28.8 | 5.2 | 3.7 | 300°C/30 min | 20.4 | 29 |

et al., 2010)

**Table 2-2. Compositions of different feedstocks containing protein contents for HTL conversion (wt.%) (cont.)**

| Category | Crude Fat | Crude Protein | Carbohy-drates[b] | Ash Content | C | H | N | Optimum Conditions for Biocrude Oil Production | Optimum Biocrude Oil Yields[f] | Optimum HHV of Biocrude Oil |
|---|---|---|---|---|---|---|---|---|---|---|
| Mixed-culture Algae | | | | | | | | | | |
| Mixed-culture algae from wastewater (Chen et al., 2014c) | 1.70 | 27.2 | 23.6 | 47.5 | 27.9 | 3.0 | 3.9 | 300°C/60 min | 49.9[g] | 33 |
| Wastewater-fed algae (Roberts et al., 2013) | 14.0[g] | N/A[c] | N/A[c] | 29.0[g] | 48.9[g] | 7.1[g] | 8.4[g] | 350°C/60 min | 44.5[g] | 39 |
| High-ash algae from Dianchi Lake (Tian et al., 2015) | 1.04 | 13.5 | 40.0 | 41.6 | 23.7 | 4.5 | 3.3 | 300°C/60 min | 18.4[g] | 37 |
| **Sewage Sludge** | | | | | | | | | | |
| Sewage Sludge (Yu, 2012) | 0.10 | 41.6 | 32.0 | 26.3 | 38.0 | 7.8 | 7.3 | N/A[c] | 33-35[h] | N/A[c] |
| Anaerobic sludge (Vardon et al., 2011) | <1 | 15.0 | 54.0 | 31.0 | N/A[c] | N/A[c] | N/A[c] | N/A[c] | 9.4 | 32[i] |
| Sludge (Li et al., 2010a) | N/A[c] | N/A[c] | N/A[c] | N/A[c] | 41.7 | 5.8 | 3.2 | 380-400°C/10 min | 50-55 | 40 |

[a]Unpublished data from our own laboratory; [b]Calculated by difference (*i.e.*, carbohydrate (wt.%)=100-%Crude Fat-%Protein-%Ash);
[c]N/A: Not Available; [d]Fresh swine manure ;[e]Grower-finisher pig stored for different days; [f]Based on dry weight of feedstock; [g]Based on dry ash free of feedstock;
[h]HTL was carried out at 280°C for a 30 min reaction time; [i]HTL was carried out at 300°C for a 30 min reaction time.

Compared to food processing waste, animal manure contains less crude fat and more crude proteins and carbohydrates. This results in a higher HTL reaction temperature to achieve an optimum biocrude oil yield. HTL of swine manure were reported at 240-350°C at reaction time of 5-180 min in batch reactor system (Chen et al., 2014b; Dong et al., 2009; He et al., 2000a; He et al., 2001a; He et al., 2001b; He et al., 2000b; Vardon et al., 2011). The HTL biocrude from swine manure was found to have HHV of 35-39 MJ/kg with 71-78% carbon, 7-14% oxygen, 8.9-9.4% hydrogen, and 3.9-4.6% nitrogen. Different process gases (*e.g.*, CO, $N_2$, and $CO_2$) were also tested, with a CO as a reducing gas that improves the biocrude oil yield and quality. One study showed that the storage time changed the manure biochemical composition but did not affect the HTL biocrude oil yield (Wang, 2011b). Similar to swine manure, human feces have been demonstrated as a promising HTL feedstock (Table 2-2). An additional benefit of HTL of human feces is it completely destroys pathogens. However, HTL biocrude converted from swine manure and human feces contains higher amounts of nitrogen and oxygen compared to petroleum, thus further upgrading is needed if used for transportation fuel.

Swine manure and crude glycerol was co-liquefied under hydrothermal conditions (Xiu et al., 2011b). However, HHV of the co-liquefied HTL biocrude oil was drastically decreased from 36 to 25 MJ/kg due to its dominant esterification that results in high oxygen content in the biocrude oil.

HTL of cattle manure was investigated with the presence of NaOH as catalyst and initial process gas (air, $N_2$, CO, and $H_2$), for a 500 ml of cattle manure slurry (solid content was 23.6 wt.%). The higher initial pressure, longer reaction time, and high solids content of the cattle manure led to the production of gases and char/tar instead of biocrude (Yin et al., 2010). Dairy manure was studied as HTL feedstock at 250-350°C and 15 min reaction time with carbon monoxide as the process gas (Theegala & Midgett, 2012). The highest energy recovery (68%), defined as the energy in the biocrude oil divided by that of raw manure, was achieved at 350°C (Theegala & Midgett, 2012).

Algae is considered as one of the promising HTL feedstocks for next generation biofuel because of their superior photosynthetic efficiency and lower crop-land demand (Tsukahara & Sawayama, 2005). Algae can be classified as microalgae, macroalgae, and mixed-culture algae that may contain both micro- and macroalgae (Table 2-2). High-lipid microalgae has been favored as HTL feedstocks (Yu et al., 2011a). Dote converted *Botryococcus branunii* into

biocrude oil via HTL with biocrude oil yield higher than the original oil content in the algal biomass (Dote et al., 1994), indicating non-lipid fraction in algae contributed to the biocrude oil formation under HTL [2].

In contrast to high-lipid algae, low-lipid high-protein algae species, such as *Chlorella* and *Spirulina*, typically have higher biomass productivity under stressed environment such as wastewater (Chen et al., 2002; Sheehan et al., 1998). Therefore, HTL of low-lipid algae have been an increasing interest in the past five years (Eboibi et al., 2014a; Gai et al., 2014a; Vardon et al., 2012; Yu et al., 2011a; Yu et al., 2011b; Zhang et al., 2013b). HTL parameters including reaction temperature, reaction time, initial pressure, biomass to water ratio, total volume of feedstocks, heating rate, reaction mode, catalysts, and reaction solvents were studied to enhance the algal biocrude oil yield and/or improve its heating value (Anastasakis & Ross, 2011; Brown et al., 2010; Chen et al., 2014c; Duan & Savage, 2010; Elliott et al., 2013; Faeth et al., 2013; Gai et al., 2014a; Jazrawi et al., 2013; Yu et al., 2014; Yu et al., 2011a; Yu et al., 2011b; Zhang et al., 2013a; Zhang et al., 2013b; Zou et al., 2010). Among all the HTL parameters investigated, reaction temperature and reaction time are recognized as the two dominant factors affecting algal biocrude oil yield and biocrude oil quality (*e.g.*, heating value and elemental compositions).

Macroalgae were also investigated as HTL feedstocks due to their fast-growing rates and large quantity (Anastasakis & Ross, 2011; Cole et al., 2016; Elliott et al., 2014; He et al., 2016; Zhou et al., 2010). However, macroalgae generally has high contents of lignocellulose and ash, both adversely affect the HTL conversion efficiency (Yu, 2012) (Table 2-2).

Mixed-culture algae from wastewater environment have attracted increasing attention for HTL conversion. Coupling algal bioenergy production with wastewater treatment can alleviate the burden of nutrients in algae growing by uptaking nutrients from wastewaters instead of petroleum-based fertilizers (Clarens et al., 2010; Zhou et al., 2013). In an Environment-Enhancing Energy paradigm centered on HTL, nutrients in wastewater from post HTL can be reused three times (through laboratory study) to ten times (through modeling) to amplify algae growth and biocrude oil production (Figure 2-1) (Chen et al., 2014b; Chen et al., 2014c; Zhou et al., 2013). Wastewater algae was proved to be a promising HTL feedstock in a separate study (Roberts et al., 2013). In addition to mitigate eutrophication, high-ash low-lipid algal biomass from lakes were harvested for HTL (Tian et al., 2015).

Municipal sludge is another promising feedstock and present comparable heating value of the HTL biocrude oil as those from animal manure and algae (Vardon et al., 2011; Yu, 2012). The SlurryCarb™ process reported that a scaled-up (a 20 ton per day facility) HTL conversion of sewage sludge could produce a biofuel product up to 22 MJ/kg (dry basis) and can be utilized in conventional combustion infrastructure with less than 20% excess air (Bolin, 2001). However, the pretreatment processes for the municipal sludge in a wastewater treatment plant can substantially alter the biochemical compositions of the harvested sludge, which in turn impact the resulting HTL biocrude oil yield and quality. Vardon et al converted anaerobic sludge from a wastewater treatment plant into biocrude oil via HTL, but the biocrude oil yield was much lower than other types of sludge (Vardon et al., 2011; Yu, 2012). Systematic studies regarding HTL of different types of sewage sludge and process parameters such as reaction temperature and reaction time are identified as a research gap in the area of HTL of municipal waste (Leng et al., 2015; Leng et al., 2016; Zhao et al., 2014).

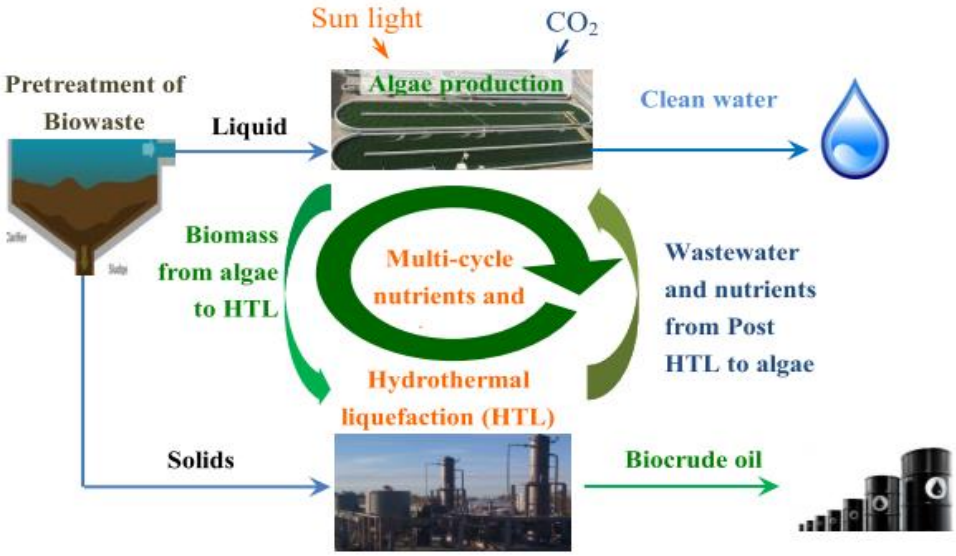


**Figure 2-1. A schematic Environment-Enhancing Energy (E2-Energy) system that can simultaneously produce biocrude oil and treat wastewater by reusing nutrients (Chen et al., 2014c).**

### 2.2.2 Process mode

Hydrothermal liquefaction (HTL) of protein-containing biomass has been mostly investigated in a batch mode. There is only limited information yet available on continuous-flow HTL reactor design and experiment, even fewer studies on scale-up reactors (Elliott et al., 2015).

Discussion about the reactor design and scale-up implementation is provided in later section (2.4 Examples of plants/implementations).

Continuous HTL conversion has been investigated with algae and swine manure (Elliott et al., 2014; Elliott et al., 2013; Jazrawi et al., 2013; Ocfemia et al., 2006a; Ocfemia et al., 2006b). Comparisons of the yields and quality of biocrude oil converted from different feedstocks in continuous and batch modes are summarized in Table 2-3. According to currently available literature (Table 2-3), the algal biocrude oil yields with continuous plug-flow mode are usually higher than those with batch modes, while the carbon, hydrogen, nitrogen contents and heating values of the algal biocrude oil are the same (Elliott et al., 2013; Jazrawi et al., 2013). This reveals that the continuous plug-flow HTL systems can produce algal biocrude oil with the same quality as those from batch reactors. In another study, it is reported that the biocrude oil yields converted from swine manure under continuous modes are closely resemble to those under batch modes, but the energy contents and elemental compositions are slightly lower than those from batch modes. This may be that the swine manure was hydrothermally processed in a continuous-stirred reactor (CSTR), rather than a plug-flow reactor (PFR) (Ocfemia et al., 2006a). Considering a reactor with the same volume, PFR typically can achieve a higher conversion yields than CSTR. Although CSTR systems could be more easily operated and maintained (Fogler, 2016), it bears an inherent disadvantage of mixing mode compared with plug-flow system as part of the feedstock will always subjected to undesirable reaction time – some undercooked, and some overcooked. Comparing continuous HTL systems with batch HTL systems are difficult as the products from the batch are often equilibrium limited (Elliott et al., 2015).

**Table 2-3. Comparison of batch and continuous HTL conversions of wet biowaste**

| Feedstocks | Batch | Continuous |
|---|---|---|
| Algae (Anastasakis & Ross, 2011; Brown et al., 2010; Elliott et al., 2015; Elliott et al., 2014; Elliott et al., 2013; Jazrawi et al., 2013; Jena et al., 2011b; Vardon et al., 2011; Yu et al., 2011a; Zhou et al., 2010) | | |
| Yields (d.a.f.%) | 21-43 | 27(macroalgae)-64(microalgae) |
| C in Biocrude oil (wt.%) | 64-82 | 69(macroalgae)-79(microalgae) |
| H in Biocrude oil (wt.%) | 7-11 | 8(macroalgae)-11(microalgae) |
| N in Biocrude oil (wt.%) | 4-6 | 3(macroalgae)-8(microalgae) |
| HHV of Biocrude oil (MJ/kg) | 29-39 | 28-40 |
| Swine Manure (He et al., 2000a; Ocfemia et al., 2006a; Ocfemia et al., 2006b) | | |
| Yields (d.a.f.%) | 59-70 | 62-70 |
| C in Biocrude oil (wt.%) | 71-78 | 66-74 |
| H in Biocrude oil (wt.%) | 8.9-9.4 | 9.2-10 |
| N in Biocrude oil (wt.%) | 3.9-4.6 | 3.7-4.5 |
| HHV of Biocrude oil (MJ/kg) | 34-39 | 25-31 |

Although the yields and heating values of the biocrude oil converted from algae and swine manure are similar under continuous modes, the optimum reaction conditions are significantly different for these two feedstocks in a continuous HTL reactor. For algal biomass, it is generally agreed that more severe reaction conditions can lead to higher yields, lower oxygen but increased nitrogen contents in the HTL biocrude (Elliott et al., 2015; Elliott et al., 2013; Jazrawi et al., 2013). In addition, very short residence time (*e.g.,* 1-5 min) in a continuous reactor can produce algal biocrude oil yields similar to that of longer residence time under batch modes (*e.g.*, 60-120 min) (Elliott et al., 2015; Elliott et al., 2013; Jazrawi et al., 2013). Both recent batch and continuous HTL studies also suggest that higher heating rate and lower residence time favor the production of biocrude. This feature would also help improve the energy efficiency and techno-economic feasibility of algal biomass to fuel systems via a continuous HTL (Elliott et al., 2015; Faeth et al., 2013).

Continuous HTL of swine manure requires a longer retention time compared to algal feedstocks. Ocfemia et al. has conducted a continuous HTL of swine manure with a CSTR reactor at 285-325°C for 40-80 min. The highest oil yield was achieved at about 285-305°C for a 60 min retention time, which is very similar to those obtained at a batch reactor (He et al., 2000a; He et al., 2000b). In this continuous HTL study, it was reported that increasing the reaction temperature from 305°C to 325°C decreased the oil yield by 22-25 wt.% at the same residence

time, while extending the residence time from 60 min to 80 min only increased the oil yield by 1-2 wt.% at 285°C-325°C (Ocfemia et al., 2006b). According to the literature, swine manure is composed of 25 wt.% proteins and 35 wt.% of carbohydrate, while the algal feedstocks used in these continuous HTL studies contain much more proteins (*e.g.*, 60-68 wt.% in *Chlorella* and *Spirulina*) (Chen et al., 2014b; He et al., 2000a; He et al., 2000b; Jazrawi et al., 2013; Ocfemia et al., 2006a; Vardon et al., 2011). Moreover, the continuous HTL of swine manure has been examined in a CSTR, but the continuous HTL of algal biomass has been investigated in a PFR or the combinations of CSTR and PFR.

### 2.2.3 Process Conditions

Process conditions of HTL include reaction temperature, reaction (also refers to as retention) time, pressure, feedstock/water ratio (solid content) and catalyst applications. Figure 2-2 summarizes the effects of major process parameters (reaction temperature, reaction time, and total solid content of feedstocks) on the distribution of HTL product yields converted from algal biomass based on a number of studies.

Reaction temperature has been identified as the most significant factor affecting HTL product yields and the quality of biocrude oil converted from wet biowaste such as animal manure, algae, and food processing waste (He et al., 2000b; Yoshida et al., 1999; Yu et al., 2011b). In general, reaction temperatures from 250-375°C were used for biocrude oil production from protein-containing biomass. Reaction temperature varies largely depending on feedstock species. Yu et al. (2011) and Gai et al. (2014) converted microalgae (Chlorella) into biocrude oil via HTL without catalyst and suggested that 280-300°C are the optimal reaction temperature to achieve the highest biocrude oil yield, heating value, and energy recovery (Gai et al., 2014a; Yu et al., 2011b). Brown et al (2010) and Valdez et al (2012) converted Nannochloropsis into biocrude oil via HTL and concluded that 300-350°C is the best reaction temperature to reach the highest biocrude oil yield (Brown et al., 2010; Valdez et al., 2012). Considering heating rates, mixing versus non-mixing, and reactor systems (*e.g.*, batch versus continuous), optimal reaction temperatures are quite different. Therefore, it is important to elucidate the reaction mechanisms of HTL in terms of feedstock composition, reaction temperature, reaction time and catalyst.

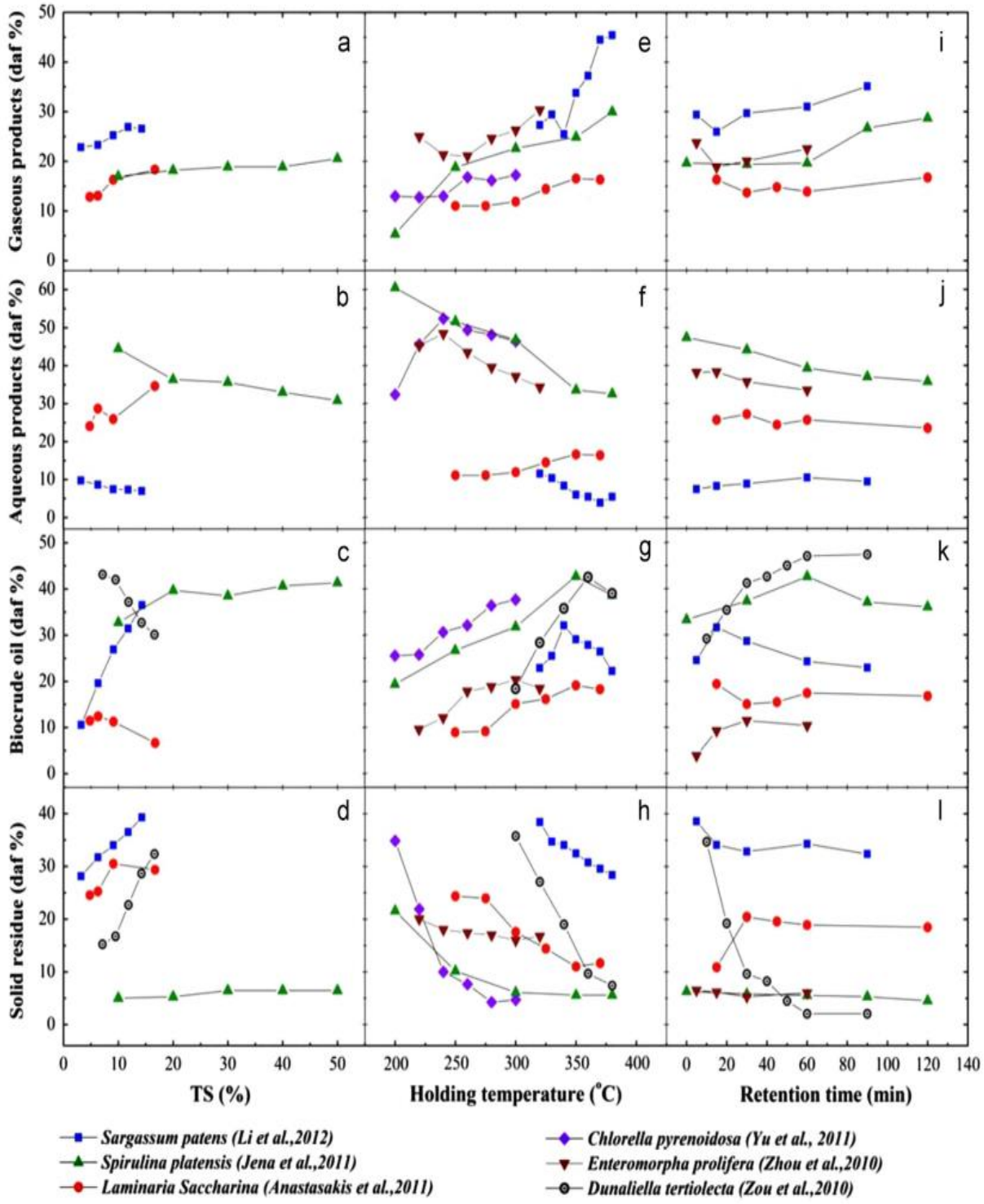


**Figure 2-2. Effects of major operational parameters on distribution of product yields converted from algae via HTL (Tian et al., 2014) (The blue dot is from Li et al., 2012 (Li et al., 2012); the purple dot is from Yu et al., 2011 (Yu et al., 2011a); the green dot is from Jena et al., 2011 (Jena & Das, 2011); the brown dot is from Zhou et all, 2010 (Zhou et al., 2010); the red dot is from Anastasakis et al., 2011 (Anastasakis & Ross, 2011); the grey dot is from Zou et al., 2010 (Zou et al., 2010)).**

Multiple studies have reported that more gases products were formed when the HTL reaction temperature is above 320°C (Brown et al., 2010; Jena et al., 2011a; Li et al., 2012; Tian et al., 2014). Li et al (2012) found that the gas product yields were drastically enhanced when the HTL reaction temperature increased from 320°C to 380°C (Li et al., 2012). Hydrolysis and depolymerization of feedstock is the governing reaction at the initial stage, followed by repolymerization between 220-375°C, and gasification beyond 375°C (Guo et al., 2015). As the reaction temperature increased beyond the reaction regime of repolymerization, more solid residues and char would be formed (Chen et al., 2014c; He et al., 2000b; Tian et al., 2014; Valdez et al., 2012).

Reaction time is another important factor on the formation of biocrude oil. For wet biowaste such as swine manure, it takes at least 15 min reaction time to form asphalt-like biocrude products (Zhang, 2010). In the case of algal biomass, it typically takes ten minutes to form self-separated biocrude products. Reaction time is an important factor to the reaction kinetics of HTL process. While sufficient reaction time is necessary to ensure a maximum biocrude oil yield, excessive reaction time will reduce the biocrude oil yield by forming biochar or gaseous products. Other reactions such as condensation and repolymerization during HTL processes would happen and affect the quality of biocrude oil (Chen et al., 2014c; Guo et al., 2015; Yu et al., 2011b).

Heating rates could also significantly affect the completeness of HTL reaction and the biocrude oil conversion. Faeth et al. (2013) (Faeth et al., 2013) conducted a fast HTL conversion (heating rates as high as 230 ± 5°C/min) of *Nannochlorpsis* and reported that an optimum biocrude oil yield (66 wt.% based on dry ash free biomass) can be obtained within 1 min, and the biocrude oil presents a similar carbon content and HHV to those converted from conventional HTL. Jazrawi et al. (2013) reached a highest algal biocrude oil yield (41.7 wt.%) within 3-5 min at 250-350°C by a continuous-HTL reactor (Jazrawi et al., 2013).

Many HTL studies applied initial pressure by filling up a gas in the reactor headspace prior to heating up. The main purposes of applying initial pressure are to maintain water in liquid phase, reduce the enthalpy of phase change of water, enhance the solubility of biomass, and improve the energy efficiency (Akhtar & Amin, 2011; Peterson et al., 2008; Tian et al., 2014). He et al. (2001) used 0-1.30 MPa of nitrogen gas ($N_2$) as the initial pressure to convert swine manure into biocrude oil via HTL and found that no biocrude oil was formed until the initial

pressure reached 0.69 MPa (He et al., 2001a). However, multiple studies have demonstrated that further increasing the initial pressure would not improve the biocrude oil yield (He et al., 2001a; Yin et al., 2010; Yu et al., 2011a; Zhang et al., 2013b). Zhang et al (2013) has extended the initial pressure from 0.69 to 3.45 MPa to covert *Chlorella* into biocrude oil. It was indicated that the initial pressure beyond 0.69 MPa has no significant effect on HTL product yields. Yu et al (2011) showed that increasing the initial pressure from 0 to 0.69 MPa insignificantly impacted the HTL product yields converted from *Chlorella* (Yu et al., 2011a). On the other hand, Yin et al (2011) converted cattle manure with 0-0.69 MPa of CO and $N_2$ as the initial pressure. A decreasing biocrude oil yield was observed when the initial pressure increased, possibly due to the self-condensation reaction that converts biocrude oil into solid residues (Yin et al., 2010). There are still no absolute conclusions about the effect of the initial pressure on biocrude oil yields when converting wet biowaste via HTL.

Reducing gases, such as carbon monoxide (CO) and hydrogen ($H_2$), has been used as the processing gas to stabilize the fragmented products of HTL, to inhibit the condensation, cyclization, and/or repolymerization of free radicals, and thus prevent char formation (Akhtar & Amin, 2011; He et al., 2001a; Yin et al., 2010). The following equations give an example for stabilization of aromatic radicals (Ar·) in liquid oil products by $H_2$ (Shuping et al., 2010).

$$Ar\cdot + H_2 \rightarrow ArH + H\cdot \quad (2\text{-}1)$$

$$Ar\cdot + H\cdot \rightarrow ArH \quad (2\text{-}2)$$

Yin et al. (2011) has converted cattle manure into biocrude oil via HTL with reducing gases such as $H_2$ and CO (Yin et al., 2010). They summarized that using CO and $H_2$ as HTL processing gases can improve the biocrude oil yield by 5-15 wt.%. Similar results were reported by He et al. (2001) when converting swine manure into biocrude oil via HTL with CO and $H_2$ as processing gases (He et al., 2001a). Although $H_2$ and CO are effective in stabilizing the fragmented liquefaction products, they are costly and hazardous options. Alternative processing gases such as synthetic gas ($H_2$/CO) may be another option to serve the same purpose (Akhtar & Amin, 2011).

Inert gases, such as nitrogen, air, and carbon dioxide, have been used as HTL processing gases (He et al., 2001a; Yin et al., 2010). However, the role of inert gases in HTL still remains unknown other than keeping reactor headspace pressure and preventing feedstock from gasifying. Yin et al. (2010) found that using air as HTL processing gas led to a much lower biocrude oil

yield than those converted with $N_2$ , while He et al. (2001) demonstrated that using compressed air as the processing gas can reach a similar biocrude oil yield as those processed with $CO_2$ and $N_2$ (He et al., 2001a). One obvious reason for the difference was the relative mass ratio of the processing gas to feedstock. Excessive amounts of air as an initial gas could oxidize the feedstock instead of converting it into biocrude.

Total solid content (TS) of the feedstock is one of the important parameters affecting the biocrude oil yield and the quality of biocrude oil (Akhtar & Amin, 2011; Gai et al., 2014a; Tian et al., 2014). The TS of feedstock is highly dependent on the types of biomass and its collection systems. Swine manure collected from a solid floor typically contains a TS of 20-30 wt.%, while from a flushing system with settling contains a TS of 5-10 wt.%. Most studies used feedstocks with a TS of 10-30 wt.% to achieve positive energy and economic returns (Akhtar & Amin, 2011; Anastasakis & Ross, 2011; Chen et al., 2014b; Valdez et al., 2012; Vardon et al., 2012; Wang, 2011b; Yu, 2012). Additional water would result in increased expenses such as heating and wastewater treatment costs, while excessively high TS may lead to problems including poor heat transfer and material handling such as pumping. Jena et al. (2011) present that 20 wt.% of TS is the optimum for HTL of *Spirulina* and greater TS show no significant effect on product yields (Jena et al., 2011a). Similar results were reported by Zhang et al (2013) and Gai et al (2014) when using *Chlorella* as HTL feedstock (Gai et al., 2014a; Zhang et al., 2013b). When TS is lower than 15 wt.%, significantly low biocrude oil yields (<10 wt.%) were obtained (He et al., 2001b; Zhang et al., 2013b). He et al (2001) speculated that the formation of biocrude oil may need a micro-organic phase as the media and thus accumulate organic clusters that can be converted into biocrude oil (He et al., 2001b; Zhang et al., 2013b).

### 2.2.4 Catalysis

Homogeneous and heterogeneous catalysts have been investigated under HTL processes. Table 2-4 summarizes different catalysts used for HTL of wet biowaste. The results of employing catalysts in HTL were not all positive (Tian et al., 2014). Zhang et al. (2013) converted *Chlorella* into biocrude oil under supercritical ethanol (240-300°C) using heterogeneous catalysts (*e.g.,* HZSM-5 and Raney-Ni) without improvement in biocrude oil yield (Zhang et al., 2013a). Similar results were found when converting microalgae and animal manure into biocrude oil via HTL with the catalysts of $Na_2CO_3$, Co/Mo, $CoMo/Al_2O_3$, Ni/Al, $Ni/SiO_2$-$Al_2O_3$, Pt/Al, Pd/C, Ru/C, and zeolites (Biller et al., 2011; Duan & Savage, 2010; Theegala &

Midgett, 2012). Phase behavior (*i.e.*, the interaction among liquid, solid, gas, sub/super-critical phases versus heterogeneous catalysts) in HTL of wet biowaste is very complex and thus catalysts deactivations as well as strong intraparticle diffusion limitations can also attribute to the ineffectiveness of catalysts (Duan & Savage, 2010; Zhang et al., 2013a). Another reason for the catalysts having little effect on the HTL biocrude oil yields could be that the oil yield in the absence of catalyst was already near the upper bound of what is possible, given the constraint of the mass balance, availability of carbon and hydrogen (Duan & Savage, 2010). It was demonstrated that more than 80% of the C and H atoms in the algal feedstocks were recovered in the HTL biocrude oil without the addition of catalysts (Duan & Savage, 2010).

**Table 2-4. Comparison of different catalysts used in HTL of protein-containing biomass**

| Catalysts | Feedstocks | Optimal biocrude oil yield (d.w.%) | Optimal biocrude oil HHV (MJ/kg) |
|---|---|---|---|
| **Homogeneous** | | | |
| NaOH (Yu et al., 2014) | Chlorella | 45 wt.% | N/A |
| KOH (Anastasakis & Ross, 2011) | Laminaria | 15 wt.% | 34-38 |
| $Na_2CO_3$ (Jena et al., 2015; Li et al., 2012; Theegala & Midgett, 2012; Yu et al., 2014; Zhou et al., 2010) | Chlorella | 40-45 wt.% | N/A |
| | Dairy Manure | N/A[a] | 35 |
| | Enteromorpha | 25 wt.% | 30 |
| | Microcystis | 30-35 wt.% | 30-31 |
| | Sargassum | 28 wt.% | N/A |
| | Yeast | 56.4 wt.% | 37 |
| **Heterogeneous** | | | |
| Pd/C, Pd/$Al_2O_3$ (Duan & Savage, 2010; Yu et al., 2014) | Chlorella | 40-45 wt.% | N/A |
| | Nannochloropsis | 45-55 wt.% | 39 |
| Pt/C, Pt/$Al_2O_3$ (Duan & Savage, 2010; Yu et al., 2014) | Chlorella | 43-45 wt.% | N/A |
| | Nannochloropsis | 50-52 wt.% | 40 |
| Pt/Al (Biller et al., 2011) | Chlorella | 39 d.a.f.%[b] | 38 |
| | Nannochloropsis | N/A | N/A |
| Ru/C (Duan & Savage, 2010) | Nannochloropsis | 45-50 wt.% | 38 |
| Raney-type alloy (Duan & Savage, 2010; Yu et al., 2014) | Chlorella | 47-50 wt.% | N/A |
| | Nannochloropsis | 40-50 wt.% | N/A |
| Raney-Ni (Zhang et al., 2013a) | Chlorella | 50-65 wt.% | 31-35 |
| HZSM-5 (Zhang et al., 2013a) | Chlorella | 55-65 wt.% | 32-36 |
| Zeolite (Duan & Savage, 2010) | Nannochloropsis | 40-45 wt.% | 35-39 |
| Ce/HZSM-5 | Chlorella | 50 wt.% | 23-28 |
| Co/Mo (Biller et al., 2011; Duan & Savage, 2010) | Chlorella | 39 d.a.f.%[b] | 36-38 |
| | Nannochloropsis | 42-52 wt.% | 39 |
| Ni/Al (Biller et al., 2011) | Chlorella | 30.0 d.a.f.%[b] | 35-38 |
| Ni/REHY (Yang et al., 2011) | Dunaliella | 72.0 wt.% | 30 |
| $Fe(CO)_5$-S (Matsui et al., 1997) | Spirulina | 78.3 wt.% | 26 |

[a] Not available; [b] Based on dry ash free matter

The loadings of catalysts are an influential factor for HTL process. Anastasakis and Ross (2011) used 5-100 wt.% KOH to study the effect of the loadings of catalysts on HTL of macroalgae. It was reported that the HTL biocrude oil yields decreased by about 10 wt.% while the heating value of biocrude oil increased by 1.3 MJ/kg, as the amounts of catalysts increased from 5 to 100 wt.% (Anastasakis & Ross, 2011). Theegala et al. (2012) have confirmed that increasing the catalysts ($Na_2CO_3$) loading from 5 wt.% to 20 wt.% did not improve the biocrude oil yield converted from animal manure via HTL (Theegala & Midgett, 2012). Comparable results were also demonstrated when using CaO to convert olive seeds, in which the amount of catalysts increased from 5 wt.% to 40 wt.%, the HTL biocrude oil yield decreased (Tekin, 2015).

Homogeneous catalysts seem to have a positive effect on the HTL biocrude oil yield, but the recovery of homogeneous catalysts remains a challenge. Yu et al. (2014) investigated the effect of NaOH and $Na_2CO_3$ on HTL of microalgae at 280°C and reported that the algal biocrude oil yield was improved by 5-10 wt.% (Yu et al., 2014). Jena et al. (2015) converted yeast into biocrude oil via HTL and demonstrated that adding $Na_2CO_3$ can enhance the biocrude oil yield by about 7 wt.% (Jena et al., 2015).

Regeneration of catalysts has been suggested to improve the techno-economic feasibility of catalytic HTL conversion of wet biomass (Biddy et al., 2013; Ong, 2013). Ong (2013) has used NaOH to regenerate catalysts such as Raney-Ni when hydrothermally treating waste newspapers. The author demonstrated that hydrothermal reactions with in-situ Raney-Ni synthesis and routine NaOH addition can be economically and energetically viable given a catalyst lifetime greater than 55.8 g-newspaper/g-catalyst (Ong, 2013). Effective and renewable methods to regenerate catalysts under HTL processes are critically needed because the catalysts are typically expensive and their production can impact the environment (Biddy et al., 2013; Ong, 2013).

### 2.2.5 HTL Products Separation

After HTL reaction, HTL products can be separated into biocrude oil, solid residue, aqueous products, and gaseous products. Figure 2-3 presents a typical separation procedure for HTL products (Chen et al., 2014c). Depending on feedstock and process conditions, HTL products could be naturally separated via gravitation. Organic solvents such as dichloromethane, acetone, and toluene, were also used to extract the biocrude oil fraction from HTL products (Anastasakis & Ross, 2011; Chen et al., 2014c; Jena et al., 2011a; Theegala & Midgett, 2012;

Tian et al., 2015; Vardon et al., 2012; Vardon et al., 2011; Yu et al., 2011b; Zhang et al., 2013a). Valdez et al. (2011) has studied the influence of different organic solvents on HTL product yields and quality. Non-polar solvents (hexadecane, decane, hexane, and cyclohexane) and polar solvents (methoxycyclopentane, chloroform, and dichloromethane) were used to recover the biocrude oil converted from *Nannochloropsis*. It is found that non-polar solvents, such as hexadecane and decane, can provide high gravimetric yields of bio-oil (39 wt.%), but the recovered biocrude oil present a lower carbon content (*e.g.*, 69 wt.% for decane) than that recovered with polar solvents such as dichloromethane (76 wt.%). The amount of free fatty acids in the biocrude oil is highly dependent on the solvent used, with polar solvents recovering more fatty acids than nonpolar solvents (Valdez et al., 2011).

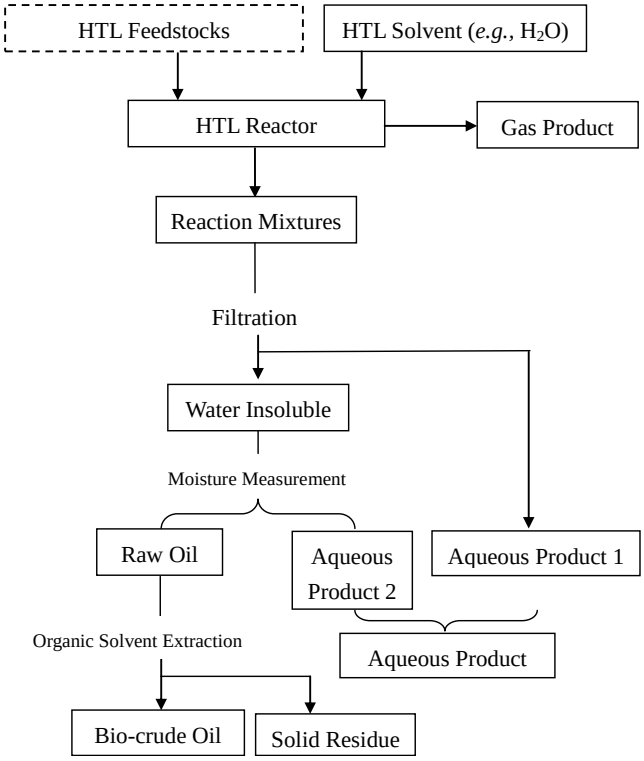


**Figure 2-3. A typical separation procedure for HTL biocrude oil**

A sequential extraction process was investigated to separate nitrogen-containing compounds from HTL biocrude oil using water and toluene in series to extract HTL biocrude oil converted from wet biowast (Chen et al., 2016b). When an ultrasonically assisted extraction by water was conducted, the nitrogen content in algal biocrude oil decreased by 16% with improved carbon and hydrogen contents. However, it was also suggested that alternative extraction

techniques should be considered to improve the extractive denitrogenation efficiency and reduce the amount of biocrude oil lost into the water extract for HTL biocrude oil (Chen et al., 2016b).

Although solvents are usually used to recover HTL biocrude oil, some studies, particularly for those focusing on continuous HTL reactor development, separate HTL biocrude oil by decanting the solid products from aqueous products. For example, the continuous hydrothermal treatment of microalgae in the PNNL studies did not use any organic solvent to recover the algal biocrude oil (Elliott et al., 2015; Elliott et al., 2013). Similar separation method is also used for continuous HTL of swine manure (Ocfemia et al., 2006a; Ocfemia et al., 2006b).

## 2.3 Characterization of HTL Products

### 2.3.1 Biocrude Oil

#### 2.3.1.1 Elemental Analyses and Heating Value

Elemental analyses including the measurement of carbon, hydrogen, nitrogen (CHN), metal, and inorganic contents are commonly used to understand and evaluate the quality of HTL biocrude oil. Carbon, hydrogen, nitrogen, and sulfur contents of the HTL biocrude oil were measured and used to calculate the higher heating value (HHV). Compared with petroleum crudes, HTL biocrude has a much higher oxygen and nitrogen contents. Further upgrading processes to lower heteroatom contents in HTL biocrude oil is recommended in order to be used as transportation fuels (Vardon et al., 2011). Similar measurement and suggestions were also reported by multiple studies converting biowaste and/or algal biomass into biocrude oil via HTL (Chen et al., 2014b; Elliott et al., 2013; Jena et al., 2011a; Valdez et al., 2011; Xiu et al., 2011b; Zhang et al., 2013a). With the elemental compositions, Van Krevelen diagrams can be constructed based on the H/C, O/C, and N/C molar ratios of HTL biocrude oil (Figure 2-4**).** From a fuel perspective, biocrude oil with a high H/C as well as a low O/C and N/C molar ratios is preferred, so that their properties would be close to those of petroleum fuels (Chen et al., 2014c; Tian et al., 2014; Yu et al., 2011b). In addition, nutrient recoveries (*e.g.*, nitrogen) can be computed with the information of elemental compositions (Chen et al., 2014c; Gai et al., 2014a; Yu et al., 2011b).

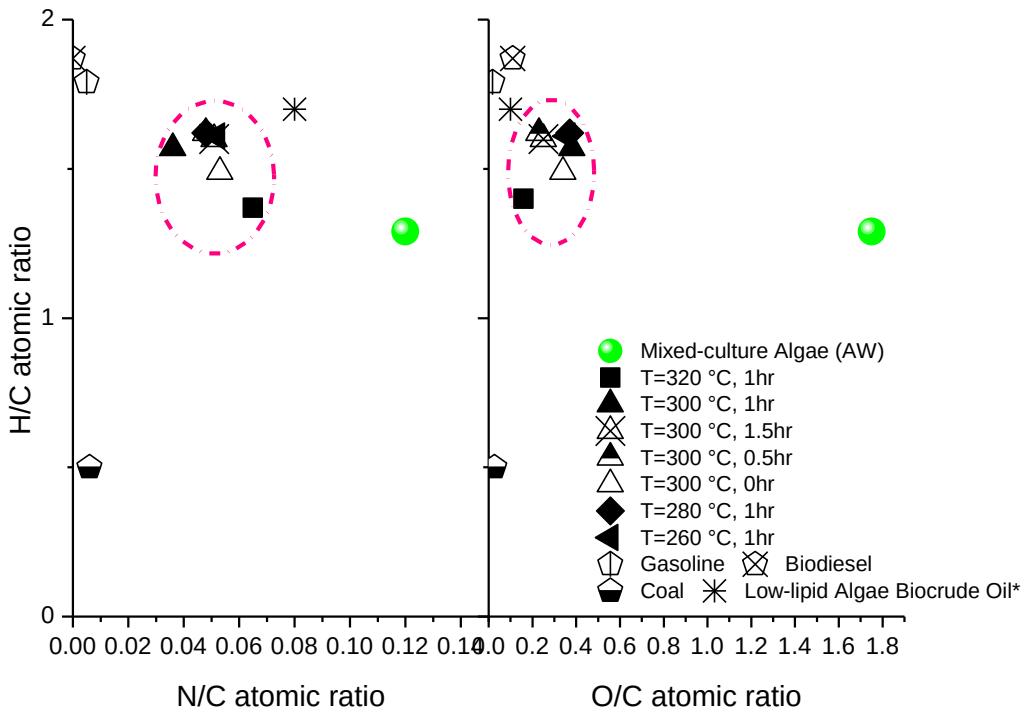


**Figure 2-4. Van Krevelen diagrams of HTL biocrude oil (Chen et al., 2014c)**

Although the HHV of HTL biocrude oil is usually calculated by Dulong formula, other equations or methods considering the effect of high ash content have been attempted. Anastasakis and Ross (2011) evaluate the HHV of biocrude oil converted from macroalgae based on the elemental compositions of carbon, hydrogen, sulfur, oxygen, nitrogen, and ash content (Anastasakis & Ross, 2011). Oxygen bomb calorimeter is commonly used to directly measure heating values of HTL biocrude oil (Tian et al., 2015; Zhang, 2014). The energy recovery (defined as the energy content in the HTL oil to the energy content in the feedstock), energy consumption ratio (defined as the energy required for HTL against the energy that can be recovered from biocrude oil combustion), and fossil energy balance (FEB, defined as the (energy in biofuel-fossil fuel input)/1 MJ biofuel produced)) of HTL biocrude oil can be further estimated with the measurement of HHV (Chen et al., 2014b; Vardon et al., 2012; Yu, 2012). To perform the techno-economic analysis for HTL (or any other bioenergy production), exergy could be a more direct indicator, which is defined as the ratio of energy in the HTL biocrude oil to the sum of energy in the feedstock and the energy required for HTL process.

Metal compositions such as Ca, Mg, K, Na, Al, Fe, *etc.* of HTL biocrude oil have also been characterized, particularly for the biocrude oil converted from high-ash biomass such as macroalgae (Anastasakis & Ross, 2011; Chen et al., 2014c; Tian et al., 2015; Xiu et al., 2011a).

Understanding the fate of the metal in feedstocks during HTL is important to assess whether they would affect HTL conversion efficiency as well as the quality of resulting biocrude oil, or recover the metal as a byproduct. Several studies have pointed out that the metal compositions such as alkaline earth metals and calcium carbonates could act as catalysts during HTL of algal biomass (Anastasakis & Ross, 2011; Chen et al., 2014c; Tian et al., 2015; Zhang, 2014). The existence of calcium carbonate can promote denitrogenation of biocrude oil during HTL of mixed-culture algae (Chen et al., 2014c). However, these metals may also poison catalyst used for upgrading processes such as desulfurization and catalytic cracking (Xiu et al., 2011a). Trade-offs between the catalytic effect and poison of the metals in biocrude oil need further investigation.

Inorganic compositions, such as phosphorus (P) , in HTL biocrude oil are also of interest, probably because phosphorus is an important element for algal cultivation and its limited quantities emphasize the need to recycle it for sustainable production of algal biofuels (Gai et al., 2014b; Valdez et al., 2012; Yu et al., 2014). A number of studies present that majority of phosphorus in algal biomass was retained in HTL aqueous product (Garcia Alba et al., 2011; Valdez et al., 2012). The phosphorus content in the HTL aqueous products could be highly affected by the metal compositions of the feedstock, because some metal elements could bond with phosphorus to form precipitates and to be recovered by solid residue (Wang, 2011b; Yu et al., 2014).

#### 2.3.1.2 TGA, Sim-Dist, GPC, and SEC analyses

Thermal gravimetric analysis (TGA) and simulated distillation (Sim-Dist) are two common tools to evaluate the boiling point distribution of HTL biocrude oil. Boiling point distribution is one of the most commonly referenced characteristics of crude oil for fuel applications (Anastasakis & Ross, 2011; Chen et al., 2014b; Chen et al., 2014c; Gai et al., 2014a; Vardon et al., 2012; Vardon et al., 2011; Yu, 2012; Zhang et al., 2013a). Boiling points of the biocrude oil converted from microalgae and swine manure predominantly fell in the range of heavy vacuum gas oil (343-538°C). Similar results were also demonstrated in other HTL biocrude converted from different types of biowaste and algal biomass (Chen et al., 2014b; Chen et al., 2014c; Gai et al., 2014a; Yu, 2012; Zhang et al., 2013a).

Gel permeation chromatography (GPC) and size-exclusion chromatography (SEC) are two typical methods to assess the molecular weight distribution of HTL biocrude oil (Barreiro et

al., 2013; Garcia Alba et al., 2011; Vardon et al., 2012; Vardon et al., 2011). Barreiro et al (2013) have conducted GPC analysis on biocrude oil converted from algal biomass at 250°C and 375°C, and found that high temperatures (375°C) and pressures (250–270 bar) seem to be severe enough to degrade the microalgae molecules into similar types of oil molecular weight distributions, while HTL at mild temperature results in an "improved" extraction, rather than a proper thermochemical conversion (Barreiro et al., 2013). On the other hand, SEC analysis can provide additional information including the weight-average molecular weights ($M_w$), the number-average molecular weights ($M_n$), and polydispersity values (PDI). In general, HTL biocrude oil presents a higher $M_w$, $M_n$ and PDI than petroleum crude. The higher PDI indicates that there is a greater difference in the minimum and maximum molecular weights of biocrude oil, which in turn is due to the high oxygen content derived from polymer-linking groups such as esters and ethers (Vardon et al., 2012; Vardon et al., 2011).

#### 2.3.1.3 Chemical composition

Chemical compositions of HTL biocrude oil are typically characterized using gas chromatography mass spectrometer (GC-MS), nuclear magnetic resonance (NMR), and Fourier-transform infrared spectroscopy (FTIR) (Chen et al., 2016b; Chen et al., 2014b; Chen et al., 2014c; Gai et al., 2014a; Vardon et al., 2012; Vardon et al., 2011; Wang, 2011b; Yu, 2012; Yu et al., 2014; Zhang et al., 2013a; Zhang, 2014). GC-MS analysis identifies compounds and NMR and FTIR reveal functionalities. HTL biocrude oil includes a variety of compounds such as hydrocarbons (*e.g.*, tridecene), fatty acids (*e.g.*, hexadecanoic acid), straight amide derivatives (*e.g.*, hexadecanamide), n-heterocyclic compounds (*e.g.*, indole), and oxygenates (*e.g.*, esters, alcohols, aldehydes and phenols). Compositions of HTL biocrude oil are extremely complex and vary widely from its original feedstocks. Only a fraction of HTL biocrude oil can be identified by GC-MS due to two reasons: 1) a large fraction of the biocrude has high molecular weight molecules; and 2) limited by the temperature of the instrument (Vardon et al., 2011). On the other hand, some low-boiling point compounds may be masked by the solvent peak or evaporated during evaporation of organic solvents used to recover biocrude oil (Chen et al., 2016b). Therefore, complementary analyses such as NMR and FTIR are usually conduced to verify the results obtained from GC-MS analysis.

FTIR analysis allows for a more comprehensive comparison of "whole" oil functional group characteristics compared to GC–MS, with spectral band assignments and interpretation

based on previous studies (Vardon et al., 2011; Xiu et al., 2011a; Yin et al., 2010; Zhang et al., 2013a). It is believed that HTL biocrude oil presents a prominent C–H stretching, –CH2 bending and CH3 bending characteristics, which suggests the existence of alkyl C–H (Gai et al., 2014a; Vardon et al., 2012; Vardon et al., 2011; Zhang et al., 2013a). On the other hand, NMR analysis gives complementary functional group information to FTIR spectra and the ability to quantify and compare integration areas between spectra (Vardon et al., 2011). To date, $^{1}$H NMR, $^{13}$C NMR, and $^{31}$P NMR have been exploited to characterize HTL biocrude oil (Gai et al., 2014a; Gai et al., 2015; Patel & Hellgardt, 2013; Vardon et al., 2012; Vardon et al., 2011; Zhang et al., 2013a; Zhang, 2014). One $^{1}$H NMR analysis of HTL biocrude oil converted from *Chlorella* observed a high percentage of aliphatic functionality (59 – 67%), which is also found in other biocrude oil products converted from *Spirulina* (53%) and duckweed (60%) (Duan et al., 2013b; Gai et al., 2014a; Vardon et al., 2011). Other techniques for quantifying biocrude oil functional groups are also employed. For example, high-resolution Fourier-transform ion cyclotron resonance mass spectrometry (FTICR-MS) has been used to fully categorize the HTL biocrude oil and relatively quantitative results of different functional groups were reported (Chiaberge et al., 2014; Faeth et al., 2016; Leonardis et al., 2013).

#### 2.3.1.4 Potential Value-added Products

In addition to transportation biofuels, HTL biocrude oil can be further processed to obtain other value-added chemicals. Chemical and rheological techniques have been used to categorize the applicability of the HTL biocrude oil converted from *Spirulina* and swine manure as raw materials for pavement construction (Dhasmana et al., 2015). It was demonstrated that HTL biocrude oil had higher asphaltene content than that of commercial binders. When HTL biocrude oil was mixed with commercial binders at a ratio of 1 to 8, the component structure resembled that of conventional petroleum binder, indicating its possible use as a softening agent for mixing with old asphalt materials, and a potential alternative surrogate for conventional asphalt.

### 2.3.2 Aqueous Product

The post-HTL aqueous product, also refers to as post-hydrothermal wastewater (PHWW), contains a significant amount of nutrients (*e.g.,* ammonia and phosphates), and toxic compounds. The PHWW of wet biowaste feedstocks is different from other feedstocks such as crop residue. First, it contains most nutrients (primarily nitrogen) in the feedstock that can be reused for biomass production. On the other hand, it contains many n-heterocyclic compounds that can be

inhibitive to the growth of microorganism, algae and plants. Therefore, PHWW must be treated prior to being used as a fertilizer or discharge to waterways.

#### 2.3.2.1 Chemical Composition

The chemical composition of PHWW can be characterized in terms of chemical oxygen demand (COD), total organic carbon (TOC), total ammonia nitrogen (TAN), total nitrogen (TN), total phosphorus (TP), and total suspended solids (TS), as well as the elemental and GC-MS analyses (Albrecht et al., 2016; Appleford et al., 2005; Biller et al., 2016; Biller et al., 2012; Cherad et al., 2016; Gai et al., 2014b; Pham et al., 2013a; Pham et al., 2013b; Tommaso et al., 2015; Valdez et al., 2012; Zhou et al., 2013). **Table 2-5** summarizes the chemical composition of PHWW converted from different feedstocks via HTL. Response surface methodology (RSM) was used to investigate the interactions of reaction temperature, retention time, and total solid ratio of feedstocks on the water quality characteristics of PHWW converted from microalgae in a batch mode [109]. The authors reported that the total solid ratio of feedstocks was the dominant factor affecting the nutrient recovery efficiencies of PHWW. Appleford et al (2005) have characterized PHWW converted from swine manure in a continuous-stirring reactor in terms of chemical compositions, biological oxygen demand (BOD), TS, pH, TAN, chloride, nitrate, phosphate, sulfate, metal ions (*e.g.*, Cr, Fe, Mg, and Zn), and total fecal coliforms (Appleford et al., 2005). Although bacterial pathogens in swine manure were completely killed during the HTL process, the level of BOD, pH, and elemental concentrations (*e.g.*, Fr, Mn, and Zn) were higher than the USEPA standard for discharge to waterways (Appleford et al., 2005; Gai et al., 2014b; Zhou et al., 2013). This is because that an HTL process essentially separates a large fraction of elements (except hydrogen and carbon) in the feedstocks into aqueous phase. For that reason, the cytotoxicity of PHWW should be thoroughly characterized. Pham et al (2013) utilized a Chinese hamster ovary (CHO) cell assay to evaluate the cytotoxicity of nine identified nitrogenous organic compounds (NOCs) in the PHWW from HTL of *Spirulina*. The authors reported that the organic mixture extracted from PHWW expressed potent CHO cell cytotoxic activity, with a $LC_{50}$ at 7.5% of PHWW. It is also found that 30% of the toxicity can be removed biologically by recycling the PHWW back into an algal cultivation system. The remaining toxicity of the PHWW could be mostly eliminated by subsequent treatment with granular activated carbon (GAC) (Pham et al., 2013a).

Chemicals of emerging concerns (CECs) that potentially cause undesirable ecological or health effects have also been characterized in the PHWW converted from the algal-bacteria biomass grown in the liquid portion of swine manure (Shin & Schideman, 2015). ELISA tests and GC-MS analysis were used to measure the concentrations of the CECs in the algal-bacterial feedstocks and HTL products. It is highlighted that a 99.9% of Florfenicol (a common environmental hormone) was removed under the HTL process at 300°C for a 35min reaction time (Shin & Schideman, 2015).

**Table 2-5. Comparison of average values of physicochemical characteristics of PHWW converted from swine manure and different algal feedstocks**

| Characteristic | Swine Manure[a] | Mixed-culture Algae[b] | *Chlorella*[c] | *Spirulina*[d] | High-Ash Algae[e] | USEPA Standard[f] | Illinois Standard[g] | Filtered Municipal Wastewater[h] |
|---|---|---|---|---|---|---|---|---|
| Biological Oxygen Demand (mg/L) | 35240 | N/A [i] | N/A [i] | N/A [i] | N/A [i] | 120 | 10 | N/A [i] |
| Chemical Oxygen Demand (mg/L) | 52030 | 30000-70000 | 62700-104000 | 89039 ±3321 | N/A [i] | N/A [i] | N/A [i] | 54 |
| Total Suspended Solids (g/L) | 33.0 | N/A [i] | 2.3-21.5 | N/A [i] | N/A [i] | 183 | 12 | N/A [i] |
| pH | 5.52 | 7.4-8.6 | 7.8-8.3 | 7.5 | N/A [i] | 6-9 | 6-9 | N/A [i] |
| **Ions (mg/L)** | | | | | | | | |
| Ammonia | 3413 | 2000-4500 | 3000-14800 | 10117±1167 | N/A [i] | N/A [i] | N/A [i] | N/A [i] |
| Total Nitrogen (TN) | 5355 | 3500-8000 | 11000-31700 | 22981±2482 | 1973-3941 | N/A [i] | N/A [i] | 33 |
| Chloride | 667 | N/A [i] | N/A [i] | N/A [i] | N/A [i] | N/A [i] | N/A [i] | N/A [i] |
| Nitrate | 0.87 | N/A [i] | N/A [i] | N/A [i] | N/A [i] | N/A [i] | N/A [i] | N/A [i] |
| Phosphate | 921 | N/A [i] | N/A [i] | N/A [i] | N/A [i] | N/A [i] | N/A [i] | N/A [i] |
| Total Phosphorus (TP) | 1499 | N/A [i] | 5440-18900 | 4400±198 | N/A [i] | N/A [i] | N/A [i] | 8 |
| Sulfate | 427 | N/A [i] | N/A [i] | N/A [i] | N/A [i] | N/A [i] | N/A [i] | N/A [i] |
| C/N ratio | N/A [i] | N/A [i] | N/A [i] | 2.4 | N/A [i] | N/A [i] | N/A [i] | N/A [i] |
| **Elements (mg/L)** | | | | | | | | |
| Aluminum (Al) | N/A [i] | N/A [i] | N/A [i] | 3.9 | N.D.[j] | N/A [i] | N/A [i] | N/A [i] |
| Boron (B) | N/A [i] | N/A [i] | N/A [i] | 22.5 | N/A [i] | N/A [i] | N/A [i] | N/A [i] |
| Calcium (Ca) | N/A [i] | N/A [i] | N/A [i] | 13.5 | 193 | N/A [i] | N/A [i] | N/A [i] |
| Chromium (Cr) | 0.27 | N/A [i] | N/A [i] | N/A [i] | N/A [i] | 2.77 | 1 | N/A [i] |

**Table 2-5. Comparison of average values of physicochemical characteristics of PHWW converted from swine manure and different algal feedstocks (cont.)**

| Characteristic | Swine Manure[a] | Mixed-culture Algae[b] | *Chlorella*[c] | *Spirulina*[d] | High-Ash Algae[e] | USEPA Standard[f] | Illinois Standard[g] | Filtered Municipal Wastewater[h] |
|---|---|---|---|---|---|---|---|---|
| **Elements (mg/L) (cont.)** | | | | | | | | |
| Copper (Cu) | N/A [i] | N/A [i] | N/A [i] | 0.6 | N/A [i] | N/A [i] | N/A [i] | N/A [i] |
| Cobalt (Co) | N/A [i] | N/A [i] | N/A [i] | 0.9 | N/A [i] | N/A [i] | N/A [i] | N/A [i] |
| Iron (Fe) | 28 | N/A [i] | N/A [i] | 4.7 | <15.7 | N/A [i] | 2 | N/A [i] |
| Magnesium (Mg) | 242 | N/A [i] | N/A [i] | 1.4 | 2.9 | N/A [i] | N/A [i] | N/A [i] |
| Manganese (Mn) | 2 | N/A [i] | N/A [i] | 0.3 | N/A [i] | N/A [i] | 1 | N/A [i] |
| Phosphorus (P) | 434 | N/A [i] | N/A [i] | N/A [i] | N/A [i] | N/A [i] | N/A [i] | N/A [i] |
| Potassium (K) | 1482 | N/A [i] | N/A [i] | 3400 | 155 | N/A [i] | N/A [i] | N/A [i] |
| Rubidium (Rb) | 0.58 | N/A [i] | N/A [i] | N/A [i] | N/A [i] | N/A [i] | N/A [i] | N/A [i] |
| Sodium (Na) | N/A [i] | N/A [i] | N/A [i] | 2254 | 115 | N/A [i] | N/A [i] | N/A [i] |
| Selenium (Se) | N/A [i] | N/A [i] | N/A [i] | 11.7 | N/A [i] | N/A [i] | N/A [i] | N/A [i] |
| Sulfur (S) | 9651 | N/A [i] | N/A [i] | N/A [i] | N/A [i] | N/A [i] | N/A [i] | N/A [i] |
| Zinc (Zn) | 1.67 | N/A [i] | N/A [i] | 1.3 | N/A [i] | N/A [i] | 1 | N/A [i] |
| **Total Fecal Coliforms (#/mL)** | <2 | N/A [i] | N/A [i] | N/A [i] | N/A [i] | N/A [i] | N/A [i] | N/A [i] |
| **$IC_{50}$ (%)** | N/A [i] | N/A [i] | 0.35-1.90 | N/A [i] | N/A [i] | N/A [i] | N/A [i] | N/A [i] |

[a] From (Appleford et al., 2005; Zhou et al., 2013)
[b] From (Chen et al., 2014c; Tommaso et al., 2015)
[c] From (Gai et al., 2014b; Zhou, 2015a)
[d] From (Mingxia Zheng, 2016; Zhou et al., 2013)
[e] From (Tian et al., 2015)
[f] Standard is 1 day maximum concentration for the Specialty Organic Chemicals industrial category
[g] Standard is categorical effluent limitation for the State of Illinois
[h] From (Zhou et al., 2013)
[i] Not applied
[j] Not detected

#### 2.3.2.2 Treatments on PHWW

PHWW treatment has been investigated using adsorption (Mingxia Zheng, 2016; Zhou, 2015a; Zhou, 2015b), anaerobic digestion (Chen et al., 2016a; Tommaso et al., 2015; Zheng et al., 2016; Zhou et al., 2015), algal cultivation (Biller et al., 2012; Pham et al., 2013a; Shin & Schideman, 2015), recirculation to the HTL processes (Biller et al., 2016; Ramos-Tercero et al., 2015; Zhu et al., 2015), and catalytic hydrothermal gasification (Breinl & Zhang, 2015; Cherad et al., 2016; Elliott et al., 2014; Elliott et al., 2013). A photobioreactor (PBR) was used to monitor the long-term performance when treating a combination of municipal wastewater and PHWW for an about 800-day operation (Zhou, 2015a). Different operating conditions (retention time, various PHWW loading rate, with and without the addition of GAC) were performed and the results show that the PBR can achieve an efficient removal of organic carbon (79%-93% COD) and nitrogen (50%-99% $NH_4^+$ and 27-30% total nitrogen) (Zhou, 2015a). Increasing the PHWW loading rates reduced the removal efficiency of COD and $NH_4^+$. Adding GAC facilitated a stable PBR performance and allowed higher PHWW loading rate. GAC addition also resulted in shorter retention times with an improved removal efficiency of COD (from 70% to over 90%), $NH_4^+$ (from 26% to 100%) and cytotoxicity (from 40% to 60%). Similarly, zeolite, GAC, and polyurethane matrices (PM) were used for detoxification during a two-round anaerobic batch test with PHWW converted from cyanobacteria (e.g. *Spirulina*). GAC was considered promising due to its highest methane yield of 124 mL/g COD at the second feeding, indicating a good recovery of adsorption capacity (Zheng et al., 2016).

Anaerobic digestion (AD) could be also used to treat PHWW. Zhou et al (2015) have investigated the feasibility of using AD to treat PHWW converted from swine manure (Zhou, 2015a; Zhou et al., 2015). It is demonstrated that successful AD occurred at relatively low concentrations of PHWW ($\leq$ 6.7%) and led to a biogas yield of 0.5 ml/mg COD removed. On the other hand, higher concentrations of PHWW (e.g., $\geq$ 13.3%) present an inhibitory effect on the AD process (Zhou, 2015a; Zhou et al., 2015). Tommaso et al (2015) has also examined the anaerobic degradability of PHWW converted from mixed-culture algae grown in a wastewater treatment system (Tommaso et al., 2015). The effect of HTL reaction temperature (260-320°C) and reaction time (0-90 min) on the anaerobic degradability of PHWW was studied. The highest cumulative methane production (with a moderate lag phase) was realized when PHWW was obtained at 320°C. The second highest accumulated methane production (obtained with the

PHWW converted at 300°C) was achieved after overcoming the longest lag phase in this study. Further, the authors have identified acetogenesis as a possible rate-limiting pathway in AD of PHWW (Tommaso et al., 2015).

Cultivating algal biomass in PHWW can help develop a sustainable system that couples bioenergy production with nutrient recovery, wastewater treatment, as well as biomass augmentation. Multiple studies have utilized diluted PHWW to grow algal biomass (Biller et al., 2012; Jena et al., 2011a; Zhang et al., 2016b; Zhou, 2015a). Biller et al (2012) cultured microalgae strains of *Chlorella* and *Scenedesmus* as well as the cyanobacteria of *Spirulina* and *Chlorogloeopsis* with diluted PHWW converted from the same microalgae and cyanobacteria strains. It is found that the optimum dilution is strain dependent but ranges between 200 and 400 times (Biller et al., 2012). Zhang et al (2016) investigated the nutrient recovery efficiency (C, N and P) from PHWW prepared with two biocrude-aqueous separation methods (vacuum filtration and ethyl ether extraction). With ethyl ether extraction as a biocrude-aqueous separation method, a higher algal biomass growth rate was reached. In contrast, a more advantageous nutrient recovery efficiency (about 1.4 times nitrogen recovery, 1.5 times phosphorus recovery, and 2.3 times carbon recovery) was realized when the vacuum filtration was utilized to separate the PHWW converted from *Chlorella* (Zhang et al., 2016b).

Alternatively, PHWW still contains 10-40% of original carbon in the feedstock than can be added back to HTL processes as a reaction substrate. PHWW converted from microalgae was recirculated to HTL processes to recover the organic content and to develop a solvent-free process (Ramos-Tercero et al., 2015). It was demonstrated that the biocrude oil yield increased to a constant level after six recycles at 240°C. The authors also summarized that recycling the PHWW not only increased the biocrude oil yield, but also reduced the operating temperature of HTL (*e.g.*, from 300°C to 240°C) to achieve an optimal biocrude oil yield.

PHWW can also be converted into hydrogen via catalytic hydrothermal gasification (CHG) (Breinl & Zhang, 2015; Cherad et al., 2016). Breinl (2015) has hydrothermally treated the PHWW converted from swine manure with a number of catalytic and non-catalytic batch tests at 350-600°C with a reaction time of 1 h. Activated carbon (AC), $\alpha$-$Al_2O_3$, $TiO_2$, diatomaceous earth (DE), $MnO_2$ and Raney-nickel were employed as catalysts for CHG processes. Raney-nickel and AC can lead to the highest catalytic activities, while the highest COD removal efficiency (91.3-98.1%) was reached at 600°C (Breinl & Zhang, 2015). PHWW converted from

microalgae was upgraded into hydrogen via CHG with sodium hydroxide. The high yields of hydrogen can be produced (30 mol $H_2$/kg algae) with near complete gasification of the organics (98%) in PHWW (Cherad et al., 2016). Compared with HTL, the energy recovery of CHG for PHWW is quite low due to its low energy content in the PHWW and high energy input of the CHG process.

### 2.3.3 Gas Products

The chemical compositions of HTL gas products are mainly composed of carbon dioxide ($CO_2$), and small fraction of carbon monoxide (CO), hydrogen ($H_2$), methane ($CH_4$), ethane ($C_2H_6$), ethene ($C_2H_4$), benzene, toluene, and styrene (Appleford et al., 2005; Chen et al., 2014c; Faeth et al., 2016; Jazrawi et al., 2013; Yu et al., 2011b; Zhang et al., 2013a). Gas products converted from swine manure in a continuous-stirring HTL reactor were reported at concentrations (167-288 ppm) of total hydrocarbons as gas ($C_4$-$C_{12}$). Faeth et al (2016) also characterized the compositions of gaseous products converted from microalgae in a batch reactor. Carbon dioxide is found to be the primary compound (0.301-0.857 mmol/g dry algae), along with some CO (0.002-0.120 mmol/g dry algae), $H_2$ (0.0002-0.035 mmol/g dry algae), $CH_4$ (0.001-0.046 mmol/g dry algae), $C_2H_6$ (0.004-0.013 mmol/g dry algae), and $C_2H_4$ (0.009-0.043 mmol/g dry algae).

Since the HTL gaseous products contain mostly carbon dioxide (>95%), it is suggested to recycle the gas product to grow biomass (Yu et al., 2011b; Zhou et al., 2013). The University of Illinois Group has proposed a synergistic system, namely Environment-Enhancing Energy ($E^2$-Energy), that can re-utilize the nutrients in PHWW and the carbon source in HTL gaseous products to achieve biomass amplification by growing more algal-bacteria biomass (Yu et al., 2011b; Zhou et al., 2013). Several compounds (*e.g.*, $C_2H_4$) in the HTL gaseous products have been identified as USEPA Hazardous Air Pollutant (HAP) (Appleford et al., 2005). Although these levels are exempt from the regulation of HAP because of low concentrations, health and safety precautions, such as gas masks, for those working around the process should be used (Appleford et al., 2005). Moreover, abatement facilities such as activated carbon filters are highly suggested to treat the HTL gaseous products before they are vented out to the atmosphere (Jazrawi et al., 2013).

### 2.3.4 Solid Residue

Elemental, TGA, FTIR and surface analyses are conducted on HTL solid residues to understand their CHN and mineral contents, boiling point distribution, chemical compositions, and surface area, so their potential utilization can be elucidated. For HTL of mixed-culture algae from wastewater treatment systems, 12%–18% of the carbon remained in the solid residue, while TGA suggests that the solid residues can be possibly used as asphalt (Chen et al., 2014c). Most of the potassium and sodium could be recovered in the PHWW, while most of the calcium and magnesium is distributed in the solid residue. It is possible that the solid residue can be potentially combustible without problems associated with fouling, based on the low concentration of alkalis in the solid residue.

Ash content, surface area ($S_{BET}$), bulk density, and helium density of the solid residue converted from swine carcasses via HTL is close to the biochar converted from plant biomass via pyrolysis and can be potentially used as soil amendments (Zheng et al., 2015). The solid residue can also be used as an alternative of activated carbon for metal adsorption or as a renewable solid fuel, based on their CHN contents and HHV (Zheng et al., 2015). Aliphatic, carboxylic, primary and secondary amides, as well as primary amine functional groups were identified in the solid residue (Li et al., 2015). Similar results were also reported when macroalgae were used as HTL feedstocks (Singh et al., 2015). Lignocellulosic fraction in feedstocks could not be completely reacted and remain as solid residue such as biochar (Kruse et al., 2013).

## 2.4 HTL Reaction Mechanism

Though many different feedstocks have been converted into biocrude oil via HTL, the reaction mechanism of HTL remains unclear, largely due to the complexity of the feedstock biochemical property. Several studies have attempted (Chen et al., 2014c; Gai et al., 2015; Wang, 2011b; Yu, 2012; Zhang et al., 2016a; Zhang et al., 2013a) to elucidate the reaction mechanisms, and it is generally believed that there are three basic HTL reaction pathways: (1) depolymerization of various biomolecules (*e.g.*, lipids, proteins, carbohydrates, *etc.*); (2) decomposition of different biomass monomers (*e.g.*, fatty acids, amino acids, glucoses, *etc.*) by cleavage, decarboxylation, deamination; and (3) recombination and repolymerization of reactive compounds (*e.g.*, radicals) (Demirbaş, 2000a; Peterson et al., 2008; Toor et al., 2011; Vardon et al., 2011; Zhang, 2010).

To elucidate reaction mechanisms, HTL of model compounds such as albumin (representative of proteins), butter, fatty acids (representatives of crude fats), starch, and glucose (representatives of carbohydrates), were conducted (Biller & Ross, 2011b; Wang, 2011a; Zhang et al., 2016a). Lipid can be further converted into hydrocarbons, possibly via decarboxylation (Chen et al., 2014c; Gai et al., 2015; Peterson et al., 2008; Vardon et al., 2014; Wang, 2011b; Yu, 2012; Zhang et al., 2013a). Protein can experience either deamination or decarboxylation and is potentially converted into amines, amides, nitriles, ammonia and carbon dioxide (Chen et al., 2016b; Chen et al., 2014b; Chen et al., 2014c; Gai et al., 2015; Peterson et al., 2008; Toor et al., 2011; Zhang et al., 2013a). It is generally believed that lignocellulosic materials are first hydrolyzed and then decomposed into char during HTL processes (Guo et al., 2012; Guo et al., 2013; Toor et al., 2011). Further, the monomers of various biomolecules (*e.g.*, proteins) can have inter-reactions. For example, amino acids could react with reduced glucose and then produce melonoidins (Peterson et al., 2008). The reaction kinetics of HTL has been investigated by using model compounds (*e.g.*, soy protein) and different HTL products (*e.g.*, aqueous products and solid residue from HTL reactions) (Luo et al., 2016; Valdez & Savage, 2013). HTL tests with both model compounds and real feedstock (*e.g.*, animal manure) were conducted to understand reaction pathways regarding the major inter-reactions under HTL reactions (Wang, 2011a; Zhang et al., 2016a). It is concluded that an excessive amount of protein in the feedstock would negatively impact the biocrude oil quality, while the addition of carbohydrates (such as glucose) would promote the biocrude oil formation.

A modified reaction network for HTL of wet biowaste is present in Figure 2-5. The reaction network of HTL of microalgae has also been established, while the reaction constants and the activation energy of respective reaction paths have been reported (Valdez & Savage, 2013; Valdez et al., 2014).

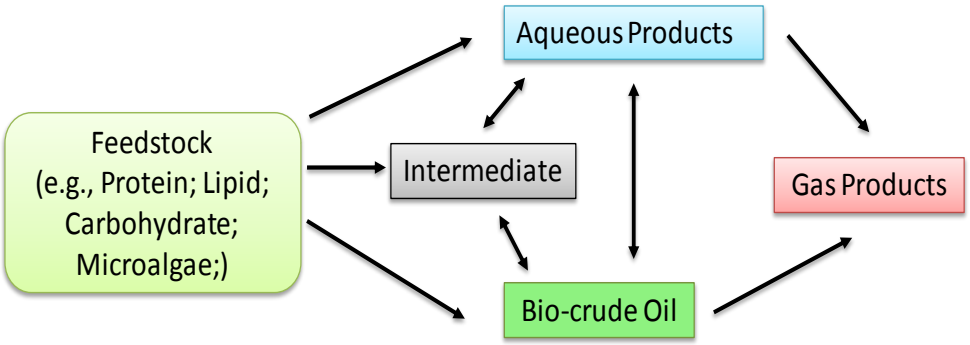


**Figure 2-5. A generic reaction network for HTL of protein-containing feedstocks (modified from (Luo et al., 2016; Sheehan & Savage, 2016; Valdez & Savage, 2013; Valdez et al., 2014)).**

The reaction mechanism of HTL of wet biowaste mostly relies on the speculation from characterization results of GC-MS, NMR, FTIR, *etc*. In order to validate this speculation, insightful techniques such as isotopes (*e.g.*, deuterium oxide or isotopic labeling proteins) with representative model compounds in HTL process will greatly enhance the understanding of the reaction kinetics and network in this biomass conversion system. Considering HTL reactions involve complex free-radical reactions between hundreds of reaction intermediates, it is extremely difficult to elucidate its mechanism via experiment. Computational studies using quantum chemistry could be an effective tool to provide fundamental information on HTL reaction mechanisms.

## 2.5 Upgrading of HTL Biocrude

Table 2-6 summarized current available techniques for upgrading HTL biocrude oil converted from wet biowaste, while Figure 2-6 categorized those techniques according to their upgrading temperature and pressure. Available upgrading techniques for HTL biocrude include steam reforming (Saber et al., 2016; Trane-Restrup & Jensen, 2015; Vagia & Lemonidou, 2008; Xiu & Shahbazi, 2012; Xu et al., 2010), sub-/super-critical fluid (SCF) treatment (Cole et al., 2016; Duan et al., 2013a; Duan & Savage, 2011c; Li et al., 2011; Peterson et al., 2008; Savage, 2009; Xu et al., 2014; Zhang et al., 2013a), hydrocracking (Li & Savage, 2013; Mortensen et al., 2011; Zhu et al., 2013), zeolite cracking (Cheng et al., 2014a; Mortensen et al., 2011; Saber et al., 2016), thermal cracking (Li & Savage, 2013; Roussis et al., 2012), hydrotreating (Biller et al., 2015; Furimsky & Massoth, 2005; Huber et al., 2006b; Mullen et al., 2013; Zacher et al., 2014), solvent addition (Hilten et al., 2010; Oasmaa et al., 2004; Xiong et al., 2009; Xu et al., 2011), chemical extraction from HTL biocrude oil (Cao et al., 2010; Chen et al., 2016b; Cheng et al.,

2014b; Eboibi et al., 2014a; Hoffmann et al., 2016b; Ott et al., 2008), and emulsification (Chiaramonti et al., 2003a; Lavanya et al., 2015; Leng et al., 2015; Li et al., 2010b). Sub-/super-critical fluid (SCF) treatments can inhibit the char formation (Peterson et al., 2008; Savage, 2009) and significantly improve the HTL biocrude oil quality such as reducing oxygen and nitrogen contents as well as viscosity. SCFs such as water can serve as a hydrogen donor. However, the upgrading mechanism (*e.g.*, how SCFs participate in the reaction) under SCFs still remains unclear.

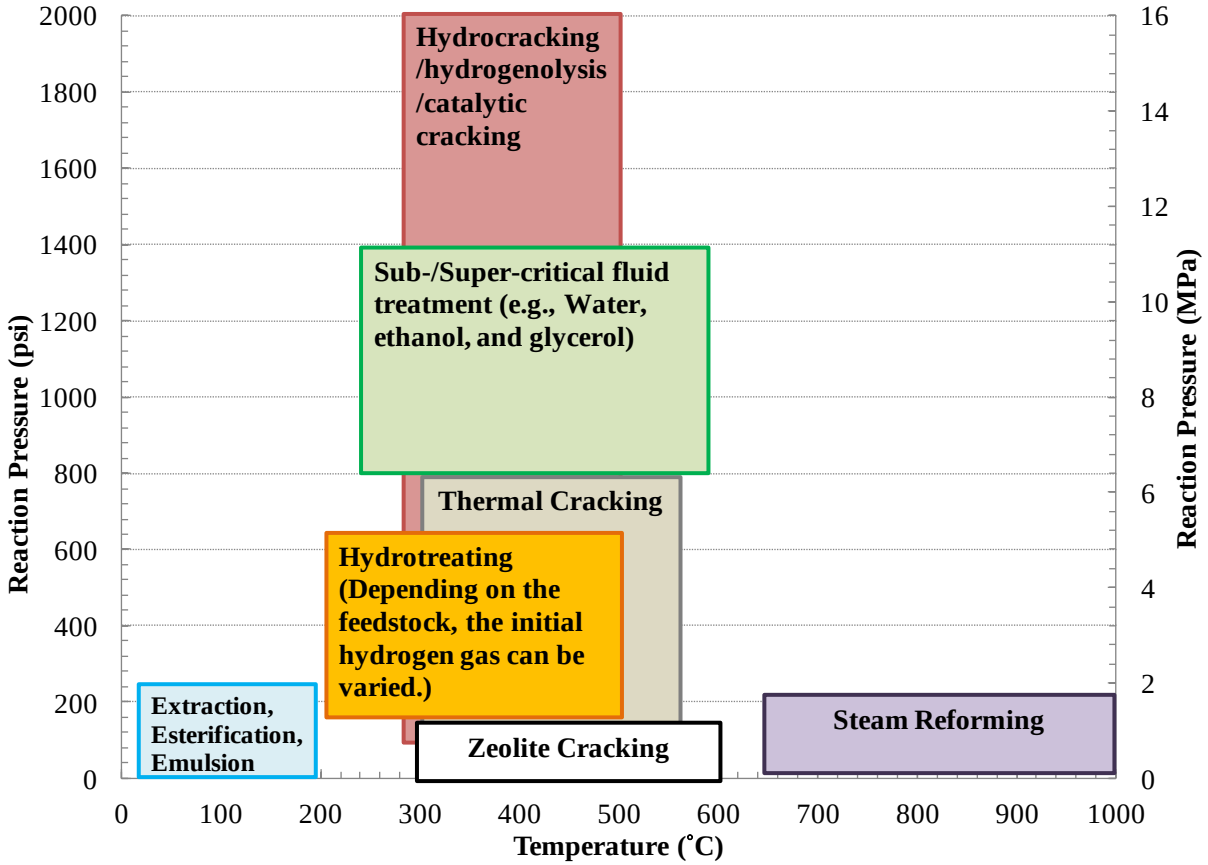


**Figure 2-6. Reaction conditions of different HTL biocrude oil upgrading strategies**

**Table 2-6. Brief description and technical feasibility of current techniques for upgrading HTL biocrude oil converted from wet biowaste**

| Method | Features | Upgrading Mechanism | Upgraded Products | Pros | Cons |
|---|---|---|---|---|---|
| Steam reforming | Has been extensively studied in fixed and fluidized bed reactors, Ni-based catalysts are the most common catalysts | Water-gas shift and steam reforming reactions | $H_2$-containing gases (e.g., synthesis gas) | Produce a relatively clean energy resource (i.e., hydrogen gas) | High temperature is needed (700-1000°C), coking of catalysts |
| Sub-/ Super-critical fluid (SCF) treatment | Water or organic solvents are needed, faster rates of mass/heat transfer | Dissolve materials not soluble in either liquid or gas phases of organic solvents | Similar to petroleum-based fuels | Increase HHV, reduce viscosity, decrease O and N, inhibit char formation | High pressure is needed (up to 3000 psi), organic solvent is expensive |
| Hydrocracking/ Hydrogenolysis/ Catalytic cracking | A thermal process (> 350°C) under high pressure hydrogen (up to 2000 psi) with catalysts | Hydrogen breaks C-C bonds, hydrogenation and cracking happens simultaneously | Light saturated olefins | Produces large quantities of light oil | High pressure hydrogen is needed, economical and energy inefficient, catalysts deactivation |
| Zeolite Cracking | Occurs at 300-600°C under atmospheric pressure with zeolites | Crack heavy molecules to light compounds | Light oil with low H/C, aromatic compounds | Produces large quantities of light oil | Catalyst deactivation; upgraded oil with low H/C ratio |
| Thermal Cracking | Occurs at 350-500°C under atmospheric pressure without catalyst | Crack heavy molecules to light compounds | Light oil with low H/C | No catalysts, operate with existing refinery equipment | upgraded oil with low H/C ratio, low upgraded oil yield |
| Hydrotreating/ Hydroproceesing/ Hydrorefining/ Hydrodeoxygenation/ Hydrodenitrogenation | Occurs up to ~ 500°C under atmospheric pressure with catalysts such as $CoMo/Al_2O_3$ (No simultaneous cracking) | Remove N and O as $NH_3$ and $H_2O$ | Saturated olefins, converting aromatics to naphthenes | Operate with current petroleum upgrading infrastructure; increase HHV | High coking (8-25%), low yield of upgraded oil, catalyst deactivation, high pressure hydrogen is needed |
| Solvent addition, Esterificatoin/ Alcoholysis | Occurs under mild conditions, polar solvents needed (*e.g.*, alcohols) | Esterification, alcoholysis, acetalization | Esters and acetals | Simple and economic | Organic solvents needed, unable to remove N |

**Table 2-6. Brief description and technical feasibility of current techniques for upgrading HTL biocrude oil converted from wet biowaste (cont.)**

| Method | Features | Upgrading Mechanism | Upgraded Products | Pros | Cons |
|---|---|---|---|---|---|
| Chemical Extractions and Separations from HTL biocrude oil | Occurs under mild conditions, solvents needed | Solvent extraction, distillation, and/or absorption | A wide range of chemicals | Valuable chemical extracted from HTL biocrude oil | Removal of solvents, application of the rest of the HTL biocrude oil |
| Emulsification/ Emulsions | Occurs under mild conditions with surfactant | Emulsification | Drop-in biofuel | Simple | High energy consumption due to high production of emulsions, no chemical reaction to reform undesired compounds |

Traditionally, cracking reactions (*e.g.*, zeolite cracking) and hydrotreating are two major approaches to upgrade petroleum crude because they can reform undesired chemicals into hydrocarbons through chemical reactions. Cracking reactions mainly fragment one heavy molecule into two light molecules whilst hydrotreating can achieve saturation of olefins, hydrodeoxygenation (remove O as $H_2O$), hydrodenitrogenation (remove N as $NH_3$), and hydrodesulfurization (remove S as $H_2S$).

Steam reforming of pyrolysis bio-oil has been extensively studied but not of HTL biocrude oil (Ortiz-Toral, 2008). Steam reforming could be a promising method to upgrade HTL biocrude oil because it can produce a synthesis gas as a renewable fuel. Further, steam reforming is a relatively well-established technique (*e.g.*, reactor development) and the reaction mechanisms are better understood (Saber et al., 2016; Xiu & Shahbazi, 2012). However, the catalysts involved in steam reforming can be significantly deactivated by coking, which is typically caused by oligomerization of carbonaceous materials such as tar. Steam reforming of HTL biocrude oil can be inherently complex due to the need of different decomposition reactions in order to obtain single carbon species to react with the water on the surface of catalysts (Ortiz-Toral, 2008; Takanabe et al., 2006).

Less severe upgrading, such as solvent addition, improves the viscosity and acidity of pyrolysis bio-oil through esterification and alcholysis. The removal of nitrogen-containing compounds presents a challenge when solvent-addition technique is adapted to upgrading HTL biocrude oil. In contrast, chemical extraction/separations and emulsification involves no chemical reactions during upgrading processes. This feature makes these two methods relatively simple and economic. However, they cannot reform undesired compounds such as phenols and pyridines.

Most upgrading techniques have been exclusively developed for petroleum which nitrogen is not a concern. HTL biocrude oil converted from wet biowaste typically contains a relatively high nitrogen content (3-7%) (Audo et al., 2015; Chen et al., 2014b; Yu, 2012). The high nitrogen content in HTL biocrude oil would cause fouling of conventional oil-upgrading catalysts (*e.g.*, zeolites) because the high basicity of the heterocyclic nitrogen (N-ring) compounds can result in adhesion to acidic active catalytic sites and poison the catalysts (Chen et al., 2016b; Furimsky & Massoth, 2005; Vardon et al., 2012). If the upgraded HTL biocrude oil is used as drop-in transportation fuel (*e.g.*, blending 5-10% upgraded HTL biocrude with

petroleum fuel), the nitrogen content could be diluted to an acceptable level. Identifying what types of nitrogen-containing compounds would negatively affect combustion processes is essential such as nitrogen-heterocyclic compounds versus nitrogen-containing alkyl compounds. Engine tests are highly needed to examine the effect of nitrogen-containing compounds on combustion performance and emissions.

Most of the upgrading techniques such as hydrotreating need catalysts to enhance the heteroatom removal efficacy. Deactivation of catalysts is commonly observed in steam reforming, cracking, and hydrotreating of pyrolysis bio-oil. Deactivation of catalysts has also been found when hydrothermally treating HTL algal biocrude oil under supercritical water in batch reactor systems (Duan et al., 2013a). Duan et al. has recycled the spent Pt/$\gamma$-$Al_2O_3$ to hydrothermally upgrade HTL algal biocrude oil at 400°C for 1 h with an added 6 MPa hydrogen under supercritical water. The spent catalyst presented modest activity loss on the performance of hydrodeoxygenation but not hydrodenitrogenation. On the contrary, catalyst deactivation was not observed when hydrotreating HTL algal biocrude oil in a continuous reactor system during a short-term testing (Elliott et al., 2013; Tian et al., 2014).

**2.6 Continuous HTL Reactor Development**

Efforts have been made to scale-up the HTL process of protein-containing biomass by University as well as industry. The major findings are summarized in Table 2-7.

The University of Sydney group developed a plug-flow reactor system with a total volume of 2L for converting algal biomass into biocrude oil under HTL. In their system, high-pressure triplex piston pump was used to pump up to 10 wt.% microalgae slurries with high viscosities. Heat exchangers were employed to preheat the algal slurries (to about 170°C) before entering the reactor (Jazrawi et al., 2013). The flow rates investigated in this study were in the range of 15–30 L/h and led to residence times of 3–5 min. In addition, the authors claimed that the blockage of the reactor coils has never happened in any of their operations (with a maximum duration of 2h in a single run) (Elliott et al., 2015; Jazrawi et al., 2013). Overall, the University of Sydney group reported that the higher temperatures and longer residence times increased the yields, which is in agreement with results from batch HTL experiments of algal feedstocks (Jazrawi et al., 2013).

**Table 2-7. Summary of plants/implementation of HTL feedstocks containing protein contents**

| Group | Capacity of the plant to process feedstocks | Biocrude oil yield/conversion efficiency | Process Condition & Features |
|---|---|---|---|
| **University of Sydney Group** | | | |
| He et al., 2016 (He et al., 2016) | Up to 90 L/h of feed microalgae & macroalga slurries | Up to 25 wt.% (dry ash-free basis) | Co-processed with 10 wt.% n-heptane, toluene, or anisole at 300–350°C for 3–5 min with 2–5 wt.% loadings of algal feedstocks to achieve in-situ fractionation of HTL biocrude oil |
| Jazrawi et al., 2013 (Jazrawi et al., 2013) | 15-90 L/h of feed algal feedstocks (total reaction volume: 2 L) | Up to 41.7 wt.% (dry ash-free basis) | Processed at 250–350°C for 3–5 min with 1–10 wt.% loadings of microalgae under 150-200 bar |
| **PNNL Group** | | | |
| Elliott et al., 2013 (Elliott et al., 2013) | 1.5 L/h of microalgae (total reaction volume: 1 L tubular reactor) | 38.0-63.6 wt.% (dry ash-free basis) | Processed at 350°C for 3–5 min with 1–10 wt.% loadings of microalgae under 200 bar |
| Elliott et al., 2013 (Elliott et al., 2014) | 1.5 L/h of macroalgae (total reaction volume: 1 L tubular reactor) | 8.70-27.7 wt.% (dry ash-free basis) | Processed at 350°C with 5–22 wt.% loadings of macroalgae under 200 bar |
| **UIUC Group** | | | |
| Ocfemia et al., 2006 (Ocfemia et al., 2006a; Ocfemia et al., 2006b) | Up to 3 kg/h of swine manure (total reaction volume: 2L continuous stirred reactor) | 62.0-70.4 wt.% (dry ash-free basis) | Processed at 285-305°C for 40-80 min hydraulic residence time with 20 wt.% loadings of swine manure under 90-121 bar |

Continuous HTL conversions of algal feedsctoks with organic solvents has been conducted by the University of Sydney group recently (He et al., 2016). Co-solvent HTL with 10 wt.% n-heptane, anisole, or toluene was conducted to achieve in-situ fractionation and reduce heteroatoms (*e.g.*, nitrogen) of the algal biocrude oil. Techno-economic (TEC) analyses are suggested to evaluating if the co-solvent HTL process is cost-effective, since the organic solvents are more expensive and less accessible than water. Life-cycle analysis (LCA) of the co-solvent HTL is also needed, because the production of organic solvents from petroleum crude can negatively impact the environment (*e.g.*, produce greenhouse gases). Further, it is recommended to explore if the organic solvents can be produced from renewable sources to prevent the additional emission of greenhouse gases. Besides, recycling the organic solvents back to HTL produces could be an option too.

Pacific Northwestern National Laboratory (PNNL) has developed a continuous HTL process consisting of a high-pressure pump feeding system, a product recovery system, a 1L continuous stirred tank reactor (CSTR) for preheating algal feedstocks, and a 1L tubular catalytic reactor (Elliott et al., 2013). In order to avoid potential plugging problems, the PNNL group combined CSTR and plug flow in their continuous HTL process. The authors reported that as the temperature in the CSTR preheater maintained below 200°C, no plugging with algal feedstocks was observed. Trace components (*e.g.*, minerals) were also removed by processing steps so that they would not cause process difficulties during HTL conversions and/or catalytic hydroprocessing stages (Elliott et al., 2013). For example, before the algal biocrude entering the fixed catalysts bed for catalytic hydroprocessing, the algal biocrude would be pretreated in the CSTR and then passed through the solid separator as well as a sulfur stripping bed.

In addition to algal biocrude oil production, the PNNL group is also interested in recovering the nutrients from HTL byproducts. The PNNL group studied the compositions of the HTL gaseous products and pointed out that the depressurization of the high-pressure liquid collecting system reveals possibility to recover unaccounted ammonia. Development of an alternate collection method to allow the ammonia to be collected as dissolved ammonium in the HTL aqueous byproduct is therefore recommended in their studies (Elliott et al., 2013). Further, improving the recovery system of the solid residues is also suggested, so that a better recovery efficiency of trace elements (*e.g.*, Phosphorus) can be achieved (Elliott et al., 2014).

Different from the studies reported by the University of Sydney group, the PNNL group not only produces biocrude in a continuous HTL reactor, but also upgrades the algal biocrude oil through catalytic hydroprocessing. By using molybdenum sulfide as catalysts, the nitrogen content in the HTL algal biocrude can be effectively reduced from 4.0-4.7 d.w.% to <0.05-0.25 d.w.%, depending on the types of algal biocrude oil. Nevertheless, the catalysts activity for a long-term operation would need further investigation, since the PNNL group typically operates the continuous HTL reaction over a range of days. Additionally, the PNNL group also noted that the mineral residues in the HTL biocrude oil may remain as a concern for a long-term operation. Further removal of the trace elements are thus proposed (Elliott et al., 2015).

Compared to the continuous HTL of microalgae in the PNNL studies, the process design and reactor set-up of the University of Sydney group's unit exhibit some differences. The reactor employed by the University of Sydney group is unstirred and the reactants flow through coiled stainless steel tubes submerged into a fluidized sand bath (Elliott et al., 2015). Moreover, the University of Sydney group utilized solvents to recover biocrude, while PNNL studies recovered the biocrude by gravity separation without the requirement of solvent handling (Elliott et al., 2013).

In contrast to the previously mentioned studies in the University of Sydney and PNNL, the University of Illinois at Urbana-Champaign (UIUC) group focuses on using agricultural biowaste—swine manure and food processing waste —as their HTL feedstocks. The UIUC group has developed a CSTR system to process 20 wt.% loadings of swine manure under HTL condition (Figure 2-7). Different from algal slurry, the swine manure slurry was very viscous (~32,000 cp) and contains solid particles as well as other compositions such as pig hair that cannot be well homogenized before entering the CSTR system. Therefore, a special high-end metering pump, the valveless rotary piston pump, was utilized in their study, because the valveless design would avoid blockage and undesired backflow caused by flaky particles in the swine manure (Ocfemia et al., 2006a).

The UIUC group reported that no clogging or accumulation was experienced in using the continuous stirred tank reactor (Ocfemia et al., 2006a). However, there was a pump durability issue as the piston and sleeve wore out quickly, which was possibly caused by the abrasive nature of swine manure slurries. Similar to the PNNL group's unit, the UIUC group separated the HTL products by gravity without any organic solvents. A decanting method was used to

separate the HTL biocrude oil and aqueous products. (Ocfemia et al., 2006a). Different from the results reported by the University of Sydney and PNNL groups, a longer residence time (60 min v.s. 3-5 min) was employed by the UIUC group. The authors stated that the continuous mode operation of their reactor showed that steady state could be achieved in about 60 min (Ocfemia et al., 2006a)

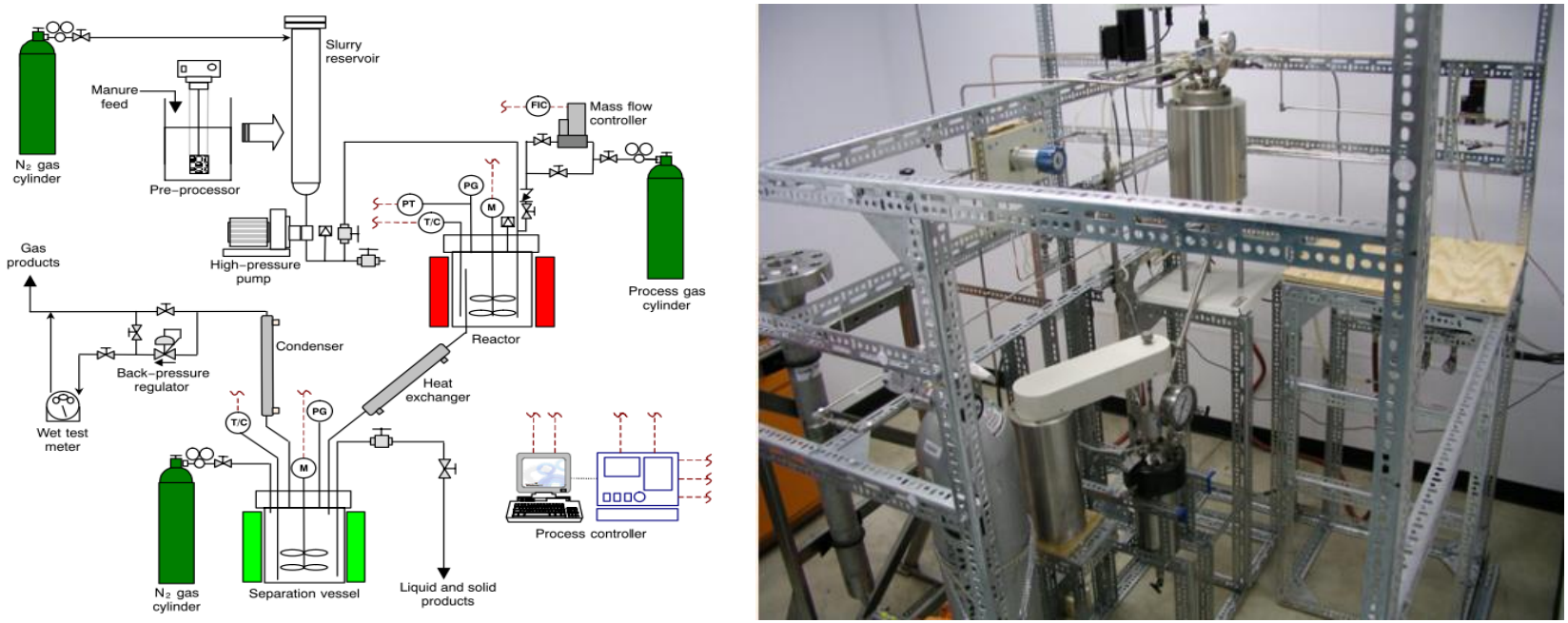


**Figure 2-7. UIUC HTL Laboratory continuous reactor system: (a) schematic of the continuous hydrothermal process (CHTP) reactor system, and (b) photo of the CHTP reactor system setup (Ocfemia et al., 2006a; Ocfemia et al., 2006b)**

In summary, technical challenges associated with HTL of wet biowaste are highly dependent on the feedstock compositions, optimization of the liquefaction/upgrading process variables, and effective separation techniques to recover biocrude oil/remove precipitated nutrients (Elliott et al., 2013). The physiochemical properties of the oil could be different due to the separation methods alone (*e.g.*, solvent extraction and centrifugation) (Ocfemia et al., 2006a; Ocfemia et al., 2006b). Further studies to investigate different types of wet biowaste feedstocks, various separation techniques, and HTL operation strategies are needed. In addition, high pressure feeding systems for wet biowaste slurries have been recognized as a process development challenge for a continuous HTL system (Elliott et al., 2015; Ocfemia et al., 2006a). Moreover, the above mentioned studies mostly focus on pilot-scale implementations (the total reactor volume is generally 1-2L), a demonstration scale (*e.g.*,1-2 ton processing capacity) would be highly recommended to more practically realize the potential of using HTL to produce biofuel from wet biowaste.

# CHAPTER 3. OBJECTIVES

The ultimate goal of this study is to develop a viable technology to upgrade biocrude oil converted from wet biowaste into transportation fuels and carry out engine tests. To achieve this research goal, the following objectives are established for this study:

1. Pretreat the mixed-culture algal feedstock by reducing its ash content so as to improve the HTL biocrude oil conversion efficiency. Previous studies have revealed that the excessive ash content in the mixed-culture algal biomass (AW) would deteriorate the biocrude oil quality in terms of heating value and chemical compositions. As a consequence, a series of physical pretreatment on AW biomass were conducted to reduce the ash content and improve the biocrude oil quality in this study. Moreover, the role of the ash content in HTL processes was further investigated by converting the model algae with different amounts of representative ash content.
2. Separate the biocrude oil converted from wet biowaste via HTL by distillation to upgrade the heating value of biocrude products**.** The distillation of biocrude oil converted from swine manure (SW), food processing waste (FPW), and *Spirulina* (SP) via HTL is performed in this study. Physicochemical characterizations of the distillates are conducted to understand the similarity/difference between biocrude oil and petroleum transportation fuels. With a distillation separation, it is expected to reduce the viscosity and improve the heating value of biocrude oil for preparing drop-in biofuel.
3. Upgrade the distillates from biocrude oil to improve their fuel specification properties. Further upgradation on the distillates from SW-, FPW-, and/or SP-derived biocrude oil will be carried out to make the distillates more compatible with petroleum fuel (*e.g.,* meeting the ASTM standards). Different concentrations of catalysts, reaction temperature, reaction time, and molar/weight ratio of distillates to reactants (*e.g.,* methanol in esterification) will be tested with HTL distillates.
4. Carry out engine tests with the distillates from biocrude oil. Drop-in biodiesel will be prepared with the most promising upgraded distillates and petroleum diesel for a diesel engine test. The power generated, particulate matter (PM), unburned hydrocarbons (UHC), CO, $CO_2$, and $NO_x$ emitted by the drop-in biodiesel will be evaluated. Simultaneously, drop-

in biodiesel utilization issues such as the oxidation stability and engine compatibility will be realized.

Through different upgrading processes, scientific justifications to develop a viable technology to upgrade biocrude oil converted from wet biowaste into transportation fuels are expected to be realized. Ultimately, the multi-phase biorefineries will be developed to expedite the downstream application of biocrude oil into aviation biofuel, biodiesel, and other potential value-added chemicals (*e.g.*, phenosl and functional materials).

# CHAPTER 4. EXPERIMENTAL DESIGNS AND PROCEDURES

## 4.1 Feedstock

The wastewater algal (WA) biomass was harvested from a local wastewater treatment plant (Urbana-Champaign Sanitary District, U.S.A.). Before pretreatments, WA biomass was washed with tap water for 1 hour to remove entrained garbage and then dried at 85°C to achieve sterilization. Next, the dry WA biomass was pulverized with a commercial blender (MX 1000XT, Waring commercial *Inc.*, U.S.A.). The dry solid content and the ash content of WA biomass were measured as the weight fraction after drying at 105°C and the residual fraction after combustion at 550°C, respectively. The particle sizes were analyzed by a laser scattering particle size distribution analyzer (LA-300, Horiba Instruments *Inc.*, U.S.A.). The median mass diameters (MMD) were reported.

The mixed-culture algal biomass was directly harvested from a wastewater treatment plant with algae wheel systems (AW biomass) (One Water Inc., Indianapolis, IN). More details about AW biomass have been reported in previous publication (Chen, 2013; Chen et al., 2014b; Chen et al., 2014c).

*Chlorella pyrenoidosa* (CP) and eggs were obtained respectively from a health food store and a grocery store as a food grade material (Now Foods and County Market, IL). The tested algal biomass was evenly pulverized with a commercial blender (MX 1000XT, Waring Commercial *Inc.*, Torrington, CT) and then stored in a refrigerator below 4°C. The dry content of the solid residue and combustion residue (*i.e.*, ash content) were measured at 105°C and 550°C, respectively. Elemental analysis of feedstock was operated by a CHN analyzer (CE-440, Exeter Analytical *Inc.*, North Chelmsford, MA). Duplicate analysis was conducted for each sample and the average value was reported. Other macromolecules and chemical compositions were analyzed according to the standard methods of the Association of Official Analytical Chemists (AOAC) (Chen et al., 2014c; Gai et al., 2014a; Yu, 2012). Detailed chemical compositions of above mentioned algal biomass are summarized in Table 4-1.

**Table 4-1. Chemical and elemental compositions of AW biomass (AW) and *Chlorella pyrenoidosa* (CP)**

| Compositions (wt.%) | AW | CP[b] |
|---|---|---|
| Crude protein | 27.2 | 71.5 |
| Crude fat | 1.70 | 0.20 |
| Carbohydrate[a] | 17.8 | 22.6 |
| Ash content | 53.3 | 5.70 |
| C | 27.9 ± 2.6 | 51.4 |
| H | 3.01 ± 0.5 | 6.60 |
| N | 3.90 ± 0.4 | 11.1 |
| O[a] | 65.2 | 30.9 |

[a] calculated by difference; [b]Modified from (Yu, 2012; Yu et al., 2011a; Yu et al., 2011b)

Swine manure (SW) was sampled from the floor of a grower-finisher barn, which was the same type used in previous studies (Chen et al., 2014b; Vardon et al., 2011; Wang, 2011b; Yu, 2012). Food processing waste (FPW) was sampled from a full-scale salad dressing plant (Kraft Company, *Inc.*, Champaign, IL). *Spirulina platensis* (SP) were purchased in dry powder form from Cyanotech (Kailua-Kona, HI). The total solid content of feedstock was measured as the dry residue at 105°C for 24 h. Before HTL experiments, SM was pulverized using a commercial blender (MX 1000XT, Waring Commercial Inc., CT) while FPW and SP naturally existed in one homogeneous phase. The feedstocks used in this study were all stored in a refrigerator at 4°C before HTL tests. The total solid content of feedstock was measured as the dry residue at 105°C for 24 h. The contents of crude protein (AOAC 990.03), crude fat (AOAC 954.02), and lignin (AOAC 973.18) were measured using AOAC standard methods while acid and neutral detergent fibers were determined by Ankom Technology standard methods (MWL DF 021) (Gai et al., 2014a; Gai et al., 2015; Yu, 2012). Elemental analysis of feedstock was operated by a CHN analyzer (CE-440, Exeter Analytical *Inc.*, North Chelmsford, MA) and duplicate analysis was conducted for each sample and the average value was reported. ICP analysis was employed to measure the contents of total sulfur (S), phosphorus (P), potassium (K), magnesium (Mg), calcium (Ca), sodium (Na), iron (Fe), manganese (Mn), copper (Cu), and zinc (Zn) in the feedstocks, according to the AOAC standard methods (AOAC 985.01). Detailed analyses of SM, FPW, and SP biomass were summarized in Table 4-2. Notably, the biochemical compositions of SM can be different due to the swine conditions (*e.g.*, age, diet, *etc.*), and therefore multiple replicates of dataset (n=5) were used to compute their compositions.

**Table 4-2. Chemical and elemental compositions of swine manure, food processing waste, and Spirulina (dry weight basis, d.w.%)**

| Compositions (d.w.%)[a] | Swine Manure[e] | Food processing waste | Spirulina[f] |
|---|---|---|---|
| Crude protein | 24.3 ± 1.6 (n=5) | 2.76 | 64.4 |
| Crude fat | 19.9 ± 1.6 (n=5) | 40.8 | 5.1 |
| Hemicellulose | 26.6 ± 2.4 (n=5) | N.D.[c] | 1.4 |
| Cellulose | 5.1 ± 3.2 (n=5) | N.D.[c] | 0.5 |
| Lignin | 2.9 ± 1.9 (n=5) | N.D.[c] | 0.2 |
| Non-fiber carbohydrates[b] | 6.4 ± 4.5 (n=5) | 50.3 | 18.9 |
| Ash content | 14.3 ± 2.0 (n=5) | 6.17 | 9.5 |
| C | 41.1 ± 0.3 (n=2) | 54.0 ± 1.6 (n=2) | 49.3 |
| H | 5.42 ± 0.1 (n=2) | 7.93 ± 0.3 (n=2) | 6.4 |
| N | 3.36 ± 0.1 (n=2) | 0.57 ± 0.01 (n=2) | 11.0 |
| O[b] | 50.1 | 37.5 | 33.3 |
| Heating Value (MJ/kg) | 18.2 | 22.9 | 19.9 |
| S | 0.34 ± 0.04 (n=4) | 0.04 | 0.73 |
| P | 2.38 ± 0.4 (n=4) | 0.12 | 1.06 |
| K | 1.65 ± 0.4 (n=4) | 0.12 | 1.71 |
| Mg | 0.97 ± 0.1 (n=4) | N.D.[c] | 0.47 |
| Ca | 2.42 ± 0.4 (n=4) | 0.12 | 0.18 |
| Na | 0.32 ± 0.05 (n=4) | 2.33 | 1.25 |
| Fe | 0.16 ± 0.01(n=2) | 0.02 | 0.02 |
| Mn (ppm)[d] | 264 ± 26.2 (n=2) | N.D.[c] | 75 |
| Cu (ppm)[d] | 91.7 ± 0.9 (n=2) | N.D.[c] | 6 |
| Zn (ppm)[d] | 845.5 ± 164.8 (n=2) | N.D.[c] | 29 |

[a]unless specified, otherwise reported by dry weight basis; [b] calculated by difference (*i.e.*, non-fibrous carbohydrate (%)=100-crude fat(%)-crude protein(%)-hemicellulose(%)-cellulose(%)-lignin(%)-ash content (%); [c]not detected; [d]part per million; [e]Average values were reported based on the previous studies using the same type of swine manure (Chen et al., 2014b; Dong, 2009; Dong et al., 2009; Vardon et al., 2011; Wang, 2011b; Yu, 2012); [f]Modified from (Yu, 2012; Yu et al., 2011a; Yu et al., 2011b)

### 4.2 Pretreatments

After pulverization, WA biomass was divided into several sizes (≥300 μm, 300-180μm, 180-106μm, 106-45μn and ≤45μm) by screening with a Sieve Shakers (D-4325, DUAL Manufacturing Co. *Inc.*,U.S.A.). The size (106-45 μm) with lower ash content was chosen for further pretreatments. 2 g of screened biomass and 40 mL of deionized water were loaded into a 50 mL centrifuge tube for centrifugal and ultrasonic pretreatments. Centrifugation of algae was carried out at speeds of 3000 and 4000 rpm for 15 and 25 minutes, respectively (CENTRA-7,

International Equipment Co. *Inc*., U.S.A.). The design of experiments (DOE) of centrifugation pretreatments was based on the Stoke's law as well as preliminary tests after obtaining reasonable rotation speeds from the Stoke's law. According to Coulson (Coulson et al., 2002), it is known that the required residence time for separating fine particles from liquid layer can be written as,

$$t_R = \frac{18\mu}{d^2(\rho_s - \rho)\varpi^2} \ln \frac{R}{r_o} \qquad 4\text{-}1$$

$$\varpi = \frac{2\pi N}{60} \qquad 4\text{-}2$$

where $t_R$ is the residence time (sec), μ is the viscosity of fluid (kg/ms), d is the diameter of particles (m), $\rho_s$ is the density of particle (kg/m$^3$), ρ is the density of liquid (kg/m$^3$), R is the radius of the centrifugation bowl (m), $r_0$ is the radius of the inner surface of the liquid (m), ω is the angular velocity (radians/s), and N is the rotation speed (rev/min, also known as r.p.m., revolution per minute) (Coulson et al., 2002). Table 4-3 displays the parameters and their references used in this study.

Assuming that the required residence time for separating proteins from water should be more than 1 second ($t_R \geq 1$sec), it is computed that the minimum rotation speed (r.p.m.) should be around 3008 rpm. Thus, 3000 rpm and 4000 rpm were selected in this study.

**Table 4-3. Parameters used in calculating the required rotation speed (r.p.m.) in this study**

| Parameters in equation (1) | Notation | Values | References | Note |
|---|---|---|---|---|
| Viscosity of algae solution (kg/ms) | $\mu$ | 0.005 | (Allen, 1974; Normah & Nazarifah, 2003) | |
| Diameter of algae (m) | d | 0.00005 | (Becker, 2007) | Also confirmed by a laser scattering particle size distribution analyzer in this study. The average size (50 μm) of algae from the upper and middle layers after centrifugation was used (Figure 5-2). |
| Density of proteins ($kg/m^3$) | $\rho_s$ | 1300 | (Schramm et al., 2006; Singh, 1995) | Assuming the volatile contents in wastewater algae mainly are proteins based on previous studies (CHEN ET AL., 2014C; ROBERTS ET AL., 2013). |
| Density of water ($kg/m^3$) | $\rho$ | 1000 | N/A | |
| Angular velocity (radians/s) | $\omega$ | Unknown | N/A | Assuming $t_R \geq 1$sec |
| Radius of the centrifugation bowl (m) | R | 0.16 | N/A | Measured in this study |
| Radius of the inner surface of the liquid (m) | $r_0$ | 0.07 | N/A | Measured in this study |

After selecting the rotation speeds, we have tested three centrifugation times: 5, 15 and 25 minutes. When the wastewater algae were centrifuged with 3000 and 4000 rpm for 5 minutes, the layering was not apparent (Figure 4-1). Furthermore, it was observed that there were some algae particles still suspending in the liquid with rotation speed of 4000 rpm. Consequently, this present study selected 15 and 25 minutes as the centrifugation times for further tests.

(a) (b)

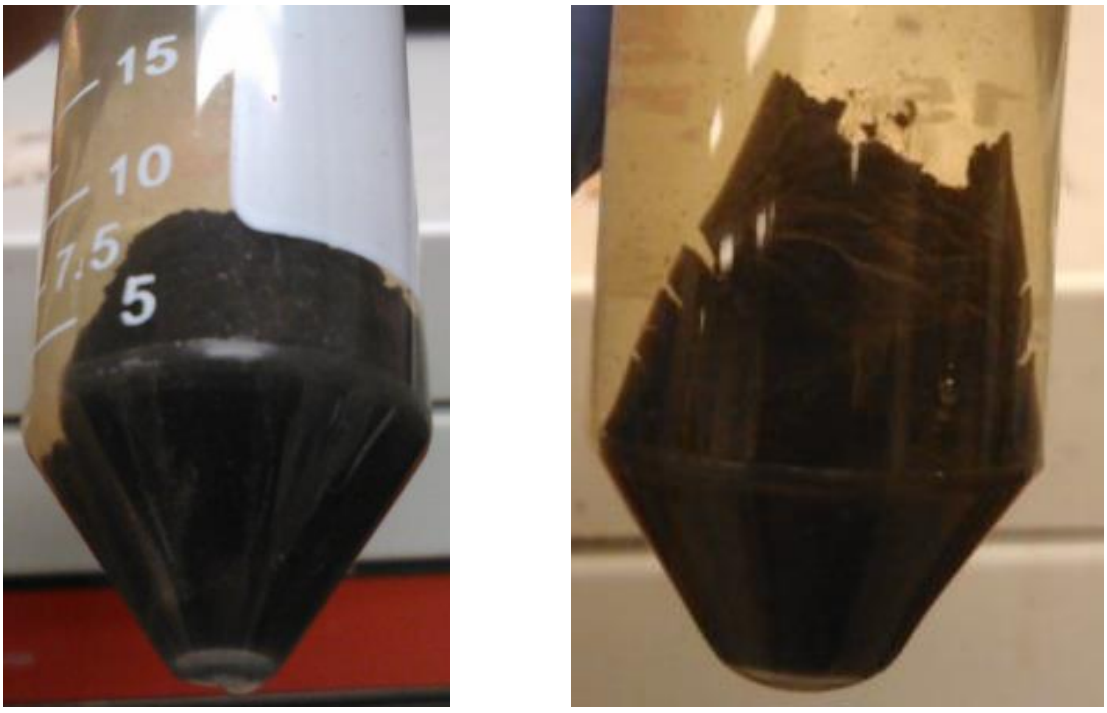


**Figure 4-1. Centrifugation of wastewater algae for 5 minutes with (a) 3000 rpm and (b) 4000 rpm**

Ultrasonicaction of algae was operated by an ultrasonic cleaner (CD-4800, Syhann Co. Ltd., Canada) for 1 hour with a 42k Hz frequency (Shi et al., 2013b). The algal biomass was spontaneously separated into three layers after the centrifugation due to the different densities and particle sizes of different compositions in the WA biomass (Coulson et al., 2002). The upper and middle layers were removed by a spatula to another centrifuge tubes with 20 times deionized water and then the two layers were treated with the ultrasonic bath for both 0.5 and 1 hour, which were selected based on previous studies about improving bio-oil yields converted in hot-compressed water using ultrasonic-pretreated cellulose and rice husk (Shi et al., 2013a; Shi et al., 2012).

## 4.3 HTL experiments

### 4.3.1 Batch HTL experiments

HTL tests were operated in 100 ml stainless steel cylinder batch reactors with a magnetic drive stirrer and removable vessel (Model 4593, Parr Instrument Co., U.S.A.) with at least two independent experiments (Yu, 2012). HTL was operated at 300°C and 1 hour reaction time (previously obtained optimal condition for converting algal biomass into bio-crude oil) (Chen et

al., 2014c). For WA biomass, the reactor was fed with a total 4 g of algal slurry (1 g solids and 3 g water), due to the limited amounts of pretreated algae, and then sealed and purged with nitrogen three times. For AW and CP biomass, each HTL test contains 30 g slurry feedstock with 25% total solid content by weight. Next, nitrogen gas was added to the reactor headspace to build 0.69 MPa pressure to prevent water from boiling during the test. Once the HTL was completed, the reactor was cooled down to 30°C in 0.5 h by circulating tap water via the cooling coil outside the reactor.

### 4.3.2 Continuous HTL experiments

The HTL experiments were conducted according to the previously reported methods (Chen et al., 2014a; Gai et al., 2015; He et al., 2000a; Ocfemia et al., 2006a; Yu et al., 2011b), using a tubular plug-flow reactor (Snapshot Energy *Inc.*, Danville, IL). Briefly, the HTL reaction was carried out at the previously determined optimum conditions for converting biowaste into biocrude oil (for SW: 280°C and 2 h reaction time; for FPW: 260°C and 0.5 h reaction time) (Chen et al., 2014b; He et al., 2000b; Ocfemia et al., 2006b; Wang, 2011b). The reactor was sealed and purged with nitrogen gas at least three times to remove the residual air in the reactor. Nitrogen gas was again added to the reactor to build a 0.69 MPa gauge initial pressure inside the reactor to prevent water boiling during the tests. All parameters, including pressure and temperature, were recorded continuously and available in Supplementary Information (in Appendix Figure A1). After the HTL reaction at the designated temperature and reaction time, the reactor was cooled down to approximately 60°C by the heat exchangers. The biocrude oil was naturally self-separated from the aqueous fraction by decanting (Ocfemia et al., 2006a; Ocfemia et al., 2006b). A series of HTL tests was conducted to determine the optimum reaction condition for converting FPW into biocrude oil, based on previous studies with similar biomass feedstocks (Dong, 2009; Gai et al., 2014a; Li et al., 2014; Yu, 2012). As Table 4-4 shows, the optimum reaction condition for converting FPW into biocrude oil was at 260°C for 0.5 h to achieve the highest liquefaction yield and the highest heating value (HHV) of the biocrude oil.

**Table 4-4. A screen test to determine the optimum reaction condition for converting FPW via HTL**

| | 200°C | 220°C | 240°C | 260°C | | 280°C | | |
|---|---|---|---|---|---|---|---|---|
| **Property** | **2 h** | **2 h** | **2h** | **0.5 h** | **2 h** | **0 h** | **0.25 h** | **0.5 h** |
| Liquefaction yield (d.w.%)[a] | 56.5% | 81.0% | 78.5% | 80.2% | 77.1% | 85.2% | 72.1% | 74.0% |
| HHV (MJ/kg) | 29.9 | 33.0 | 37.3 | 40.1 | 33.8 | 29.4 | 29.5 | 40.6 |

[a]Defined as the weight of dry solid oil product obtained per weight of dry feedstock

## 4.4 Separation Procedure for HTL Products

### 4.4.1 Products from Batch Reactor

As the reactor was cooled down, the gas products were collected through a control valve into a Tedlar® gas sampling bag (CEL Scientific CORP., Cerritos, CA). The rest of the products were separated with Whatman® 55 mm glass-fiber filter. The aqueous portion is defined as the water-soluble portion (which can pass through the filter) while the rest of the filtration cake is defined as the raw-oil. The moisture content of the water-insoluble product was measured with a distillation apparatus based on ASTM Standard D95-99 (ASTM, 2004a); the solid residue fraction of the raw oil product was determined with the Soxhlet extraction method according to the ASTM Standards D473-02 and D4072-98 (ASTM, 2015a; ASTM, 2004b). The recovery procedure is shown in Figure 4-2.

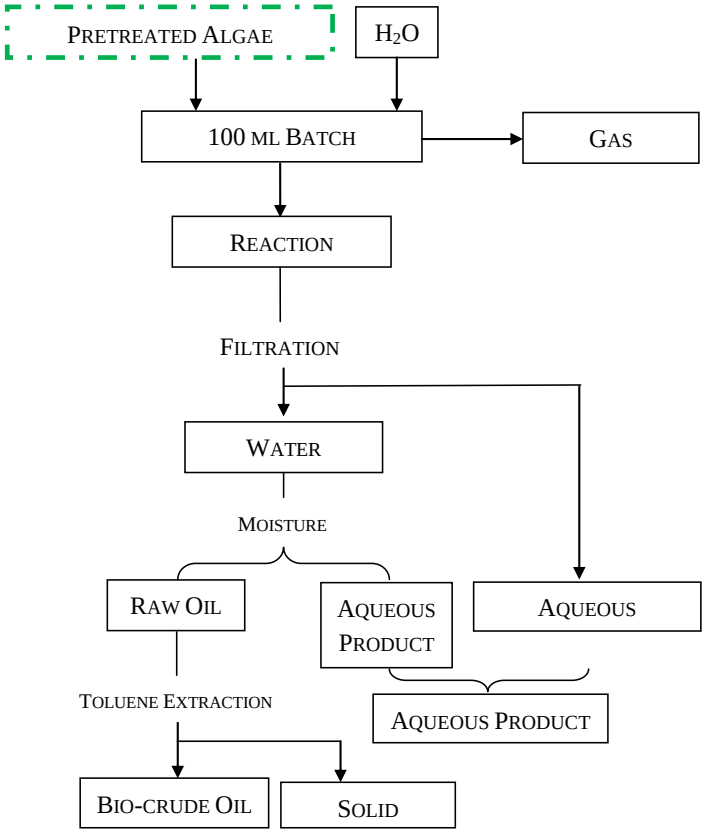


**Figure 4-2. Experimental process schematic for separation of HTL products**

The product distribution was calculated based on the dry weight (d.w.) or dry ash free matter (d.a.f) of the feedstock (feed) by the following equations (Chen et al., 2014a; Chen et al., 2016b; Chen et al., 2014b; Chen et al., 2014c):

$$\text{Biocrude oil yield (d.w.\%)} = \frac{W_{oil}}{W_{feed}} \times 100 \quad (4\text{-}3)$$

$$\text{Biocrude oil yield (d.a.f.\%)} = \frac{W_{oil}}{W_{feed-volatiles}} \times 100 \quad (4\text{-}4)$$

$$\text{Solid residue yield (d.w.\%)} = \frac{W_{residue}}{W_{feed}} \times 100 \quad (4\text{-}5)$$

$$\text{Gas product yield (d.w.\%)} = \text{Based on the ideal gas law equation} \quad (4\text{-}6)$$

$$\text{Aqueous product yield (d.w.\%)} = \text{100-(biocrde oil+solid residue+gas)} \quad (4\text{-}7)$$

The gas yield was estimated by the ideal gas law with the initial/final temperature and pressure. The gas composition was analyzed in a Varian CP-3800 Gas Chromatograph equipped with an Alltech HayeSep D 100/120 column and a thermal conductivity detector (TCD). Biocrude oil was dried at room temperature in the fume hood for 24 h prior to the elemental test. Elemental compositions of biocrude oil were determined using a CE 440 elemental analyzer (Exeter Analytical, Inc., MA). Duplicate analysis was conducted for each sample and the average value was reported. The higher heating value (HHV) of biocrude oil was calculated by using the *Dulong* formula based on the elemental composition: HHV= 0.3383×C+1.422× (H-O/8), where C, H, and O are the carbon, hydrogen, and oxygen mass percentages of the dry material (Yu et al., 2011b; Zhang et al., 2013a). Carbon, nitrogen, and energy recoveries for HTL products were defined as the carbon, nitrogen, or the HHV of the HTL products divided by those of feedstock (Chen et al., 2014b; Gai et al., 2014a; Yu et al., 2011b).

### 4.4.2 Products from Continuous Reactor

The HTL products converted from SM and FPW containing both solid and liquid phases can be separated by decanting because the biocrude oil (solid phase) is naturally self-separated from the aqueous products. The solid phase product was defined as the biocrude oil. The biocrude oil was extracted with toluene in a Soxhlet extractor for 3 h to determine toluene soluble fraction and the refined oil was obtained in this stage (ASTM, 2004b). The fraction that cannot be extracted by toluene was defined as the solid residue. The moisture content of the biocrude oil was measured with a distillation apparatus based on ASTM Standard D95-99 (ASTM, 2004a). The separation flow was shown in Figure 4-3.

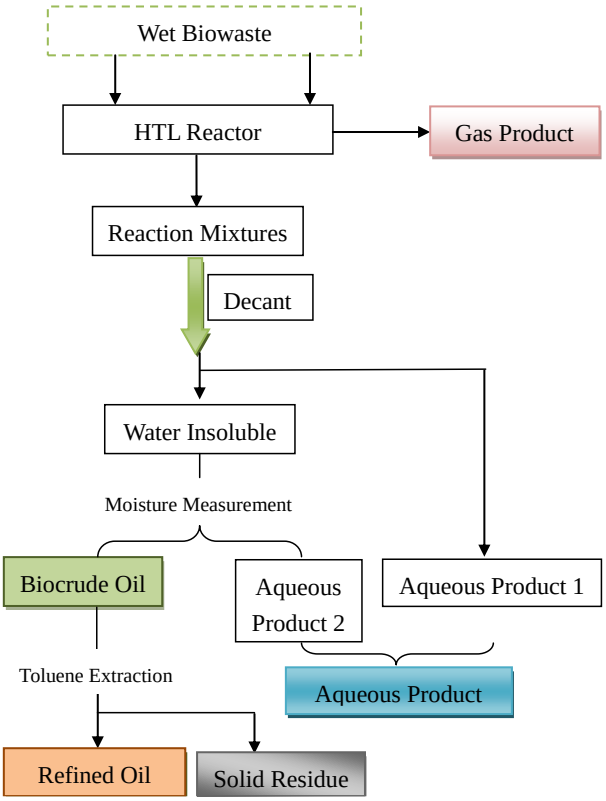


**Figure 4-3. Separation processes for continuous HTL products**

### 4.5 Distillation of Biocrude Oil

The distillation was conducted according to the previously reported standard methods (ASTM, 2015a; Cheng et al., 2014b) and the distillation curves were measured. For each distillation test, approximately 200 g biocrude oil was loaded into a 300 ml round-bottom flask, which was heated with a stirring heating mantle (Azzota SHM-250, LabShops, Claymont, DE). To avoid quick distillations that may cause ineffective separation and safety issues, the heating rate was set at about 1°C/min. The biocrude in the flask was homogenized with a stir bar to enhance the heat transfer. In order to reduce the heat loss, glass wool was wrapped around the distillation equipments. The distillation was conducted under an atmospheric pressure. The vapor distillate was refluxed into an inclined condenser and then condensed by circulating tap water. Distillate fractions at a weight of 10 g (~5 wt.% of feed biocrude) each were collected at different distillation temperatures in sequence (Cheng et al., 2014b; Ott et al., 2008). Distillation experiments were conducted for at least three independent tests with three types of biocrude and average values were reported. The distillation set-up is present in Figure 4-4.

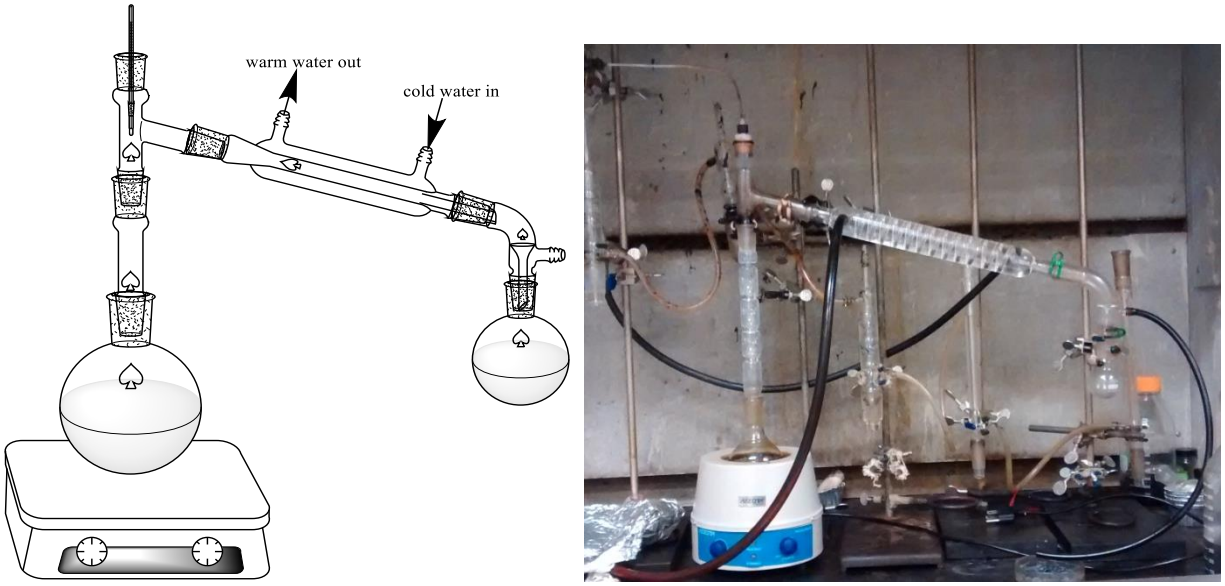


**Figure 4-4. The distillation set-up for separating biocrude oil**

## 4.6 Physicochemical Analysis of HTL products

### 4.6.1 Thermogravimetric Analysis (TGA) experiments

#### 4.6.1.1 TGA analysis for pretreated WA biomass

Thermogravimetric analysis (TGA) of algal biomass were performed on a Q50 TGA (TA Instruments, Schaumburg, IL), from 25ºC to 800ºC in 60 ml/min $N_2$ at a heating rate of 10ºC/min, to assess the decomposition kinetics of WA biomass with various pretreatment methods. The tested sample weight for each test was 15±0.1 mg (dry basis) to avoid the heat-transfer limitation generated by the sample itself. To determine the decomposition kinetics of algae with various pretreatments based on the TGA data, the mathematical procedure used in this study is based on the integral method employed by many other studies (Jaber & Probert, 2000; White et al., 2011). Assuming that a first-order reaction model (White et al., 2011) occurred during TGA tests, the rate of decomposition can be described as:

$$\frac{dx}{dt} = k(1 - X) \qquad 4\text{-}8$$

Where k is the reaction rate constant, which can be calculated by the Arrhenius expression (equation 4-9). X represents the fraction of conversion (equation 4-10).

$$k = Ae^{\frac{-E}{RT}} \qquad 4\text{-}9$$

$$X = \frac{W_o - W_t}{W_o - W_\infty} \quad 4\text{-}10$$

Where $W_o$ and $W_\infty$ respectively represents the initial and final weights of the sample while $W_t$ refers to the sample weight at reaction time t. Due to a constant heating rate (h=dT/dt) selected during TGA tests, the integration of equation 4-8 can be converted into equation 4-11 :

$$\ln[-\ln(1-X)] = \ln[\frac{ART^2}{hE}(1-\frac{2RT}{E})] - \frac{E}{RT} \quad 4\text{-}11$$

For a given fraction of conversion, the plot of ln[-ln (1-X)] against 1/T is a straight line with a slope of –(E/R), the magnitude of which can be used to calculate the activation energy (E).

#### 4.6.1.2 TGA analysis for HTL products

Thermogravimetric analysis (TGA) of biocrude oil, solid residue, and distillates were performed on a Q50 TGA (TA Instruments, Schaumburg, IL) from 110ºC to 800ºC in 60.0 ml/min $N_2$ at 10ºC/min to estimate the boiling point distribution. Biocrude oil and solid residue were dried naturally in the fume hood for 24 h and then subject to TGA analysis.

### 4.6.2 SEM (Scanning Electron Microscope) Analysis

Morphologies of the pretreated algae was probed by SEM (JEOL 6060LV, JEOL Ltd., Japan). A small amount of algae was spread on conductive adhesive tapes on a sample holder followed by gold sputter coating.

### 4.6.3 Gas Chromatograph Mass Spectrometer (GC-MS) Analysis

The chemical composition of the biocrude oil, distillates, and aqueous products were analyzed using GC-MS (Agilent Technologies, Santa Clara, CA). All data were normalized according to internal standards: 0.1μM 3-methyl butanoic acid for aqueous products and 0.5μM pentadecanoic acid methyl ester for the biocrude oil extracted in toluene as well as the distillates extracted in hexane. Detailed analytical methods were described in previous literature (Chen et al., 2014b; Gai et al., 2014a). The spectra of all chromatogram peaks were evaluated using the HP Chem Station (Agilent, Palo Alto, CA) and AMDIS (NIST, Gaithersburg, MD) programs. The spectra of all chromatogram peaks were compared with an electron impact mass spectrum

from NIST Mass Spectral Database (NIST08) and W8N08 library (John Wiley & Sons, Inc., Hoboken, NJ).

In order to probe relatively non-volatile organic compounds, derivatization treatment was also applied to the HTL products (*e.g.*, distillates extracted with hexane) before GC-MS analysis. Dried extracts (600 μL) were derivatized with 100 μL methoxyamine hydrochloride (40 mg/mL in pyridine) for 1.5h at 50°C, then with 100 μL MSTFA (N-Methyl-N-(trimethylsilyl) trifluoroacetamide) at 50°C for 2h and following a 2-h incubation at room temperature. The internal standard, hentriacontanoic acid (10 mg/mL), was added to each sample prior to derivatization. The derivatized sample was then injected with the split ratio of 7:1. Metabolites were analyzed using a GC-MS system (Agilent Inc, CA) consisting of an Agilent 7890 gas chromatograph, an Agilent 5975 mass selective detector, and a HP 7683B autosampler. Gas chromatography was performed on a ZB-5MS capillary column (Phenomenex, CA). The inlet and MS interface temperatures were 250°C, and the ion source temperature was adjusted to 230°C. The helium carrier gas was kept at a constant flow rate of 2 mL/min. The temperature program was: 5-min isothermal heating at 70°C, followed by an oven temperature increase of 5°C /min to 310°C and a final 10 min at 310°C. The mass spectrometer was operated in positive electron impact mode (EI) at 69.9 eV ionization energy at a m/z 50-800 scan range. The spectra of all chromatogram peaks were compared with electron impact mass spectrum libraries NIST08 (NIST, MD) and W8N08 (Palisade Corporation, NY). To allow comparison between samples, all data were normalized to the internal standard. The instrument variability was within the standard acceptance limit (5%).

### 4.6.4 Fourier Transform Infrared Spectroscopy (FTIR) Analysis

FTIR spectroscopic analaysis was operated to investigate the functionalities of biocrude oil and distillates. FTIR spectra were collected using a Thermo Nicolet Nexus 670 Fourier Transform Infrared Spectroscopy. Potassium bromide (KBr) beamsplitter was used for each analysis. With a resolution of 0.5 $cm^{-1}$, 64 scans adsorption interferogram were collected in the 4000-650 $cm^{-1}$ region for each spectra.

### 4.7 Transportation fuel compatibility analysis

In order to investigate the compatibility of biocrude oil with transportation fuels, biocrude oil converted from swine manure obtained in this study was blended with commercial fuels with different weight ratios. Diesel was purchased from a commercial gas station while aviation fuel was obtained from University of Illinois-Willard Airport (Flightstar Corporation, Savoy, IL). An ultrasonic-assisted blending was carried out with the biocrude oil and fuels under an ultrasonic bath (CD-4800, Syhann Co. Ltd., Canada) for 30 minutes with a 42k Hz frequency because ultrasonic-assisted mixing has been proven to be an efficient method for mixing biocrude oil with other solvents (Zhang et al., 2013a). The blended biofuel samples were subjected to elemental analysis, density measurement, TGA analysis, and GC-MS analysis to understand how fuel properties and compositions may be affected by biocrude oil.

### 4.8 Upgrading of distillates

The objective of this part of study is to develop processes for upgrading distillates from wet biowaste into fuel-grade diesel (*i.e.*, HTL diesel). Esterification was conducted to reduce the high free fatty acid (FFA) feedstocks. Distillates with high FFA were converted to esters with methanol and acidic catalysts (Scheme 4-1). A Bronsted acid such as $H_2SO_4$ is used for methyl esterification of FFA (Canakci & Van Gerpen, 2001; Naik et al., 2008).

$$RCOOH+R'OH \leftrightarrow RCOOR' + H_2O$$

**Scheme 4-1. Esterificiation reaction**

To investigate the effects of reaction temperature, reaction time, catalysts loadings, and molar ratio of distillates to methanol on the acid-catalyzed conversion of FFA to methyl esters, an orthogonal array design (OAD) with three levels is performed (Table 4-5 and Table 4-6). Previous studies have reported that reaction temperatures between 50°C to 80°C, reaction times between 0.5-3 h, catalysts loading of 0.5-5 wt.%, and molar ratio of feedstocks to methanol between 1:6-1:12 are suitable for converting FFA to methyl esters, depending on the feedstock types (Canakci & Van Gerpen, 2001; Leung et al., 2010; Naik et al., 2008). As a consequence, reaction temperatures of 50°C, 60°C, and 70°C was used to cover a 10°C temperature range in the present work. Excessively high reaction temperature was avoided, so the methanol would not be boiled and the reaction vessel would not need to be pressurized. Reaction time of 0.5h, 1h,

and 2h, catalysts loading of 0.5 wt.%, 1 wt.%, and 2 wt.%, and molar ratios of feedstocks to methanol of 1:5, 1:9, and 1:15 were selected to make the OAD optimization more efficient and economic. Longer reaction time, more catalysts loading, and higher molar ratio of feedstocks to methanol would be used when necessary. After the reaction, the esterified oil contained water, excess methanol, and acid catalysts that need to be removed. The oil layer was separated from the mixture with a funnel separator and passed over anhydrous $Na_2SO_4$.

**Table 4-5. Experimental parameters and their level in $L_9$ ($3^4$) Orthogonal array design (OAD)**

| Parameters | Levels | | | | | |
|---|---|---|---|---|---|---|
| | 1 | | 2 | | 3 | |
| | FPW | SW | FPW | SW | FPW | SW |
| Temperature (°C) | 50°C | 25°C | 60°C | 35°C | 70°C | 45°C |
| Time (hr) | 0.5 h | 0.5 h | 1 h | 1 h | 2 h | 2 h |
| Concentration of additives | 0.5 wt.% | 1 M | 1 wt.% | 2 M | 2 wt.% | 5 M |
| Substrate: Methanol or NaOH | 1:5 (molar) | 1:3 (weight) | 1:9 (molar) | 1:1 (weight) | 1:15 (molar) | 2:1 (weight) |

The yield of esterified oil was calculated based on the weight of distillates ($W_{distillates}$) divided by the weight of treated oil ($W_{ester}$) (*i.e.*, $W_{distillates}/W_{ester}$). The acidity of esterified oil was measured according to ASTM standards (ASTM D7467) (ASTM, 2015b).

**Table 4-6. $L_9$ ($3^4$) OAD matrix randomized experimental plan to upgrade FPW-derived distillates through esterification**

| Item | Temperature (°C) | Time (h) | Catalyst Loading (*i.e.*, $H_2SO_4$) (wt.%) | Substrate: Methanol (molar ratio) |
|---|---|---|---|---|
| 1 | 50°C | 0.5 hr | 0.5% | 1:5 |
| 2 | 50°C | 1 hr | 1% | 1:9 |
| 3 | 50°C | 2 hr | 2% | 1:15 |
| 4 | 60°C | 0.5 hr | 1% | 1:15 |
| 5 | 60°C | 1 hr | 2% | 1:5 |
| 6 | 60°C | 2 hr | 0.5% | 1:9 |
| 7 | 70°C | 0.5 hr | 2% | 1:9 |
| 8 | 70°C | 1 hr | 0.5% | 1:15 |
| 9 | 70°C | 2 hr | 1% | 1:5 |

Neutralization was carried out to reduce the phenolic compounds in feedstocks, because the phenolic compounds would lead to excessively high gum contents in fuel. Distillates with high phenolic compounds were reacted with sodium hydroxides to form sodium phenoxide and water (Scheme 4-2). Since sodium phenoxides is very soluble in water (2006), the fuel appropriate

compounds in the distillates can be simply separated by oil-water phase separation with a funnel separator.


**Scheme 4-2. Neutralization of phenols with sodium hydroxide**

To investigate the effects of reaction temperature, reaction time, concentration of sodium hydroxides, and weight ratio of distillates to sodium hydroxides on the neutralization of phenolic compounds to sodium phenoxides, an orthogonal array design (OAD) with three levels is performed (Table 4-7). Since neutralization of phenols with sodium hydroxides is an exothermic reaction (Fernandez & Hepler, 1959; Leal et al., 1991; Mishima et al., 2009), increasing the reaction temperature would shift the balance at equilibrium back toward reactants, according to Le Chatelier's principle (Atkins et al., 2016). Thus, reaction temperatures of 25°C, 35°C, and 45°C was used to cover a 10°C temperature range in the present work. Previous studies have reported that the weight ratio of HTL biocrude oil to reactants/solvents would highly affected the reaction/extraction efficiency (Chen et al., 2016b), so the weight ratio of HTL distillates to sodium hydroxide was investigated by exploring the range between 1:3 to 2:1. Reaction time of 0.5hr, 1hr, and 2hr, and the concentration of sodium hydroxides of 1M, 2M, and 5M were selected to make the OAD optimization more efficient and economic. Longer reaction time, higher concentration of sodium hydroxide, and larger weight ratio of HTL distillates to sodium hydroxide would be exploited when necessary. After the reaction, the neutralized oil contained water, excess sodium hydroxide, and sodium phenoxides that need to be removed. The oil layer was separated from the mixture with a funnel separator and passed over D.I. water to wash out most sodium phenoxides.

The yield of neutralized oil was calculated based on the weight of distillates ($W_{distillates}$) divided by the weight of treated oil ($W_{ester}$) (*i.e.*, $W_{distillates}/W_{ester}$). The gum content of neutralized oil was measured according to ASTM standards (ASTM D7467) (ASTM, 2015b).

**Table 4-7. $L_9$ ($3^4$) OAD matrix randomized experimental plan to upgrade SW-derived distillates through neutralization**

| Item | Temperature (°C) | Time (h) | Concentration of NaOH (M) | Substrate: NaOH (weight ratio) |
|---|---|---|---|---|
| 1 | 25°C | 0.5 h | 1M | 1:3 |
| 2 | 25°C | 1 h | 2M | 1:1 |
| 3 | 25°C | 2 h | 5M | 2:1 |
| 4 | 35°C | 0.5 h | 2M | 2:1 |
| 5 | 35°C | 1 h | 5M | 1:3 |
| 6 | 35°C | 2 h | 1M | 1:1 |
| 7 | 45°C | 0.5 h | 5M | 1:1 |
| 8 | 45°C | 1 h | 1M | 2:1 |
| 9 | 45°C | 2 h | 2M | 1:3 |

### 4.9 Energy Consumption Ratio and Reaction Severity of Upgrading Processes

The energy consumption ratio (ECR) was calculated for different upgrading methods using equation 4-12,

$$\mathrm{ECR}_{\mathrm{upgrading}} = \frac{E_{distillation} + E_{esterification/neutralization}}{E_{biocrude-upgraded}} = \frac{[W_i C_{pw} T + (1-W_i) C_{pm} T][1-R_h]}{[Y(HHV)(1-W_i) R_c]} \qquad 4\text{-}12$$

where $W_i$ is the moisture content of the initial feedstock prior to upgrading, $C_{pw}$ is the specific heat of water (4.18 kJ/kg·K), $C_{pm}$ is the specific heat of HTL biocrude oil (assumed to be similar to petroleum, 2.13 kJ/ kg·K) (Incropera, 2007; ToolBox), T is the difference between the designated reaction temperature and the initial temperature (assumed to be 25°C), Y is the upgraded HTL biocrude oil yield, HHV is the higher heating value of upgraded HTL biocrude oil, $R_h$ is the efficiency of heat recovery assumed to be 0.5, and $R_c$ is the efficiency of available combustion energy assumed to be 0.6 (Chen et al., 2014b; Yu, 2012). An ECR of less than 1.0 indicates a net energy gain for the system (Chen et al., 2014b; Vardon et al., 2012).

The reaction severity was also computed for different upgrading methods employing equation 4-13,

$$R_0 = \int_{t_1}^{t_2} \exp \frac{T_r(t) - T_b}{14.75}\, dt \qquad 4\text{-}13$$

where $T_r$ (°C) is the reaction temperature, $T_b$ is the base temperature (assumed to be 100°C) (Eboibi et al., 2014b; Faeth et al., 2013), and $t_1/t_2$ is the initial/final holding time. Reaction

severity combines the effect of reaction temperature and time into a single parameter (Eboibi et al., 2014b; Faeth et al., 2013).

### 4.10 Drop-in fuel preparation and fuel specification analysis

Distillates derived from SM, FPW, and SP were added into diesel to obtain a 10-20 vol.% drop-in biodiesel. The fuel specifications, including viscosity, density, acidity, net heat of combustion, gum content, ash content, Cetane number, lubricity, and oxidation stability, of drop-in biodiesel was measured and compared to those of transportation fuel standards. The characterizations of fuel specification were conducted by ASTM standard methods (ASTM, 2015b).

### 4.11 Diesel Engine Tests

#### 4.11.1 Engine Setup and Specifications

The Diesel engine tests were conducted according to the previously reported methods (Lee et al., 2016), using a an AVL 5402 single-cylinder diesel engine. Key engine specifications are presented in Table 4-8. The engine was coupled to a GE type TLC-15 class 4-35-1700 dynamometer capable of delivering up to 14.9 kW (20 HP) and absorbing up to 26.1 kW (35 HP) at a maximum rotational speed of 4500 RPM. A Dyne Systems DYN-LOC IV controller controlled the dynamometer. A Kistler type 6125B pressure transducer measured in-cylinder pressure with an AVL 3057-AO1 charge amplifier and was indexed against a crankshaft position signal from a BEI XH25D shaft encoder (Lee et al., 2016). Figure 4-5 illustrates the engine setup schematic. The control and diagnostic parameters in the engine control module (ECM) were developed and calibrated through ETAS INCA. Data acquisition and real-time recording of engine operating conditions were performed by using INCA. An ETAS ES580 interface card was used as the connection between the electronic diesel control (ECU) and the program.

**Table 4-8. Specifications of diesel engine used in this study**

| Items | Specifications |
|---|---|
| Engine | AVL 5402 Diesel engine |
| Number of cylinders | 1 |
| Bore | 85 mm |
| Stroke | 90 mm |
| Displaced volume | 510.7 cm3 |
| Number of valves | 4 |
| Compression ratio | 17.1:1 |
| Diesel injection | Direct injection |
| Diesel injection system | BOSCH common rail CP3 |
| Number of injection holes | 5 |
| Diameter of injection holes | 0.18 mm |

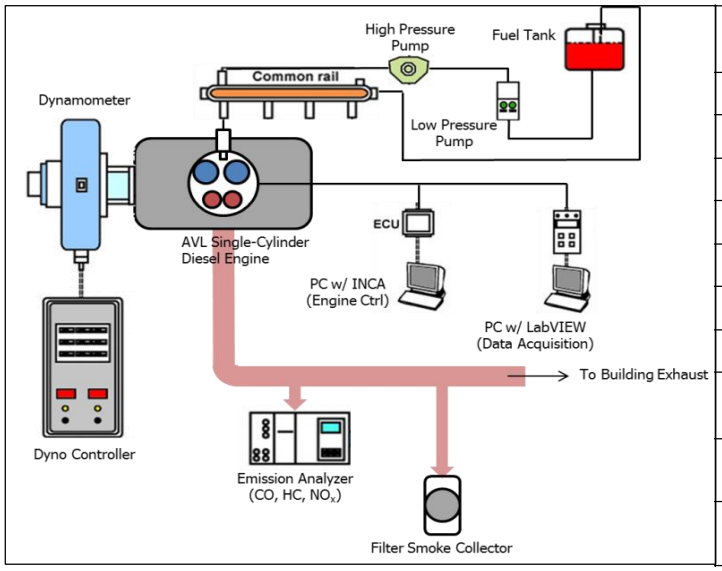


| | |
|---|---|
| Engine | AVL 5402 Diesel engine |
| Number of cylinders | 1 |
| Bore | 85 mm |
| Stroke | 90 mm |
| Displaced volume | 510.7 $cm^3$ |
| Number of valves | 4 |
| Compression ratio | 17.1:1 |
| Diesel injection | Direct injection |
| Diesel Injection system | BOSCH common rail CP3 |
| Number of injection holes | 5 |
| Diameter of injection holes | 0.18 mm |

**Figure 4-5. Experimental Setup for Diesel Engine Tests**

### 4.11.2 Emission Analysis

Nitrogen oxides ($NO_x$) was measured by a Horiba MEXA-720 $NO_x$ non-sampling type meter in the exhaust manifold of the engine. The measurement range of $NO_x$ was 0-3000 ppm (with ±30 ppm accuracy for 0-1000 ppm, ±3% accuracy for 1000-2000 ppm, and ± 5% accuracy for 2000-3000 ppm). Carbon monoxide, carbon dioxide, and unburned hydrocarbons (UHC) emissions were sampled by a Horiba MEXA-554JU sampling type meter. In order to transport the exhaust gases to the meter, a probe was fabricated to fit in the exhaust manifold of the engine. The measurement range were 0.00-20.00% by volume for carbon dioxide, 0.00-10.00% by volume for carbon monoxide, and 0-10,000 ppm for unburned hydrocarbons.

Exhaust gas temperature (EGT) located in the exhaust manifold is measured by a type-K thermocouple.

Soot content was determined by a standard filter paper method reported in previous studies (Lee et al., 2016; Zhang et al., 2015). In short, raw exhaust gases were drawn through a 7/8" round filter paper using a vacuum pump. Rectangular strips of filter papers (Grainger Industrial Supply, #6T167) were placed in a filter holder taken from a Bacharach True-Spot smoke meter. The sampling flow rate is constantly monitored by a flow meter. After the samples were collected, a digital scanner was used to measure the filter paper blackening.

The paper blackening (PB) is defined as:

$$PB = \frac{100 - R_R}{10} \tag{4-14}$$

where

$$R_R = (\frac{R_p}{R_f}) \times 100\% \tag{4-15}$$

$R_p$ = reflectometer value of sample

$R_f$ = reflectometer value of unblackened paper

$R_R$ = relative brightness of the sample (relative radiance factor)

With the sampled volume at 1 bar and 298 K, the paper blackening value could be considered as the filter smoke number (FSN).

# CHAPTER 5. PHYSICAL PRETREATMENTS OF WASTEWATER ALGAE TO REDUCE ASH CONTENT AND IMPROVE THERMAL DECOMPOSTION CHARACTERISTICS

## 5.1 The effect of pretreatments on macroscopic structures of WA biomass

HTL of wastewater algae (WA) biomass involves with complicated physicochemical processes. To provide insight into the mechanism of these heterogeneous reactions, it is essential to determine the solid-state decomposition kinetics of WA biomass, which is typically conducted by thermogravimetric analyses (TGA) (Gai et al., 2013). TGA encompasses two major processes: isothermal and non-isothermal. In recent decades, non-isothermal method is more predominant because of its high sensitivity and accuracies (Gai et al., 2013; White et al., 2011). Kinetic parameters such as apparent activation energy can be calculated with the thermogravimetric (TG) and differential thermogravimetric (DTG) curves obtained from the TGA tests.

Algal biomass harvested from wastewater typically contains 30%-50% (dry weight basis) ash content (Chen et al., 2014c; Yu, 2012). The relatively high ash content was not desirable to yield biocrude oil during HTL (Chen et al., 2014b; Yu, 2012). The pretreatment of WA biomass could help address this issue. As a result, the physical pretreatments such as centrifugation and ultrasonication were used to help decrease the ash content in algae and thus improve the thermal decomposition behavior of WA biomass. Pretreatment processes for WA biomass and physicochemical analyses of the resulted biocrude oil were illustrated in Figure 5-1.

Abbreviations[1]

S-2: Screen size between 45-106 μm; C-1: Centrifuge at 3000 rpm for 15 minutes; C-2: Centrifuge at 3000 rpm for 25 minutes; C-3: Centrifuge at 4000 rpm for 15minutes; C-4: Centrifuge at 4000 rpm for 25 minutes; U: Ultrasonic for 1 hour; C+U-1: C-1 treatment plus ultrasonic for 0.5 hour; C+U-2: C-1 treatment plus ultrasonic for 1 hour

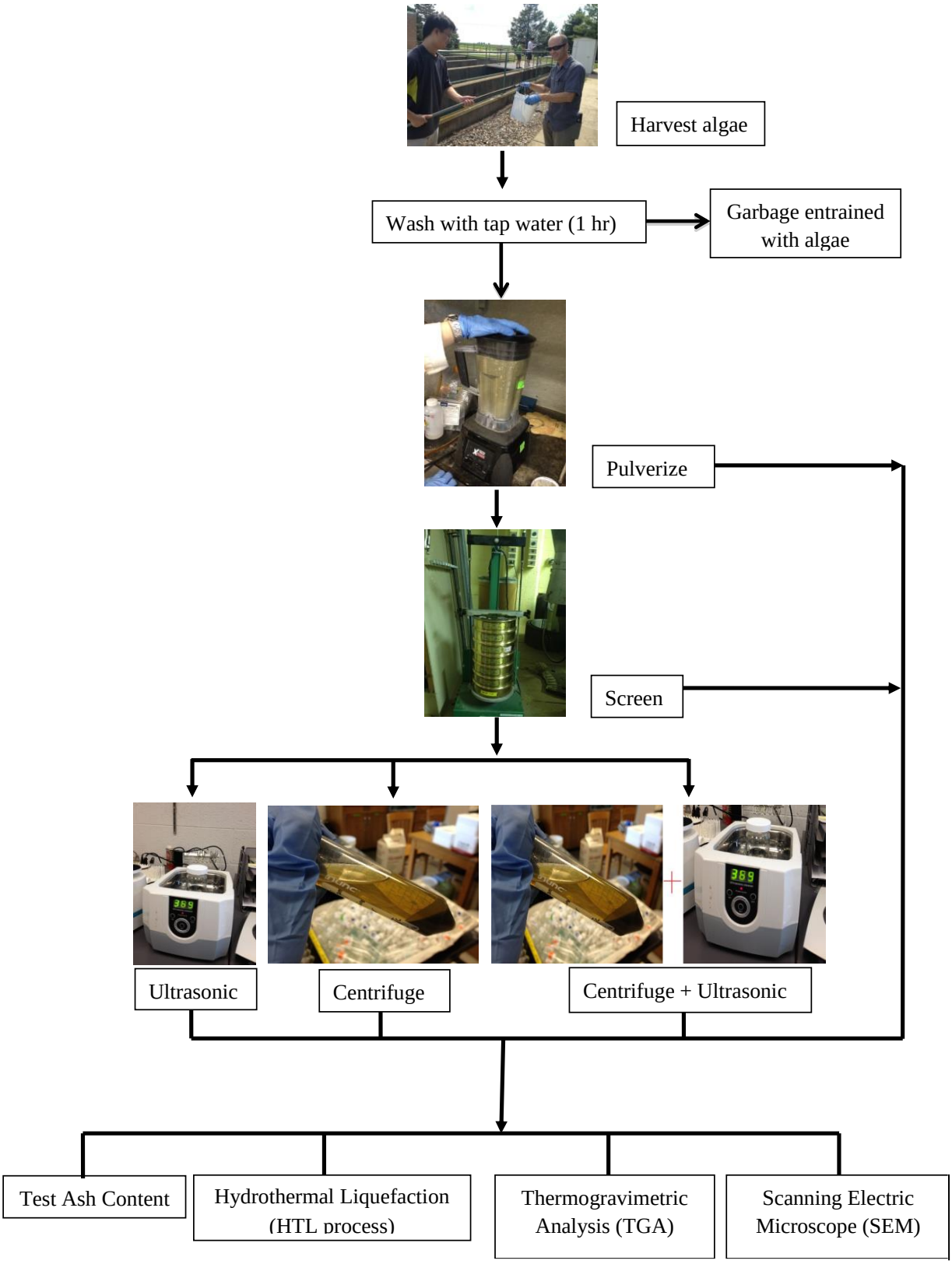


**Figure 5-1. Pretreatment processes for WA biomass and physicochemical analyses for resulting biocrude oil**

Table 5-1 shows the ash content of the algae samples with various pretreatments. The upper layer algal biomass obtained by the centrifugal pretreatment contained more ash content than the algae with only screening. However, the algal biomass collected from the middle fraction via centrifugal pretreatments (Figure 5-2), typically contained less ash than the raw algae and those from the upper layer. The result infers that centrifugation can help segregate the volatile solids from the ash content in WA biomass. This may be explained by that the density of ash content such as snail shell fragments are typically heavier than that of volatile solids such as proteins (Lide, 2004; Noureddini et al., 1992). However, ash content with relatively small sizes (Figure 5-2) may tend to remain in the upper layer, and thus the ash content of the algae obtained from upper layer via centrifugation were increased.

**Table 5-1. The ash content and weigh percentage of algal biomass with different centrifugation treatments (n=2)**

| Pretreatment condition | | Ash content | Weight percentage after centrifugation |
|---|---|---|---|
| Pulverized | | 27.6 ± 0.07% | N/A |
| S-2 | | 28.6 ± 1.9% | 100% |
| C-1 | Upper | 32.5 ± 1.2% | 26.4 ± 4.27% |
| | Middle | 18.6 ± 0.8% | 29.0 ± 0.73% |
| C-2 | Upper | 36.7 ± 3.1% | 24.5 ± 2.15% |
| | Middle | 21.8 ± 0.8% | 27.0 ± 0.50% |
| C-3 | Upper | 34.1 ± 3.5% | 24.4 ± 0.18% |
| | Middle | 21.0 ± 0.04% | 33.0 ± 7.35% |
| C-4 | Upper | 34.4 ± 1.7% | 26.7 ± 0.63% |
| | Middle | 19.2 ± 1.9% | 33.5 ± 1.38% |

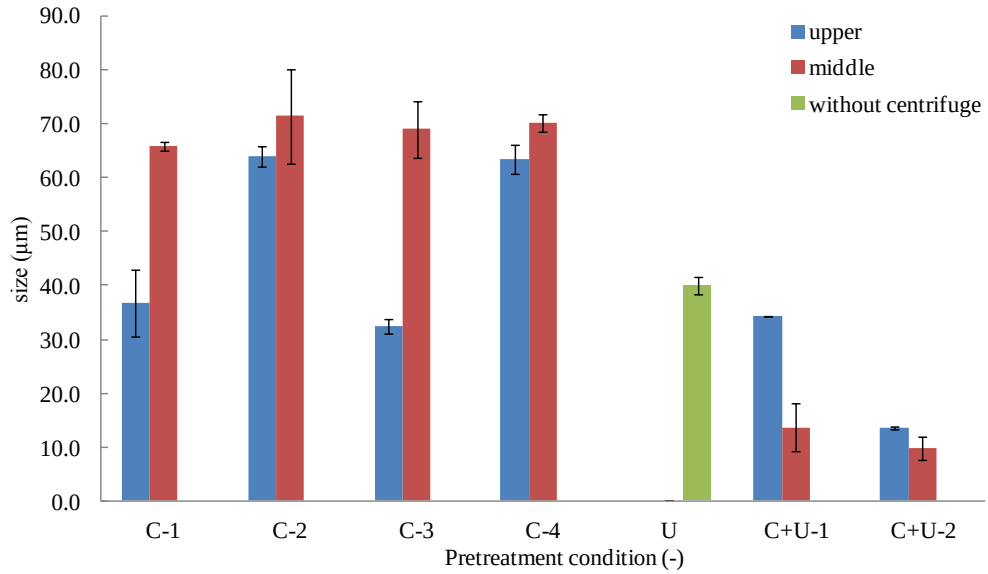


**Figure 5-2. Particle size of algal biomass with different pretreatment conditions (n≥2)**

Table 5-1 also showed that the ash content of most algal biomass samples decreased as the centrifugal test time and speed decreased, particularly for the centrifuged sample obtained at 3000 rpm for 15 minutes. This indicates that increased centrifugation time and speed were not essential for separating volatile solids from ash content. It is worth of pointing out that when the pretreatment of C+U-1 and C+U-2 applied to WA biomass, the particle sizes of the middle part of algae were greatly reduced from 65.8-71.4 μm to 9.78-13.7 μm, which may be carried out by the strong shockwaves and shear forces generated during ultrasonication, as compared to that of the upper part. This also reveals that there were more easily breakdown macromolecules in the middle layer of WA biomass.

**5.2 Thermogravimetric analysis of WA biomass with different pretreatments**

Figure 5-3 shows the thermogravimetric (TG) curves of algal biomass with different pretreatments. It can be found that the TG curves of these samples were similar, which all showed three stages during the heating process. The first stage was from the initial temperature (about 25°C) to about 150°C. This stage of mass loss probably results from the dehydration of the algal cells (Gai et al., 2013; White et al., 2011). The second mass loss stage began at about 275°C and ended at around 400°C. This stage exhibited a major weight loss of algae with various pretreatments, which can be contributed by the decomposition or depolymerization of algal organic substances such as carbohydrates and proteins. The third stage was ranged from 400°C to 800°C (final temperature), possibly caused by the degradation of carbonaceous materials retained in the solid residues (Liu et al., 2013).

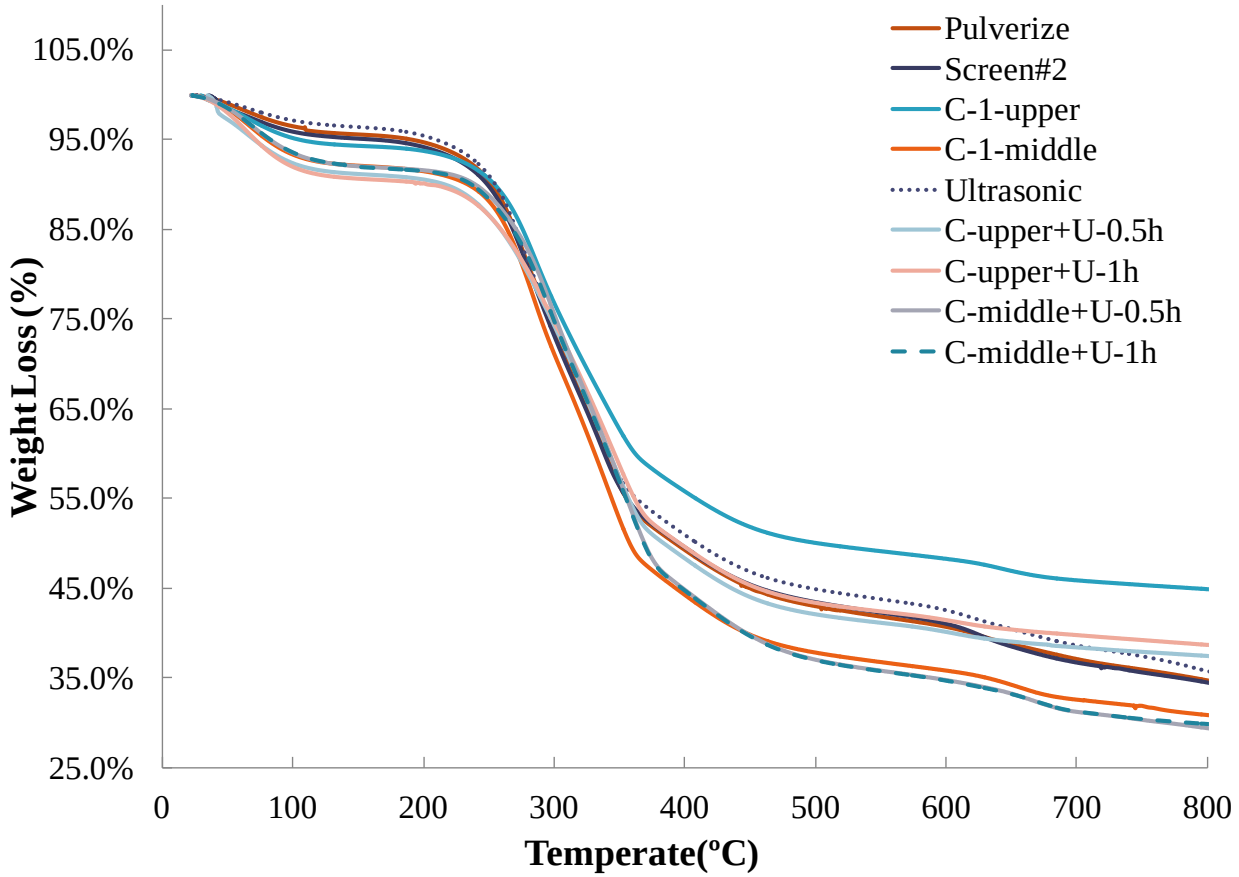


**Figure 5-3. Thermogravimetric (TG) curves of algal biomass with different pretreatment conditions in the thermal decomposition process**

Although the trends of all curves are similar, slight differences existed among various pretreatments. Table 5-2 presents the apparent activation energies of stage 1 ($E_{a1}$) and 2 ($E_{a2}$) for thermal decomposition of algal biomass with various pretreatments. Detailed regression results for determining apparent activation energies of thermal decomposition of algal biomass with different pretreatment methods are demonstrated in Figures 5-4 and 5-5.

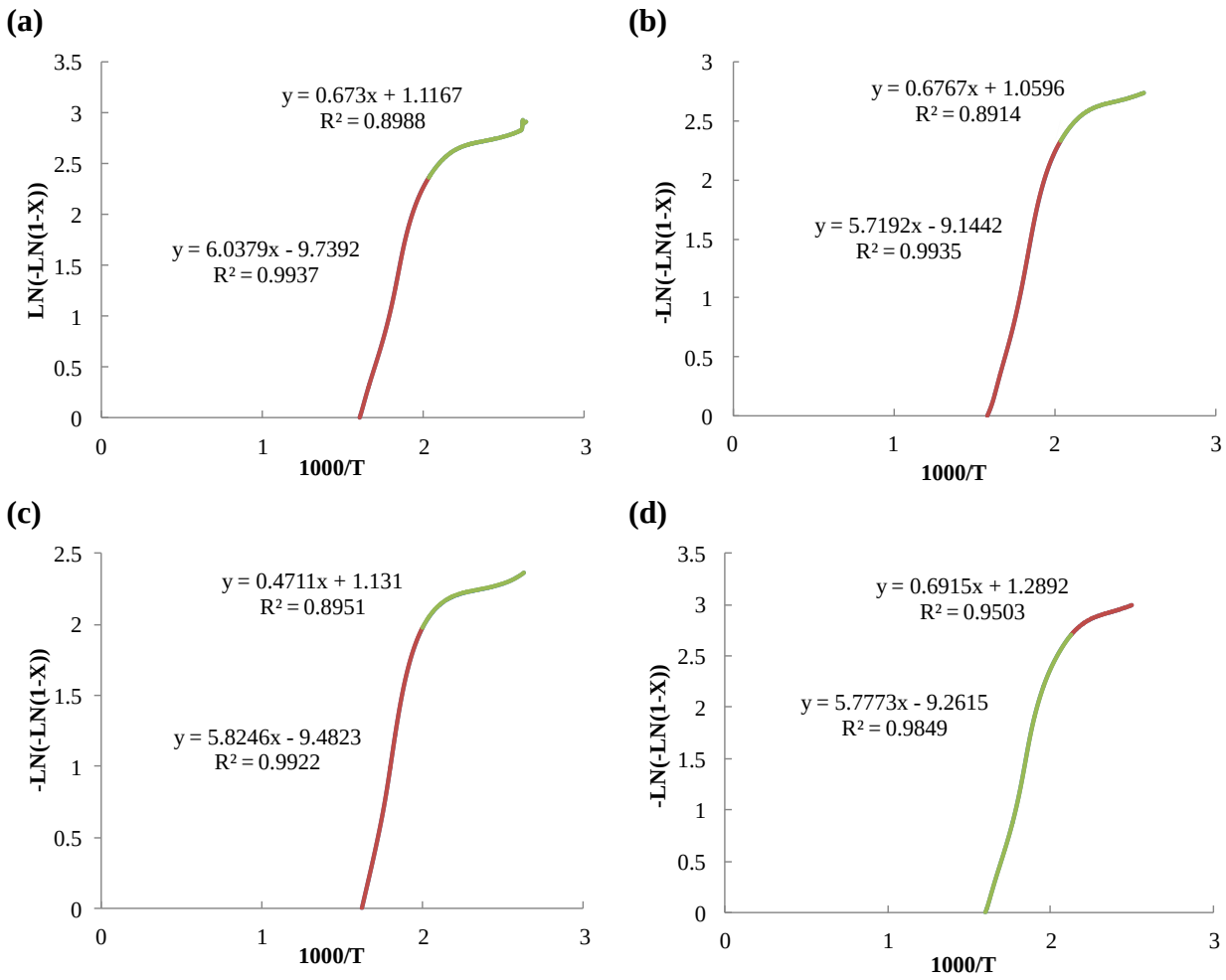


**Figure 5-4. Determination of apparent activation energy of thermal decomposition of algal biomass with different pretreatment conditions: (a) pulverize (b) screen size between 45-106µm (c) upper layer from centrifuge at 3000rpm for 15minutes (d) ultrasonic for 1 hour**

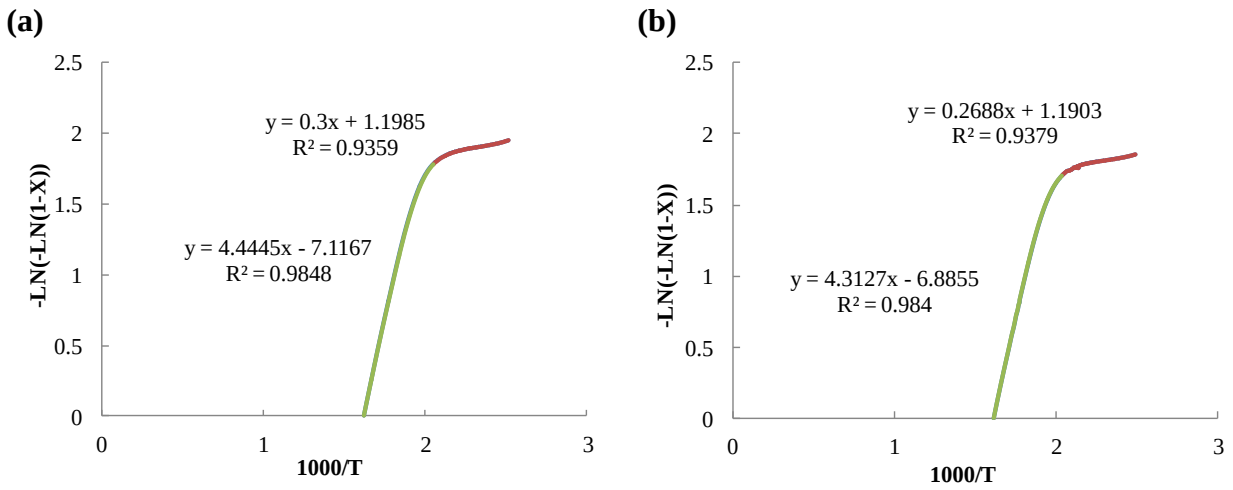


**Figure 5-5. Determination of apparent activation energy of thermal decomposition of algal biomass (upper layer) with different pretreatment conditions: (a) centrifugation followed by ultrasonic bath for 0.5h (b) centrifugation followed by ultrasonic bath for 1h**

As Table 5-2 shows, single centrifugation or ultrasonic bath had little effect on improving thermal decomposition behavior of WA biomass. For instance, $E_{a2}$ remained almost constant (about 48 kJ/mol) in those cases. In contrast, the combination of centrifugation and ultrasonication (C+U) greatly reduced the $E_{a2}$ of the thermal degradation process of WA biomass from 48 kJ/mol to36-41 kJ/mol. The related $E_{a2}$ was also lower than those of pure microalgae (*e.g.*, *Chlorella*). This may be that the physical structures of partial WA biomass (*e.g.*, lignocelluloses fractions) can be effectively changed by ultrasonic bath after centrifuge separation. SEM images also confirmed that the pretreatment of C+U changed the physical structure of algal biomass from intact to furry, which was mainly caused by the mechanism of ultrasound disruption (*e.g.*, cavitation) (Luo et al., 2013). Besides, previous similar studies also found that the ultrasonic pretreatment can help increase the surface area and decrease the crystallinity and the degree of polymerization of lignocelluloses (Shi et al., 2013a; Shi et al., 2012). Overall, the above results infer that the WA biomass with the pretreatment of C+U can be regarded as a better feedstock for biocrude oil conversion. Yet, increasing the ultrasonic bath retention time appeared to hardly impact the $E_{a1}$ and $E_{a2}$ of the thermal decomposition processes.

**Table 5-2. Slope and apparent activation energy ($E_a$) for stage 1 and 2 of WA biomass with different pretreatment methods during thermal decomposition processes; and the yield and heating value of the biocrude oil converted from pretreated algae via HTL**

| Sample | Pretreatment method | Slope[b] | | | | $E_a$ (kJ/ mol) | | Biocrude Oil Yields from HTL (%)[c] | Higher Heating Value (MJ/kg) |
|---|---|---|---|---|---|---|---|---|---|
| | | $S_1$ | $r_1^2$ | $S_2$ | $r_2^2$ | $E_{a1}$ | $E_{a2}$ | | |
| **Algae from a waste-water treatment plant** | Pulverize | 0.67 | 0.90 | 6.04 | 0.99 | 5.60 | 50.2 | 30.9 ± 1.87% | 28.2 |
| | S-2 | 0.68 | 0.89 | 5.72 | 0.99 | 5.63 | 47.6 | 29.2 ± 3.35% | 28.4 |
| | C-1-upper | 0.47 | 0.90 | 5.82 | 0.99 | 3.92 | 48.4 | | |
| | C-1-midddle | 0.35 | 0.93 | 5.35 | 0.98 | 2.91 | 47.5 | 30.6 ± 4.32% | 29.9 |
| | U | 0.69 | 0.95 | 5.78 | 0.98 | 5.75 | 48.0 | 35.4 ± 5.13% | 30.9 |
| | C+U-1-upper | 0.30 | 0.94 | 4.44 | 0.98 | 2.49 | 37.0 | | |
| | C+U-2-upper | 0.27 | 0.94 | 4.31 | 0.98 | 2.23 | 35.9 | | |
| | C+U-1-middle | 0.30 | 0.96 | 4.94 | 0.98 | 2.53 | 41.1 | | |
| | C+U-2-middle | 0.31 | 0.97 | 4.83 | 0.98 | 2.56 | 40.2 | 55.3 ± 1.54% | 32.4 |
| **Chlorella[a]** | N/A | 0.78 | 0.97 | 5.46 | 0.98 | 6.32 | 44.4 | 39.6 ± 0.79%[d] | 37.8 [d] |
| **Spirulina[a]** | N/A | 0.57 | 0.93 | 5.87 | 0.96 | 4.70 | 48.8 | | |

[a] Adopted from *(Gai et al., 2013),* which was operated at the same condition under TGA.

[b] Detailed regression results for determining apparent activation energies of thermal decomposition of algal biomass with different pretreatment methods are available in Figure 5-4 and 5-5.

[c] HTL processes were conducted with 25% total solids content of feedstocks at reaction temperature of 300°C with reaction time of 1 hour ($n \geq 2$).

[d] Adopted from *(Gai et al., 2013),* which was operated at the same condition under HTL.

### 5.3 SEM images of WA biomass with different pretreatments

Since the pretreatment of C+U appeared to significantly improve the thermal decomposition behavior of the upper layer algal biomass obtained after centrifugation, SEM was applied to observe the surface morphology of the specific algae sample. SEM images of WA biomass with single pretreatments (*e.g.*, centrifugation only) were also listed for comparison and summarized in Figure 5-6. It was found that the surface of screened algae sample was intact, relatively smooth, and flatted while that of algae with single centrifugation were destroyed, separated and found with many holes. With the pretreatment of C+U, the upper layer algal biomass obtained after centrifugation were completely shattered into smaller fragments as compared to the same scalar bar. Additionally, partial fibrillation of algal biomass was observed (Figure 5-6 (d)), which was also shown in another study about pretreating celluloses with ultrasonic bath for bio-oil production in hot-compressed water (Shi et al., 2012). The changing morphology of algae also reveals that why the apparent activation energies of the algal biomass with C+U pretreatments were greatly decreased during the thermal decomposition process.

a

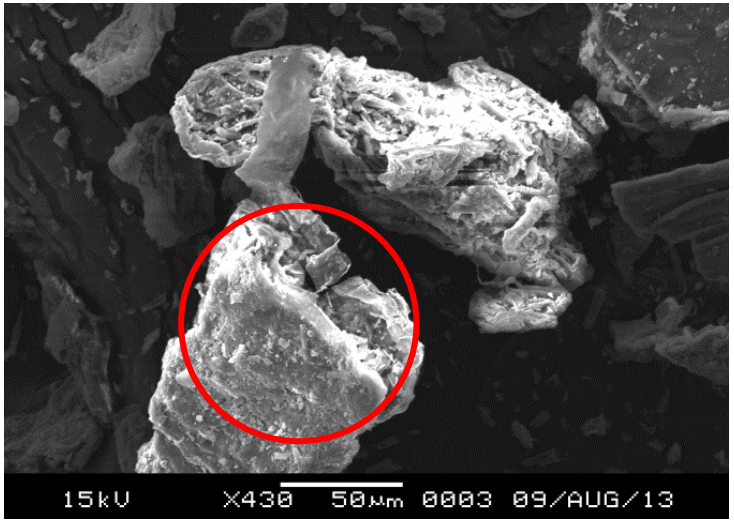


c

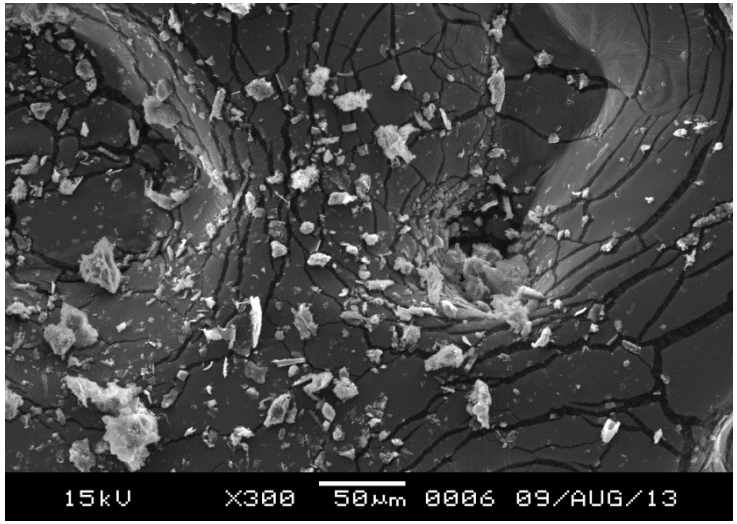


b

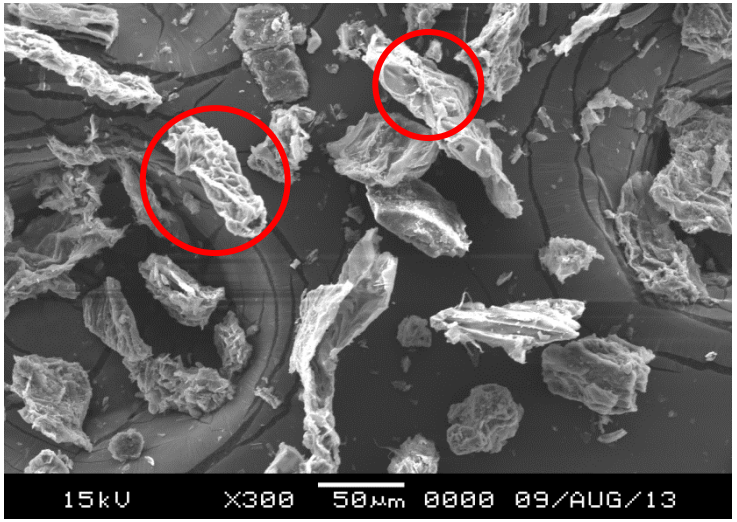


d

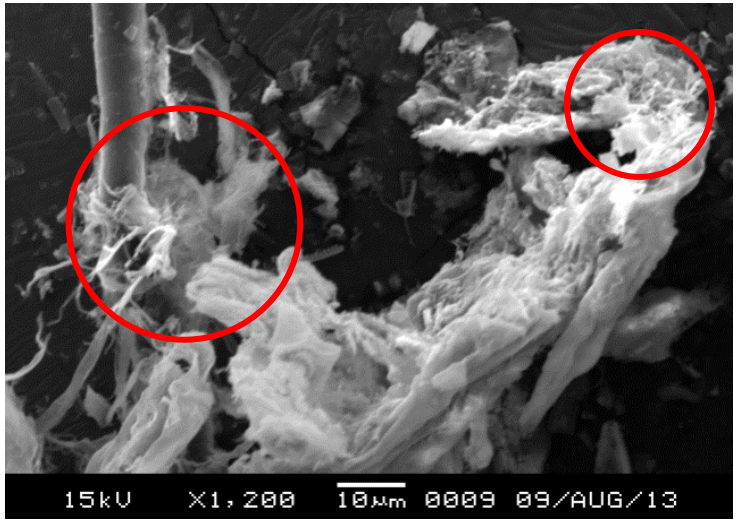


**Figure 5-6. SEM images of algal biomass with different pretreatments: (a) S-2, (b) C-1, and (c) C+U-1 (upper), (d) zooming image of C+U-1 (upper)**

## 5.4 HTL of WA biomass with different pretreatments

HTL tests were conducted on selected samples to examine if the pretreatment of C+U on WA biomass can effectively improve the yield and heating value of the bio-crude oil. Compared to the algae with single-stage pretreatment or only pulverization, the bio-crude oil yield of the algae with C+U pretreatment were substantially improved from about 30-35% to 55% and the heating value increased from 28-30 MJ/kg to 32 MJ/kg (Table 5-2). This indicates centrifugal separation and ultrasonication may effectively change the structure of WA biomass (*e.g.*, increasing the surface area, eroding lignin structure, and leading to more exposure of the volatile components such as lignocelluloses) (Shi et al., 2013b). In addition, ultrasonication can lyse the whole algal cells and help excrete the contents in the cells (*e.g.*, proteins) to the exposed surface, promoting the accessibility of the volatile materials in the algal cells and thus benefiting the subsequent conversions toward biofuels (Luo et al., 2013). Table 5-2 also confirms that WA biomass with the pretreatment of C+U can be regarded as a better feedstock for bio-crude oil conversion in terms of yield and heating value. Besides, Table 5-2 shows that the thermal decomposition behavior of pretreated algae (*e.g.*, $E_{a2}$) positively correlated to their bio-crude oil yields, which indicates that TGA could be a reliable tool to evaluate the thermal degradation performance of pretreated algae. However, although the ash content in the feedstock reduced from 28% (S-2) to 18% (C-1 middle fraction) after centrifugation, the biocrude oil yields did not increase as expected (Table 5-2). This reveals that how ash content interacts with volatile components in the feedstock under HTL processes still requires additional investigation.

# CHAPTER 6. EFFECT OF ASH ON HYDROTHERMAL LIQUEFACTION OF HIGH-ASH CONTENT ALGAL BIOMASS

Batch HTL of mixed-culture algal biomass from wastewater environment (AW) has been thoroughly investigated in terms of reaction temperature and reaction time, which are the two dominant factors during the HTL processes (Chen et al., 2014c; Elliott et al., 2013; Gai et al., 2014a; Gai et al., 2015; Jazrawi et al., 2013; Yu, 2012). However, the relatively high ash content in AW biomass (~50 wt.%) appeared to retard the biocrude oil formation and deteriorate the biocrude oil quality in terms of heating value and light oil fraction (Chen et al., 2014a; Chen et al., 2014b; Chen et al., 2014c; Rojas-Pérez et al., 2015). Few studies have reported the effect of ash content on HTL conversion of algal feedstock (Rojas-Pérez et al., 2015). How the ash content interact with volatile components in the feedstock under HTL processes still remains unknown and requires additional investigation to elucidate the role of the ash content in HTL processes.

Therefore, this chapter aims to explore the relationship between the ash content of algal feedstock and the yield and quality of the biocrude oil. The snail shell fragment is the major ash content in AW biomass (Chen et al., 2014c). As a result, the screen pretreatment was used to remove the ash content in AW biomass. In order to probe the effect of ash content on HTL processes, the AW biomass was screened into two fractions (AW-41.8 and AW-38.5) and then converted into biocrude oil at 300°C for a 60 minute reaction time via HTL (Chen et al., 2014c; Gai et al., 2014a). In addition, the mass balance of HTL products was calculated. Elemental, GC-MS and TGA analyses were also conducted on biocrude oil samples to study how the ash content may influence the quality of biocrude oil. Finally, HTL of model algae, *Chlorella pyrenoidosa*, with different concentrations of representative ash content, was conducted to examine the effect of ash content on HTL of algal biomass.

## 6.1 Hydrothermal Liquefaction of Screened AW biomass

By screening, some large particles, such as snail shell, can be removed and therefore reduce the ash content by 10-15% in AW biomass. Table 6-1 also demonstrates that the calcium carbonates were the major ash content in the AW biomass and they decreased with the screen pretreatment.

**Table 6-1. Elemental analysis of AW biomass with different ash content**

| Component (d.w.%) | Without screening | AW-41.8 | AW-38.5 |
|---|---|---|---|
| C | 27.9±3.7 | 29.6±0.2 | 31.2±0.5 |
| H | 3.01±0.6 | 3.84±0.1 | 4.14±0.02 |
| N | 3.90±0.6 | 4.28±0.1 | 4.94±0.11 |
| Ca | 16.0 | 13.9 | 11.0 |
| Estimated $CaCO_3$[a] | 40.0 | 34.8 | 27.5 |
| Ash content of feedstock | 53.3±1.3 | 41.8±2.4 | 38.5±0.6 |

[a]Assume calcium carbonate ($CaCO_3$) is the major components (Chen et al., 2014c)

In order to understand how the ash content influence HTL processes, HTL of AW biomass with different ash content was conducted at 300°C for a 60 minute reaction time, which is the previously determined optimal condition for converting algal biomass into biocrude oil (Chen et al., 2014c; Gai et al., 2014a). The effect of particle sizes was presumed to be negligible in batch HTL processes, based on multiple previous studies researching the influence of particle size under thermochemical conversion processes in a batch reactor (Akhtar & Amin, 2011; Bae et al., 2011; Zhang et al., 2009). Further, sub/supercritical water generally acts both as a heat transfer medium as well as an extractant and thereby can help overcome the heat and mass transfer limitations caused by particle size in HTL processes (Akhtar & Amin, 2011).

The HTL product yields of AW biomass with different ash content were presented in Figure 6-1. Figure 6-1 shows that the solid residue yields were reduced while the aqueous product yields and gas yields increased, as the ash content reduced in the algal feedstocks. In addition, the aqueous product yields increased by about two times (from 17.0 d.a.f.% to 36.7 - 37.4 d.a.f.%) as the ash content in the AW biomass reduced by 25% (from 53.3% to 38.5 - 41.8%). Valdez and Savage have conducted HTL reactions of aqueous-phase products and concluded that the biocrude oil can be formed from aqueous-phase products under HTL processes (Valdez & Savage, 2013). Although the reduction of the ash content in AW biomass did not improve the biocrude oil yield, the precursor of the biocrude oil—the aqueous product—was substantially increased.

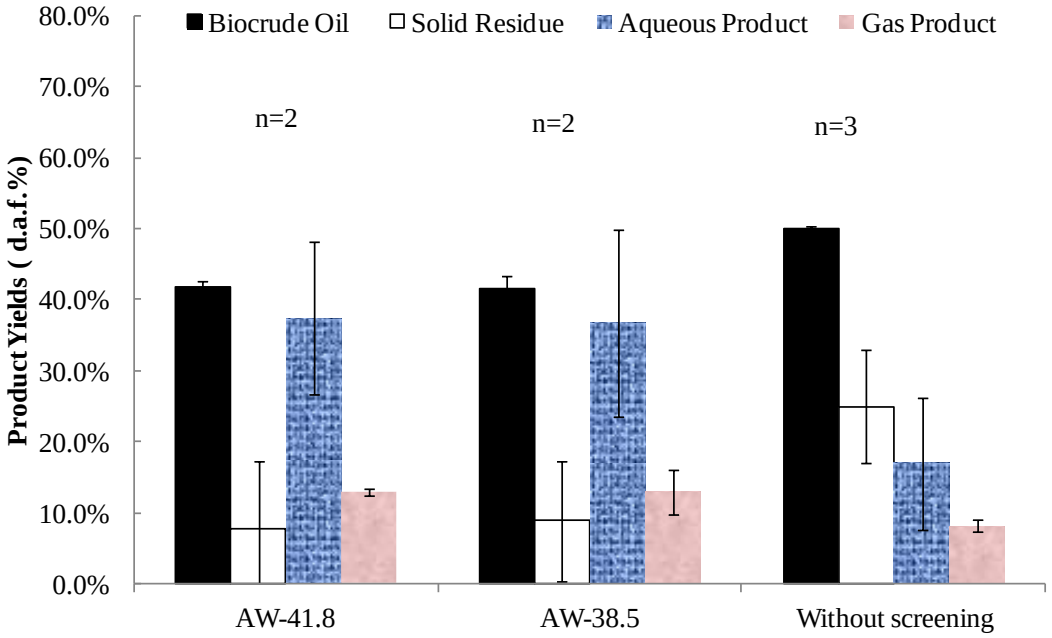


**Figure 6-1. HTL product yields of AW biomass with different ash content (dry ash free basis)**

## 6.2 Elemental Analysis of HTL Products Converted from AW Biomass with Different Ash content

Elemental compositions and the higher heating value (HHV) of biocrude oil converted from AW biomass with different ash content were summarized in Table 6-2. The carbon, hydrogen, nitrogen, and HHV of algal biocrude oil increased substantially as the ash content in the AW biomass decreased. By reducing the ash content in AW biomass and thus increasing the concentration of organic matter in the reactor, a higher degree of hydrolysis, fragmentation, and/or polymerization can be achieved (Akhtar & Amin, 2011). Further, the major components in the ash content of AW biomass, calcium carbonate, may adsorb hydrocarbons. Similar findings were found in a previous study of converting *Spirulina* with different concentrations of diatom frustules into biocrude oil via HTL (Zhang, 2014).

**Table 6-2. Elemental analysis and higher heating value (HHV) of biocrude oil converted at 300°C for a 60 minute reaction time from AW biomass with different ash content**

| Component (d.w.%) | Without screening | AW-41.8 | AW-38.5 |
|---|---|---|---|
| C | 59.4±0.1 | 64.1±0.1 | 68.9±0.5 |
| H | 7.79±0.03 | 8.21±0.01 | 8.51±0.06 |
| N | 2.50±0.2 | 4.27±0.01 | 5.08±0.01 |
| O[a] | 30.3 | 23.4 | 17.5 |
| H/C atomic ratio | 1.57 | 1.54 | 1.48 |
| O/C atomic ratio | 0.38 | 0.27 | 0.19 |
| N/C atomic ratio | 0.04 | 0.06 | 0.06 |
| Heating value (MJ/kg) | 25.8 | 29.2 | 32.3 |

[a]calculated by difference

Tracing the nutrient distributed in different HTL products helps understand whether the ash content adsorbed biocrude oil and had a negative impact on the biocrude oil quality. Figure 6-2 reveals that the ash content barely affect the carbon recovery in biocrude oil and other HTL products. On the contrary, the nitrogen recovery in biocrude oil was increased when the ash content decreased. As the ash content in AW biomass decreased from 53.3% to 38.5%, the nitrogen recovery in the solid residue increased from 11.4% to 18.2% while that in the aqueous product (and other losses) substantially reduced from 71.8% to 54.7%.

**(a)**

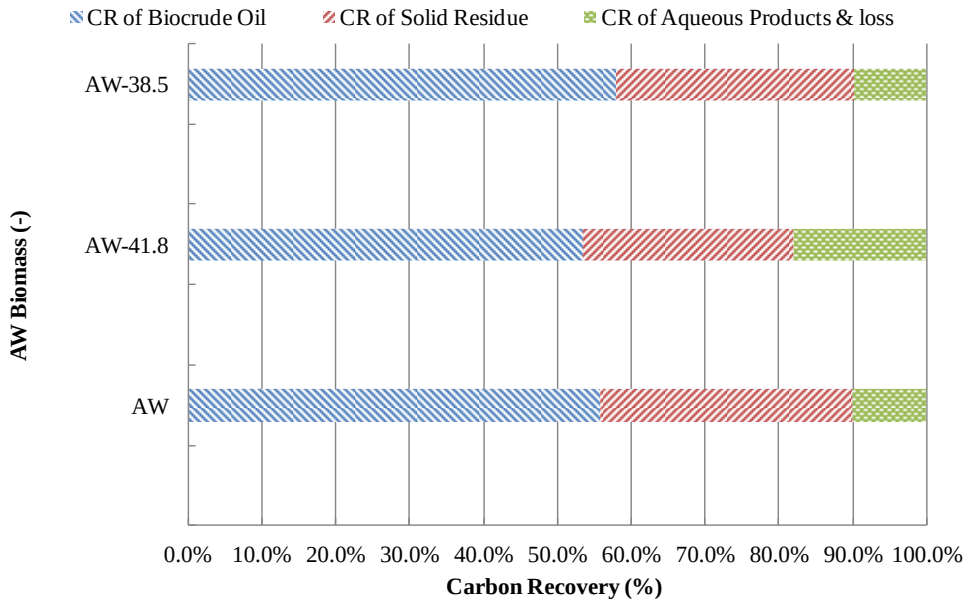


**(b)**

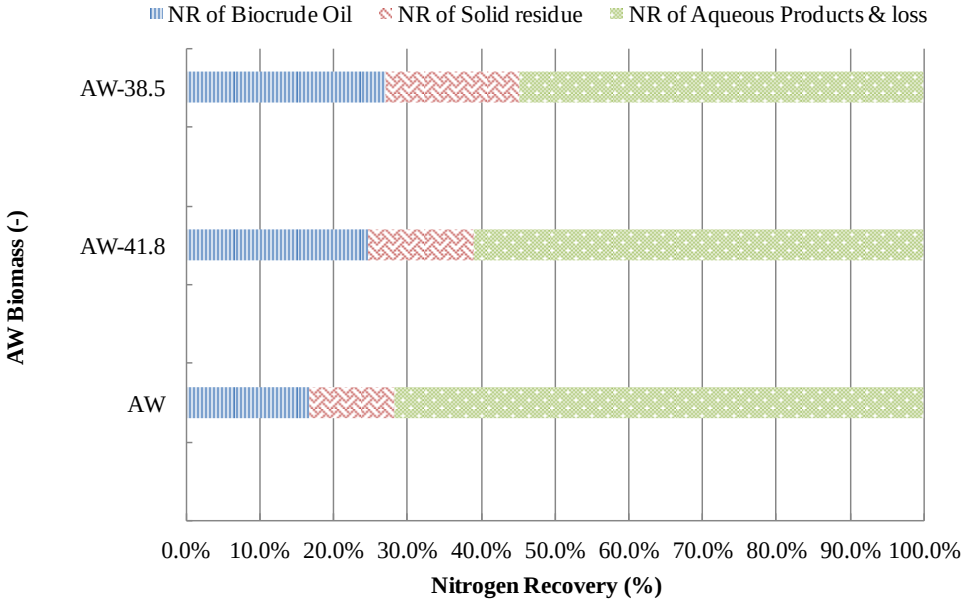


**Figure 6-2. (a) Carbon recovery (CR), and (b) nitrogen recovery (NR) distributed in different phases of HTL products converted from AW biomass with different ash content**

Under HTL processes, the major components in the ash content, calcium carbonate, would decompose into calcium ion and carbonate ion (equation 6-1). The carbonate ions then can react with ammonia, which was from deamination of amino acids degraded from proteins, and form ammonium carbonate (equation 6-2) (Chen et al., 2014c; Zhang, 2014). Upon heating,

ammonium carbonate would readily degrade to gaseous ammonia as well as carbon dioxide (equation 6-3) (Zapp et al., 2000). Thus, amino acids would be removed as ammonia and not be able to rejoin the reaction and contribute to the biocrude oil and/or solid residue formation. GC-MS results also demonstrated that the concentrations of amino acids (*e.g.*, glutamic acid) in HTL aqueous products substantially decreased when the ash content increased (details in **6.4**).

$$CaCO_3 \leftrightarrow Ca^{2+} + CO_3^{2-} \quad 6\text{-}1$$

$$CO_3^{2-} + 2\,NH_4^{+} \leftrightarrow (NH_4)_2CO_3 \quad 6\text{-}2$$

$$(NH_4)^2CO_3 \rightarrow NH_3 + CO_2 + H_2O \quad 6\text{-}3$$

### 6.3 Thermogravimetric Analysis (TGA) of Biocrude oil

TGA was performed to understand how the ash content changed the boiling point distribution of biocrude oil. The percentage of the weight loss and derivative weight loss of biocrude oil samples under thermogravimetric analysis were summarized in Figure 6-3 and Table 6-3. As the ash content reduced from 53.3% to 38.5% in AW biomass, the distilled fractions between 25-300°C in the algal biocrude oil increased from 32.2% to 53.4%. Increasing the concentration of organic matter in the reactor could lead to a higher degree of hydrolysis, fragmentation, and/or polymerization (Akhtar & Amin, 2011).

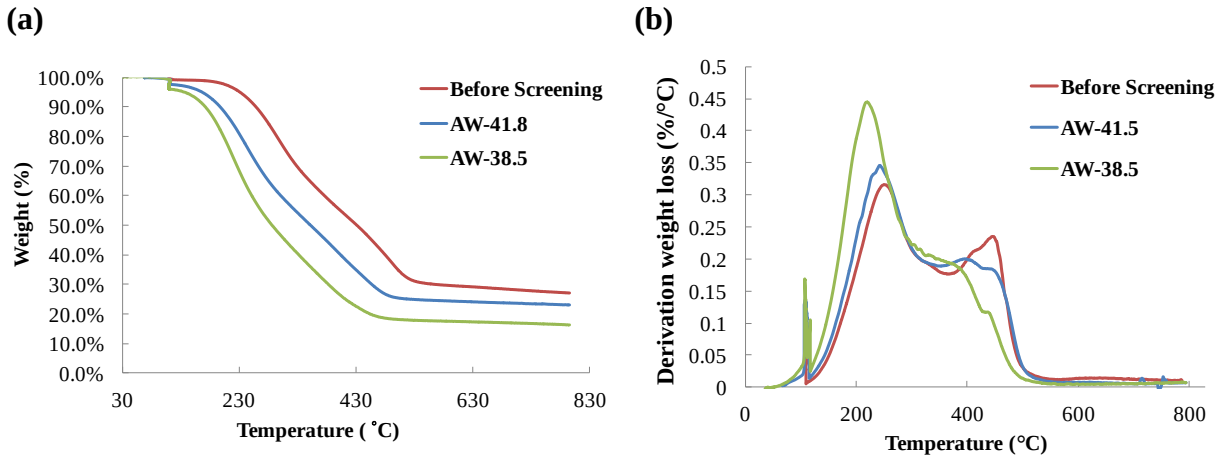


**Figure 6-3. (a) Thermogravimetric (TG) curves and (b) DTA curves of biocrude oil converted from AW biomass with different amounts of ash content via HTL at 300°C for 1 hour reaction time**

**Table 6-3. Boiling point distribution of bio-crude oil converted from AW biomass with different ash content (wt.%)**

| Distillate Range (°C) | Coke Oil Typical Application[a] | Without screening | AW-41.8 | AW-38.5 |
|---|---|---|---|---|
| 25-110 | Bottle gas and chemicals | 0.79 | 2.29 | 3.98 |
| 110-200 | Gasoline | 5.13 | 8.50 | 15.1 |
| 200-300 | Jet fuel & diesel oil | 26.3 | 29.2 | 34.3 |
| 300-400 | Lubricants & fuel for ships | 19.0 | 19.5 | 19.9 |
| 400-550 | Lubricants $ candles | 19.2 | 15.8 | 8.97 |
| 550-700 | Fuel for central heating | 1.91 | 1.04 | 0.78 |
| 700-800 | Asphalt and roofing | 1.03 | 0.60 | 0.64 |
| >800 | Residues | 26.7 | 23.1 | 16.3 |

[a] Adopted from Handbook of Petroleum Product Analysis (Speight & Speight, 2002)

### 6.4 GC-MS Analysis of Biocrude oil and Aqueous Products

GC-MS analysis was conducted to understand how ash content affect the chemical compositions of biocrude oil. The spectra of biocrude oil converted from AW biomass were listed in Figure 6-4 and the chemical compositions of biocrude oil were summarized in Table 6-4. Components characterized by GC-MS were categorized into several groups including phenols, oxygenates, hydrocarbons, amines/amides, and nitrogen-heterocyclic compounds. Compounds containing more than one functional group were classified into only one category. For example, hexadecanoic acid, pyrrolidide consists of both C=O and C-N functional groups and it was classified as nitrogen-heterocyclic compounds based on its chemical property. In addition, only a fraction of biocrude oil was identifiable by GC-MS, because the biocrude oil contained compounds with high molecular weights and high boiling points (Gai et al., 2014a; Vardon et al., 2011; Yu, 2012). Besides, some low boiling point compounds may be masked by the solvent peak or lost during evaporation of the organic solvent (*i.e.*, toluene) used to recover biocrude oil (Vardon et al., 2011).

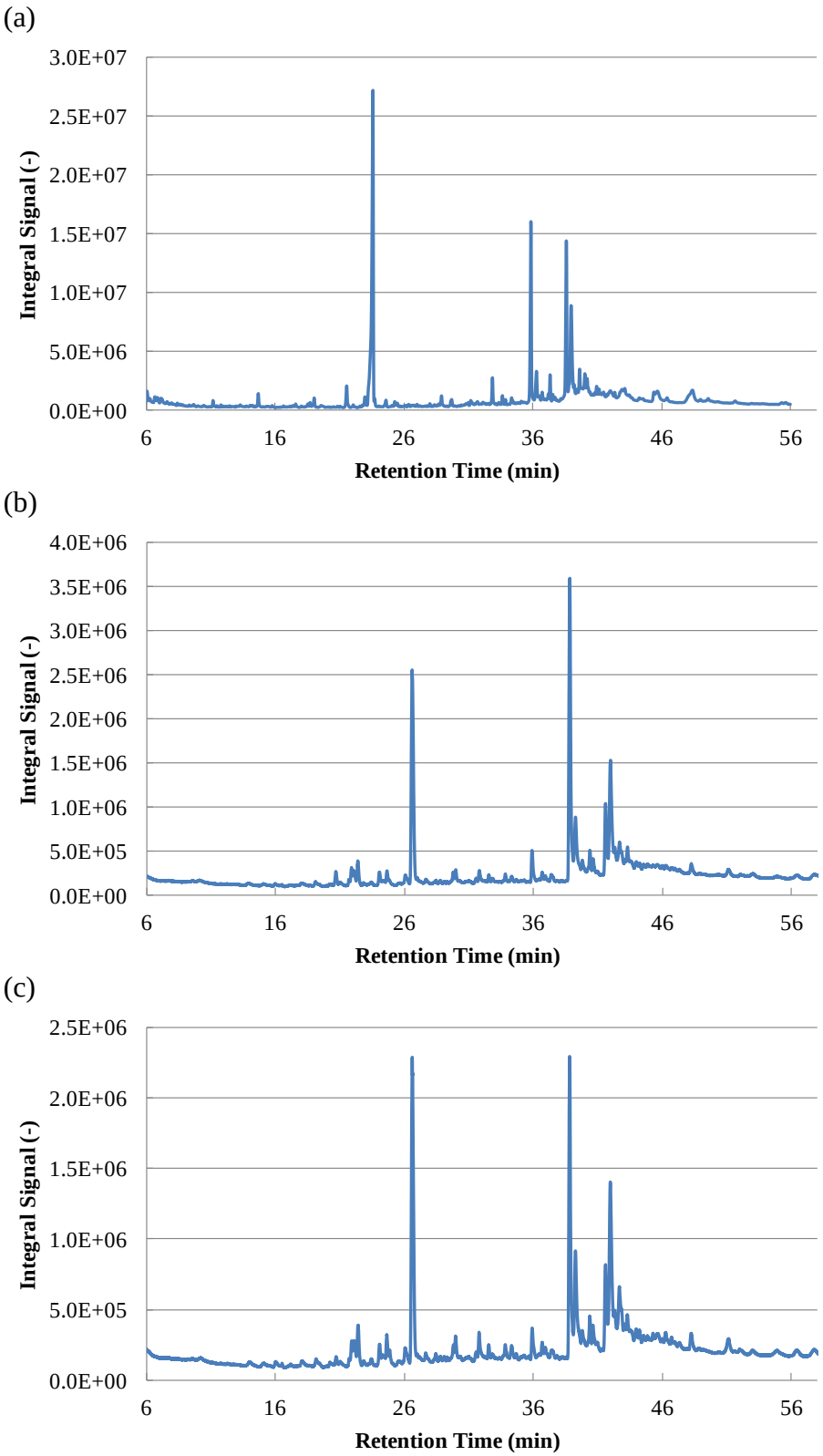


**Figure 6-4. Gas Chromatography (GC) spectra of biocrude oil converted from AW biomass (a) without screening, (b) AW-41.8, and (c) AW-38.5**

**Table 6-4. Normalized GC-MS signals of components identified in biocrude oil converted from AW biomass with different ash content; "×" indicates the chemical was not detected**

| Compound Name | Normalized Signal (-)[a] | | |
|---|---|---|---|
| | Before screening | AW-41.8 | AW-38.5 |
| **Esters, Alcohols & Aldehydes** | | | |
| Dodecanol | × | 0.10 | 0.10 |
| **Hydrocarbons** | | | |
| Trimethyl dodecane | 0.31 | × | × |
| Tridecane | 0.03 | × | × |
| Tetradecane | × | × | 0.01 |
| Hexadecane | 0.05 | × | × |
| Tetramethyl hexadecane | 0.03 | 0.45 | 0.33 |
| Heptadecane | × | 0.01 | 0.02 |
| **Phenol Derivatives** | | | |
| Phenol | 0.05 | 0.09 | 0.15 |
| Methyl phenol | 0.02 | 0.02 | 0.08 |
| Ethyl phenol | 0.01 | 0.01 | 0.03 |
| Di-t-butylphenol | × | 0.11 | 0.08 |
| **Amine/Amide Derivatives** | | | |
| Acetamide, N-(2-Phenyethyl)- | × | × | 0.03 |
| Hexadecanamide | 0.03 | 0.06 | 0.14 |
| Methyl Hexadecanamide | 0.04 | 0.13 | 0.13 |
| Dimethyl Hexadecanamide | 0.01 | 0.12 | 0.07 |
| Methyl Octadecanamide | 0.02 | 0.004 | 0.03 |
| **N-Heterocyclic Compounds** | | | |
| Indole | 0.02 | 0.08 | 0.15 |
| Methyl indole | 0.01 | 0.04 | 0.02 |
| Dimethyl indole | × | 0.04 | 0.06 |
| Hexadecanoic acid, pyrrolidide | × | 0.10 | 0.13 |
| 1-Methyl-5H-pyrido[4,3-b]indole | 0.02 | × | 0.002 |
| Hexanoic acid, morpholide | × | 0.04 | 0.03 |
| Cyclo(leucylpolyl) | × | × | 0.03 |
| **Fatty Acids** | | | |
| Tetradecanoic acid | 0.05 | 0.26 | 0.12 |
| Pentadecanoic acid | 0.01 | 0.02 | 0.03 |
| Hexadecanoic acid | 0.39 | 1.28 | 1.45 |
| Hexadecenoic acid | 0.08 | 0.28 | 0.40 |
| Octadecanoic acid | 0.34 | 0.34 | 0.30 |
| Octadecenoic acid | 0.27 | 0.83 | 1.54 |
| **Sterols** | | | |
| Stigmast-5-en-3-ol | 0.03 | × | × |
| Cholesta-3,5-diene | 0.03 | × | 0.02 |
| Stigmastanol | 0.03 | × | × |

[a]The normalized signal ($N_i$) is defined as the peak area of target compounds ($X_i$) divided by that of internal standard ($X_{is}$) (*i.e.*, $N_i=X_i/X_{IS}$).

Figure 6-5 demonstrates that the signals of fatty acids (Figure 6-5a), phenol derivatives (Figure 6-5b), n-heterocyclic compounds (Figure 6-5c), and amine/amide derivatives (Figure 6-5d) increased as the ash content in AW biomass decreased. For example, the normalized GC-MS signals of hexadecanoic acid (Figure 6-5a), indole (Figure 6-5c), and methyl hexadecanamides (Figure 6-5d) were increased by 3-4 times when the ash content reduced from 53.3% to 38.5% in AW biomass. This result indicated that a higher concentration of organic compounds in the reactor enhanced the degree of hydrolysis, fragmentation, and/or polymerization by reducing the ash content in the feedstock (Akhtar & Amin, 2011). In addition, the relative concentration of nitrogen-containing compounds, such as amine/amide derivatives and n-heterocyclic compounds, increased as the ash content decreased in AW biomass. Denitrogenation would be promoted if the ash content were increased in the feedstock, because the major component in the ash content, calcium carbonates, would react with nitrogen atoms from the deamination of proteins and prevent nitrogen to rejoin the HTL reaction to form amides/amines (Chen et al., 2014c; Zhang, 2014). Similar results were also found in previous reports of using CaO and frustules derived from mussel and diatom shells, respectively, as catalysts to convert biomass into biocrude oil under HTL (Tekin, 2015; Zhang, 2014).

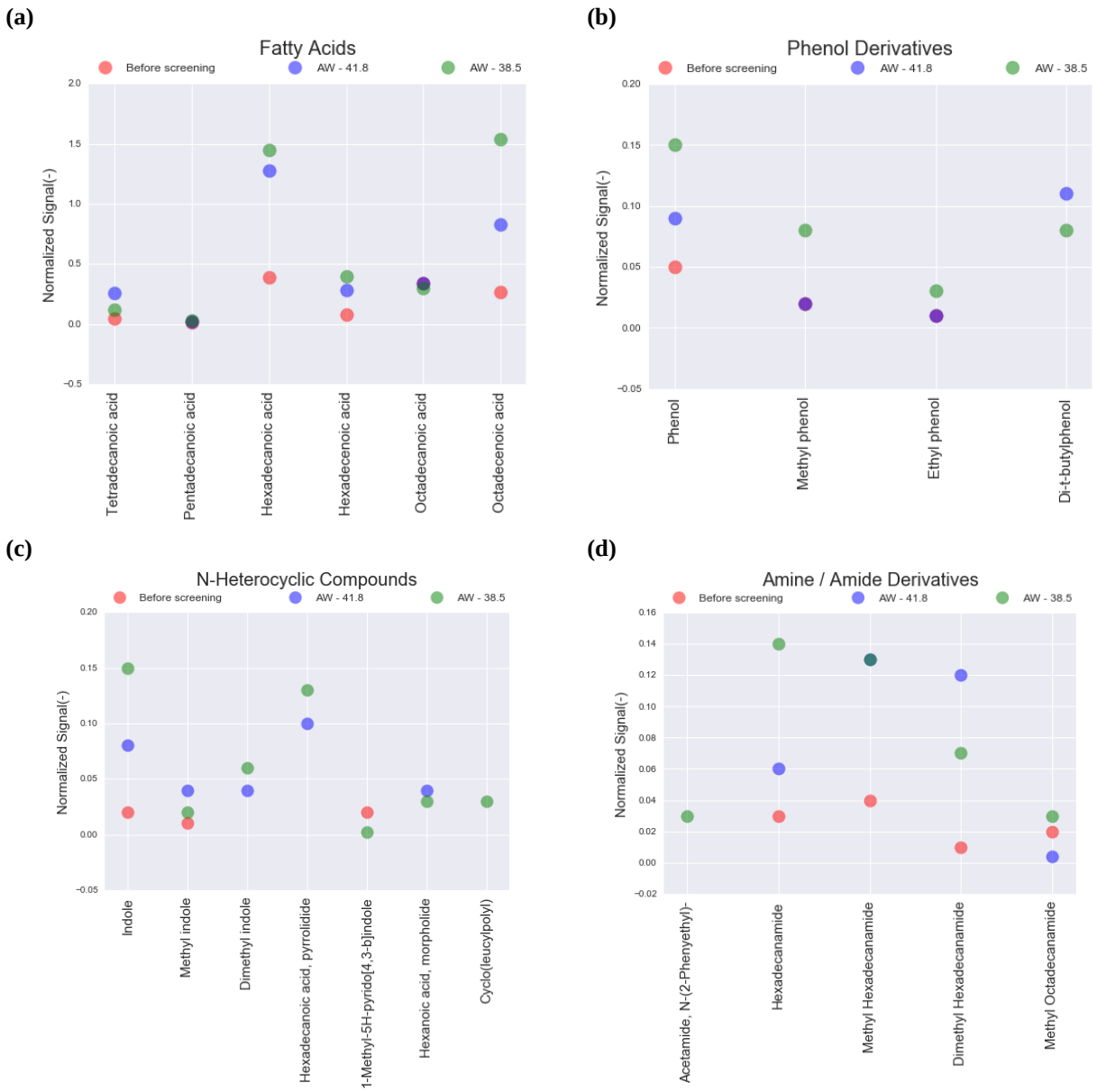


**Figure 6-5. Normalized GC-MS signals of (a) fatty acids, (b) phenol derivatives, (c) n-heterocyclic compounds, and (d) amine/amide derivatives identified in biocrude oil converted from AW biomass with different ash content**

Furthermore, the concentrations of hydrocarbons (Table 6-4) increased as the ash content increased in AW biomass. The ash content, calcium carbonates, can play a role as a catalyst during the HTL processes. High alkalinity was reported to promote the hydrolysis of polymers in cellulose and hemicelluloses by breaking glycosidic bonds and in lignin by cleavage of ester and ether bonds (Nazari et al., 2015; Zhang et al., 2011). Under alkaline treatment, the water-gas shift reaction can be accelerated with CO from cellulose/hemicelluloses decomposition and thus

favors $H_2$ and $CO_2$ formation, increasing the quality of the biocrude oil (Toor et al., 2011; Zhang, 2010). In addition, alkaline salts (*e.g.*, $K_2CO_3$) have a higher catalytic activity than their hydroxides (*e.g.*, KOH) (Karagöz et al., 2005; Wang et al., 2013). Carbonate ion (*i.e.*, $CO_3^{2-}$) from alkaline salts can further react with water and form bicarbonates, which can act as secondary catalysts and promote the water-gas shift reaction as described below (Sınağ et al., 2004; Sinag et al., 2003). Formate salts, $(HCOO^-)_2Ca^{2+}$, are formed as the alkali salt reacts with CO from the lignocellulose's degradation:

$$2CaCO_3+2H_2O \rightarrow Ca(HCO_3)_2+Ca(OH)_2 \quad 6\text{-}4$$

$$Ca(OH)_2+2CO \rightarrow (HCOO)_2Ca \quad 6\text{-}5$$

Hydrogen is obtained when formates react with water molecules.

$$(HCOO)_2Ca+2H_2O \rightarrow Ca(HCO_3)_2+2H_2 \quad 6\text{-}6$$

Then, $CO_2$ can be generated from $Ca(HCO_3)_2$.

$$2Ca(HCO_3)_2 \rightarrow 2H_2O+2CaCO_3+2CO_2 \quad 6\text{-}7$$

The overall reaction can be summarized as:

$$H_2O+CO \leftrightarrow HCOOH \leftrightarrow H_2+CO_2 \quad 6\text{-}8$$

With the promoted water-gas shift reaction, simultaneously, the decarboxylisation and/or hydrogenation of fatty acids may be more effective by providing a higher reductive environment in the HTL system (He et al., 2000a; Toor et al., 2011). For instance, Watanabe *et al.* studied the decomposition of stearic acid under HTL processes and improved the conversion of stearic acid to saturated alkanes from 2% to 32% by adding alkaline hydroxides as catalysts (Watanabe et al., 2006).

In order to further investigate how the ash content affect the compositions of HTL aqueous products and influence the reaction pathways under HTL processes, GC-MS analysis was conducted with the aqueous products converted from AW biomass with different ash content. The GC spectra of aqueous products converted from AW biomass with different ash content were listed in Figure 6-6 and the GC-MS characterization results were summarized in Table 6-5.

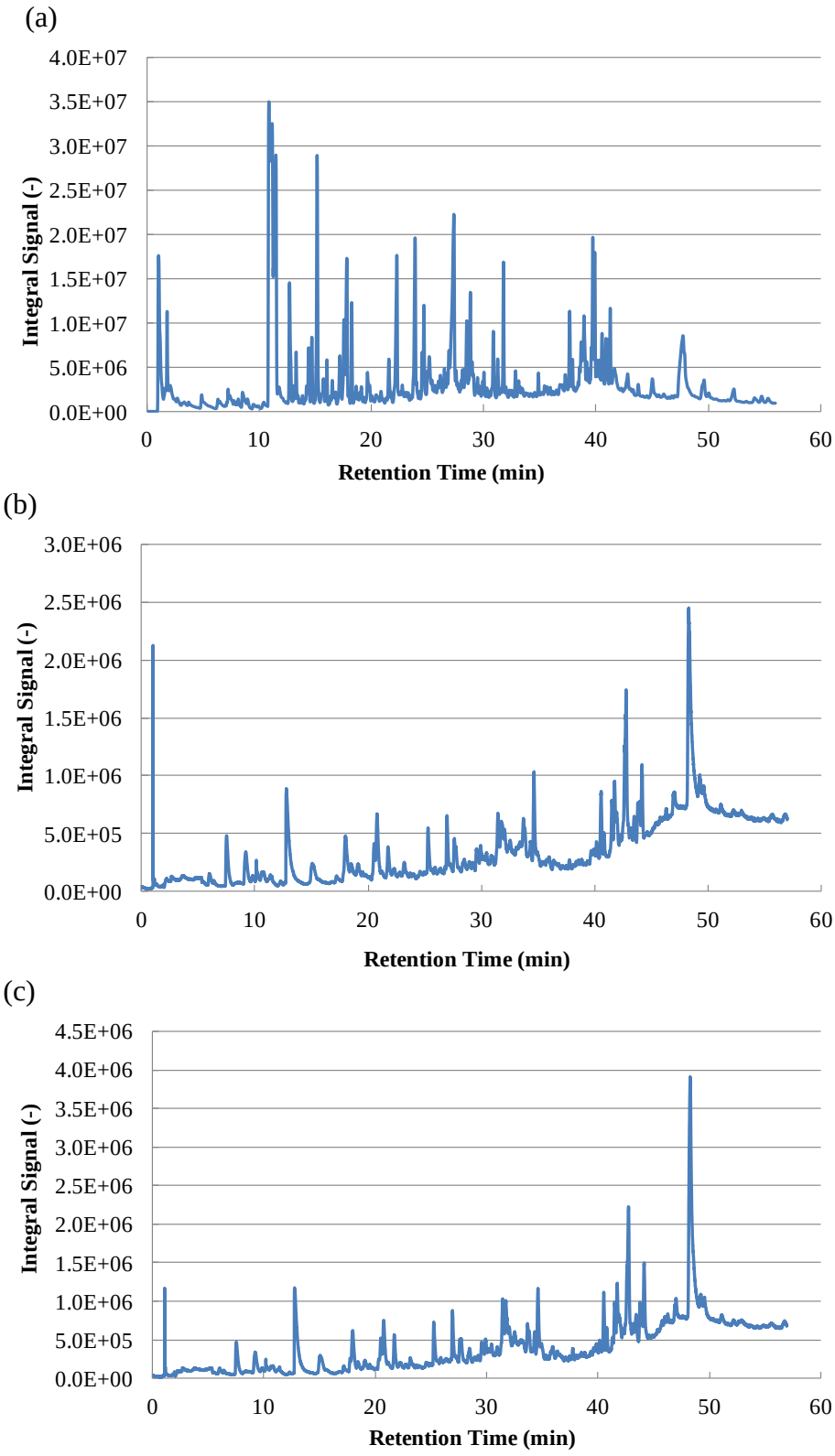


**Figure 6-6. Gas Chromatography (GC) spectra of aqueous products converted from AW biomass (a) without screening, (b) AW-41.8, and (c) AW-38.5**

**Table 6-5. Normalized GC-MS signals of components identified in the aqueous products converted from AW biomass with different ash content; "×" indicates the chemical was not detected**

| Compound Name | Normalized Signal (-)[a] | | |
|---|---|---|---|
| | Before screening | AW-41.8 | AW-38.5 |
| **Oxygenates** | | | |
| Acetic acid | 5.61 | 19.9 | 12.1 |
| Propanoic acid | 0.79 | 0.34 | 0.06 |
| Pentanoic acid | 0.05 | 0.32 | 0.41 |
| Benzeneacetic acid | 0.17 | 1.56 | 2.54 |
| Benzenepropanoic acid | 0.40 | 7.05 | 4.47 |
| Benzeneethanol, 4-hydroxy- | 0.09 | 1.88 | 0.94 |
| **Phenol Derivatives** | | | |
| Phenol | 0.13 | 0.57 | 0.49 |
| **Amine/Amide Derivatives** | | | |
| Trimethylamine | 0.04 | 4.53 | 1.21 |
| Acetamide, N-(2-phenylethyl)- | 0.12 | 2.77 | 1.80 |
| **N-Heterocyclic Compounds** | | | |
| Pyrazine, methyl | 0.08 | 9.62 | 4.87 |
| Pyrazine, ethyl | × | 1.74 | 0.51 |
| Pyrrolidinone, methyl- | 0.30 | 0.17 | 0.08 |
| Pyrrolidine, acetyl | 0.38 | 4.45 | 3.71 |
| Pyrrolidinone | 0.95 | 8.89 | 5.80 |
| Piperidinone | 0.81 | 11.6 | 6.80 |
| Hydroxypyridine,dimethyl | 0.06 | 1.64 | 1.06 |
| Pyridinol, methyl | 0.34 | 3.27 | 1.73 |
| Pyridinol | 0.23 | 2.52 | 3.72 |
| 3,6-Diisopropylpiperazin-2,5-dione | 0.57 | 22.7 | 15.5 |
| Cyclo(leucylprolyl) | 0.62 | 6.86 | 5.82 |

[a]The normalized signal ($N_i$) is defined as the peak area of target compounds ($X_i$) divided by that of internal standard ($X_{is}$) (*i.e.*, $N_i=X_i/X_{IS}$).

Figure 6-7 shows that the HTL aqueous product from AW with lower ash content had higher concentrations of n-heterocyclic compounds (Figure 6-7a), oxygenates and phenols (Figure 6-7b) than those from AW biomass with higher ash content. For example, Figure 6-7a demonstrated that the aqueous products with lower ash content contained 27-40 times of 3,6-Diisopropylpiperazin-2,5-dione, indicating that more proteins were reacted by reducing the ash content in the algal feedstock (Chen et al., 2014c; Gai et al., 2015). Another example is that the concentrations of acetic acid (Figure 6-7b) increased by 2-4 times when the ash content decreased by 20-25% in AW biomass.

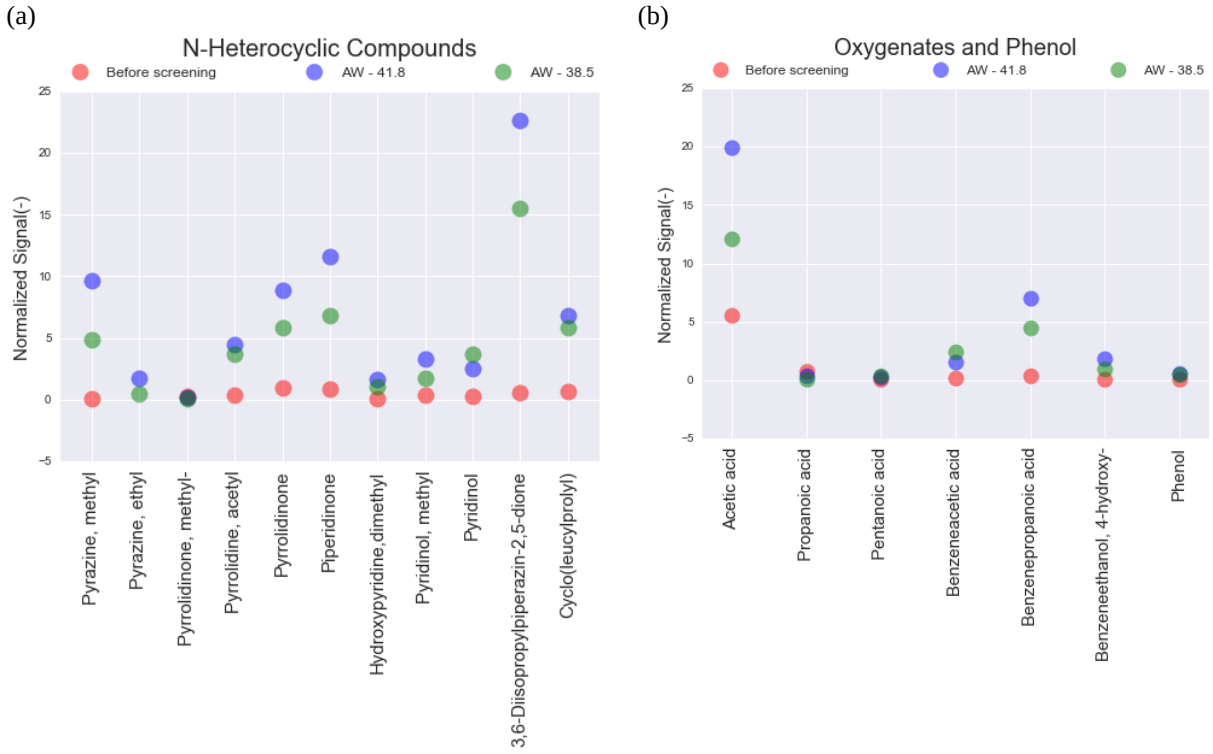


**Figure 6-7. Normalized GC-MS signals of (a) n-heterocyclic compounds and (b) oxygenates and phenol derivatives identified in the aqueous products converted from AW biomass with different ash content**

### 6.5 HTL of Model Algae with the Addition of Ash content

Based on the results obtained from 6.1-6.4 in this chapter, it was hypothesized that algal biomass with certain amounts of ash content can be converted into reasonable quality and quantity of biocrude oil. In order to study the range of ash content where it may present a positive effect on the biocrude oil yield or quality, HTL tests with model algae and representative ash content were conducted at the same reaction condition. *Chlorella* was selected as the model algae because it contains few amounts of ash content (5-6%) and can be cultured in a wastewater environment (Yu et al., 2011b; Zhou et al., 2013). Eggshells were used as representative ash content since they are mainly composed of calcium carbonates (95-97%) and physicochemically similar to the major ash content (*i.e.*, snail shell) in AW biomass (Chen et al., 2012; Hunton, 2005). HTL tests of *Chlorella* with 0%, 27.5%, 35%, and 40% of eggshells were carried out to simulate the amounts of the major ash content (calcium carbonates) in AW biomass with and without the screen pretreatment. Figure 6-8 summarizes the HTL product yields (dry ash free basis) converted from *Chlorella* with different amounts of eggshells. Similar to Figure 6-1,

Figure 6-8 validated the previous hypothesis that the algal biomass with certain amounts of ash content can be converted into biocrude oil with a reasonable quantity. On the other hand, as the ash content increased in the algal feedstock, the solid residue yield increased while the gas product yield decreased.

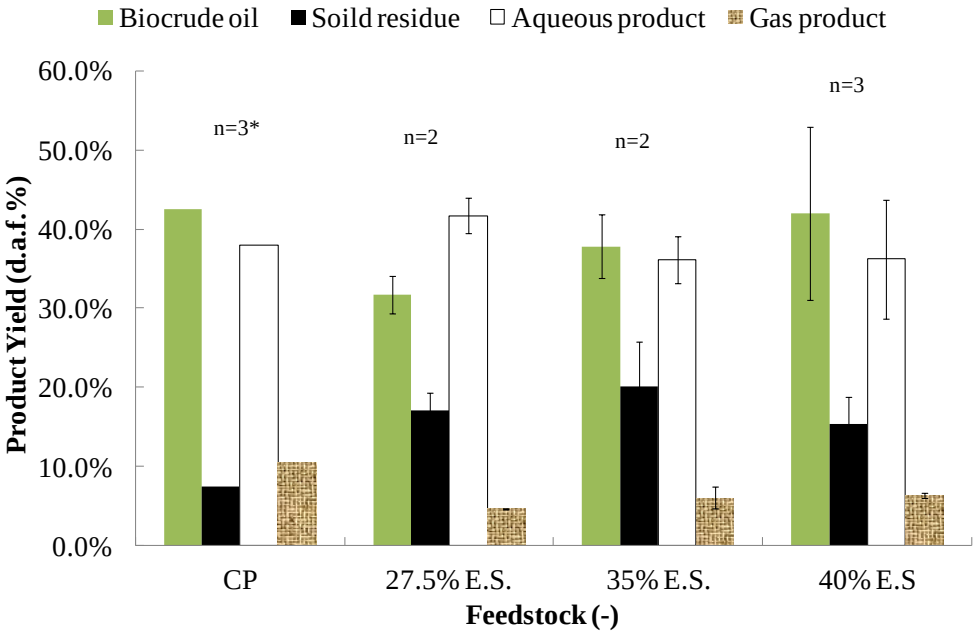


**Figure 6-8. The effect of different amounts of ash content on HTL conversion of *Chlorella* (CP) (*Product yields from CP are adopted from previous studies (Gai et al., 2014a; Gai et al., 2015) at the same reaction condition)**

Table 6-6 demonstrated the elemental compositions and HHV of biocrude oil converted from *Chlorella* with different amounts of ash content. Table 6-6 showed that the contents of carbon, hydrogen, and nitrogen in the biocrude oil decreased as the ash content in the feedstock increased. Notably, as the addition of eggshells increased from 35 wt.% to 40 wt.%, the contents of carbon, hydrogen, and nitrogen as well as the heating value of the biocrude oil substantially decreased. A similar trend was also present in Table 6-2—when the ash content in the algal feedstock was below about 40 wt.%, the contents of carbon, hydrogen, and nitrogen as well as the heating value of the algal biocrude oil were significantly increased.

**Table 6-6. Elemental compositions of biocrude oil converted from *Chlorella* (CP) with different amounts of ash content via HTL at 300°C for a 60 minute reaction time**

| Property | CP | CP+27.5% Egg Shell | CP+35% Egg Shell | CP+40% Egg Shell |
|---|---|---|---|---|
| C (wt.%) | 75.9±0.05 | 72.3±0.01 | 72.3±1.5 | 58.7±0.3 |
| H (wt.%) | 9.55±0.01 | 9.33±0.1 | 8.87±0.2 | 7.03±0.2 |
| N (wt.%) | 6.07±0.1 | 5.02±0.1 | 5.04±0.3 | 3.59±0.02 |
| O (wt.%)[a] | 8.47 | 13.3 | 13.8 | 30.7 |
| HHV (MJ/kg) | 37.8 | 35.4 | 34.6 | 24.4 |
| Ash content in the algal feedstock (wt.%) | 5.70 | 33.2 | 40.7 | 45.7 |
| Calcium in the algal feedstock (wt.%) | 0.23 | 11.2 | 14.2 | 16.2 |

[a]calculated by difference

Thermogravimetric analysis of the biocrude oil converted from *Chlorella* with different amounts of ash content was also conducted. Figure 6-9 and Table 6-7 showed that the addition of the ash content reduced the amount of light components in the resulting algal biocrude oil.

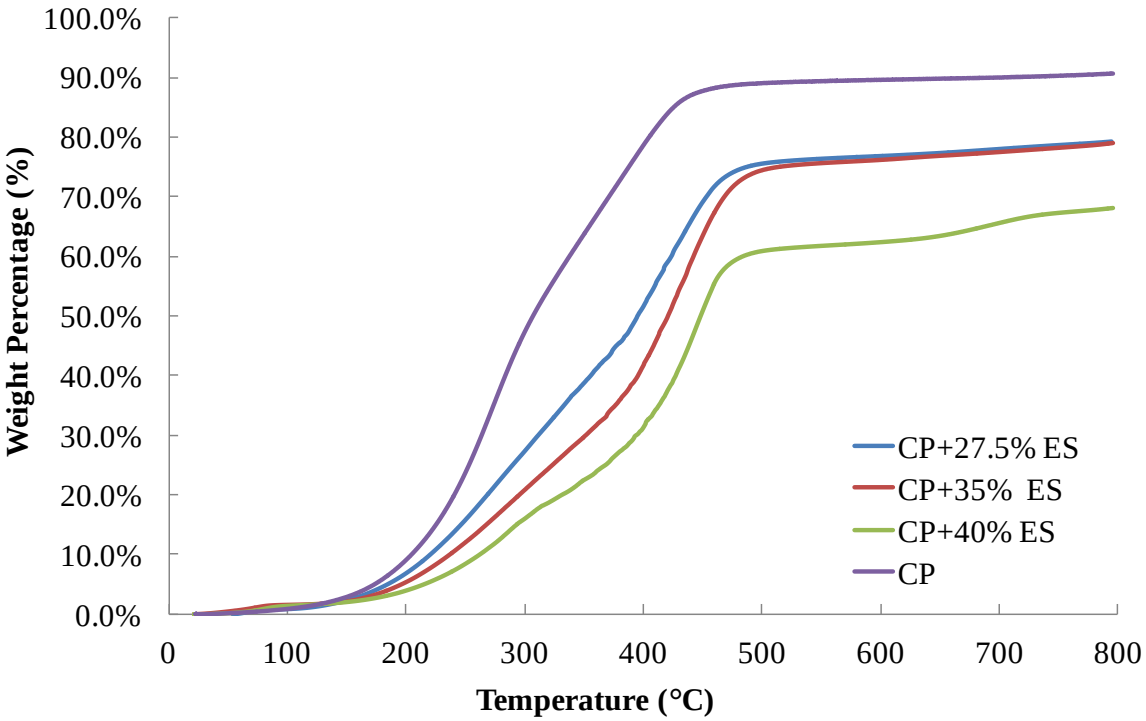


**Figure 6-9. Thermogravimetric analysis (TGA) of biocrude oil converted with different amounts of ash content and Chlorella via HTL at 300°C for 1 hour reaction time**

**Table 6-7. Boiling point distribution of biocrude oil converted with different amounts of ash content and *Chlorella* via HTL at 300°C for 1 hour reaction time (d.w.%)**

| Distillate Range (°C) | Coke Oil Typical Application[a] | CP | 27.5% E.S. | 35% E.S. | 40% E.S. |
|---|---|---|---|---|---|
| 25-110 | Bottle gas and chemicals | 1.08 | 1.00 | 1.63 | 1.52 |
| 110-200 | Gasoline | 7.95 | 5.89 | 3.80 | 2.50 |
| 200-300 | Jet fuel & diesel oil | 38.2 | 20.5 | 15.5 | 12.1 |
| 300-400 | Lubricants & fuel for ships | 31.3 | 24.2 | 20.9 | 15.4 |
| 400-550 | Lubricants $ candles | 10.8 | 24.7 | 33.9 | 30.3 |
| 550-700 | Fuel for central heating | 0.60 | 1.63 | 1.47 | 2.39 |
| 700-800 | Asphalt and roofing | 0.66 | 1.25 | 0.40 | 1.45 |
| >800 | Residues | 9.44 | 20.8 | 22.4 | 33.3 |

[a] Adopted from Handbook of Petroleum Product Analysis (Speight & Speight, 2002)

GC-MS analyses of biocrude oil converted from *Chlorella* with different amounts of ash content were conducted to verify if the addition of eggshells would promote the denitrogeantion and catalyze the formation of hydrocarbons under HTL processes. The spectra of biocrude oil converted from *Chlorella* with different amounts of ash content were included in Figure 6-10 and the chemical compositions of biocrude oil were exhibited in Table 6-8.

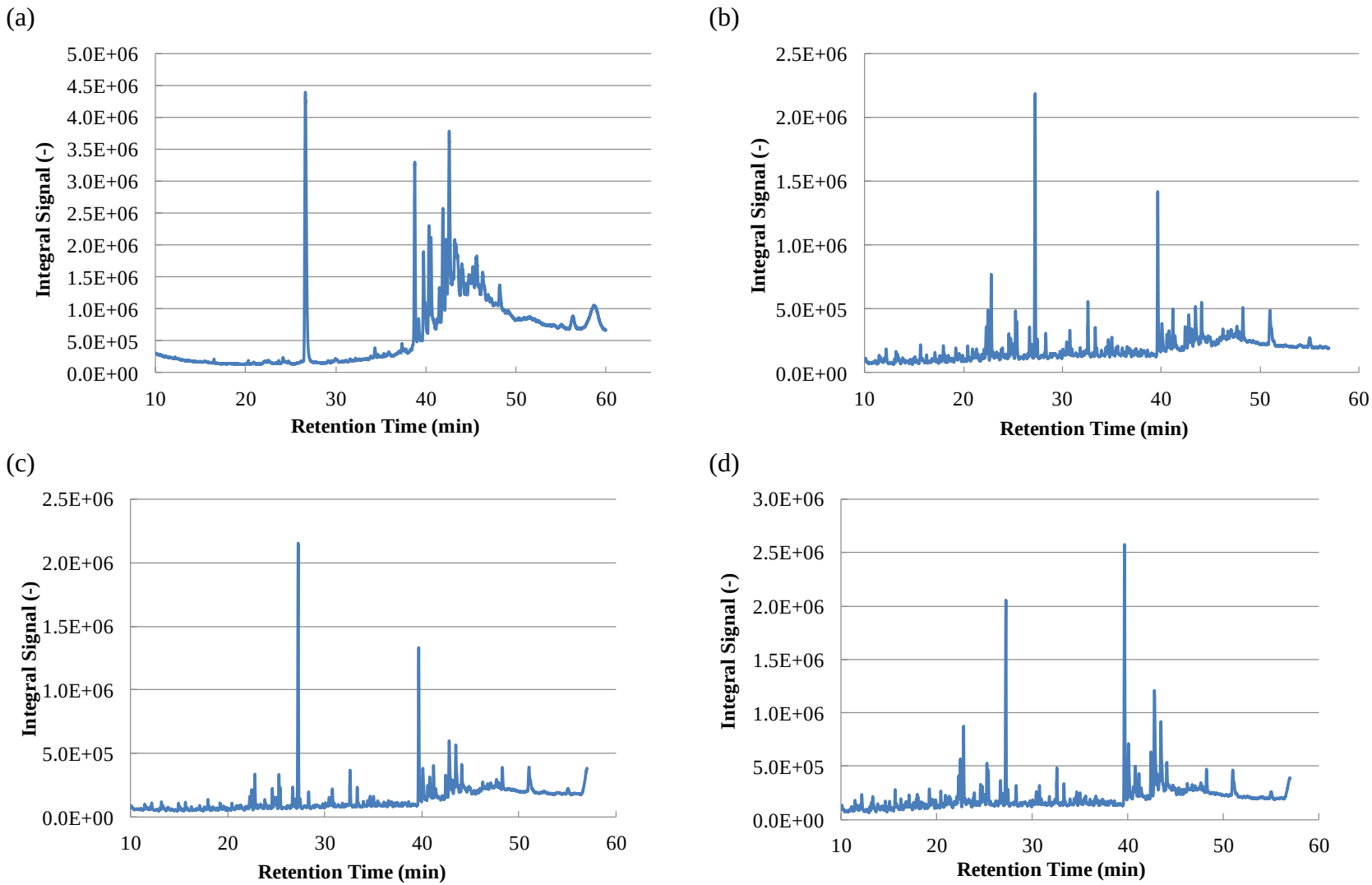


**Figure 6-10. Gas Chromatography (GC) spectra of biocrude oil converted from *Chlorella* with (a) 0%, (b) 27.5%, (c) 35%, and (d) 40% egg shell**

**Table 6-8. Normalized GC-MS signals of components identified in biocrude oil converted from *Chlorella* with different amounts of eggshells (E.S.); "×" indicates the chemical was not detected**

| Compound Name | Normalized Signal (-)[a] | | | |
|---|---|---|---|---|
| | 0% E.S. | 27.5% E.S. | 35% E.S. | 40% E.S. |
| **Hydrocarbons** | | | | |
| Tetradecene | × | 0.04 | 0.03 | 0.04 |
| Pentadecane | 0.01 | 0.01 | 0.02 | 0.02 |
| Pentadecene | 0.11 | × | × | × |
| Hexadecene | × | 0.05 | 0.03 | 0.05 |
| Tetramethyl hexadecane | 0.81 | 0.59 | 0.24 | 0.74 |
| Heptadecane | × | 0.05 | 0.02 | 0.09 |
| Nonadecene | × | 0.05 | 0.02 | 0.07 |
| **Phenol Derivatives** | | | | |
| Phenol | 0.53 | 0.20 | 0.13 | 0.21 |
| Methyl phenol | 0.41 | 0.18 | 0.03 | 0.11 |
| Ethyl phenol | 0.16 | 0.13 | 0.05 | 0.09 |
| Di-t-butylphenol | × | 0.09 | 0.05 | 0.08 |
| **Amides/Amines** | | | | |
| Hexadecanamide | 1.06 | × | × | × |
| Methyl hexadecanamide | 0.93 | 0.15 | 0.12 | 0.09 |
| Octadecanamide | 0.23 | × | × | × |
| Octadecenamide | 0.37 | × | × | × |
| Dimethyl octadecanamide | 0.69 | × | × | × |
| Butyl octadecanamide | 0.65 | × | × | × |
| Hydroxyethyl octadecanamide | 0.26 | × | × | × |
| Dimethyl nonenamide | 0.27 | × | × | × |
| Methyl dodecanamide | 0.20 | × | × | × |
| Oleic diethanolamide | 0.21 | × | × | × |
| Hydroxyethyl succinimide | 0.13 | × | × | × |
| Heptynonylamine | 0.11 | × | × | × |
| Hydroxycyclododecanimine | 0.28 | × | × | × |
| Trimethyl benzonitrile | 0.23 | × | × | × |
| **N-Heterocyclic Compounds** | | | | |
| Indole | 0.20 | 0.21 | 0.13 | 0.19 |
| Methyl indole | 0.14 | 0.11 | 0.06 | 0.11 |
| Ethyl-methyl, pyrazine | 0.19 | 0.09 | 0.05 | 0.06 |
| Hexadecanoic acid, pyrrolidide | 0.82 | 0.15 | 0.09 | 0.13 |
| Diphenyl (methoxyphenyl)pyrrole | 0.68 | × | × | × |
| 9H-Pyrido[3,4-b]indole | 0.34 | × | × | × |
| **Acids, Alcohols, Aldehydes, Esters** | | | | |
| Dodecyl acrylate | × | 0.04 | 0.03 | 0.03 |
| Hexadecanol | × | 0.03 | 0.01 | 0.03 |
| Tetramethyl hexadecenol | 0.03 | 0.11 | 0.05 | 0.14 |
| Hexadecanoic acid | 0.49 | 0.67 | 0.60 | 1.35 |
| Hexadecenoic acid | × | 0.07 | 0.06 | 0.29 |
| Octadecanoic acid | × | 0.06 | 0.08 | 0.22 |
| Octadecenoic acid | × | 0.06 | 0.09 | 0.59 |
| Octadecadienoic acid | × | 0.18 | 0.27 | 0.34 |
| Diethylene glycol dibenzoate | × | 0.18 | 0.09 | 0.10 |

[a]The normalized signal ($N_i$) is defined as the peak area of target compounds ($X_i$) divided by that of internal standard ($X_{is}$) (*i.e.*, $N_i=X_i/X_{IS}$).

Compounds identified by GC-MS were grouped into several categories such as amides/amines. Figure 6-11 demonstrates that the relative concentrations of n-heterocyclic compounds (Figure 6-11a) and amides/amines (Figure 6-11b) reduced as eggshells increased in the algal feedstock, confirming that the addition of calcium carbonates can promote denitrogenation under HTL processes. For example, fourteen kinds of amines/amides were identified in the algal biocrude converted from *Chlorella* while only one amide (*i.e.*, methyl hexadecanamide) was detected after eggshells were added in the HTL feedstock (Figure 6-11b). On the other hand, it is noted that increasing the addition of eggshells cannot greatly enhance the denitrogenation efficacy. For instance, the normalized signal of hexadecanoic acid, pyrrolidide ((Figure 6-11a) was reduced from 0.82 to 0.09 and back to 0.13, as the addition of eggshells increased from 0 wt.% to 35 wt.% and to 40 wt.%. Similar trend occurred on the catalytic formation of hydrocarbons under HTL processes. For example, the normalized signal of tetradecene was kept constant as 0.04 when the addition of eggshells increased from 27.5 wt.% to 40 wt.% ((Table 6-8). Comparable results were also reported when using CaO catalysts derived from mussel shells to convert olive seeds into bio-oil under HTL processes (Tekin, 2015). In short, the addition of eggshells can promote the denitrogeantion and catalyze the formation of hydrocarbons, but increasing the amount of calcium carbonates can barely enhance the efficacy of denitrogenation and catalytic formation of hydrocarbons under HTL processes.

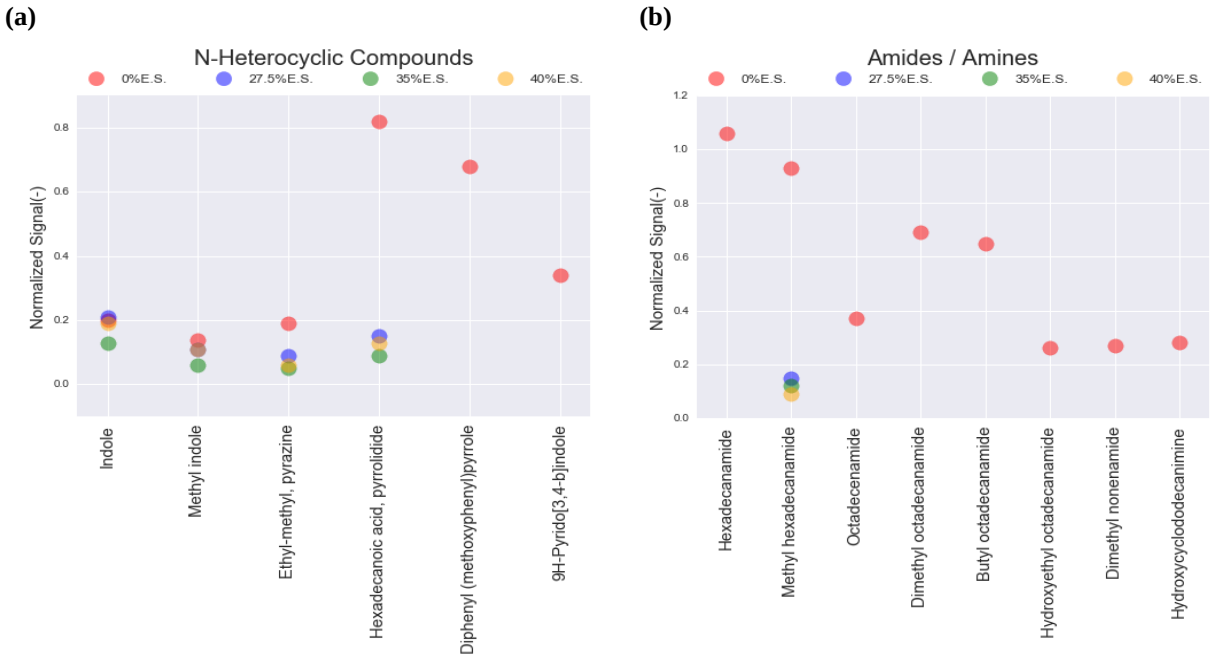


**Figure 6-11. Normalized GC-MS signals of (a) n-heterocyclic compounds and (b) amides/amines identified in biocrude oil converted from *Chlorella* with different amounts of eggshells (E.S.)**

In order to examine if the addition of ash content can help mitigate recalcitrant compounds in the HTL aqueous products, GC-MS analysis was performed with the aqueous products converted from *Chlorella* with different amounts of eggshells. The GC spectra of aqueous products converted from *Chlorella* with different amounts of eggshells were also available in Figure 6-12. GC-MS characterization results were included in Table 6-9, which demonstrated that lower concentrations of nitrogen-heterocyclic compounds, phenols, and oxygenates were measured in the HTL aqueous products converted from *Chlorella* with higher ash content. For example, Table 6-9 showed that the aqueous products with 27.5-40 wt.% of eggshells contained 3-4 times lower amount of pyrrolidinone.

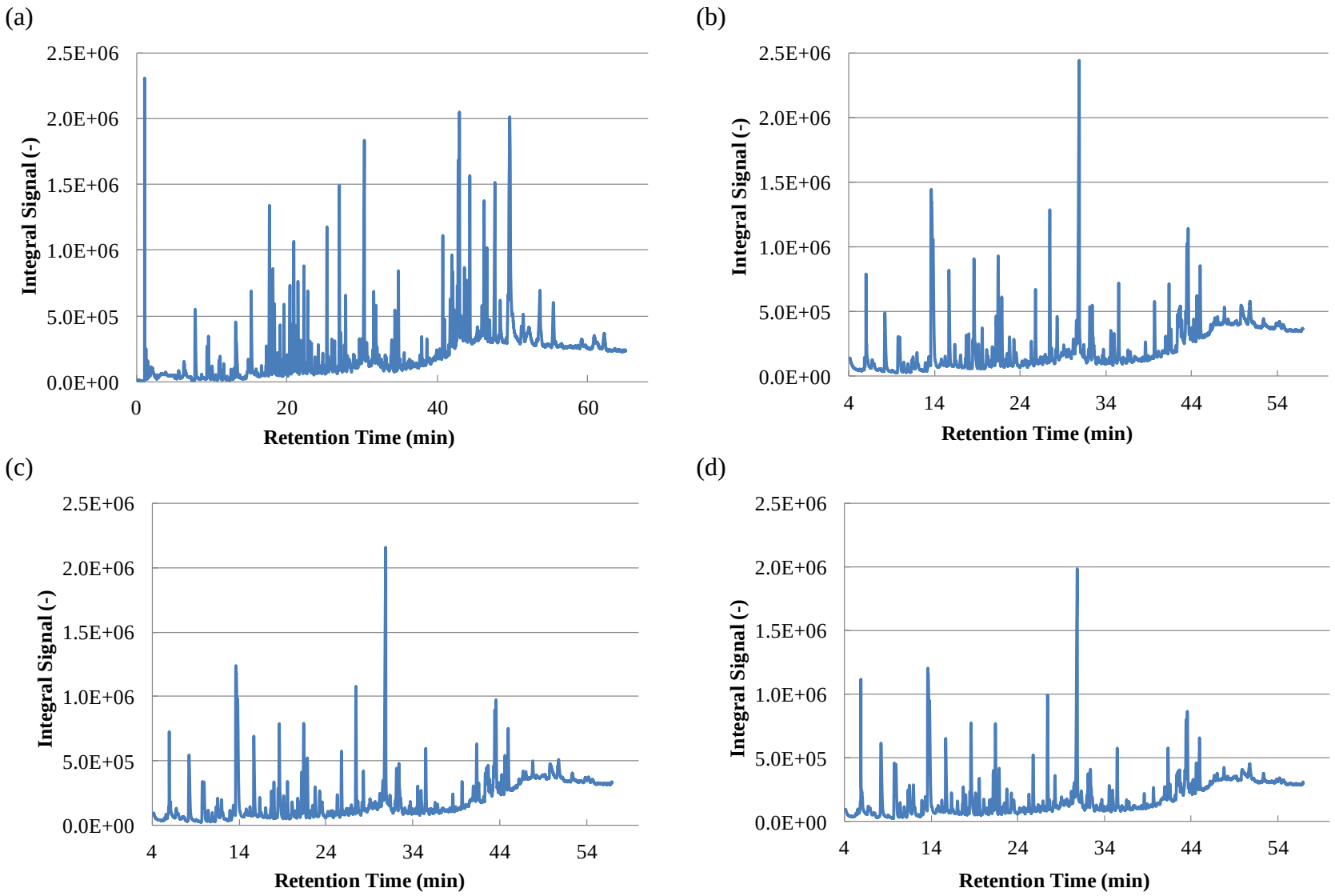


**Figure 6-12. Gas Chromatography (GC) spectra of aqueous products converted from *Chlorella* with (a) 0%, (b) 27.5%, (c) 35%, and (d) 40% egg shell**

**Table 6-9. Normalized GC-MS signals of components identified in aqueous products converted from *Chlorella* with different amounts of eggshells (E.S.); "×" indicates the chemical was not detected**

| Compound Name | Normalized Signal (-) [a] | | | |
|---|---|---|---|---|
| | 0% E.S. | 27.5% E.S. | 35% E.S. | 40% E.S. |
| **Phenol Derivatives** | | | | |
| Phenol | 0.23 | 0.22 | 0.21 | 0.18 |
| Methyl phenol | 0.06 | × | 0.07 | 0.05 |
| Dimethylamino phenol | × | 0.09 | 0.09 | 0.08 |
| Amino phenol | × | 0.25 | 0.16 | 0.10 |
| Ethoxy methoxyphenol | 0.89 | × | × | × |
| **Amides/Amines** | | | | |
| Methyl acetamide | × | 0.31 | 0.38 | 0.17 |
| Acetamide | × | 0.17 | 0.18 | 0.13 |
| Phenylmethyl acetamide | 0.19 | 0.31 | 0.30 | 0.23 |
| Tyramines | 0.32 | 0.19 | 0.10 | 0.06 |
| **N-Heterocyclic Compounds** | | | | |
| Pyrazine | 0.02 | 0.03 | 0.05 | 0.14 |
| Methyl pyrazine | 1.10 | 0.78 | 1.11 | 1.07 |
| Dimethyl, pyrazine | 0.57 | 0.59 | 0.74 | 0.94 |
| Ethyl methyl pyrazine | 0.29 | 0.28 | 0.53 | 0.50 |
| Methyl pyrrolidinone | × | 0.29 | 0.33 | 0.23 |
| Ethyl pyrrolidinone | 0.32 | × | 0.23 | 0.22 |
| Methyl pyrrolidinedione | 1.12 | 0.24 | × | 0.19 |
| Pyrrolidinone | 2.01 | 0.74 | 0.74 | 0.59 |
| Piperidinone | 2.53 | 1.58 | 1.53 | 1.23 |
| Caprolactam | 0.99 | 0.62 | 0.67 | 0.51 |
| Pyridinol | 0.83 | 0.59 | 0.58 | 0.46 |
| Methyl pyridinol | 0.94 | 0.43 | 0.15 | 0.37 |
| Butyl hydantoin | 0.58 | 0.29 | 0.28 | 0.23 |
| Cyclo(leucylprolyl) | 2.38 | 1.24 | 1.23 | 1.59 |
| Prolines | 4.16 | 0.72 | 0.16 | 0.26 |
| 5,10-Diethoxy-2,3,7,8-tetrahydro-1H,6H-dipyrrolo[1,2-a;1',2'-d]pyrazine | 2.40 | 0.71 | 0.67 | 0.55 |
| **Acids, Alcohols, Aldehydes, Esters** | | | | |
| Methyl cyclopentenone | 0.12 | 0.09 | 0.11 | × |
| Dimethyl cyclopentenone | × | 0.09 | 0.10 | 0.13 |
| Acetic acid | 0.86 | 2.95 | 2.48 | 2.34 |
| Propanoic acid | 1.16 | 0.98 | 1.00 | 0.86 |
| Methyl propanoic acid | 0.09 | 0.19 | 0.18 | 0.19 |
| Butanoic acid | 0.34 | 0.30 | 0.32 | 0.26 |
| Pentanoic acid | × | 0.15 | 0.12 | 0.11 |
| Methyl pentanoic acid | 2.15 | 0.86 | 1.00 | 0.85 |
| Hexanoic acid | × | 0.44 | 0.41 | 0.34 |
| Benzeneacetic acid | 0.34 | 0.31 | 0.30 | 0.23 |
| Benzenpropanoic acid | 1.35 | 0.78 | 0.73 | 0.59 |
| Glycerol | 2.57 | 2.78 | 2.89 | 2.60 |

[a] The normalized signal ($N_i$) is defined as the peak area of target compounds ($X_i$) divided by that of internal standard ($X_{is}$) (*i.e.*, $N_i=X_i/X_{IS}$).

### 6.6 The Effect of Ash content under Hydrothermal Liquefaction Processes

The ash content in algal biomass would reduce the total solid content of the feedstock, which is one of the important parameters affecting the biocrude oil yield and the quality of biocrude oil (Akhtar & Amin, 2011; Gai et al., 2014a; Tian et al., 2014). Several previous studies have demonstrated that when the total solid content in HTL feedstock (*e.g.,* swine manure and *Chlorella*) was lower than 15 wt.%, significantly low biocrude oil yields (<10 wt.%) were obtained (He et al., 2001b; Zhang et al., 2013b). Analogous to the micellization processes (Equation 6-9), the formation of biocrude oil may also require a specific concentration of volatile solid content (Equation 6-10) (Balat, 2008; Demirbaş, 2000b; Havre, 2002; He et al., 2001b; Zhang et al., 2013b). Micelle ($M_n$) forms when the concentration of surfactants ([M]) reaches the critical micelle concentration (CMC). Likewise, assuming that the concentration of the volatile solid content in feedstock is [V], the biocrude oil ($V_n$) can be produced once [V] achieves the threshold concentration—critical volatile content concentration (CVC). In other words, if [V] is too small, the biocrude oil formation would not happen under batch HTL (He et al., 2001b).

$$nM \leftrightarrow M_n \qquad 6\text{-}9$$

$$nV \leftrightarrow V_n \qquad 6\text{-}10$$

Therefore, the ash content can be deemed as the "non-convertible" components in the biocrude oil formation processes. When the ash content in the algal feedstock increased, the volatile solid content decreased. Incorporating results from this study and literature investigating the effect of total solid content on HTL processes (Anastasakis & Ross, 2011; Duan et al., 2013b; Jena et al., 2011a; Xu & Savage, 2015), Figure 6-13 demonstrates that the energy recovery in biocrude oil reduced as the total volatile solid content in feeding slurry reduced. Further, Figure 6-13 shows that the total volatile solid content has a nonlinear *(e.g.,* exponential) effect on the energy recovery in biocrude oil. This result also indicates that the volatile solid content has to achieve a certain concentration (*i.e.,* CVC) under HTL processes, so that an efficient energy recovery in biocrude oil can be obtained. For example, Figure 6-13 presents that the energy recovery in biocrude oil would significantly decrease from 70.3% to 45.8% (orange circle) when the total volatile solid content of *Nannochloropsis* reduced from 18.7 wt.% to 8.6 wt.% (Xu & Savage, 2015). Moreover, calcium carbonates in the algal feedstocks may be bounded by volatile matter (*e.g.,* amino acids) (Chen et al., 2014c; Zhang, 2014), which may further reduce the

concentration of the volatile solid content. The adsorption of the non-convertible components on the surface of the biocrude oil may also hinder effective conversions of other biocrude oil precursors into biocrude oil with higher heating values. As a result, the HTL processes would be more complex than the system described in equation 6-10.

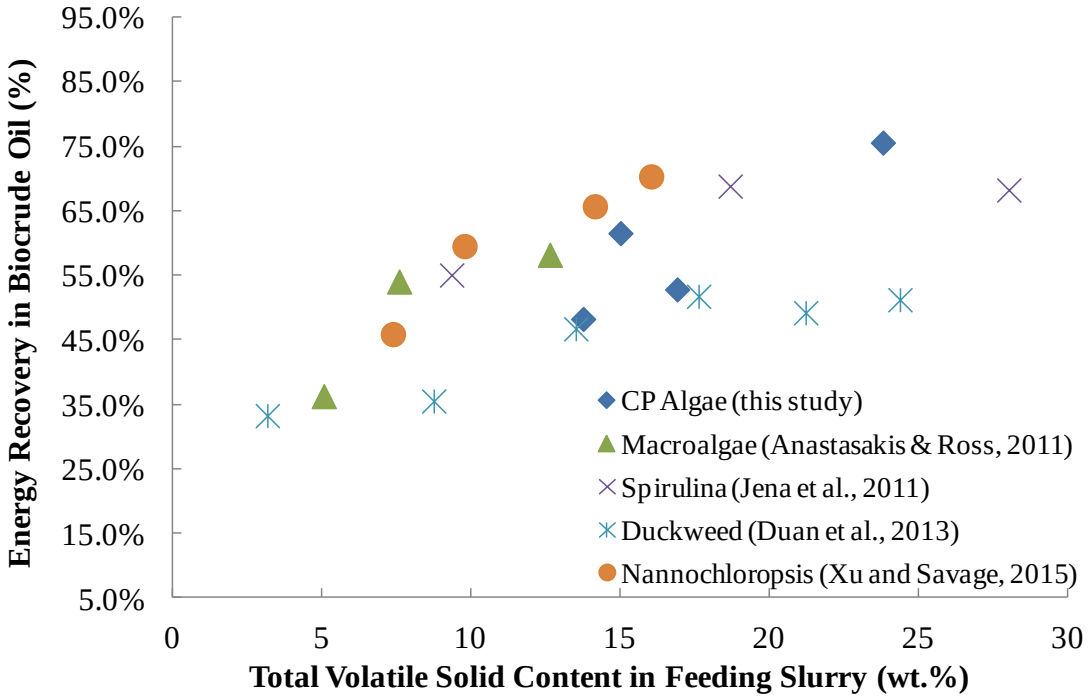


**Figure 6-13. The effect of total volatile solid content in feeding slurry on the energy recovery in biocrude oil (%) (with data adopted from (Anastasakis & Ross, 2011; Duan et al., 2013b; Jena et al., 2011a; Xu & Savage, 2015))**

# CHAPTER 7. RENEWABLE TRANSPORTATION BIOFUEL FROM WET BIOWASTE VIA HYDROTHERMAL LIQUEFACTION

Biocrude oil converted from wet biowaste generally contains 10-20% oxygen, 3-7% nitrogen, and up to 20% moisture contents (Chen et al., 2014b; Chen et al., 2014c; Gai et al., 2014a; He et al., 2000a; He et al., 2000b; Yu, 2012; Yu et al., 2011b). These impurities will result in corrosion of the engine when the biocrude oil is used as transportation fuels (Chiaramonti et al., 2003a; Chiaramonti et al., 2003b). Thus, further upgrading or separation of the biocrude oil is critically needed. Several previous studies have demonstrated that commercially available catalysts (*e.g.,* zeolites, Pt/C, Raney-Ni, Rh) had little effect on upgrading the quality of biocrude oil when the upgrading reaction temperature was below 450°C (Cheng et al., 2014a; Duan & Savage, 2011c; Duan & Savage, 2010; Torri et al., 2013; Yu et al., 2014; Zhang et al., 2014; Zhang et al., 2013a). On the other hand, it was reported that after proper separations, such as distillation, the oxygen content in the biocrude oil could be reduced to 5% and the heating values could be increased to 41-45 MJ/kg (Cheng et al., 2014b). This indicates that there is a high potential to utilize biocrude oil as drop-in fuels.

Biocrude oil converted from wet biowaste, such as swine manure or algal biomass, mainly contains fractions (26-44 wt.%) that could be used as diesel and aviation fuel (boiling point between 200-300°C) (Chen et al., 2014b; Gai et al., 2014a). In the past five years, the diesel and aviation industries respectively consumed 22% and 11% of energy supplied to the U.S. transportation sector and accounted for 24.3% and 8.3% of green house gas (GHG) emissions by the U.S. transportation sector (United States. Environmental Protection Agency. Office of Policy & Evaluation, 2017; USEIA). In response to growing environmental concerns, the transportation industry is exploring economical, societal, and environmental solutions to reduce its GHG emissions for sustainable growth (Han et al., 2013; Hoekman, 2009).

This chapter aims to develop an integrated process that could effectively separate HTL biocrude oil into fuel appropriate fractions (Figure 7-1). More specifically, distillation was used to separate biocrude oil converted from wet biowaste—including swine manure, food processing waste, and *Spirulina platensis*—via HTL into different fractions that could be used as drop-in fuels. Different distillate fractions were characterized in terms of elemental compositions, density, viscosity, acidity, and chemical compositions. Related results were compared to those obtained from petroleum transportation fuels such as diesel.

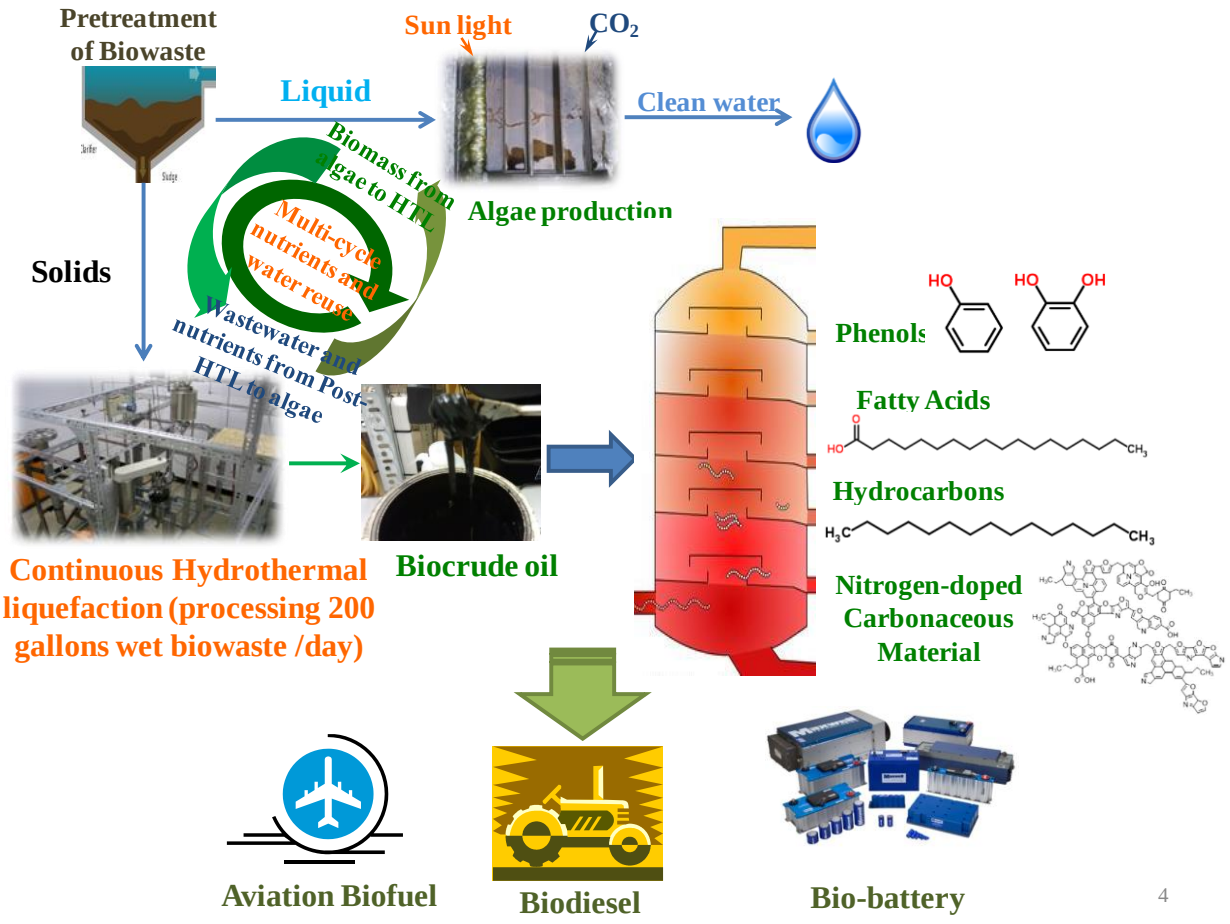


**Figure 7-1. Integrated process scheme to produce drop-in biofuels from wet biowaste**

### 7.1 Compatibility of biocrude oil in transportation fuels

In order to study the compatibility of biocrude oil in transportation fuels, the biocrude oil converted from swine manure (SW) via HTL was mixed with diesel at a weight ratio of 1 to 9. The mixing process was conducted under ultrasonication, which has been reported as an effective extraction and homogenization technique for biocrude with organic solvents (Zhang et al., 2013a). Physicochemical properties of diesel, biocrude, and their blends are given in Table 7-1 and Figure 7-2. As Table 7-1 shows, when the biocrude was blended with diesel at a weight ratio of 1 to 9, the density, heating value, carbon, hydrogen, and nitrogen contents were insignificantly affected. On the other hand, Figure 7-2 reveals that the biocrude slightly shifted the boiling point distribution of blended diesel to a higher temperature range, which could be attributed to the heavier fractions that distributed from biocrude oil to diesel. In short, the above results demonstrate that the biocude oil is compatible with diesel.

**Table 7-1. Physicochemical properties of diesel blended with the biocrude converted from swine manure at different ratios under ultrasonication for 1h (dry weight sample basis)**

| Property | SW:Diesel=1:9 | Diesel | SW-Biocrude |
|---|---|---|---|
| Density (g/cm$^3$) | 0.8 | 0.8 | 0.92 |
| HHV (MJ/kg) | 47.3 | 47.9 | 34.1 |
| C (wt.%) | 84.5±0.1 | 85.4±0.07 | 72.1±0.5 |
| H (wt.%) | 13.3±0.04 | 13.4±0.06 | 8.61±0.2 |
| N (wt.%) | 1.60±0.1 | 1.53±0.00 | 5.09±0.0 |
| O[a] (wt.%) | 0.55 | N.D. [b] | 14.3 |

[a] calculated by difference; [b] Not detected

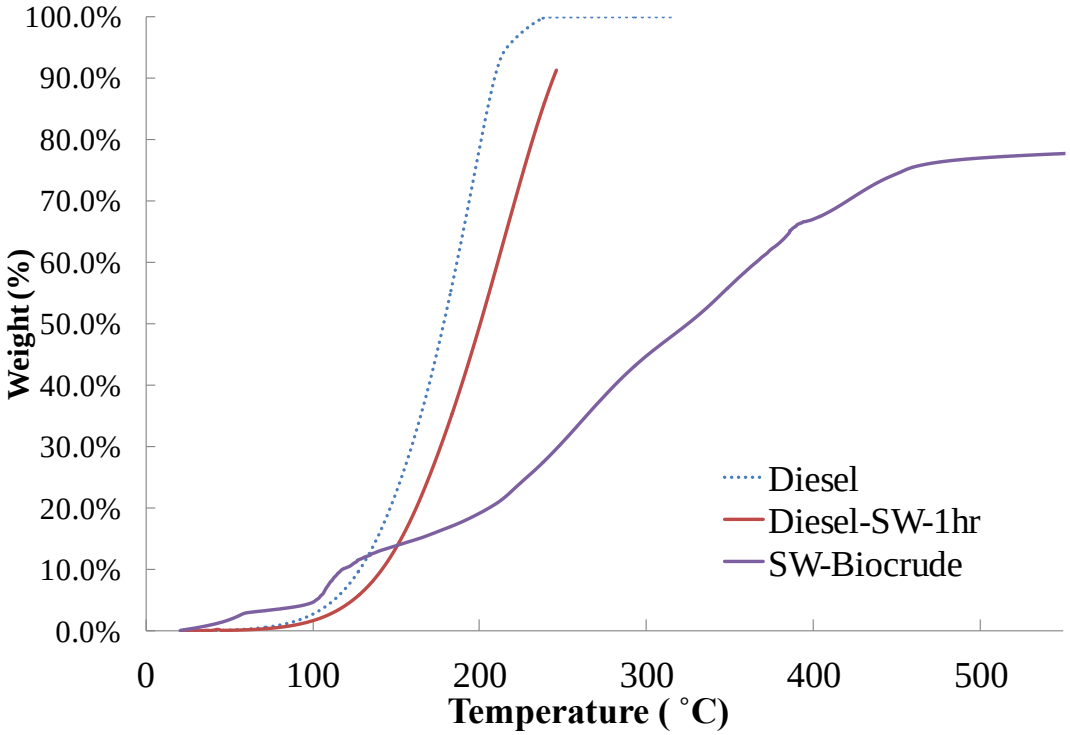


**Figure 7-2. Boiling point distribution of SW-biocrude oil blended diesel**

The biocrude oil converted from swine manure (SW) via HTL was also mixed with jet fuel at a weight ratio of 1 to 9 to examine its compatibility with aviation fuel. Physicochemical properties of jet fuel, biocrude oil, and their blends are summarized in Table 7-2 and Figure 7-3, which show that the elemental compositions, heating value, boiling point distribution of blended jet biofuel were very close to those of regular jet fuel.

**Table 7-2. Physicochemical properties of jet fuel (JA), kerosene (K), and kerosene blended with biocrude oil converted from swine manure (SW) at a weight ratio of 1 to 9 under ultrasonication for 1h (SW:K=1:9)**

| Property | SW:K=1:9 | Kerosene | Jet Fuel | SW-Biocrude Oil |
|---|---|---|---|---|
| Heating Value (MJ/kg)[a] | 45.2 | 47.4-47.9 | 45.6 | 31.7-33.7 |
| HHV (MJ/kg) | 49.3 | 49.6 | 49.5 | 34.1 |
| C (wt.%) | 85.6±0.04 | 86.0±0.2 | 86.0±0.06 | 72.1±0.5 |
| H (wt.%) | 14.3±0.08 | 14.4±0.1 | 14.4±0.02 | 8.61±0.2 |
| N (wt.%) | 1.25±0.07 | 1.08±0.06 | 0.25±0.02 | 5.09±0.0 |
| O[b] (wt.%) | N.D. [c] | N.D. [c] | N.D. [c] | 14.3 |

[a]Measured by Oxygen Bomb Calorimeter [b]calculated by difference; [c] Not detected

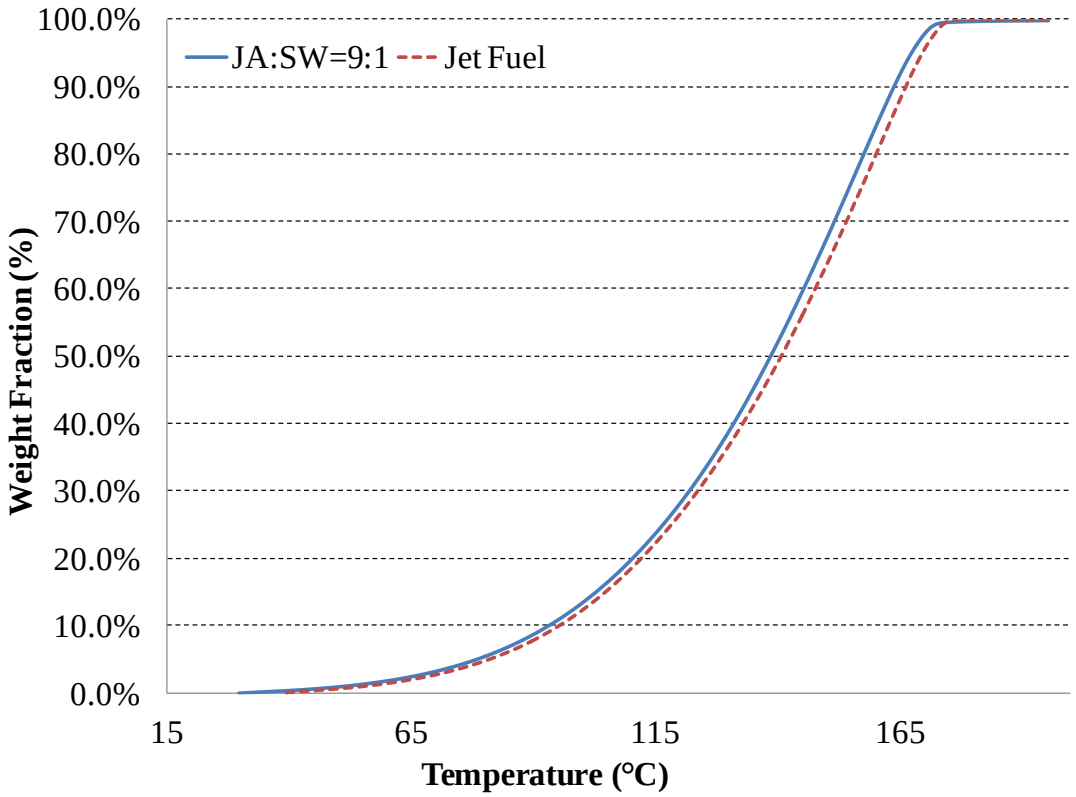


**Figure 7-3. Boiling point distribution of blended jet biofuel**

To further understand the chemical compositions of heavier fractions that may diffuse from biocrude oil to transportation fuels, the blended jet biofuel, jet fuel, and biocrude oil were subjected to GC-MS analysis. The GC spectra produced are presented in Figure 7-4. GC-MS analysis with derivative treatment was also conducted to explore if relatively non-volatile organic compounds may partition into jet fuel and those GC spectra are shown in Figure 7-5.

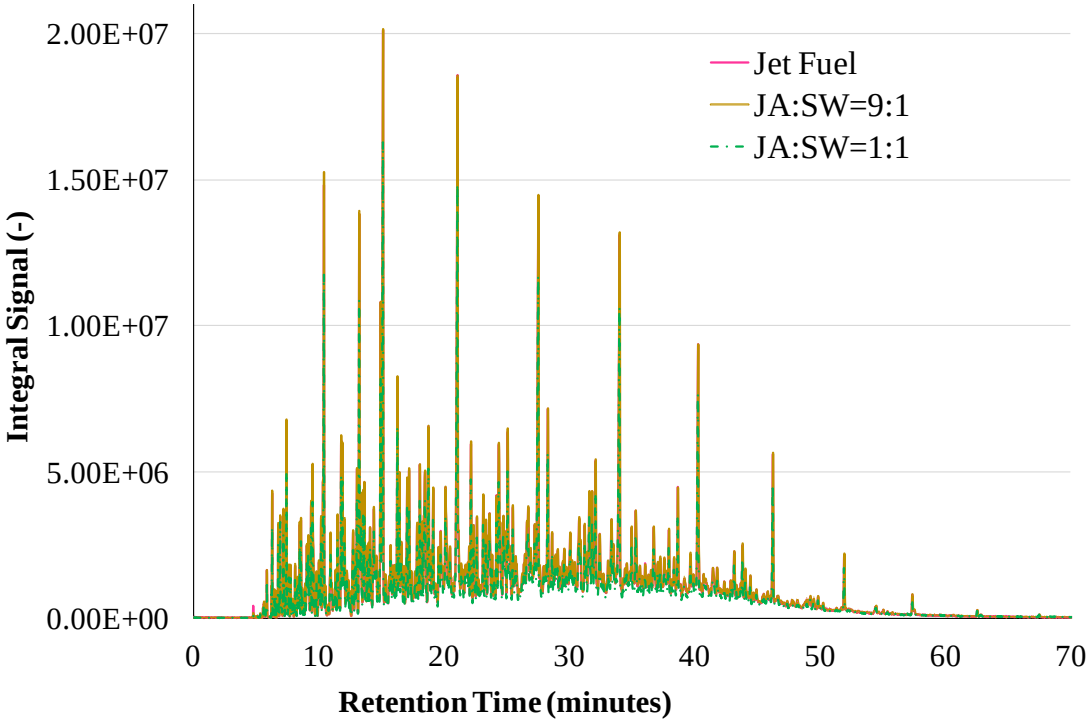


**Figure 7-4. GC spectra of blended jet biofuel at different weight fractions of SW-derived biocrude oil and petroleum jet fuel**

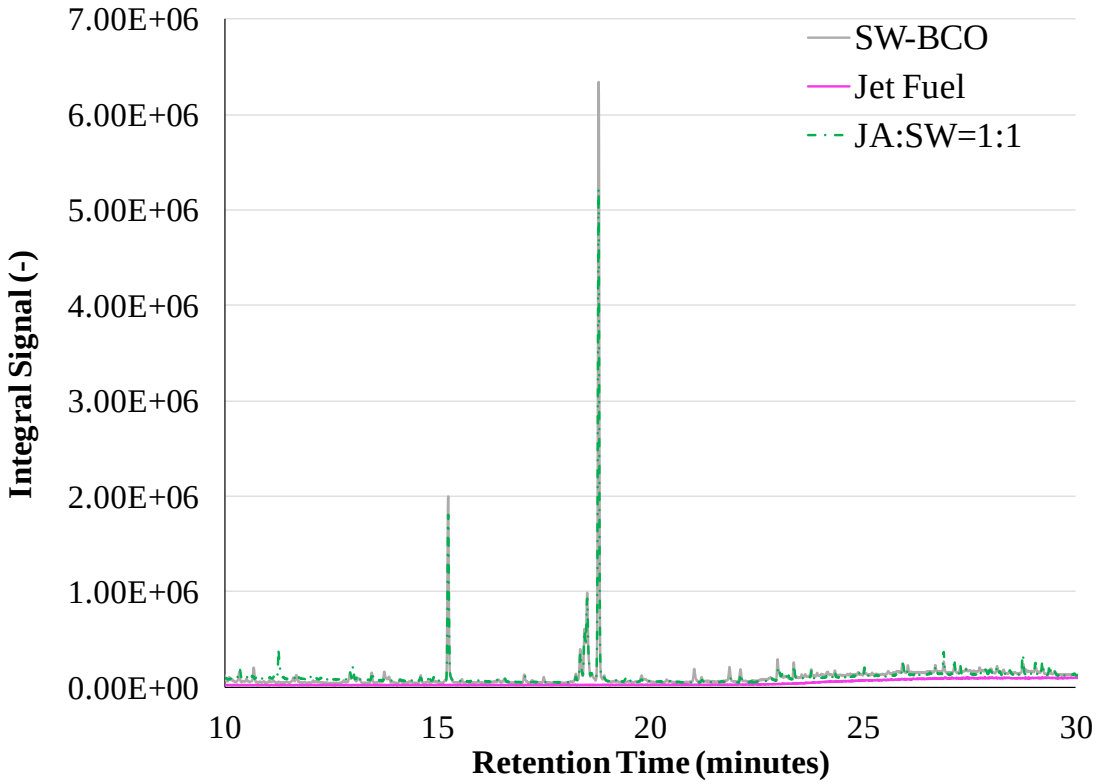


**Figure 7-5. GC spectra of blended jet biofuel with derivative treatment at different weight fractions of SW-derived biocrude oil and petroleum jet fuel**

As Figure 7-4 shows, the chemical compositions of blended jet biofuel at a 1 to 9 weight ratio of biocrude oil to jet fuel is very close to that of regular jet fuel. Further, the blended jet biofuel at a higher weight ratio (*i.e.,* 1 to 1) of biocrude oil to jet fuel was prepared and characterized under GC-MS to more accurately identify chemicals that can partition from biocrude oil to jet fuel. Table 7-3 summarizes the chemical compounds that partitioned from biocrude oil to jet fuel. The purpose of this analysis is to identify compounds that typically would not be present in jet fuel but can be blended from biocrude oil to jet fuel. As Table 7-3 shows, fatty acids (*e.g.,* hexadecanoic acid and octadecanoic acid), fatty acid esters (*e.g.,* hexadecanoic acid methyl ester), fatty amides (*e.g.,* ocadecanamide), and sterols (*e.g.,*cholestene) are non-hydrocarbon compounds that can partition from biocrude oil to jet fuel. The presence of these oxygen- and nitrogen-containing compounds distinguishes the blended jet biofuel from petroleum jet fuel. This result is also similar to the previous study co-processing 10% algal biocrude oil with 90% petrocrude (Lavanya et al., 2015).

In short, the above results all suggest that the biocude oil is compatible in petroleum diesel and jet fuel. Although the oxygenated and nitrogen-containing compounds were mixable with transportation fuels, they may remain critical for preparing drop-in fuels. In fact, it is worth noting that the blended diesel and jet biofuel were not stable and indicated partial phase separation (solid phase products were precipitated in the bottom of blended biofuels). Further separation of biocrude oil is critically needed to synthesize stable drop-in fuels for engine tests.

**Table 7-3. Integral signals of major compounds in SW-derived biocrude oil (SW-BCO) and blended jet biofuel with one weight fraction of jet fuel and one weight fraction of SW-derived biocrude oil (JA:SW=1:1)**

| Name | JA:SW=1:1 | SW-BCO |
|---|---|---|
| **Regular GC-MS** | | |
| Hexadecanoic acid | 6825092 | 589401617 |
| n-Octadecenoic acid | 4306246 | 528032555 |
| Octadecanoic acid | 20947458 | 950753114 |
| Octadecanamide derivatives | 224252 | 94560136 |
| Fatty acid, pyrrolidides | 298797 | 20178135 |
| Cholestene | 614540 | 13597542 |
| Stereol derivatives | 777545 | 11693352 |
| **Derivative treatment on samples before GC-MS** | | |
| Tetradecanoic acid | 136183 | 208457 |
| Tetradecanoic acid, 12-methyl ME[a] | 185234 | 208406 |
| Hexadecanoic acid ME[a] | 6825092 | 8327288 |
| Heptadecanoic acid ME[a] | N.D. [b] | 293966 |
| Octadecenoic acid ME[a] | 1309190 | 4679720 |
| Octadecanoic acid | 20947458 | 26515792 |
| Eicosanoic acid ME[a] | 283113 | 366727 |
| Octadecanamide | 562206 | 697696 |
| N-Methyldodecanamide | 472549 | 465317 |

[a]methyl ester; [b] Not detected

### 7.2 Distillation of Biocrude Converted from wet biowaste

Distillation was conducted to separate the biocrude converted from swine manure (SW), food processing waste (FPW), and Spirulina (SP) into several distillates. The properties of the SW-, FPW-, and SP-derived biocrude are listed in Table 7-4. As Table 7-4 shows, SW-, FPW-, and SP-derived biocrude all contain heating values closer to that of petroleum transportation fuels, indicating SW, FPW and SP are promising HTL feedstocks. However, the biocrude still contains 12-28% oxygen contents that need to be separated to improve their heating values to those of petroleum transportation fuels. In addition, all tested biocrude demonstrated high viscosity at room temperature before distillation. This feature also makes biocrude oil hard to be used as drop-in fuel—diffusion of biocrude oil to transportation fuel is challenging.

**Table 7-4. Properties of the biocrude converted from swine manure (SW) and food processing waste (FPW) (dry weight basis)**

| Property | SW-Biocrude | FPW-Biocrude | SP-Biocrude |
|---|---|---|---|
| Toluene Insoluble Fraction | 25.5±3.7% | 0% | 19.0±6.2% |
| HHV (MJ/kg) | 34.1 | 40.4 | 26.4 |
| C (wt.%) | 72.1±0.5 | 76.1±0.02 | 58.3±0.2 |
| H (wt.%) | 8.61±0.2 | 11.7±0.1 | 8.12±0.3 |
| N (wt.%) | 5.09±0.0 | 0.42±0.01 | 6.00±0.2 |
| O[a] (wt.%) | 14.3 | 11.7 | 27.6 |

[a]calculated by difference

Figure 7-6 summarizes the distillation curves of the SW-, FPW-, and SP-derived biocrude. The three types of biocrude show distinct distillation characteristics. Distillation can respectively separate 41%, 75%, and 62% distillates from SW-, FPW-, and SP-derived biocrude. This also implies that FPW- and SP-derived biocrude oil is more volatile than SW-derived one. In fact, the morphologies of SW-, FPW-, and SP-derived biocrude are very different from each other at room temperature as well. Typically, SW-derived biocrude is in the solid form; FPW-biocrude is in the liquid form; and SP-biocrude is in slurry form at room temperature. This is mainly due to the different compositions in the three feedstocks. As Table 4-2 presents, FPW mainly contains crude fat and non-fiber carbohydrates. In contrast, SP mostly includes proteins and non-fiber carbohydrates while SW is composed of crude protein, crude fat, hemicelluloses, and celluloses. It is generally believed that crude fat degrades into fatty acids or is further converted into hydrocarbons under HTL processes (Chen et al., 2014c; Gai et al., 2015; Peterson et al., 2008; Vardon et al., 2014; Watanabe et al., 2006). On the other hand, proteins and carbohydrates may react through the Maillard reaction and be converted into complex heterocyclic compounds (Chen et al., 2014c; Gai et al., 2015). In short, the reaction pathways can be very different for different biological compounds under HTL processes. Further chemical analyses will help elucidate more details.

(a)

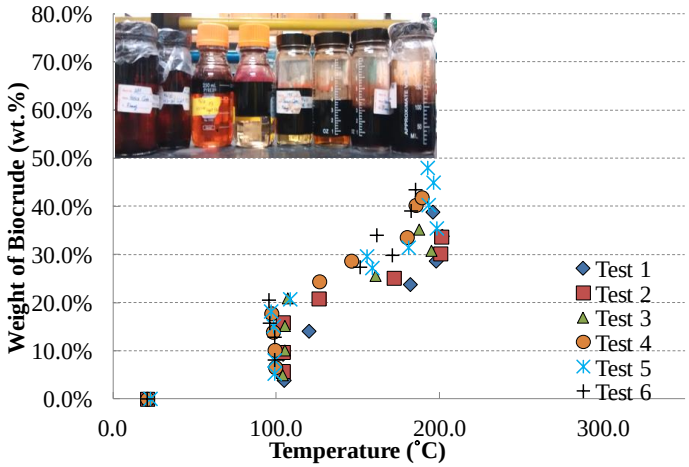


(b)

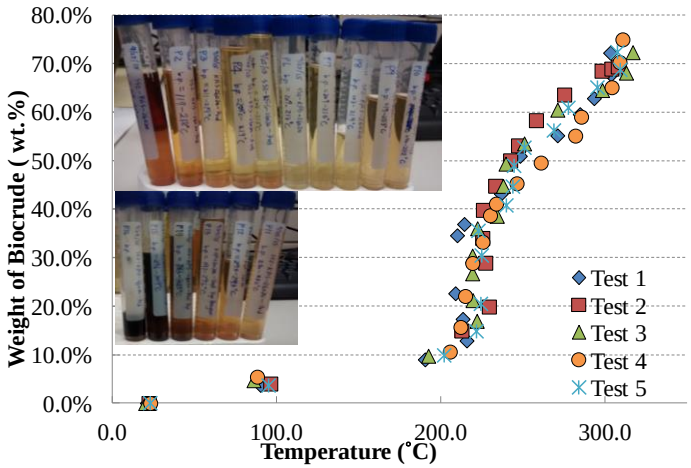


(c)

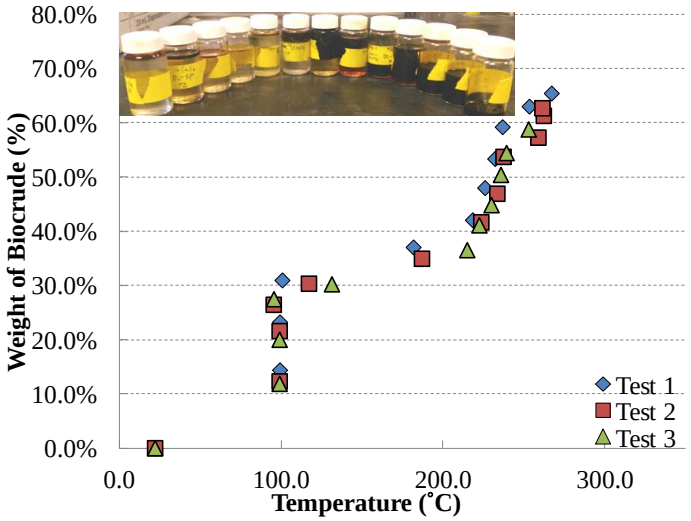


**Figure 7-6. Distillation curves of the biocrude converted from (a) swine manure, (b) food processing waste, and (c) Spirulina via HTL**

Figure 7-6 also shows that the initial 5 and 30 wt.% were respectively distilled out from the FPW- SW-, and SP-derived biocrude at around 100°C, indicating these fractions are mostly water (data will be shown in later sections). Subsequently, 70 wt.% of distillates were separated from FPW-derived biocrude at 200-330°C whilst about 35 wt.% of distillates were recovered from SP-derived biocrude at 200-270°C and 20 wt.% of distillates were fractionated from SW-derived biocrude at 150-200°C. Compared to the distillation range of transportation fuels (ASTM, 2015c; Cheng et al., 2014b), these fractions of distillates could be suitable for aviation fuel and diesel application. Moreover, the fluidity of the distillates from the biocrude was significantly decreased from viscous phase into flowable liquid phase, suggesting that distillation makes the biocrude more appropriate for fuel applications. On the contrary, 20 wt.%, 35 wt.%, and 50 wt.% fractions were not recovered by the distillation from FPW-, SP- and SW-derived biocrude, respectively. After distillation, these fractions appeared as heavy oil or char-like products that could not be easily distilled, which would require further studies in the near future.

### 7.3 Physical Properties of different distillate fractions from various feedstocks

Density, viscosity, and the moisture content of different distillate fractions separated from SW-, FPW-, and SP-derived biocrude are listed in Table 7-5. The distillate fractions of F-H from SW-derived biocrude, B-G from FPW-derived biocrude, and G-I from SP-derived biocrude present density and viscosity closest to those of diesel and jet fuel. Particularly, the fractions of D-E from FPW-derived biocrude demonstrate the closest density and viscosity to those of jet fuel. Meanwhile, the distillate fractions of A-C from SW-derived biocrude, the fraction of A from FPW-derived biocrude, and the fractions of A-C from SP-derived biocrude, respectively contain 75-90 wt.%, 15 wt.%, and 89-99 wt.% moisture content. These distillates may also contain relatively polar compounds, such as nitrogen-containing compounds, which are inappropriate for fuel applications.

**Table 7-5. Properties of the distillates from SW-, FPW, and SP-derived biocrude**

| Fractions | Weight Fractions | Distillation Temperature (°C) | Density ($kg/m^3$)[a] | Kinematic Viscosity ($mm^2/s$ at 20°C)[b] | Moisture Content (wt.%) |
|---|---|---|---|---|---|
| **(SW-Biocrude)** | | | | | |
| A | 5.9 ± 0.9% | 102-105 | 1010 | 1.00±0.01 | 90.6% |
| B | 3.2 ± 0.6% | 103-105 | 1010 | 1.01±0.00 | 75.1% |
| C | 5.4 ± 2% | 102-105 | 990 | 4.38±0.4 | 82.1% |
| D | 11.3 ± 1% | 102-156 | 950 | 6.24±0.4 | 50.4% |
| E | 3.4 ± 1% | 141-196 | 970 | 6.27±0.03 | 9.90% |
| F | 3.4 ± 2% | 191-207 | 875 | 4.09±0.01 | 14.9% |
| G | 5.3 ± 2% | 175-210 | 845 | 9.11±0.01 | 0% |
| H | 3.2 ± 2% | 181-197 | 875 | 6.06±0.2 | 5.00% |
| **(FPW-Biocrude)** | | | | | |
| A | 9.4 ± 0.5% | 76-226 | 910 | 1.26±0.01 | 15.2% |
| B | 9.9 ± 2% | 204-221 | 850 | 1.54±0.02 | 0% |
| C | 10.2 ± 2% | 208-226 | 825 | 2.07±0.01 | N/A[c] |
| D | 8.3 ± 0.1% | 207-234 | 810 | 1.83±0.00 | N/A[c] |
| E | 12.4 ± 2% | 208-257 | 812 | 1.68±0.02 | N/A[c] |
| F | 9.9 ± 2% | 238-293 | 827 | 2.39±0.01 | N/A[c] |
| G | 7.9 ± 0.4% | 280-320 | 850 | 3.20±0.03 | N/A[c] |
| H | 7.3 ± 0.1% | 266-313 | 863 | 3.68±0.2 | N/A[c] |
| **(SP-Biocrude)** | | | | | |
| A | 12.9 ± 1% | 97-99 | 1004[f] | 1.09±0.01 | 99.9% |
| B | 8.8 ± 0.6% | 97-99 | 1003[f] | 1.04±0.00 | 99.2% |
| C | 8.9 ± 1.3% | 88-151 | 1024[f] | 1.53±0.02 | 88.7% |
| D | 5.7 ± 0.9% | 151-219 | 909[f] | 3.21±0.3 | 29.0% |
| E | 5.4 ± 1.1% | 211-227 | 899[f] | 4.64±0.02 | 14.9% |
| F | 5.0 ± 1.1% | 218-231 | 882[f] | 12.6±0.04 | 0% |
| G | 5.9 ± 0.8% | 223-237 | 888[f] | 5.33±0.02 | N/A[c] |
| H | 4.5 ± 1.2% | 219-244 | 880[f] | 8.85±0.11 | N/A[c] |
| I | 5.3 ± 0.9% | 244-268 | 901[f] | 12.8±0.2 | N/A[c] |
| Jet Fuel | | ≦ 300[d] | 805 | 1.75±0.00 | |
| Diesel | | ≦343[e] | 835 | 3.75±0.02 | |

[a] Measured by hydrometer (ASTM D7566); [b] Measured by Cannon-Fenske Viscometer (ASTM D7566); [c] Not applied; [d] Reported by ASTM D7566; [e] Reported by ASTM D7467; [f]Calculated by the equation of (Mass/Volume) due to the limited amount of SP-distillates.

Viscosity plays an important role in the fuel injection, atomization, and combustion processes (Lu et al., 2009). Table 7-5 demonstrates that the viscosity of HTL distillates increased as the distillation temperature increased because the amounts of large molecules increased with the distillation temperature (Cheng et al., 2014b). In general, aliphatic and aromatic hydrocarbons display low viscosities due to their lack of oxygen and other heteroatoms (Knothe & Steidley, 2005). In the case of SW-derived distillates, their viscosities first increased from

fraction A to E, then reduced from E to F, which can be attributed to the reduction of phenolic compounds (data shown in GC-MS analysis). For example, the viscosity of phenol at room temperature is about 12 $mm^2/s$ (Haynes, 2016), while that of diesel is 3.75. Subsequently, the viscosity of SW-distillates increased again from F to G. This can be attributed to the higher concentration of fatty esters (*e.g.*, Propanoic acid, 3-mercapto-, dodecyl ester) in fraction G than in fraction F (Knothe & Steidley, 2005). Yet, the viscosity reduced again from G to H, which is possibly due to the reduction of phenolic compounds. Similarly, the viscosities of SP-derived distillates first increased from fraction A to F, then reduced from F to G, which may be due to the high concentration of nitrogen-heterocyclic compounds (*e.g.*, Methylindole) residing in fraction F. Afterwards, the viscosity increased again from the fraction G to I. In contrast, the viscosities of FPW-derived distillates generally increased with the distillation temperature. This is mainly since FPW contains less complex compositions than SW and SP. This fact also indicates that the FPW-derived distillates are the most promising candidate for drop-in diesel synthesis among the three investigated feedstocks. Nevertheless, the compositions of HTL distillates are far more complex than conventional biofuels (*e.g.*, biodiesel and bioethanol). Further investigation (*e.g.*, exploration of phase transition points) is suggested to understand the rheological properties of HTL distillates.

### 7.4 Chemical compositions of different distillate fractions from various feedstocks

#### 7.4.1 Elemental Analysis of different distillate fractions from various feedstocks

Table 7-6 gives the heating value along with carbon, hydrogen, nitrogen, and oxygen contents of different distillates from SW-, FPW-, and SP-derived biocrude. The fractions A-C from SW-and SP-derived biocrude were not subjected to elemental composition analysis because they mainly contain water. The fractions E-H, D-H, and F-I of SW-, FPW-, and SP-derived biocrude respectively present the closest heating values, carbon, and hydrogen contents to those of diesel and jet fuel. Notably, the distillate fractions D-H of FPW-derived biocrude demonstrate the closest levels of carbon, hydrogen, nitrogen, and heating values to those of jet fuel and diesel. Compared to the distillates from the biocrude converted from woody biomass, microalgae, or swine manure with glycerol via HTL (Cheng et al., 2014b; Eboibi et al., 2014a; Hoffmann et al., 2016a), the distillates from FPW-derived biocrude achieve a similar or higher level of heating values, suggesting the food processing waste is a very promising HTL feedstock for fuel

applications. In fact, in the United States alone, it is estimated that the energy embedded in the food waste represents about 2% of annual energy consumption nationwide while 133 billion pounds of waste biomass were attributed by the food waste (Buzby et al., 2014; Cuéllar & Webber, 2010). Nevertheless, the food processing waste typically contains high water contents and thereby is not suitable for pyrolysis or conventional oilseed extraction processes that would require additional energy to dewater feedstock. As a consequence, HTL is an advantageous and energy-efficient route to treat the food processing waste and can be a promising technique to address the issues within the food-water-energy nexus.

**Table 7-6. Elemental compositions of the distillates from SW-, FPW-, and SP-derived biocrude**

| SW-Biocrude | HHV (MJ/kg) | C (%) | H (%) | N (%) | O[a] (%) |
|---|---|---|---|---|---|
| A | N/A[b] | N/A[b] | N/A[b] | N/A[b] | N/A[b] |
| B | N/A[b] | N/A[b] | N/A[b] | N/A[b] | N/A[b] |
| C | N/A[b] | N/A[b] | N/A[b] | N/A[b] | N/A[b] |
| D | 37.2 | 74.3±0.1 | 10.1±0.02 | 3.21±0.07 | 12.4 |
| E | 44.4 | 81.5±0.06 | 12.3±0.2 | 2.62±0.03 | 3.64 |
| F | 46.3 | 82.9±0.06 | 13.1±0.06 | 2.37±0.00 | 1.72 |
| G | 44.7 | 82.7±0.00 | 12.1±0.08 | 3.33±0.00 | 1.97 |
| H | 43.2 | 82.7±0.02 | 11.0±0.02 | 3.81±0.11 | 2.53 |
| I[c] | N/A[b] | 74.9±0.23 | 2.52±0.06 | 6.07±0.09 | 16.5 |
| **FPW-Biocrude** | | | | | |
| A | 40.6 | 74.2±0.04 | 12.5±0.03 | 0.17±0.01 | 13.1 |
| B | 42.9 | 76.3±0.01 | 13.3±0.1 | 0.17±0.01 | 10.3 |
| C | 44.2 | 80.4±0.09 | 12.8±0.7 | 0.18±0.08 | 6.62 |
| D | 47.2 | 83.5±0.02 | 13.7±0.04 | 0.14±0.1 | 2.71 |
| E | 47.6 | 84.3±1.1 | 13.7±0.04 | 0.20±0.00 | 1.87 |
| F | 47.4 | 85.8±0.01 | 13.1±0.2 | 0.21±0.02 | 0.93 |
| G | 47.0 | 86.2±0.03 | 12.7±0.04 | 0.21±0.00 | 0.92 |
| H | 47.1 | 86.6±0.05 | 12.6±0.01 | 0.24±0.00 | 0.56 |
| I[c] | N/A[b] | 74.9±1.11 | 9.32±0.14 | 0.42±0.11 | 15.4 |
| **SP-Biocrude** | | | | | |
| A | N/A[b] | N/A[b] | N/A[b] | N/A[b] | N/A[b] |
| B | N/A[b] | N/A[b] | N/A[b] | N/A[b] | N/A[b] |
| C | N/A[b] | N/A[b] | N/A[b] | N/A[b] | N/A[b] |
| D | 41.8 | 78.2±0.08 | 11.5±0.03 | 4.94±0.03 | 5.37 |
| E | 40.3 | 76.8±0.06 | 10.8±0.1 | 6.25±0.01 | 6.10 |
| F | 41.9 | 77.9±0.1 | 11.5±0.2 | 6.00±0.03 | 4.60 |
| G | 42.6 | 79.8±0.1 | 11.4±0.1 | 5.23±0.08 | 3.59 |
| H | 44.2 | 80.8±0.01 | 12.1±0.01 | 4.83±0.00 | 2.25 |
| I | 42.5 | 80.4±0.1 | 11.1±0.3 | 5.88±0.3 | 2.61 |
| J[c] | N/A[b] | 57.6±0.04 | 1.75±0.01 | 6.45±0.01 | 34.2 |
| **Diesel** | 47.2-48.0 | 85.4±0.07 | 13.4±0.06 | 1.53±0.00 | N.D.[d] |
| **Jet Fuel** | 46.0-49.5 | 86.0±0.06 | 14.4±0.02 | 0.25±0.02 | N.D.[d] |

[a] Calculated by difference; [b] Not applied; [c] The fraction that cannot be recovered by the distillation; [d] Not detected

Although the fractions E-H, D-H, and F-I of SW-, FPW-, and SP-derived biocrude contain 2-5% oxygen contents, this oxygen content may enhance the combustion efficiency of transportation fuels, particularly for diesel (Zhou et al., 2014). Normally, the fuel is injected directly into the diesel engine cylinder just before the combustion process begins without pre-

mixing. Partially oxygenated biofuels can enhance the air-fuel ratio and thus improve the combustion efficiency (Heywood, 1988). For example, it has been reported that butanol-fueled diesel can lead to lower carbon dioxide, total hydrocarbons, and particulate matter emissions than those from petroleum diesel, since butanol contains 22% of oxygen contents (Liu et al., 2011; Zhou et al., 2014).

Notably, the nitrogen contents were in the range of 2-6% in the distillates from SW- and SP-derived biocrude. This is due to the fact that swine manure and low-lipid algae typically contain 25% and 65% proteins, respectively (Chen et al., 2014b; Wang, 2011b; Yu, 2012). In general, biocrude oil converted from swine manure and algae contains a relatively high nitrogen content (3-7%) (Audo et al., 2015; Chen et al., 2014b; Yu, 2012) for the application of transportation fuels. The high nitrogen content in biofuel would cause fouling of conventional oil-upgrading catalysts (*e.g.*, zeolites) because the high basicity of the heterocyclic nitrogen compounds can result in adhesion to acidic active catalytic sites and poison the catalysts (Chen et al., 2016b; Furimsky & Massoth, 2005; Vardon et al., 2012). Moreover, from the perspective of combustion, the nitrogen-containing compounds, such as fatty amines and nitriles, could potentially increase the $NO_x$ emissions (Reiter & Kong, 2011). With distillation, the nitrogen content was reduced from 5% to 2-3% in the biofuel products, which could benefit the following catalytic denitrogenation processes.

Table 7-6 indicates that the nitrogen-containing compounds (*e.g.*, fatty nitriles) tend to partition into the heavy fractions in the SW-derived biocrude. This is since nitrogen-containing compounds (*e.g.*, fatty nitriles) usually have a higher boiling point than hydrocarbons with the same carbon number. For example, the boiling point of dodecanenitrile ($C_{12}H_{23}N$) is 276.1°C, while that of dodecane ($C_{12}H_{26}$) is 216.3°C (Haynes, 2016). In contrast, the nitrogen content of SP-derived distillates increased from the fraction D to E, and then decreased from fraction E to H, and increased again from fraction H to I. Similarly to the SW-distillates, the first and second increases of nitrogen contents in SP-distillates are mainly due to the increase of fatty nitriles. More details regarding chemical compositions will be provided in later sections.

### 7.4.2 GC-MS analysis of different distillate fractions from various feedstocks

GC-MS analysis was conducted to understand the chemical compositions in the distillates from different types of HTL biocrude. Identified compounds were categorized into several groups such as hydrocarbons and phenols. It should be noted that only a fraction of the distillates

are identifiable by GC-MS. This is since the distillates may contain compounds with high molecular weights and chemicals that are not volatile (Gai et al., 2014a; Vardon et al., 2011; Yu, 2012).

Figure 7-7a and Table 7-7 show that the distillate fractions E-H mainly contained hydrocarbons, which indicates that the distillation can effectively separate hydrocarbons from non-hydrocarbon compounds, such as oxygen- and nitrogen-containing compounds. Hydrocarbons ranging from C10 to C18 in the distillate fractions E-H are suitable for drop-in transportation fuel application (Colket et al., 2007), while phenols, fatty acids, nitrogen-heterocyclic compounds, and fatty nitriles remain concerns for fuel application. Particularly, both phenols and fatty acids would lead to an acidity too high for fuel application. Further upgrading of SW-derived distillates is esstential to remove phenols and fatty acids. Once removed, those phenols and fatty acids can find alternative function in the form of commodity chemical application. For instance,  phenols can be used as precursors for epoxies (Asada et al., 2015).

Figure 7-7b and Table 7-8 demonstrates that hydrocarbons and oxygenates are the major compounds in the distillates from FPW-derived biocrude. The distillate fractions D-H mainly contain alkanes and alkenes with carbon numbers from 8-17, which are in the range for jet fuel (10-14) (Colket et al., 2007) and diesel (8-21) (Collins, 2007) application. In addition, these fractions also contain saturated and unsaturated fatty acids with carbon numbers from 6-18, which indicates that further upgrading would be needed to modify and/or remove these fatty acids. Compared to the distillates from SW-derived biocrude, the chemical compositions for the distillates from FPW-derived biocrude are less complex. This is because FPW is primarily composed of crude fats and non-fibrous carbohydrates whilst SW contains proteins, crude fats, and fibrous carbohydrates.

**Table 7-7. Normalized GC-MS signals of components identified in the distillates from SW-derived biocrude; "×" indicates the chemical was not detected**

| Compound Name | Normalized Signal (-) | | | | |
|---|---|---|---|---|---|
| | D | E | F | G | H |
| **Hydrocarbons** | | | | | |
| Decane | 0.06 | 0.72 | 0.59 | × | × |
| Undecane | 0.09 | 0.97 | 0.62 | × | × |
| Dodecane | 0.17 | 1.22 | 0.72 | 0.51 | 0.44 |
| Tridecane | 0.34 | 1.87 | 1.05 | 0.84 | 0.55 |
| Tetradecane | 0.74 | 2.57 | 1.34 | 1.39 | 0.78 |
| Pentadecane | 1.52 | 3.85 | 2.11 | 1.96 | `1.3 |
| Hexadecane | 0.59 | 2.59 | 1.90 | 1.38 | 1.45 |
| Heptadecane | 0.81 | 3.21 | 2.95 | 1.78 | 2.48 |
| Octadecane | × | 0.49 | 0.98 | 0.38 | 0.91 |
| **Phenols** | | | | | |
| Phenol | 0.58 | 0.94 | × | × | × |
| Methyl phenol | 1.26 | 1.25 | 0.47 | 0.31 | 0.25 |
| Ethyl phenol | 1.63 | 2.21 | 0.36 | 0.5 | 0.15 |
| Ethyl-methyl phenol | 0.69 | 2.08 | 0.39 | 0.25 | 0.15 |
| Ethyl-methoxy phenol | 2.19 | 0.98 | × | × | × |
| Methoxy phenol | 0.97 | 0.14 | × | × | × |
| **Nitrogen Heterocyclic Compounds** | | | | | |
| Pyridines | × | × | × | × | × |
| Pyrazines | 0.53 | 0.18 | 0.04 | × | × |
| Pyridinols | × | × | × | × | × |
| Indoles | 0.23 | 1.97 | 0.98 | × | × |
| Pyrroles | × | × | × | × | × |
| **Fatty Nitriles** | | | | | |
| Hexadecanenitrile | × | 0.38 | 0.52 | × | × |
| **Amino acids, Amines and Amides** | | | | | |
| Dimethylaminoanisole | × | × | × | × | × |
| **Fatty Acids & Fatty Alcohols** | | | | | |
| Benzoic acid | × | × | × | × | × |
| Benzenepropanoic acid | × | × | × | × | × |
| Acetic acid | × | × | × | × | × |
| Propanoic acid | × | × | × | × | × |
| Butanoic acid | 0.42 | × | × | × | × |
| Pentanoic acid | 0.43 | × | × | × | × |
| Hexanoic acid | 0.66 | × | × | × | × |
| Hexadecanoic acid | 0.02 | 0.06 | × | 0.1 | 0.16 |
| Octadecanoic acid | 0.01 | 0.01 | × | 0.01 | 0.01 |
| Octadecenoic acid | × | 0.03 | 0.04 | 0.05 | 0.07 |
| Propanoic acid mercapto-dodecyl ester | × | × | × | 0.11 | 0.11 |
| Propenoic acid, oxybis(methyl, ethanediyl) ester | × | × | × | 0.18 | 0.20 |
| Hexadecanoic acid, methyl ester | × | 0.51 | × | × | |

**(a)**

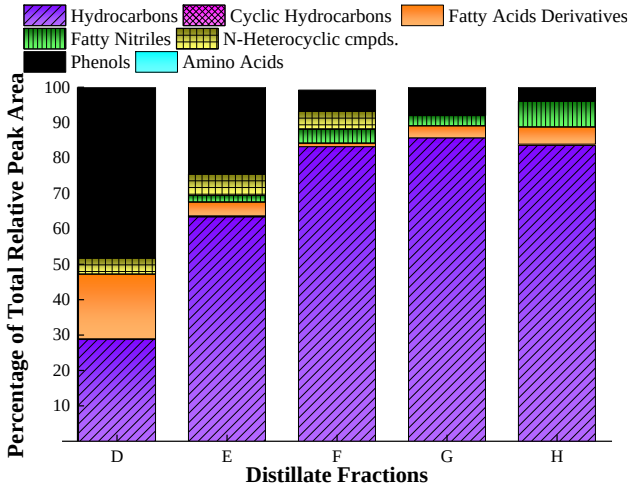


**(b)**

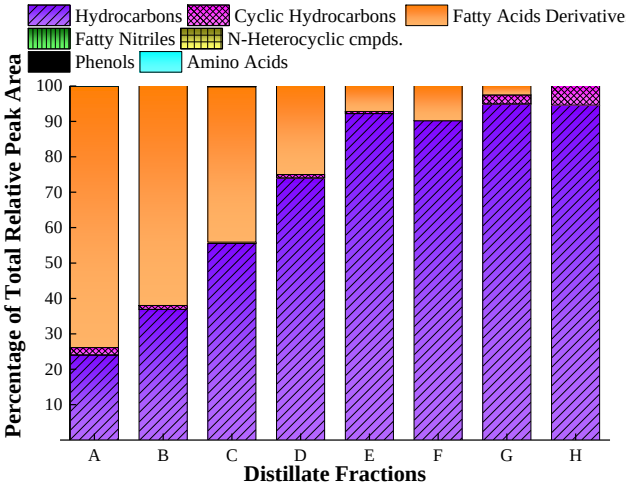


**(c)**

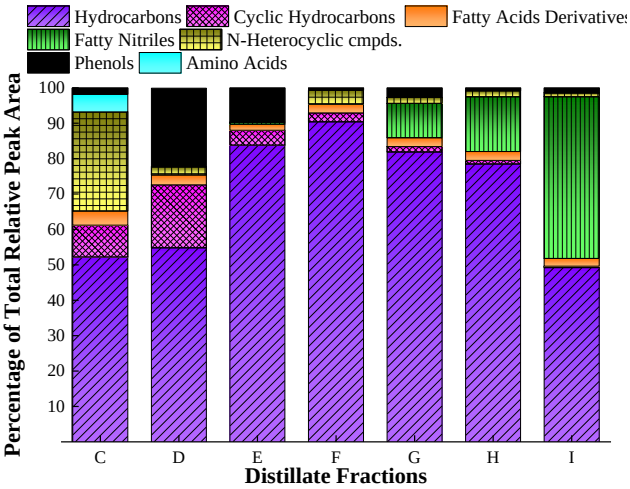


**Figure 7-7. Percentage of the total relative peak area of different chemical compositions obtained under GC-MS analysis for the distillates from (a) SW-, (b) FPW-, and (c) SP-derived biocrude oil**

**Table 7-8. Normalized GC-MS signals of components identified in the distillates from FPW-derived biocrude; "×" indicates the chemical was not detected**

| Compound Name | Normalized Signal (-) | | | | | | | |
|---|---|---|---|---|---|---|---|---|
| | A | B | C | D | E | F | G | H |
| **Hydrocarbons** | | | | | | | | |
| Octane | 0.26 | 0.43 | 0.46 | 0.58 | 0.53 | 0.51 | 0.42 | 0.33 |
| Nonane | 0.29 | 0.53 | 0.53 | 0.61 | 0.50 | 0.44 | 0.52 | 0.34 |
| Nonene | 0.21 | 0.20 | 0.23 | 0.33 | 0.26 | 0.25 | 0.30 | 0.19 |
| Decane | 0.12 | 0.28 | 0.41 | 0.50 | 0.43 | 0.42 | 0.51 | 0.36 |
| Undecane | 0.18 | 0.18 | 0.31 | 0.44 | 0.42 | 0.38 | 0.47 | 0.37 |
| Undecene | 0.18 | 0.18 | 0.31 | 0.44 | 0.42 | 0.38 | 0.47 | 0.37 |
| Dodecane | 0.24 | 0.11 | 0.17 | 0.25 | 0.19 | 0.20 | 0.26 | 0.21 |
| Dodecene | 0.24 | 0.11 | 0.17 | 0.25 | 0.19 | 0.20 | 0.26 | 0.21 |
| Tridecane | 0.14 | 0.26 | 0.43 | 0.59 | 0.50 | 0.42 | 0.46 | 0.33 |
| Tridecne | 0.23 | 0.17 | 0.27 | 0.39 | 0.28 | 0.28 | × | 0.22 |
| Tetradecane | 0.18 | 0.41 | 0.83 | 0.89 | 0.73 | 0.56 | 0.54 | 0.35 |
| Tetradecene | 0.15 | 0.40 | 0.36 | 0.66 | 0.42 | 0.39 | 0.47 | 0.32 |
| Pentadecane | 0.71 | 1.91 | 2.15 | 1.97 | 1.23 | 0.82 | 0.65 | 0.43 |
| Pentadecene | 0.20 | 0.29 | 0.38 | 0.49 | 0.34 | 0.33 | 0.35 | 0.24 |
| Hexadecane | × | 0.18 | 0.42 | 0.84 | 0.74 | × | 0.39 | 0.24 |
| Hexadecene | 0.04 | 0.11 | 0.15 | 0.24 | 0.28 | 0.28 | 0.27 | 0.19 |
| Heptadecane | 0.08 | 0.55 | 0.91 | 1.36 | 1.19 | 0.99 | 0.42 | 0.24 |
| Heptadecene | 0.08 | 0.68 | 0.45 | 0.27 | × | × | 0.14 | 0.10 |
| Octadecane | × | × | × | 0.11 | 0.26 | 0.48 | 0.25 | 0.17 |
| Nonadecane | × | × | 0.10 | 0.08 | 0.11 | 0.38 | 0.36 | 0.15 |
| Eicosane | × | × | × | × | × | 0.12 | 0.28 | × |
| **Cycloalkanes** | | | | | | | | |
| Nonyl Cyclohexene | × | 0.05 | 0.03 | 0.03 | × | × | × | × |
| Indene derivatives | × | × | 0.02 | 0.11 | 0.06 | × | 0.22 | 0.12 |
| Methyl naphthalene | 0.01 | 0.01 | 0.02 | 0.03 | × | × | × | 0.14 |
| **Phenols** | | | | | | | | |
| Phenol | × | × | × | × | × | × | × | × |
| Ditertbutyl phenol | 0.03 | × | 0.03 | 0.03 | × | × | × | × |
| **Oxygenates** | | | | | | | | |
| Heptadecanone | × | × | × | 0.03 | 0.06 | 0.21 | 0.14 | × |
| Cyclopentenone Derivatives | 0.07 | × | × | × | × | × | × | × |
| Acetic acid | 2.68 | × | × | × | × | × | × | × |
| Hexanoic acid | 0.78 | 0.60 | 0.36 | 0.23 | × | × | × | × |
| Heptanoic acid | 2.97 | 1.37 | 0.57 | 0.36 | × | × | × | × |
| Ocatanoic acid | 1.64 | 1.90 | 0.88 | 0.44 | × | × | × | × |
| Nonanoic acid | 0.61 | 2.41 | 1.54 | 0.74 | 0.14 | × | × | × |
| Dodecanoic acid | 1.32 | 0.05 | 0.14 | 0.10 | × | × | × | × |
| Hexadecanoic acid | 1.09 | 0.15 | 0.67 | 0.31 | × | × | × | × |
| Octadecanoic acid | 0.16 | 0.03 | 0.07 | 0.06 | × | × | × | × |
| Octadecenoic acid | 0.99 | 0.1 | 0.22 | 0.18 | 0.20 | 0.22 | × | × |
| Octadecadienoic acid | 0.75 | 0.09 | 0.15 | 0.24 | 0.32 | 0.44 | × | × |
| Methyl furancarboxaldehyde | 0.25 | × | × | × | × | × | × | × |
| Furfural | 0.09 | × | × | × | × | × | × | × |

Figure 7-7c and Table 7-9 summarized the chemical compositions of the distillates from SP-derived biocrude. GC-MS analysis was not conducted on fractions A and B, because they mainly contain water. Similarly to the distillates from SW- and FPW-derived biocrude, the middle fractions (E-I) from SP-derived biocrude are mostly composed of alkanes and alkenes with carbon numbers from 10-18. Notably, these distillates also contains branched alkanes and alkenes (*e.g.,* tetramethylhexadecane), which could be converted from Chlorophyll (Warneck, 1999). Furthermore, the distillates from SP-derived biocrude also contain phenols, nitrogen-heterocyclic compounds, and fatty nitriles. This is because SP feedstock majorly consists of proteins and therefore their distillates tend to include more nitrogen-containing compounds. Figure 7-7c and Table 7-9 also show that the fatty nitriles (*e.g.,* hexadecanenitrile) tend to distribute to the heavy fractions in the distillates from SP-derived biocrude, since fatty nitriles typically have a higher boiling point than hydrocarbons with the same carbon number. Additional upgrading processes would be essential for the distillates from SP-derived biocrude oil as well. Unlike for the distillates from SW- and FPW-derived biocrude oil, denitrogenation would be the major upgrading approach for SP-derived biocrude. Based on multiple previous studies upgrading algal HTL biocrude (Duan et al., 2013a; Duan & Savage, 2011b; Duan & Savage, 2011c; Zhao et al., 2012), catalysts such as Pd/Pt and HZSM-5 may effectively promote denitrogenation and deoxygenation of the distillates. Noble metals such as Pd and Pt have demonstrated an effective and highly selective deoxygenation and denitrogenation through hydrodeoxygenation of phenolic compounds, decarboxylation of fatty acids, and hydrodenitrogenation of pyridines under near- and super-critical water (Duan & Savage, 2011b; Fu et al., 2010; Zhao et al., 2009). Zeolites such as HZSM-5 have also been found effective in denitrogenating algal biocrude oil under supercritical water media (Duan & Savage, 2011c).

**Table 7-9. Normalized GC-MS signals of major components identified in the distillates from SP-derived biocrude; "×" indicates the chemical was not detected**

| Compound Name | Normalized Signal (-) | | | | | | |
|---|---|---|---|---|---|---|---|
| | C | D | E | F | G | H | I |
| **Hydrocarbons** | | | | | | | |
| Decane | × | 0.06 | 0.17 | 0.06 | 0.12 | 0.18 | 0.11 |
| Decene | × | 0.02 | 0.07 | 0.01 | 0.04 | 0.10 | 0.15 |
| Methyldecane | × | × | × | × | 0.02 | 0.02 | 0.01 |
| Undecane | 0.03 | 0.08 | 0.20 | 0.08 | 0.18 | 0.24 | 0.13 |
| Undecene | × | 0.01 | 0.14 | 0.01 | 0.09 | 0.13 | 0.18 |
| Demethylundecane | × | 0.03 | 0.05 | 0.04 | 0.03 | 0.03 | 0.03 |
| Dodecane | 0.02 | 0.09 | 0.26 | 0.12 | 0.24 | 0.30 | 0.15 |
| Dodecene | 0.05 | 0.09 | 0.28 | 0.23 | 0.44 | 0.49 | 0.47 |
| Trimethyldodecane | × | 0.02 | 0.06 | 0.05 | 0.06 | 0.02 | 0.02 |
| Tridecane | 0.03 | 0.15 | 0.36 | 0.25 | 0.40 | 0.39 | 0.20 |
| Tridecene | 0.01 | × | 0.12 | 0.05 | 0.15 | 0.20 | 0.18 |
| Methyltridecane | × | × | 0.03 | 0.02 | 0.02 | 0.03 | 0.02 |
| Tetradecane | × | 0.21 | 0.41 | 0.50 | 0.64 | 0.53 | 0.25 |
| Tetradecene | × | 0.03 | 0.07 | 0.09 | 0.10 | 0.10 | 0.06 |
| Pentadecane | 0.07 | 0.44 | 0.75 | 1.47 | 1.36 | 0.86 | 0.34 |
| Pentadecene | × | 0.05 | 0.09 | 0.18 | 0.26 | 0.23 | 0.17 |
| Tetramethylpentadecane | × | 0.01 | 0.03 | 0.13 | 0.15 | 0.07 | × |
| Hexadecane | 0.04 | 0.08 | 0.14 | 0.39 | 0.56 | 0.45 | 0.17 |
| Hexadecene | 0.01 | × | 0.03 | 0.16 | 0.29 | 0.34 | 0.18 |
| Tetramethylhexadecane | 0.01 | 0.03 | 0.15 | 0.71 | 0.96 | 0.67 | 0.14 |
| Tetramethylhexadecene | 0.21 | 0.11 | 0.17 | 0.24 | 0.07 | 0.03 | × |
| Heptadecane | 0.52 | 0.59 | 0.93 | 1.58 | 1.10 | 0.59 | 0.21 |
| Tetramethylheptadecane | × | × | × | × | 0.09 | 0.07 | 0.05 |
| Octadecane | × | × | × | 0.06 | 0.17 | 0.23 | 0.04 |
| **Cycloalkanes** | | | | | | | |
| Cumene | 0.04 | 0.05 | × | 0.03 | 0.02 | × | × |
| Ionene | 0.14 | 0.48 | 0.19 | 0.07 | 0.06 | 0.03 | 0.01 |
| Dimethylnaphthalene | × | × | 0.04 | 0.04 | 0.03 | 0.02 | 0.02 |
| **Phenols** | | | | | | | |
| Phenol | × | 0.50 | × | 0.02 | × | × | 0.02 |
| Methyl phenol | × | 0.31 | 0.26 | 0.03 | 0.08 | × | 0.01 |
| Dimethylphenol | × | × | 0.13 | × | 0.08 | 0.03 | 0.03 |
| **Oxygenates** | | | | | | | |
| Diethylene glycol dibenzoate | 0.08 | 0.11 | 0.09 | 0.11 | 0.13 | 0.13 | 0.13 |
| Hexadecacenol | × | × | × | 0.07 | 0.10 | 0.02 | × |
| **N-Heterocyclic Compounds** | | | | | | | |
| Methyl indole | × | × | × | 0.27 | 0.07 | 0.06 | × |
| Indolizine, 2-methyl-6-ethyl- | × | × | × | × | 0.09 | 0.08 | × |
| Pyrazine, 3-ethyl-2,5-dimethyl- | 0.13 | × | × | × | × | × | × |
| Pyrazine, ethyl-methyl | 0.14 | × | × | × | × | × | × |
| 1H-Pyrrole, 3-ethyl-2,4-dimethyl- | 0.03 | 0.02 | × | × | × | × | × |
| 1-Butyl-1H-Pyrrole | 0.06 | 0.05 | × | 0.01 | × | × | × |
| **Fatty Nitriles** | | | | | | | |
| Hexadecanenitrile | × | × | × | × | 0.86 | 1.21 | 2.60 |
| Heptadecanenitrile | × | × | × | × | 0.04 | 0.04 | 0.13 |

### 7.4.3 Acidity of different distillate fractions from various feedstocks

Based on the results from GC-MS analysis (Figure 7-7), the distillates from SW-, FPW-, and SP-derived distillates contain fatty acids and phenols that may cause too high of an acidity for fuel application. As a consequence, the acidities of these distillates were investigated and are presented in Figure 7-8. Figure 7-8 compares the relationship between the oxygen contents and acidities of different fractions from three feedstocks (FPW-, SW-, and SP-derived biocrude oil). For the distillates from FPW-derived biocrude, acidities (reduced from 208 mg KOH/g sample to 1 mg KOH/g sample) and oxygen contents (reduced from 13 wt.% to 0.6 wt.%) decreased as the distillation temperature increased. The oxygen content could mainly be attributed to the fatty acids for this kind of distillates. Moreover, the acidity of distillates from FPW-derived biocrude is much higher than the maximum value (0.3) for biodiesel application (ASTM, 2015b). Mild upgrading methods such as esterification would be suggested to reduce their acidity.

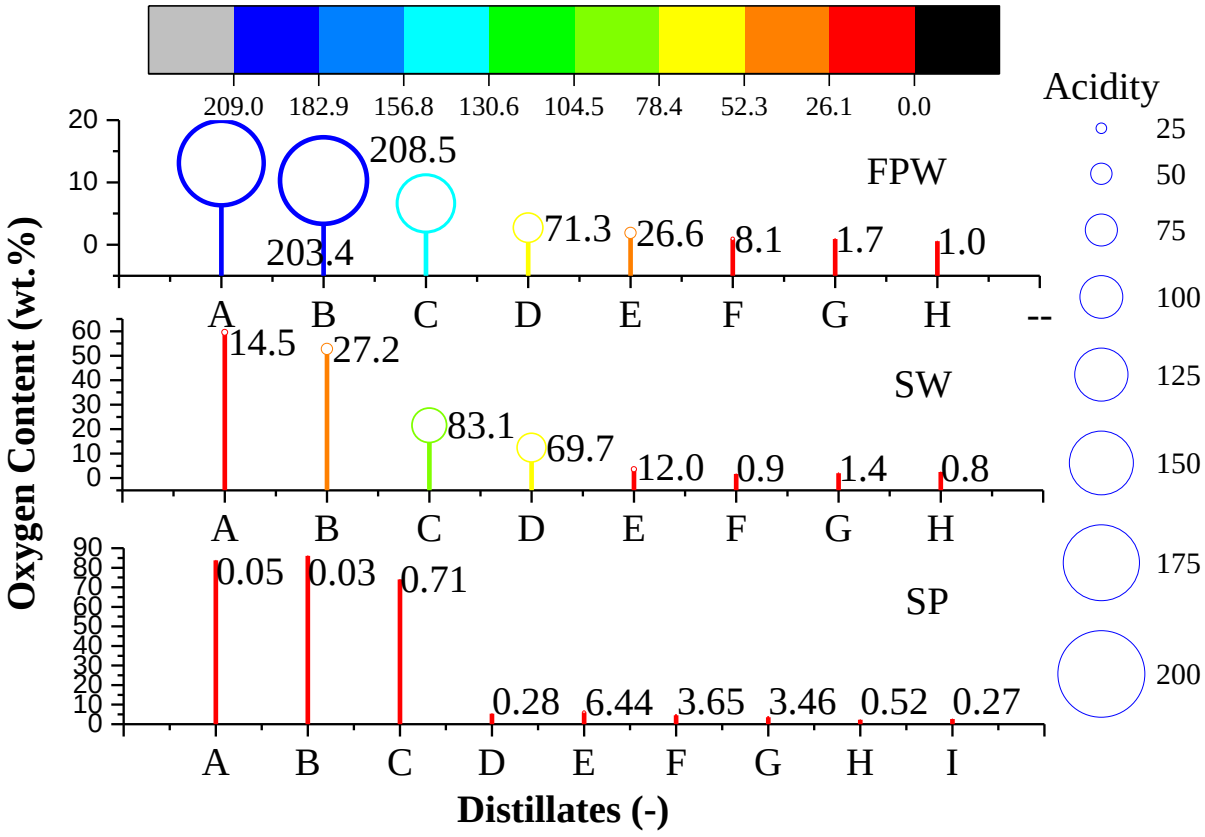


**Figure 7-8. The relationship between oxygen content and acidity of the distillates from FPW-, SW-, and SP-derived biocrude oil products**

Like the distillates from FPW-derived biocrude oil, the acidity and oxygen content of distillates from SW- and SP-derived biocrude oil both decreased with the distillation temperature.

Notably, since fractions A and B of both SW- and SP-derived biocrude oil mainly contained water, their respective acidities were lower than the acidity of fraction C. Among the three types of distillates, the acidity of the distillates from SP-derived biocrude is the smallest because these distillates also contain organic base compounds such as nitrogen-containing compounds that would neutralize the acidity attributed by phenols and acids. In contrast, the high acidity of the distillates from SW-derived biocrude oil is due to phenols and acids. Exploring approaches that can reduce their acidity caused by both phenols and acids is highly desirable for fuel application.

# CHAPTER 8. UPGRADING HTL BIOCRUDE OIL DISTILLATES CONVERTED FROM WET BIOWASTE VIA HTL

The distillate fractions with the closest physicochemical properties to transportation fuels were subjected to mild upgrading process such as esterification and neutralization. Energy efficiency and reaction severity were also compared among different upgrading methods.

## 8.1 Upgrading the distillates from FPW-derived biocrude oil

Literature has demonstrated that esterification is an effective method to reduce the acidity of high free fatty acid bio-oil from 40 mg KOH/g to <1 mg KOH/g (Canakci & Van Gerpen, 2001; Ghadge & Raheman, 2005; Naik et al., 2008). Therefore, the distillate fractions D, E, and F from FPW-derived biocrude were combined for further esterification, because of their moderate acidity (~35.3 in average), closer density (~816 kg/$m^3$ in average) and energy content (~47 MJ/kg in average) to petroleum diesel. The distillate fractions A, B, and C from FPW-derived biocrude oil contain two times higher acidity than the fractions D, E, and F, and hence were not selected for esterification. Figure 8-1 summarizes the yield and acidity of esterified oil samples through the OAD tests. It is found that the lowest acidity was achieved at experimental condition 3 (50°C, 2 hr, 2% $H_2SO_4$, and 1:15 molar ratio of FPW-distillates to methanol), while the esterification yield is about 85 wt.% for most of the experimental conditions, except the condition 8. Table 8-1 summarizes how each examined factor impacts the yield and acidity of esterified samples. By comparing the range of the mean values ($k_i$) obtained at each level of a factor, the relative importance of factors investigated can be realized. In terms of achieving the highest esterification yield, the relative importance of factors would be: time > molar ratio of feedstocks to methanol > $H_2SO_4$ concentration > temperature. It is generally believed that esterification is a slow reaction (Canakci & Van Gerpen, 2001; Leung et al., 2010). Thereby, a longer reaction time and a high molar ratio of feedstocks to methanol would help achieve a higher esterification yield. In terms of obtaining the lowest acidity, the relative importance of factors would be: temperature > time > $H_2SO_4$ concentration > molar ratio of feedstocks to methanol. High temperatures favor forward reactions and thus can reach a lower acidity. However, Figure 8-1 and Table 8-1 also suggest that an excessively high temperature is not recommended, because methanol would be vaporized over its boiling point (*i.e.*, 65°C) (Canakci & Van Gerpen, 2001; Ghadge & Raheman, 2005).

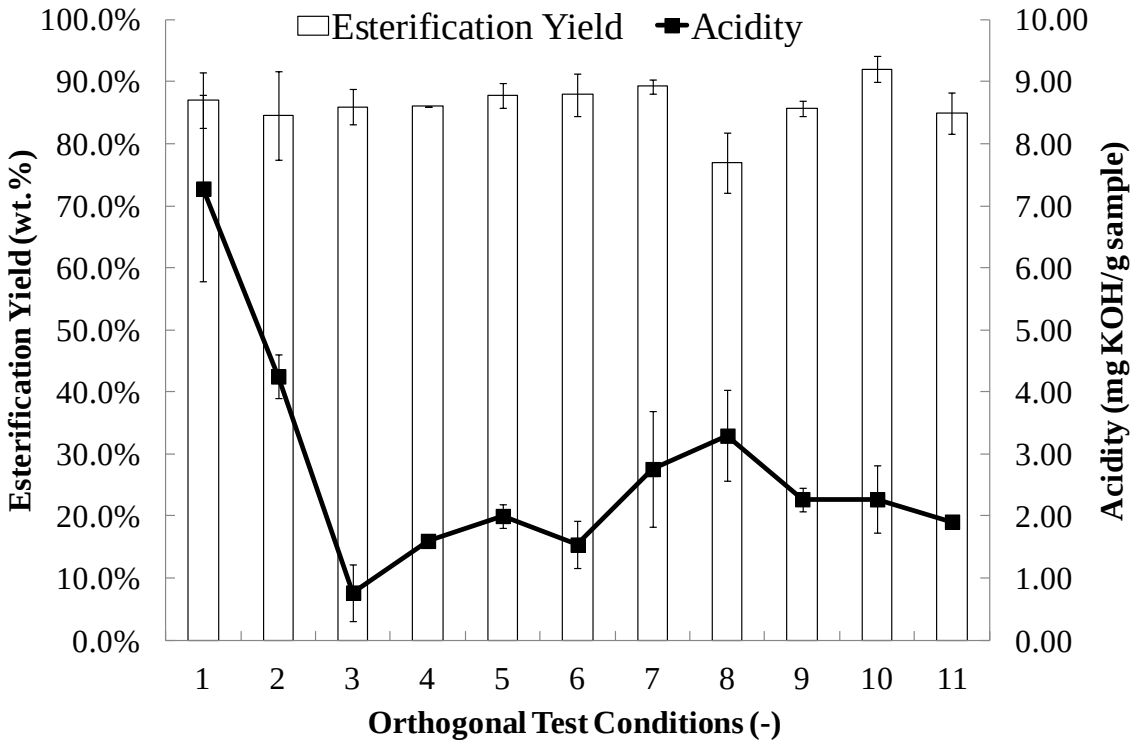


**Figure 8-1. Yield and acidity of esterified distillates obtained from the OAD tests**

**Table 8-1. The mean values ($k_i$) of yield and acidity of esterified products at each level of a factor**

| Property | $k_i$ | T (°C) | Time (hr) | Catalyst Loading (wt.%) | Molar ratio of feedstocks to methanol (-) |
|---|---|---|---|---|---|
| Esterification Yield (wt.%) | $k_1$ | 85.9 | 87.4 | 84.0 | 86.9 |
| | $k_2$ | 87.3 | 83.2 | 85.5 | 87.3 |
| | $k_3$ | 84.0 | 86.5 | 87.7 | 83.0 |
| | Range | 3.2 | 4.3 | 3.7 | 3.8 |
| Acidity (mg KOH/g distillate) | $k_1$ | 4.10 | 3.88 | 4.04 | 3.85 |
| | $k_2$ | 1.71 | 3.18 | 2.71 | 2.85 |
| | $k_3$ | 2.77 | 1.52 | 1.84 | 1.89 |
| | Range | 2.39 | 2.35 | 2.20 | 1.96 |

Esterified samples that present the highest (conditions 1 and 8) and the lowest acidities (conditions 3 and 6) were also subjected to elemental and GC-MS analysis to confirm their energy contents (Table 8-2) and chemical composition after esterification (Figure 8-2 and Table 8-3). Elemental analysis validates that the energy content of esterified samples are slightly increased (from 46 to 47 MJ/kg), because of the increasing carbon and hydrogen contents that

mainly attributed to successful esterifications of fatty acids into fatty acid methyl esters (FAME) though (Table 8-2). Further, GC-MS analysis demonstrates that esterified samples obtained at the experimental conditions 1 and 8 contain lower concentrations of FAME (Table 8-3) than those at the experimental conditions 3 and 6. These results also suggest that esterification was less efficient at those conditions.

**Table 8-2. Elemental compositions of FPW-derived distillates before and after esterification**

| Sample | C (wt.%) | H (wt.%) | N (wt.%) | O (wt.%) | HHV (MJ/kg) |
|---|---|---|---|---|---|
| D-F before esterification | 84.0 ± 0.00 | 12.9 ± 0.01 | 0.28 ± 0.00 | 2.91 | 46.2 |
| Ester-1 | 84.1 ± 0.06 | 12.9 ± 0.2 | 0.11 ± 0.03 | 2.84 | 46.3 |
| Ester-3 | 84.3 ± 0.1 | 12.8 ± 0.1 | 0.14 ± 0.01 | 2.71 | 46.3 |
| Ester-6 | 84.5 ± 0.04 | 13.3 ± 0.09 | 0.19 ± 0.03 | 2.07 | 47.1 |
| Ester-8 | 84.3 ± 0.09 | 13.3 ± 0.01 | 0.14 ± 0.00 | 2.30 | 47.0 |

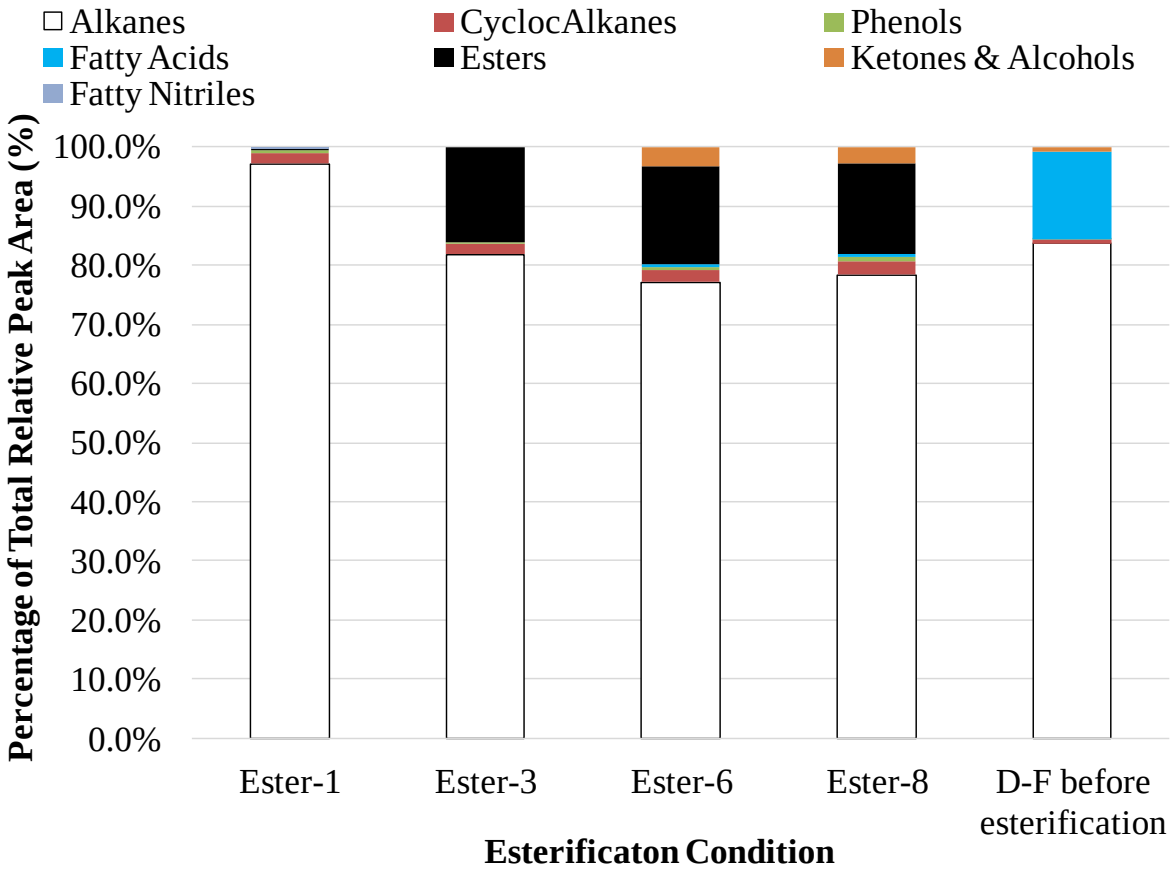


**Figure 8-2. Chemical compositions of selected FPW-distillates with different esterification conditions**

**Table 8-3. Normalized GC-MS signals of major components identified in the esterified distillates from FPW-derived biocrude; "×" indicates the chemical was not detected**

| Compound Name | Normalized Signal (-) | | | | |
|---|---|---|---|---|---|
| | 1 | 3 | 6 | 8 | D-F before esterification |
| **Hydrocarbons** | | | | | |
| Octane | 0.43 | 0.38 | 0.33 | 0.25 | 0.54 |
| Nonane | 0.39 | 0.35 | 0.35 | 0.26 | 0.52 |
| Decane | 0.31 | 0.32 | 0.30 | 0.23 | 0.45 |
| Undecane | 0.31 | 0.30 | 0.28 | 0.21 | 0.41 |
| Dodecane | 0.34 | 0.34 | 0.30 | 0.24 | 0.33 |
| Tridecane | 0.44 | 0.43 | 0.43 | 0.34 | 0.50 |
| Tetradecane | 0.61 | 0.59 | 0.60 | 0.42 | 0.72 |
| Tetradecene | 0.45 | 0.46 | 0.54 | 0.40 | 0.49 |
| Pentadecane | 1.32 | 1.24 | 1.25 | 0.96 | 1.34 |
| Pentadecene | 0.36 | 0.34 | 0.36 | 0.25 | 0.39 |
| Hexadecane | 0.70 | 0.55 | 0.55 | 0.38 | 0.53 |
| Heptadecane | 1.07 | 1.01 | 1.01 | 0.8 | 1.18 |
| Octadecane | 0.21 | 0.21 | 0.19 | 0.15 | 0.28 |
| Nonadecane | 0.23 | 0.21 | 0.20 | 0.16 | 0.19 |
| Eicosane | 0.06 | 0.05 | 0.05 | 0.04 | 0.04 |
| **Cycloalkanes** | | | | | |
| Indene derivatives | 0.11 | 0.04 | 0.04 | 0.03 | 0.06 |
| **Phenols** | | | | | |
| Ditertbutyl phenol | 0.02 | 0.02 | 0.02 | 0.02 | 0.02 |
| **Fatty Acid Methyl Esters (FAME)** | | | | | |
| Pentanoic acid, methyl ester | × | 0.05 | 0.06 | 0.04 | × |
| Hexanoic acid, methyl ester | 0.01 | 0.1 | 0.12 | 0.09 | × |
| Hexenoic acid, methyl ester | × | 0.02 | × | × | × |
| Heptanoic acid, methyl ester | 0.02 | 0.17 | 0.18 | 0.14 | × |
| Heptenoic acid, methyl ester | × | 0.03 | 0.04 | 0.03 | × |
| Octanoic acid, methyl ester | × | 0.29 | 0.25 | 0.19 | × |
| Octenoic acid, methyl ester | × | 0.07 | 0.07 | 0.06 | × |
| Nonanoic acid, methyl ester | × | 0.39 | 0.37 | 0.24 | × |
| Undecanoic acid, methyl ester | × | 0.2 | 0.17 | 0.1 | × |
| Decanoic acid, methyl ester | × | × | 0.33 | 0.24 | × |
| Hexadecanoic acid, methyl ester | × | 0.34 | 0.22 | 0.13 | × |
| Octadecenoic acid ethyl ester | × | 0.02 | × | × | × |
| Pentanoic acid, methyl ester | × | 0.05 | 0.06 | 0.04 | × |
| Hexanoic acid, methyl ester | 0.01 | 0.1 | 0.12 | 0.09 | × |
| **Ketones & Alcohols** | | | | | |
| Heptadecanone | × | × | 0.07 | × | 0.10 |

In order to make the FPW-distillates suitable for transportation fuel application, their acidity has to be reduced to as low as possible. As a result, more esterification tests regarding the effect of the molar ratio of FPW-distillates to methanol (Table 8-4) and reaction time (Table 8-5) were conducted. Considering future up-scaling of the present work, it is preferred to conduct esterification at reaction temperatures that are as low as possible, so that higher energy efficiency can be achieved and the necessity to pressurize the reaction system can be avoided. As a result, reaction temperature of 50°C is selected because the lowest acidity was gained at this

temperature via the OAD test. Further, since it is challenging to recover homogeneous catalysts ($H_2SO_4$) during esterification, the effect of higher concentrations of $H_2SO_4$ on esterification was not studied. A 2 wt.% $H_2SO_4$ is selected for additional tests.

**Table 8-4. The effect of the molar ratio of FPW-distillates to methanol on esterification yield and acidity at 50°C with 2% Sulfuric acid for 2hr reaction time**

| Sub: MeOH molar ratio (-) | Yield (wt.%) | Acidity (mg KOH/g sample) |
|---|---|---|
| 1:5 | 91.4 | 5.78 |
| 1:9 | 92.0 ± 2.1 | 2.27 ± 0.6 |
| 1:15 | 86.0 ± 2.8 | 0.76 ± 0.5 |

To reduce the amount of methanol used in esterification, lower molar ratios of FPW-distillates to methanol were studied. As the molar ratios of FPW-distillates to methanol were reduced from 1:15 (optimal conditions from ODA test) to 1:9 and then to 1:5 at 50°C for 2hr with 2 wt.% $H_2SO_4$, the acidity of the esterified sample is increased from 0.8 to 2.3 and then to 5.8 mg KOH/sample (Table 8-4). Notably, the maximum acidity for diesel is 0.3 mg KOH/sample. Assuming the esterified sample is used as B10 drop-in diesel (*i.e.*, 10% biodiesel plus 90% petroleum diesel), the maximum acidity for the esterified sample would be 3.0 mg KOH/sample. Hence, a 1:9 molar ratio of FPW-distillates to methanol was selected for further investigation, because fewer amounts of methanol would be used to achieve a qualified acidity in this case.

**Table 8-5. The effect of the reaction time on esterification yield and acidity at 50°C with 2% Sulfuric acid and a 1:9 molar ratio of methanol to FPW-distillates**

| Time (hr) | Yield (wt.%) | Acidity (mg KOH/g sample) | Note |
|---|---|---|---|
| 2 | 92.0 ± 2.1 | 2.27 ± 0.6 | Select for mass production |
| 4 | 90.7 ± 2.9 | 0.92 ± 0.04 | |
| 6 | 90.4 | 1.10 | |

Table 8-5 shows the effect of the reaction time on esterification yield and acidity at 50°C with 2% $H_2SO_4$ and a 1:9 molar ratio of methanol to FPW-distillates. As the reaction time increased from 2hr to 4 hr and then to 6hr, the acidity of the esterified samples reduced from 2.3 to 0.9 and then slightly increased to 1.1 mg KOH/sample, while the yields are around 90-92 wt.%. Thereby, a 4hr reaction time was chosen to prepare esterified FPW-distillates for fuel spec and diesel engine tests later on.

## 8.2 Upgrading the distillates from SW-derived biocrude oil

According to preliminary observation, mixing the distillate fractions F, G, and H from SW-derived biocrude with transportation fuels, such as diesel and aviation fuel (Appendix A-8), demonstrates a significant amount of existent gum in the drop-in biofuel. In fact, it was found that there were brownish precipitates in the bottom of the drop-in biofuel prepared with the distillates from SW-derived biocrude. The precipitates were extracted with toluene and ethanol for GC-MS analysis with derivative treatment (Figure A-8). Figure A-8 shows that the precipitates were mainly composed of phenols (*e.g.*, methyl phenol), acids (*e.g.*, palmitic acid), nitrogen-heterocyclic compounds (*e.g.*, pyridines), and amino acids (*e.g.*, glycines). Particularly, 50-60% percentage of relative peak area is attributed to phenols. This finding also emphasizes the necessity to upgrade the distillates from SW-derived biocrude.

Excessive gum content in the distillates from SW-derived biocrude oil could lead to potential issues (*e.g.*, storage and transportation) when using this type of distillates for fuel application. In order to reduce the gum content, which is primarily caused by phenolic compounds in the distillates from SW-derived biocrude oil, neutralization was selected for upgrading the distillates. It is hypothesized that sodium hydroxide (NaOH) would react with phenols and thus reduce the major compounds in the gum contents. The distillate fractions F, G, and H from SW-derived biocrude were combined for further neutralization because of their closer density (865 $kg/m^3$ in average) and energy content (44.7 MJ/kg in average) to petroleum diesel.

The highest neutralized biofuel yield (83.1 wt.%) is found at condition 4 (35°C, 0.5 hr, 2M NaOH, and 2:1 weight ratio of SW-distillates to NaOH). When blending the 10 vol.% neutralized distillates with 90 vol.% regular diesel (SW-HTL10), the lowest gum content (0.33 wt.%) of the drop-in biodiesel sample was achieved at experimental condition 9 (45°C, 2 hr, 2M NaOH, and 1:3 weight ratio of SW-distillates to NaOH) (Figure 8-3). Compared to the gum content in regular diesel (0.58 wt.%), the gum content of neutralized biofuel samples was reduced by 43%. Table 8-6 summarizes how each examined factor impacts the yield and gum contents of neutralized samples. By comparing the range of the mean values ($k_i$) obtained at each level of a factor, the relative importance of factors investigated in this study can be understood. In terms of achieving the highest neutralization yield, the relative importance of factors would be: reaction time > concentration of NaOH > weight ratio of distillates to NaOH > reaction

temperature. In general, neutralization of acids and bases happen readily. In other words, neutralization normally is not a rate-limited reaction. However, in the present study, reaction time turns out to be the most dominant factor affecting the neutralized biofuel yield. This is probably attributed to the viscosity of the distillates from SW-derived biocrude oil. As Table 7-5 presents, the kinematic viscosity of the fractions F-H from SW-derived biocrude oil is in the range of 4.09-9.11 $mm^2/s$, which is four to nine times higher than aqueous solution (about 1 $mm^2/s$). This relatively high kinematic viscosity may make diffusion of phenols to NaOH solutions a rate-limiting reaction. Hence, a longer reaction time and a higher concentration of NaOH may help achieve a higher neutralized biofuel yield. In terms of obtaining the lowest gum content, the relative importance of factors would be: temperature > weight ratio of distillates to NaOH > reaction time > concentration of NaOH. High temperatures favor forward reactions and thus can reach a lower gum content.

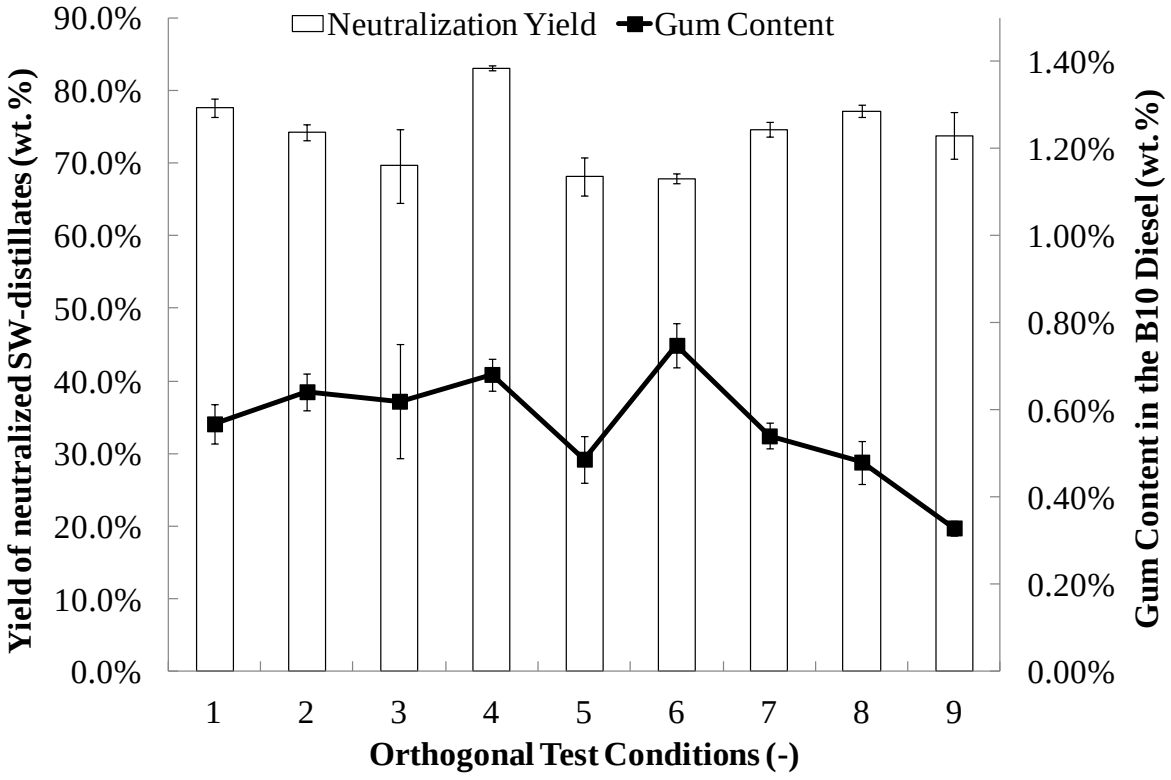


**Figure 8-3. Neutralized biofuel yield and gum content of SW-HTL10 drop-in biodiesel samples obtained from the OAD tests**

**Table 8-6. The mean values ($k_i$) of yield and gum contents of neutralized products at each level of a factor**

| Property | $k_i$ | T (°C) | Time (hr) | Concentration of NaOH (M) | Weight ratio of distillates to NaOH |
|---|---|---|---|---|---|
| Neutralization Yield (wt.%) | $k_1$ | 73.8 | 78.4 | 74.2 | 73.2 |
| | $k_2$ | 73.0 | 73.2 | 77.1 | 72.3 |
| | $k_3$ | 75.2 | 70.4 | 70.8 | 76.6 |
| | Range | 1.4 | 8.0 | 6.3 | 4.4 |
| Gum Content (wt.%) | $k_1$ | 0.61 | 0.60 | 0.60 | 0.46 |
| | $k_2$ | 0.64 | 0.54 | 0.55 | 0.64 |
| | $k_3$ | 0.45 | 0.57 | 0.55 | 0.59 |
| | Range | 0.19 | 0.06 | 0.05 | 0.18 |

Neutralized samples that present relatively higher (conditions 4 and 6) and relatively lower gum content (conditions 8 and 9) were subjected to elemental analysis to confirm their energy contents (Table 8-7). Samples with the highest (condition 4) and the lowest (condition 9) gum content were then analyzed with GC-MS to understand their chemical compositions after neutralization (Figure 8-4 and Table 8-8). Elemental analysis validates that the energy content of neutralized samples are slightly increased (from 46 to 47 MJ/kg) because of the increasing carbon and hydrogen contents that mainly attributed to effective removal of phenols and fatty acids (Table 8-8).

**Table 8-7. Elemental compositions of SW-derived distillates before and after neutralization**

| Sample | C (wt.%) | H (wt.%) | N (wt.%) | O (wt.%) | HHV (MJ/kg) |
|---|---|---|---|---|---|
| F-H before neutralization | 82.8 ± 0.3 | 12.8 ± 0.0 | 1.55 ± 0.01 | 2.88 | 45.7 |
| Neu-4 | 83.6 ± 0.03 | 13.2 ± 0.4 | 2.01 ± 0.3 | 1.27 | 46.8 |
| Neu-6 | 83.5 ± 0.3 | 12.7 ± 0.0 | 2.88 ± 0.01 | 1.00 | 46.1 |
| Neu-8 | 83.0 ± 0.6 | 12.3 ± 0.02 | 2.22 ± 0.04 | 2.53 | 45.1 |
| Neu-9 | 83.4 ± 0.07 | 13.3 ± 0.1 | 2.28 ± 0.2 | 0.98 | 47.0 |

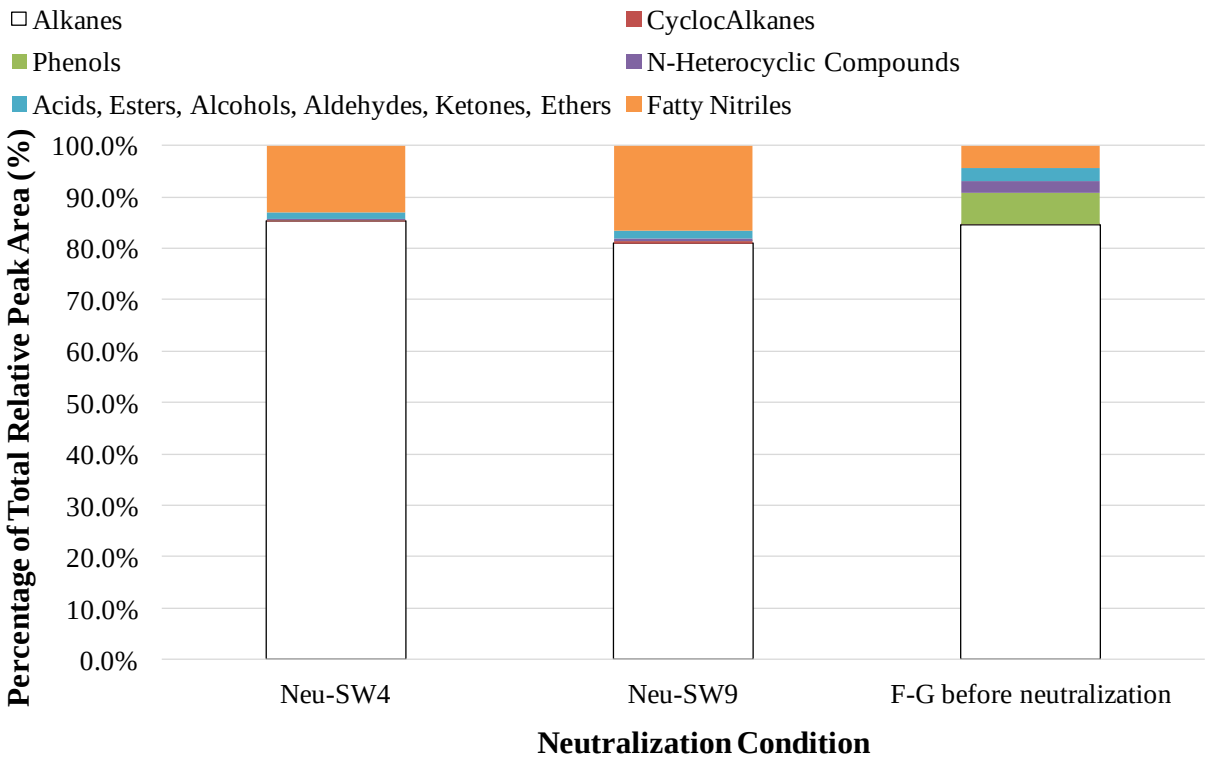


**Figure 8-4. Chemical compositions of selected SW-distillates with different neutralization conditions**

In order to make the SW-distillates suitable for transportation fuel application, their gum content has to be reduced to as low as possible. Consequently, more neutralization tests regarding the effects of the concentration of NaOH (Table 8-9), the weight ratio of NaOH to the distillates (Table 8-10), and reaction time (Table 8-11) were conducted. Considering future up-scaling of the present work, it is preferred to conduct neutralization at reaction temperature as low as possible, so that higher energy efficiency can be achieved and the operational cost can be minimized. Thus, the reaction temperature of 45°C is selected because the lowest gum content was obtained at this temperature via the OAD test. Further test regarding higher reaction temperature (*i.e.*, T> 45°C) was not studied.

**Table 8-8. Normalized GC-MS signals of major components identified in the neutralized distillates from SW-derived biocrude; "×" indicates the chemical was not detected**

| Compound Name | Normalized Signal (-) | | |
|---|---|---|---|
| | 4 | 9 | F-G before neutralization |
| **Hydrocarbons** | | | |
| Octane | × | × | 0.11 |
| Nonane | × | × | 0.13 |
| Decane | 0.28 | 0.34 | 0.20 |
| Undecane | 0.34 | 0.44 | 0.21 |
| Dodecane | 0.47 | 0.56 | 0.56 |
| Tridecane | 0.66 | 0.91 | 0.81 |
| Tetradecane | 0.91 | 1.03 | 1.17 |
| Tetradecene | 0.09 | 0.53 | 0.51 |
| Pentadecane | 1.25 | 1.38 | 1.79 |
| Pentadecene | 0.3 | 0.36 | 0.61 |
| Hexadecane | 1.17 | 1.27 | 1.58 |
| Heptadecane | 1.85 | 2.00 | 2.40 |
| Octadecane | 0.79 | 0.90 | 0.76 |
| Nonadecane | 0.33 | 0.39 | 0.22 |
| Eicosane | × | 0.14 | × |
| Heneicosane | 0.06 | 0.06 | × |
| Tricosane | 0.02 | 0.01 | × |
| **Cycloalkanes** | | | |
| Indene derivatives | × | 0.06 | 0.01 |
| Naphthalene derivative | 0.01 | 0.01 | 0.003 |
| **Phenols** | | | |
| Methylphenol | × | × | 0.34 |
| Ethylphenol | × | × | 0.34 |
| Ethyl-, Methylphenol | × | × | 0.26 |
| Dimethyl phenol | × | 0.0003 | 0.003 |
| Diethyl phenol | × | × | 0.007 |
| Benzene, 1-methoxy-4-(1-methylethyl)- | × | × | 0.01 |
| **N-Heterocyclic Compounds** | | | |
| Pyrazine Derivatives | × | × | 0.01 |
| Indole Derivative | 0.03 | 0.08 | 0.32 |
| **Fatty Nitriles** | | | |
| Tetradecanenitrile | × | 0.02 | × |
| Hexadecanenitrile | 0.76 | 0.46 | 0.17 |
| Heptadecanenitrile | × | 1.00 | 0.21 |
| Octadecanenitrile | 0.86 | 1.09 | 0.05 |
| **Acids, Esters, Alcohols, Ketones** | | | |
| Palmitic acid | × | × | 0.09 |
| Stearic acid | × | × | 0.007 |
| Octadecenoic acid | × | × | 0.05 |
| Propanoic acid, 3-mercapto-, dodecyl ester | × | × | 0.07 |
| 2-Propenoic acid, oxybis(methyl-2,1-ethanediyl) ester | × | × | 0.13 |
| Heptadecanone | × | × | 0.04 |

In order to further reduce the gum contents in the distillates from SW-derived biocrude oil, higher concentration of NaOH was used in neutralization. As the concentration of NaOH increased from 2M to 5M at 40°C for 2hr with a 1:3 weight ratio of SW-distillates to NaOH (optimal conditions from ODA test), the gum content of neutralized samples was increased from 0.33 to 0.46 wt.% while the neutralized biofuel yield was decreased from 73.8 wt.% to 64.0 wt.% (Table 8-9). This could be a result of the phenols and fatty acids in SW-distillates having completely reacted with a 2M NaOH solution. When the concentration of NaOH increased, the reaction of scheme 4-2 might be reversed because of Le Chatelier's principles and thus increase the concentration of phenols and gum contents in neutralized biofuel samples. Furthermore, excessive amounts of NaOH may react with other compounds in SW-distillates and hence reduce the neutralized biofuel yield. More chemical analyses such as GC-MS and derivative GC-MS are recommended to elucidate how excessive amounts of NaOH may affect the neutralized reaction.

**Table 8-9. The effect of the concentration of NaOH on neutralization yield and gum content of SW-distillates at 45°C for a 2hr reaction time with a 1:3 weight ratio of SW-distillates to NaOH**

| Concentration of NaOH (M) | Yield (wt.%) | Gum Content (wt.%) |
|---|---|---|
| 2 | 73.8 ± 3.2 | 0.33 ± 0.02 |
| 5 | 64.0 ± 0.5 | 0.46 ± 0.09 |

A higher molar ratio of SW-distillates to NaOH was also employed to further reduce the gum contents in the distillates from SW-derived biocrude oil. As the weight ratio of SW-distillates to NaOH increased from 1:3 (optimal conditions from ODA test) to 1:5 at 45°C for 2hr with 2M NaOH, the neutralized biofuel yield was reduced from 73.8 to 60.7 wt.% while the gum content of the neutralized sample was increased from 0.33 wt.% to 0.53 wt.% (Table 8-10). Similar to the results found in Table 8-9, when the ratio of NaOH to SW-distillates increased, the reaction of scheme 4-2 might also be reversed due to the increase of water (*i.e.*, Le'chatelier principles) and hence increase the concentration of phenols and gum contents in neutralized biofuel samples. Moreover, excessive amounts of water might extract compounds in SW-distillates (*e.g.*, N-heterocyclic compounds) and thus reduce the neutralized biofuel yield (Chen et al., 2016b).

**Table 8-10. The effect of the weight ratio of SW-distillates to NaOH on neutralization yield and gum content of SW-distillates at 45°C for a 2hr reaction time with 2M NaOH**

| Weight Ratio of NaOH to SW-distillates (-) | Yield (wt.%) | Gum Content (wt.%) |
|---|---|---|
| 1:3 | 73.8 ± 3.2 | 0.33 ± 0.02 |
| 1:5 | 60.7 ± 1.9 | 0.53 ± 0.07 |

Since a higher concentration of NaOH and molar ratio of SW-distillates to NaOH did not further decrease the gum content of neutralized biofuel, a longer reaction time was used. Table 8-11 demonstrates that when the reaction time of neutralization increased from 1hr to 24 hr, the gum content of neutralized biofuel reduced from 0.47 wt.% to 0.31 wt.%. This result implies that diffusion could be the rate-limiting reaction in this case. As a result, a 25°C and 24hr reaction time was chosen to prepare neutralized SW-distillates for fuel specification analyses.

**Table 8-11. The effect of reaction time on neutralization yield and gum content of SW-distillates for a 2hr reaction time with 2M NaOH and a 1:3 weight ratio of SW to NaOH**

| Temperature (°C) | Time (hr) | Yield (wt.%) | Gum Content (wt.%) |
|---|---|---|---|
| 25 | 24 | 70.3 ± 1.7 | 0.31 ± 0.03 |
| 55 | 2 | 80.4 ± 2.9 | 0.45 ± 0.12 |
| 45 | 1 | 72.5 | 0.47 |

### 8.3 Energy Consumption Ratio and Reaction Severity of Different Upgrading Approaches

Currently, available upgrading techniques for HTL biocrude include sub-/super-critical fluid (SCF) treatment (Duan et al., 2013a; Duan & Savage, 2011c; Peterson et al., 2008; Zhang et al., 2013a), (hydro)cracking (Cheng et al., 2014a; Mortensen et al., 2011), hydrotreating (Biller et al., 2015; Furimsky & Massoth, 2005), and separation (*e.g.*, distillation) from HTL biocrude oil (Chen et al., 2016b; Cheng et al., 2014b; Eboibi et al., 2014a; Hoffmann et al., 2016b; Ott et al., 2008). Figure 8-5 compares the energy consumption ratio and reaction severity of different available upgrading methods. Energy consumption ratio (ECR) can be considered as the energy required for upgrading against the energy that can be recovered from upgraded HTL biocrude oil combustion. Distillation plus mild upgrading (*i.e.*, esterification and neutralization) demonstrates a competitive energy consumption ratio (0.03-0.06 with 50% heat recovery) to zeolite cracking (0.07 with 50% heat recovery), SCF treatment (0.17 with 50% heat recovery), and hydrotreating (0.24 with 50% hear recovery) (Cheng et al., 2014a; Duan et al., 2013a; Elliott

et al., 2013; Zhang et al., 2013a). This is because that zeolite cracking and SCF treatment typically occur at relatively high temperature (400-425°C) and only lead to a HHV of 40-43 MJ/kg of upgraded HTL biocrude. Similarly, hydrotreating also happens under high temperature (~400°C) and with high pressure of hydrogen (*e.g.*, 6 MPa $H_2$ under batch conditions, 0.043g $H_2$/g HTL biocrude oil, and/or 85 L/hr $H_2$ under continuous conditions) (Duan et al., 2013a; Elliott et al., 2013; Jones et al., 2014). Typically, the yield and HHV of hydrotreated HTL biocrude oil can be as high as 82 wt.% and 47 MJ/kg, respectively. However, the large consumption of hydrogen and pressurized equipment may raise issues for energy efficiency, up-scaling, and techno-economic feasibility, since hydrogen gas is also a valuable energy source (120-142 MJ/kg).

Reaction severity ($R_o$) is a metric combining the effect of reaction temperature and time of a process and thus is used to evaluate the severity of different upgrading processes in this part of study (Eboibi et al., 2014b; Faeth et al., 2013). As Figure 8-5 shows, distillation (with log $R_o$ of 5.9-9.5) presents a lower reaction severity than zeolite cracking (with log $R_o$ of 11.0), SCF treatment (with log $R_o$ of 10.6), and hydrotreating (with log $R_o$ 11.5). This is mainly due to that zeolite cracking, SCF treatment and hydrotreating generally occurring at higher temperatures (400-425°C) than those for distillation (220-330°C). In short, considering the energy consumption ratio and reaction severity of different upgrading approaches, distillation is an advantageous method to upgrade HTL biocrude oil into transportation fuels.

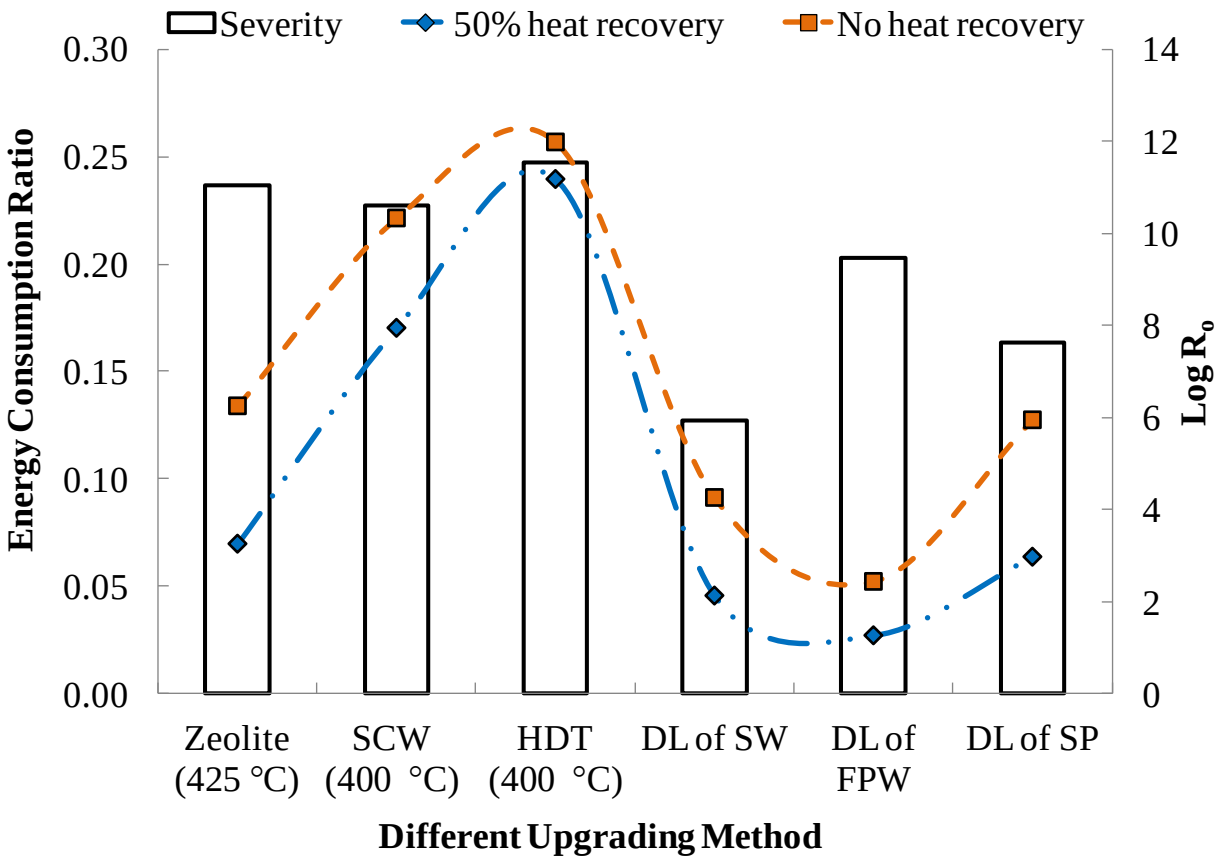


**Figure 8-5. Energy consumption ratio and severity of different strategies to upgrade HTL biocrude oil (data for zeolite cracking is adapted from Cheng et al.(2014) (Cheng et al., 2014a); data for hydrocracking is adapted from Duan et al. (2013) (Duan et al., 2013a); data for hydrotreating is adapted from Elliott et al. (2013) and Jones et al. (2014) (Elliott et al., 2013; Jones et al., 2014)**

# CHAPTER 9. FUEL SPECIFICATION ANALYSIS AND DIESEL ENGINE TEST OF UPGRADED HTL DISTILLTES

A highly desirable feature of biocrude application in practice is to produce a blendable product (*e.g.,* drop-in biofuel) with properties that fall within international standards (*e.g.,* ASTM guidelines), so that conventional distribution capabilities could be employed(Cole et al., 2016). However, fuel specification analysis and engine tests of drop-in biofuel refined from HTL biocrude oil are limited due to the amount of biocrude oil that can be produced via lab scale reactor. Furthermore, the upgradation of biocrude oil remains a bottleneck for synthesizing stable biofuels for engine tests. Thereby, the feasibility of biocrude oil as an alternative transportation fuel was unknown.

Nevertheless, this present study has demonstrated that the distillation and upgrading processes such as esterification can successfully enable HTL biocrude to be used as drop-in biofuel. The flowability, viscosity, and acidity of the HTL biocrude have been substantially improved after distillation and upgrading. As a consequence, drop-in biofuel that contains 10-20 vol.% of upgraded distillates was then subjected to fuel specification analysis and diesel engine test. Engine tests are one of the significant components to demonstrate the feasibility of using HTL biocrude oil as drop-in bifuel. Through engine tests, the power generated as well as the particulate matter (soot), unburned hydrocarbons (HC), CO, $CO_2$, and $NO_x$ emitted by the drop-in biofuel would be evaluated. Simultaneously, drop-in biofuel utilization issues such as the oxidation stability and engine compatibility will be realized.

The distillates from FPW-derived biocrude oil were selected for further fuel specification analysis and diesel engine test, because they demonstrate the lowest energy consumption ratio and closest physicochemical properties (*e.g.,* viscosity) to those of diesel. The fractions D-G (esterified fractions D-F plus fraction G) from FPW-derived biocrude oil, the upgraded fractions F-H from SW-derived biocrude oil, and the fractions G-I from SP-derived biocrude oil, were used to synthesize drop-in biodiesel. The drop-in biodiesel was prepared with 10-20 vol.% distillates and 80-90 vol.% petroleum diesel, which would be respectively named as HTL 10 (10 vol.% distillates) and HTL20 (20 vol.% distillates) for later discussion. Fuel specification analyses, including viscosity, acidity, net heat of combustion, Cetane number, lubricity, and oxidation stability, were subjected to the drop-in biodiesel.

### 9.1 Fuel Specification Analysis with Drop-in Biodesel

As Table 9-1 shows, the acidity, Cetane number, lubricity, and oxidation stability of FPW-HTL10, FPW-HTL20, SW-HTL10, and SP-HTL10 all meet the ASTM criteria for biodiesel application. Excessively high acidity would corrode storage tanks and pipelines that used to store and transfer fuel, and thus is avoided. In the present study, the high acidity of the distillates from FPW-derived biocrude oil is properly addressed via esterification, though as the addition of HTL distillate increased from 10 vol.% to 20 vol.%, the acidity of drop-in biodiesel increased from 0.10 to 0.29 mg KOH/g sample. Further increase of HTL distillate may require harsher esterification conditions to reduce their acidity. Similarly, the high acidity of the distillates from SW-derived biocrude oil is effectively reduced through neutralization. When the addition of neutralized distillates from SW-derived biocrude oil increased from 10 vol.% to 20 vol.%, the acidity of drop-in biodiesel is only increased by 0.03 mg KOH/g, which is still far lower than the ASTM standard (*i.e.,* 0.3 mg KOH/g). On the other hand, the drop-in biodiesel synthesized with 10 vol.% of the distillates from SP-derived biocrude oil, which requires no further upgrading as compared to those from FPW- and SW-derived biocrude oil, contains an acidity (0.3 mg KOH/g) that meets the ASTM standards. Yet, further increase of the distillates from SP-derived biocrude oil may need additional modification to decrease their acidity.

**Table 9-1. Fuel specification analysis and engine test of drop-in biodiesel (HTL10 and HTL 20 respectively represents 10 vol.% and 20 vol.% upgraded distillates plus 90 vol.% petroleum diesel)**

| Fuel Spec Property | Upgraded-FPW | | Upgraded –SW | | SP | Diesel |
|---|---|---|---|---|---|---|
| | HTL10 | HTL20 | HTL10 | HTL20 | HTL10 | |
| Viscosity @20°C ($mm^2/s$)[a] | 3.737 ± 0.01 | 3.050 ± 0.02 | 3.402 ± 0.02 | 3.501 ± 0.3 | 3.111 ± 0.003 | 3.746 ± 0.02 |
| Acidity (mg KOH/g)[b] | 0.10 ± 0.004 | 0.29 ± 0.05 | 0.07 ± 0.02 | 0.1 ± 0.0 | 0.3 ± 0.0 | 0.3[e] |
| Existent Gum (wt.%)[c] | 0.17 ± 0.01 | 0.21 ± 0.02 | 0.31 ± 0.03 | 0.41 ± 0.03 | 0.55 ± 0.03 | 0.63± 0.06 |
| Ash Content (wt.%)[d] | N/A[i] | N/A[i] | 0.07 ± 0.01 | 0.06 ± 0.01 | 0.05 ± 0.01 | 0.07 ± 0.002 |
| Net Heat of Combustion (MJ/kg)[f] | 44.7 ± 0.3 | 44.2 ± 0.6 | 45.6 ± 0.4 | 46.2 ± 0.4 | 45.4 ± 0.2 | 46.0 ± 0.3 |
| Cetane Number (min) | 44.2 | 43.6 | 44.5 | N/A[h] | N/A[h] | 40>[e] |
| Lubricity (μm) | 364 | 324 | 306 | N/A | 314 | <520[e] |
| Oxidation Stability (hrs) | 48> | 48> | 48> | N/A | 48> | 6>[e] |
| **Engine Test** | | | | | | |
| Power Generated (kW) | 3.68-4.26 | 3.67-4.24 | N/A | N/A | N/A | 3.41-4.26 |
| EGT (°C)[g] | 326.3- 569.6 | 303.7-554.1 | N/A | N/A | N/A | 334.9 -574.4 |
| CO emission (ppm) | 0.04-1.82 | 0.05-1.66 | N/A | N/A | N/A | 0.05-2.12 |
| $CO_2$ emission (ppm) | 7.06-11.4 | 6.22-11.7 | N/A | N/A | N/A | 7.12-11.6 |
| NOx emission (ppm) | 606-1576 | 551-1456 | N/A | N/A | N/A | 540-1549 |
| Unburnt hydrocarbons (ppm) | 14-26 | 18-29 | N/A | N/A | N/A | 14-32 |
| Particulate matter emission (Soot) | 0.01-0.12 | 0.06-0.13 | N/A | N/A | N/A | 0.01-0.11 |

[a]Measured by Cannon-Fenske Viscometer (ASTM D445); [b]Measured by ASTM D664; [c]Modified ASTM D381, heat the sample in the furnace from room temperature to 240°C for 60 minutes; [d] Measured by ASTM D482; [e] ASTM D7467; [f]Measured by bomb Calorimeter (ASTM D4809); [g]Exhaust Gas Temperature; [h]Not applied due to the limit amounts of distillates; [i]Not applied because of the low existent gum contents.

Cetane number indicates the readiness of a fuel to auto-ignite when injected into a diesel engine (Lu et al., 2009). A high Cetane number refers to a low ignition delay before combustion and hence is favored. In this study, the Cetane number reduced from 44.2 min to 43.6 min, as the addition of HTL distillate increased from 10 vol.% to 20 vol.%. This fact suggests that the distillates from FPW-derived biocrude oil may contain compounds with lower volatility than petroleum diesel. For example, the enthalpy of vaporization for Hexadecane is 66 kJ/mol (~80°C), while that for Hexadecanoic acid, methyl ester is 93 kJ/mol (~80°C) (NIST). SW-HTL10 also presents a Cetane number similar to that of FPW-HTL10 (44.5 min), indicating that neutralized distillates from SW-derived biocrude oil could be a promising drop-in diesel as well.

Lubricity of a fuel infers the ability to reduce wear and friction (Lu et al., 2009). Poor lubricity would lead to severe wear problems because the fuel injection system is mainly lubricated by the fuel itself. For most petroleum fuels, viscosity is positively related to a fuel's lubricity. As Table 9-1 exhibits, the lubricity and viscosity respectively decreased by 11% and 18% when the addition of HTL distillates from FPW-derived biocrude increased from 10 vol.% to 20 vol.%. This could be that HTL distillates from FPW-derived biocrude (C8-C20) contains hydrocarbons with smaller carbon chain than petroleum diesel (C14-C20) and thus reduce the viscosity of HTL10 and HTL 20 (Gai et al., 2014a). For instance, the viscosity of Decane ($C_{10}H_{22}$) is 0.8 mPa·s (25°C), whilst that of Tetradecane ($C_{14}H_{30}$) is 2.1 mPa·s (25°C) (Haynes, 2016). Furthermore, HTL distillates from FPW-derived biocrude also contain FAME with smaller carbon chain (C5-C18) than regular biodiesel (C16-C18) and thereby lead to a lower viscosity as well as lubricity (Pratas et al., 2010). Moreover, the lubricity and viscosity of HTL10 from SW- and SP-derived biocrude oil is even lower than that from FPW-derived biocrude oil. Neutralized distillates from SW-derived biocrude oil and the distillates from SP-derived biocrude oil contain more fatty nitriles (17-24% total relative peak area identified under GC-MS) than those from FPW-derived biocrude oil (no fatty nitriles were identified). Fatty nitriles such as Heptadecanenitrile may serve as a role of surfactants, which can act as emulsifiers and dispersants in an oil-aqueous phase, and thus help improve the flowability and reduce lubricity in this case (Chen et al., 2016b). Further rheology studies with SW-HTL10, SP-HTL10, and model compounds (*e.g.,* Heptadecanenitrile with diesel) would elaborate the effect of fatty nitriles on viscosity and lubricity.

It is generally believed that the oxidation stability of biodiesel is link to the presence of unsaturated compounds, particularly unsaturated FAME and fatty acids, because they tend to degrade during storage (Kumar, 2017). Normally, oxidation stability for biodiesel is 4-12 hours (Kumar, 2017). In the present work, FPW-HTL10, FPW-HTL20, SW-HTL10, SW-HTL20, and SP-HTL10 all demonstrate an oxidation stability of more than 48 hours, which indicates there is no rapid oxidation. According to GC-MS results (Tables 8-3, 8-8, and 7-9), the major components in the distillates from FPW-, SW-, and SP-derived biocrude are alkanes (51-61% total relative peak area) and saturated FAME (15% total relative peak area in esterified FPW-distillates). Alkenes and unsaturated FAME are only composed of 19-25% and 1% total relative peak area, respectively. In fact, no fatty acids were identified in samples of SW-HTL10, SW-HTL20, and SP-HTL10 under GC-MS. Derivative GC-MS analysis is suggested to further validate if there are any fatty acids in these two samples, since some fatty acids (especially for those with chain length longer than 18) could be less volatile and thus are not identifiable under regular GC-MS.

Heat of combustion is mainly affected by the elemental compositions of fuel samples (ASTM, 2015b; ASTM, 2015c). FPW-HTL 10 and FPW-HTL 20 present a lower heat of combustion because the distillates from FPW-derived biocrude oil contain 1.82 wt.% oxygen contents. Although this extra oxygen contents lead to a lower heat of combustion, they would make the drop-in biodiesel combust more completely. More results regarding diesel engine test would be discussed in **9.2**. In contrast, SW-HTL10 and SP-HTL10 demonstrate a slightly higher heat of combustion than those of FPW-HTL10 and FPW-HTL20. This is probably due to that SW-HTL10, SW-HTL20, and SP-HTL10 contain fewer oxygenates such as FAME and fatty acids.

Existent gum contents and ash content of drop-in biodiesel samples are also measured to investigate if additional upgrading processes are needed to remove compounds that cannot stably mix with petroleum diesel. Three types of drop-in biodiesel all contain a lower or comparable existent gum contents and ash content (Table 9-1). This feature also indicates that esterification and neutralization have effectively improved the fuel specifications of the distillates from FPW- and SW-derivied biocrude oil—compounds that were not well mixed petroleum diesel were properly reformed through the proposed mild upgrading approaches.

(a)

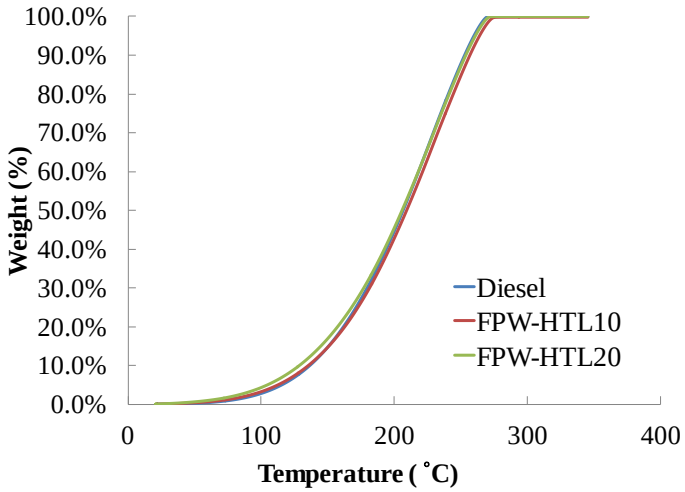


(b)

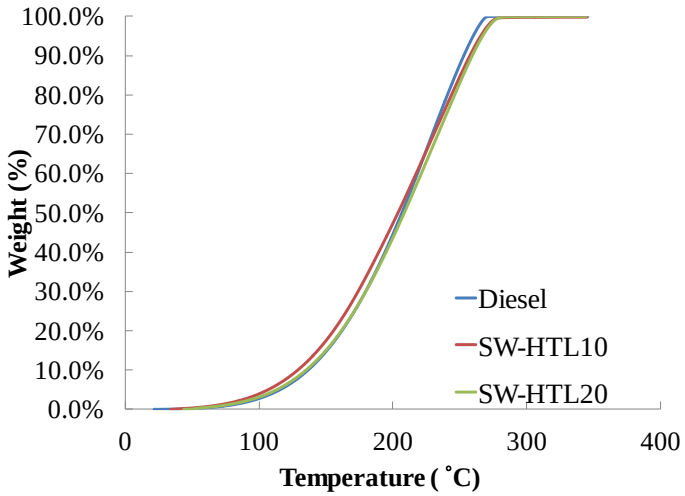


(c)

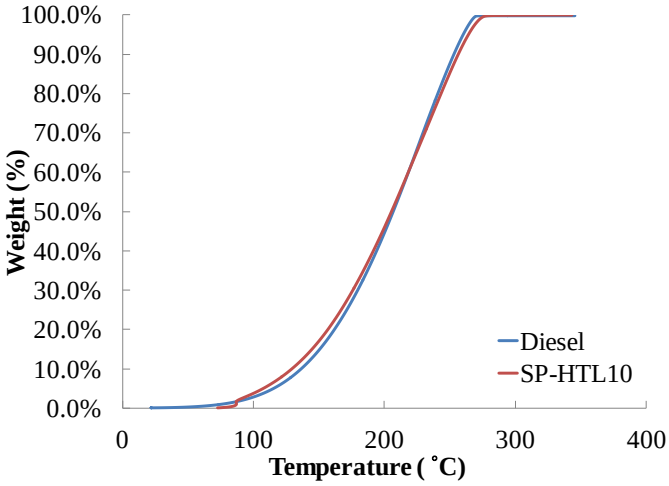


**Figure 9-1. Boiling point range of drop-in biodiesel prepared by (a) esterified FPW-derived biocrude oil (b) neutralized SW-derived biocrude oil, and (c) SP-derived biocrude oil**

Boiling point range of FPW-HTL10, FPW-HTL20, SW-HTL10, SW-HTL20, and SP-HTL10 are present in Figure 9-1. As Figure 9-1 shows, three types of drop-in biodiesel all demonstrate a similar boiling point range to that of diesel—99.9 wt.% of diesel, FPW-HTL10, and FPW-HTL20; 99.6% of SW-HTL10 and 99.3% of SW-HTL20; as well as 99.7% of SP-HTL10 can be distilled before 278°C.

**9.2 Diesel Engine Tests with Drop-in Biodiesel Prepared**

Engine tests are one of the significant components to demonstrate the feasibility of using HTL biocrude oil as transportation fuels. Since the fuel specification analysis has validated that the distillate from FPW-derived biocrude is a promising diesel alternative and can stably mix with petroleum diesel, HTL10 and HTL20 were used for diesel engine test. Diesel engine was operated at 1200-2000 rpm under different fuel injection timing with 20 mg fuel/stroke. Fuel injection timing is governed by the crank angle (CA, unit: degree) before top dead center (BTDC) in a typical compression ignition engine (*e.g.*, diesel engine). Thus, a 0-12 CA BTDC has been explored in this study. In general, diesel engine performs at 0 CA BTDC to reach the highest power output, but running at 0 CA BTDC would result in an incomplete pre-mixing as a trade-off (Heywood, 1988).

Power output, exhaust gas temperature, and pollutant emissions of HTL10, HTL20, and regular diesel are summarized in Table 9-1 and Figures 9-2~9-5. Table 9-1 and Figure 9-2a present HTL10 and HTL20 can achieve a competitive power output, as compared to regular diesel. In fact, Figure 9-2a shows that HTL 10 can achieve a slightly higher power output (8%) than regular diesel at 0 CA BTDC for high speed condition (2000 rpm). This is probably due to that HTL 10 contains extra oxygen contents (0.2 wt.% ) that can make diesel combustion more completely. This result also demonstrates that HTL distillates are promising diesel fuel alternative, because they can be operated in diesel engine without premixing and/or harsh modification. In contrast, conventional drop-in fuels such as butanol-based biodiesel usually require premixing to be fired in a diesel engine (Lee et al., 2016).

Figure 9-2b illustrates the emissions of $NO_x$, which is influenced by volumetric efficiency, combustion duration, and temperature (can be indicated by power output) (Buyukkaya, 2010). In general, it is preferred to run diesel engine at higher speed (*e.g.*, 2000rpm) with 0-4 CA BTDC to achieve a higher power output and lower $NO_x$ emission. This is primarily due to the increase in volumetric efficiency and gas flow motion within the engine

cylinder under higher engine speeds, which would lead to faster mixing between fuel and air and thus shorten ignition delay (Buyukkaya, 2010). Figure 9-2b reveals that running with HTL 10 and HTL20 leads to a lower $NO_x$ emission (6-13%) than regular diesel, particularly at speeds of 1500-2000 rpm for all tested CA. This could be attributed to a lower exhaust gas temperature of HTL10 and HTL20, as compared to regular diesel (Figure 9-5). Similar results were found when using palm oil methyl ester (Masjuki et al., 1997) and preoxidized soybean oil methyl ester (Lin & Lin, 2006) for diesel engine tests.

Figure 9-3 displays the emissions of soot and unburned hydrocarbons at 1200-2000 rpm with 0-12 CA BTDC. In diesel engines, fuel is injected into the engine cylinder near the end of the compression stroke. As the piston moves closer to top dead center, the temperature of fuel mixture reaches the fuel's ignition point, causing ignition of some premixed quantity of fuel and air that were atomized and vaporized during ignition delay (Heywood, 1988). The rest of fuel that had not participated in premixed-dominant combustion is consumed in the rate-controlled combustion phase. As a consequence, higher soot indicates that premixed combustion is a minor combustion mechanism. Rather, a rate-controlled combustion is the major one in this case (Figure 9-3a). In the present study, the distillates from FPW-derived biocrude oil could contain less volatile compounds (*e.g.*, phenols) than regular diesel and thereby delay the atomization and vaporization, especially for HTL 20 (Figure 9-3a). An in-depth combustion study with HTL10 and HTL20 is recommended to elucidate their combustion characteristics and soot formation mechanisms.

On the other hand, Figure 9-3b shows that HTL10 can lead to a 10-21% lower unburned hydrocarbon (HC) emission than regular diesel. This could be explained by that HTL10 has a higher Cetane number and power output than regular diesel and HTL20. The higher power output would lead to a higher temperature of burned gases, which helps prevent condensation of the heavier hydrocarbons in the sampling line. Besides, a higher Cetane number makes the combustion delay shorter and thus decreased HC emissions.

Figure 9-4 summarized the emission of CO (Figure 9-4a) and $CO_2$ (Figure 9-4b). The emission of CO decreased by 6%-42% as the addition of HTL distillates increased from 0 to 10-20 vol.%, particularly for those emitted at delayed injection timing (*e.g.*, 8-12 CA BTDC) (Figure 9-4a). In general, the emission of CO is derived from incomplete combustion. This reducing CO emission is probably due to the extra oxygen content inherently present in HTL10

and HTL20, which will make combustion in the diesel engine more completely. Further, Figure 9-4a also suggests that HTL10 and HTL20 are less volatile than regular diesel. Delayed injection timing would enable a more complete combustion and thus lead to a lower CO emission.

Figure 9-4b presents that the emission of $CO_2$ decreased as the engine speed and the addition of HTL distillates increased. Moreover, HTL20 can lead to a 7-10% lower carbon dioxide emission at lower engine speed (*i.e.*, 1200 rpm), as compared to HTL10 and regular diesel. This could be attributed to that the distillates from FPW-derived biocrude oil contain lower carbon contents than regular diesel (Xue et al., 2011). Besides, HTL20 may lead to a less complete combustion than HTL10 and regular diesel (Figure 9-4a), and hence result in a lower $CO_2$ emission.

Combining the results of power output and pollutant emission of HTL10, HTL20, and regular diesel, it is believed that the distillate from FPW-derived biocrude is a promising drop-in biodiesel. Compared to regular diesel, a competitive power output (8% higher) and soot emission, as well as a lower $NO_x$ (3-7%), CO (1-44%), $CO_2$ (1-4%), and HC (10-21%) emissions are demonstrated with HTL10.

(a)

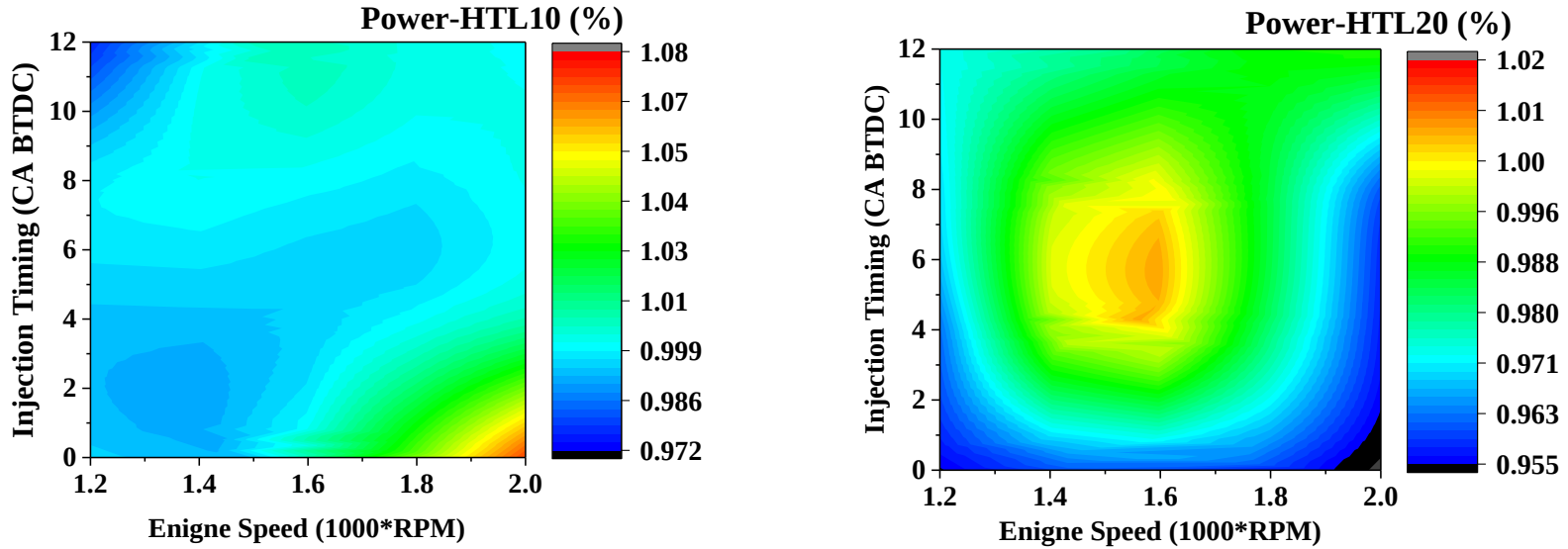


(b)

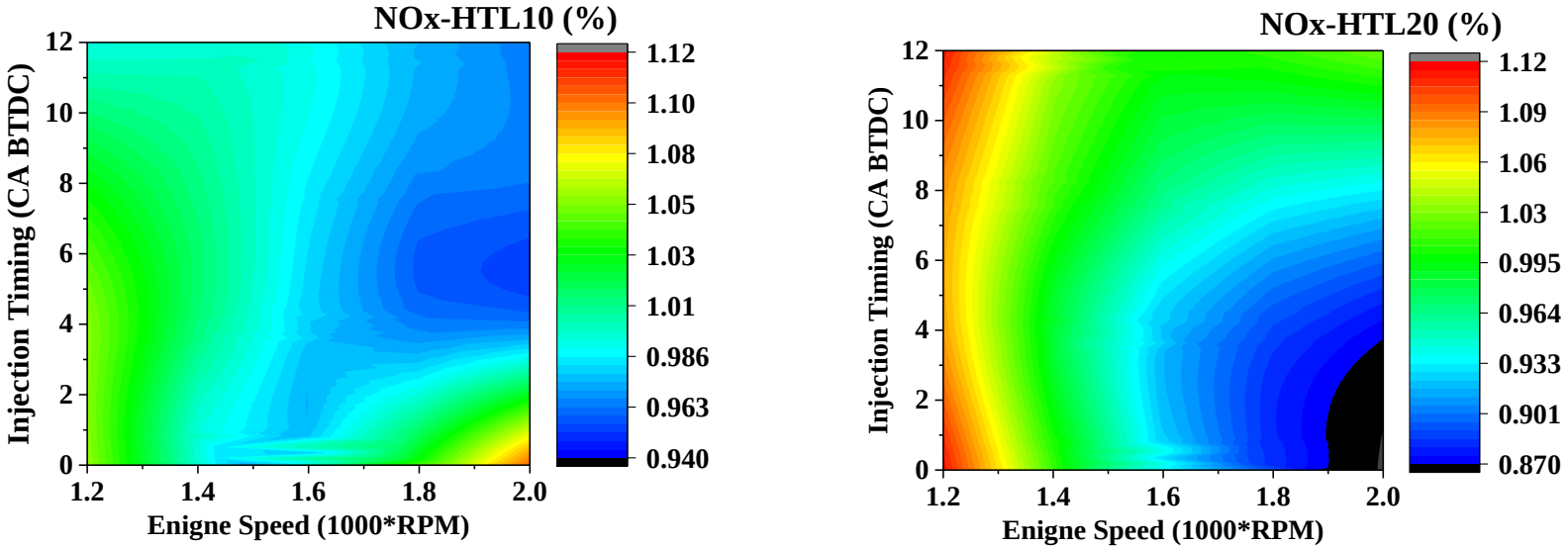


**Figure 9-2. The effect of engine speed and injection timing on (a) power output and (b) $NO_x$ emission of drop-in biodiesel prepared with HTL distillates (Exclude HTL20 at 2000 RPM/0 CA BTDC because of misfire)**

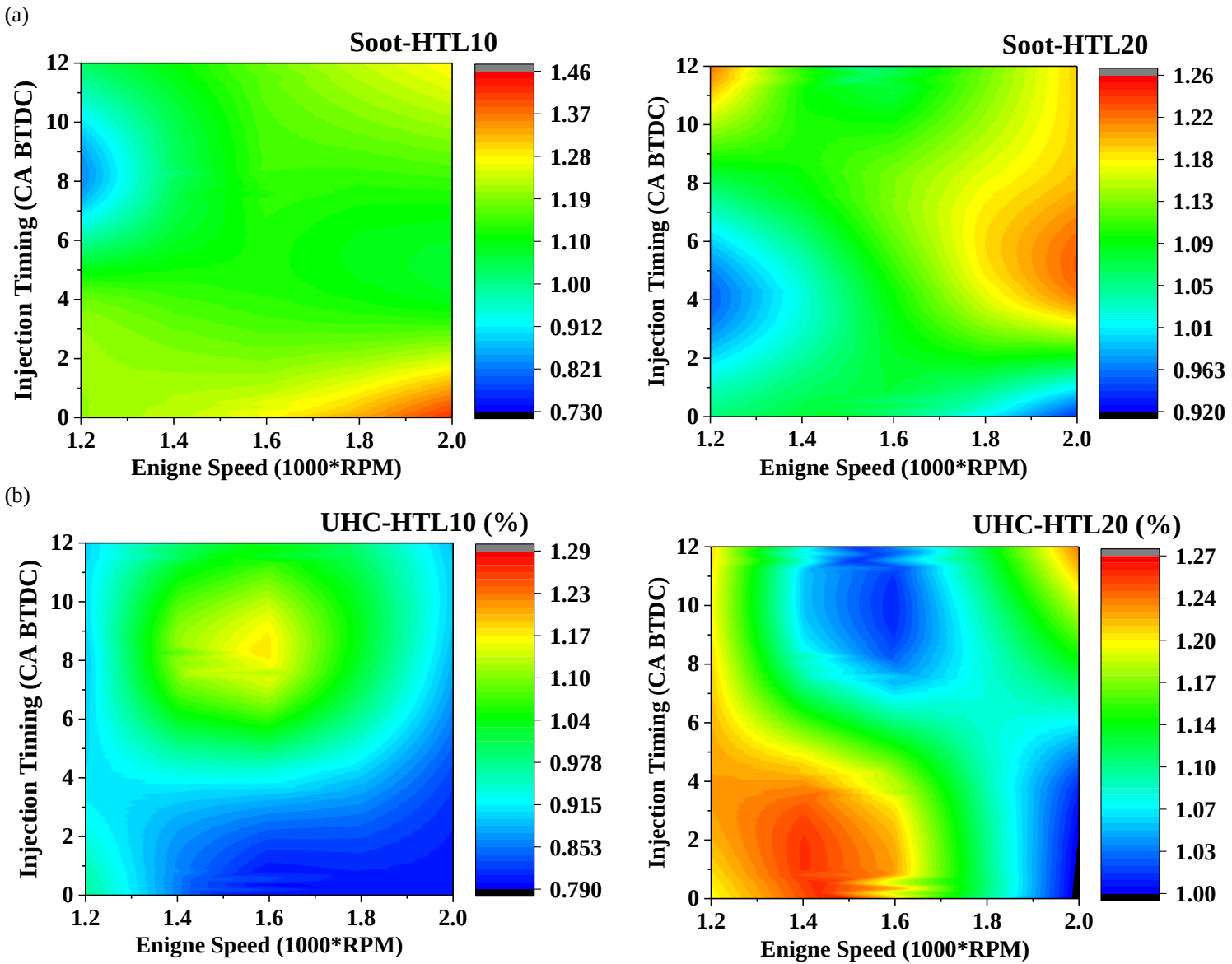


**Figure 9-3. The effect of engine speed and injection timing on (a)Soot formation and (b) unburned hydrocarbon (UHC) emissions from drop-in biodiesel prepared with HTL distillates**

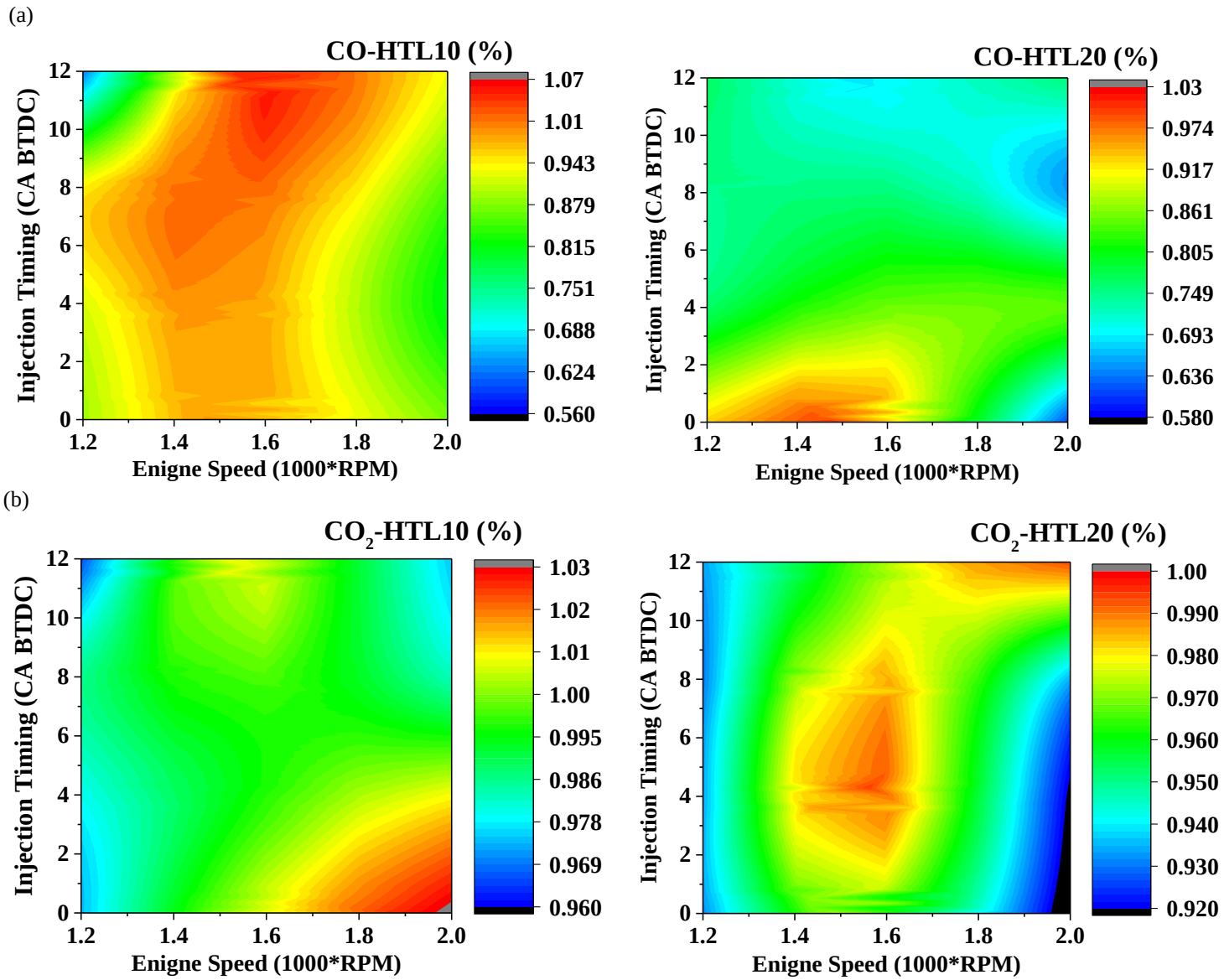


**Figure 9-4. The effect of engine speed and injection timing on (a) CO and (b) $CO_2$, emission from drop-in biodiesel prepared with HTL distillates**

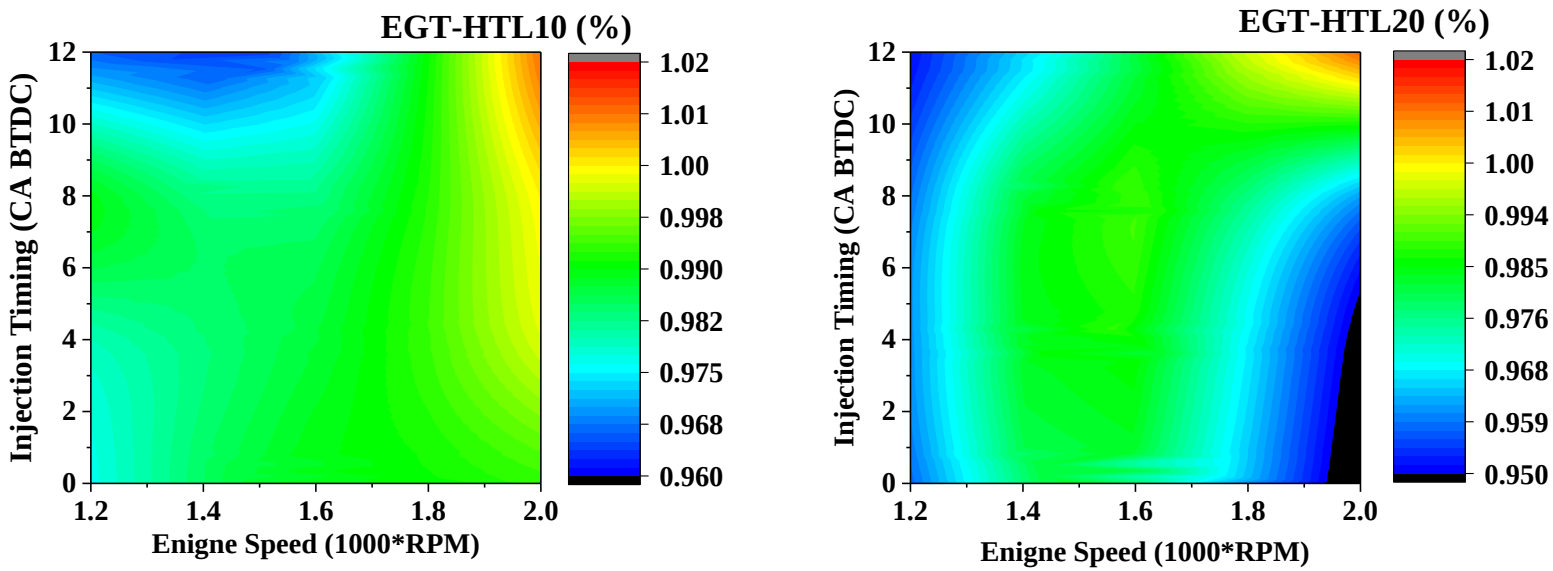


**Figure 9-5. The effect of engine speed and injection timing on exhaust gas temperature (EGT) from drop-in biodiesel prepared with HTL distillates**

# CHAPTER 10. SUMMARY AND RECOMMENDATIONS

## 10.1 Summary

Single-stage and two-stage physical pretreatments of WA biomass were investigated in terms of the ash content, bio-crude oil yield via HTL processes, and apparent activation energy of the thermal decomposition ($E_{a2}$). In contrast to untreated algae, the ash content of WA biomass was reduced from 28.6% to 18.6% with the pretreatment of centrifugation; $E_{a2}$ and the bio-crude oil yield were respectively decreased from 50.2 kJ/mol to 35.9 kJ/mol and increased from about 30-35% to 55% with the two-stage pretreatment of centrifugation followed by ultrasoication. The morphology of pretreated algae also supported this finding.

By screening AW biomass into the sizes of <106 μm and 106-180 μm, the ash content were reduced from 53% to 43% and 39%. The biocrude oil yields were barely affected by the reducing ash content of HTL algal feedstock. Nevertheless, the reducing ash content of HTL algal feedstock could effectively improve the biocrude oil quality in terms of higher heating values and light fraction components with lower boiling points. Moreover, the ash content could promote denitrogenation, catalyze the formation of hydrocarbons, and alleviate recalcitrant compounds in the aqueous products under HTL processes. HTL of model algae with representative ash content validates that the algal feedstock with no more than 40 wt.% of ash content can be converted into liquefaction products with a reasonable quantity and quality of biocrude oil. This fact significantly enables the ash-rich biomass as a feasible HTL feedstock and concurrently diminishes the necessity of multi-step pretreatments and modifications of ash-rich biomass for biofuel applications.

Distillation can effectively separate biocrude converted from swine manure (SW), food processing waste (FPW), and algal biomass (SP), via HTL into different fractions that can be used to synthesize drop-in biodiesel. The distillates from SW-, FPW-, and SP-derived biocrude respectively contains 15 wt.%, 56 wt.%, and 15% fractions that present heating values of 43-46 MJ/kg, densities of 810-900 kg/m$^3$, kinematic viscosities of 1.68-12.8 mm$^2$/s (at 20°C) and alkanes with carbon numbers of 8-18, which are similar to those of petroleum diesel. Although the distillates from FPW-derived biocrude demonstrate the most resemble density and energy content to petroleum diesel, as compared to the distillates from SW- and SP-derived biocrude oil, the distillates from FPW-derived biocrude displayed a significantly higher acidity that need to be

reduced from 35.3 mg KOH/g to ≤ 3 mg/g (the requirements suggested by the ASTM standard for a 10 vol.% biodiesel). Consequently, an orthogonal array design (OAD) of esterification experiment was conducted to reduce the acidity of the distillates from FPW-derived biocrude. The reaction temperature (50-70°C), reaction time (0.5h-6h), catalysts concentration (0.5 wt.%-2 wt.%), and the molar ratio of FPW-distillates to methanol (1:5-1:15) were explored through the OAD esterification experiment. An optimized esterification condition was realized at 50°C for 4 hr with 2 wt.% $H_2SO_4$ and a FPW-distillates to methanol ratio of 1:9. Assuming 50% heat is recovered from the upgrading processes, the integrative upgrading approach proposed by this study (distillation plus esterification) present a competitive energy consumption ratio (0.02-0.06) to zeolite cracking (0.26), supercritical fluid (SCF) treatment (0.28), and hydrotreating (0.02). Further, ignoring the need of high pressure hydrogen gas, the reaction severity of the upgrading approach used in this study (with log $R_o$ of 5.9-9.5) is much lower than those of zeolite cracking (with log $R_o$ of 11.0), SCF treatment (with log $R_o$ of 10.6), and hydrotreating (with log $R_o$ of 11.3). Lastly, the fuel specification analysis and engine test were conducted with drop-in biodiesel prepared with 10 vol.% (HTL10) and 20 vol.% (HTL20) upgraded distillates and 80-90 vol.% petroleum diesel. With a qualified Cetane number (<40 min), lubricity (<520 μm), oxidation stability (>6 min), viscosity (0.2%-19% lower) and net heat of combustion (3%-4% lower) to those of petroleum diesel, HTL10 result in a competitive power output (8% higher) and lower emissions of $NO_x$ (3-7%), CO (1-44%), $CO_2$ (1-4%), and unburned hydrocarbons (10-21%). An energy-efficient and technically cohesive approach to produce renewable high-quality drop-in biofuels for demanding transport applications is successfully demonstrated in the present study.

## 10.2 Recommendations for Future Works

### 10.2.1 Upgrading HTL Distillates for Aviation Biofuel Application

Since the physicochemical characterization all suggests that the distillates from SW- and FPW-derived biocrude are similar to aviation fuel in terms of density, viscosity, heating values, and chemical functionalities, drop-in biofuel were prepared with the distillate fractions from SW- and FPW-derived biocrude and petroleum transportation fuels. The distillate fraction F from SW-derived biocrude and the fractions C to G (C-G) from FPW-derived biocrude were selected as drop-in aviation biofuel because they present the closest HHV, density, and chemical compositions to those of petroleum transportation fuels. On the other hand, jet fuel A ($3.7-

4.1/gallon in Urbana-Champaign) is selected due to its higher value compared to other fuels such as diesel ($2.00-2.03/gallon) (U.S. EIA, 2016). Moreover, changing the fuel source is one of the few available options to reduce the GHG emissions in the aviation industry.

The drop-in aviation biofuel was prepared with 10 wt.% distillates and 90 wt.% jet fuel A. Fuel specification analyses, including density, viscosity, acidity, flash point, copper corrosion, net heat of combustion, total sulfur content, and existent gum, were subjected to the drop-in aviation biofuel. Table A-11 compares the fuel specifications of drop-in aviation biofuel and petroleum jet fuel. Notably, the drop-in aviation biofuel has close density, viscosity, copper corrosion performance, total sulfur content, and net heat of combustion to those of petroleum jet fuel. This indicates that the distillates from FPW- and SW-derived biocrude can be well blended into petroleum jet fuel without modifications. However, Table A-11 also reveals that the drop-in aviation biofuel prepared with the distillates from FPW-derived biocrude presented a higher acidity and lower flash point than petroleum jet fuel. The higher acidity may be due to the oxygenates such as fatty acids while the lower flash point may be attributed to unsaturated hydrocarbons (*e.g.*, alkenes) in the distillates from FPW-derived biocrude. For instance, the vapor pressure of dodecene is eight times lower than dodecane (Information, 2016). In order to reduce the acidity and increase the flash point of the distillates from FPW-derived biocrude, upgrading processes including esterification and hydrotreating are suggested.

On the contrary, the drop-in aviation biofuel prepared with the distillates from SW-derived biocrude demonstrate a significant amount of existent gum, which may be attributed to the phenolic compounds. In fact, it was found that there were brownish precipitates in the bottom of the drop-in aviation biofuel prepared with the distillates from SW-derived biocrude. The precipitates were extracted with toluene and ethanol for GC-MS analysis with derivative treatment (Figure A-8). Figure A-8 shows that the precipitates were mainly composed of phenols (*e.g.*, methyl phenol), acids (palmitic acid), nitrogen-heterocyclic compounds (*e.g.*, pyridines), and amino acids (*e.g.*, glycines). Particularly, 50-60% percentage of relative peak area is attributed to phenols. This finding suggests that the distillates from SW-derived biocrude are not perfectly suitable for aviation biofuel application. In fact, it is recommended to refine the phenolic compounds from the SW-derived biocrude for value-added chemical production (*e.g.*, biopolymer, biobinder, *etc.*).

### 10.2.2 Super/Sub-critical Fluids Applications on Algal Biomass and Wet Biowaste

Microalgae and wet biowaste such as animal manure are potential feedstocks for biofuels, bulk chemicals, and bioactive compounds with nutraceutical and pharmaceutical importance, because of their fast growth, high lipid content (20-70%), and relatively low environmental impact(Ahmad et al., 2011; Ghatak, 2011; Gouveia & Oliveira, 2009). Most lipids from microalgae and wet biowaste contain fatty acids. Lipids with fatty acids containing 14 to 20 carbons (C14-C20) are desired for biodiesel production, while polyunsaturated fatty acids (PUFA) with 20 or more carbons are targeted for the health food market (Yen et al., 2013). One of the main reasons this energy and value-added products are not effectively harvested is the high water content (80-99%) of algal biomass, which becomes a bottleneck for a number of bioenergy conversion/extraction technologies that could have a net positive energy balance. It has been shown that over 75% of the total energy input toward refinement comes from the drying process (Vasudevan et al., 2012). Newer technologies can exploit the potential of wet biomass. Use of supercritical carbon dioxide ($scCO_2$) has been recognized as a sustainable solvent for extraction processes due to its unique efficacy, relative lack of intrinsic hazard, and robust tolerance of water contents (Soh & Zimmerman, 2011). Research has demonstrated that using scCO2 to extract lipids from algal biomass can lead to a comparable yield and an increased selectivity to conventional extractions with organic solvents (Soh & Zimmerman, 2011). Moreover, $scCO_2$ entrainers such as ethanol have been used to enhance solubility and increase yield of triacylglycerols (TAG) and value-added chemicals such as carotenoids (*e.g.*, astaxanthin, AX) from microalgae, as well as proteins (*e.g.*, phycocyanin, PY) from cyanobacteria (Crampon et al., 2011; Deniz et al., 2016; Reyes et al., 2014). Further, the solvation ability of $scCO_2$ can be tuned based on its solvent density by changing the reaction temperature and pressure or by adding $scCO_2$ entrainers. Thus, it is suggested that $scCO_2$ can be used for sequential extractions of non-polar compounds such as biodiesel precursors and carotenoids, as well as polar compounds, such as proteins, by employing system conditions that are favorable to the desired products and unfavorable to the remaining compounds. Moreover, by demonstrating the continuous use of a single extraction vessel in this proposal, the cost of large-scale scCO2 technologies can be greatly reduced by eliminating the need for additional refining processes after extraction.

# APPENDIX A: TEMPERATURE AND PRESSURE OF A CONTINUOUS HTL

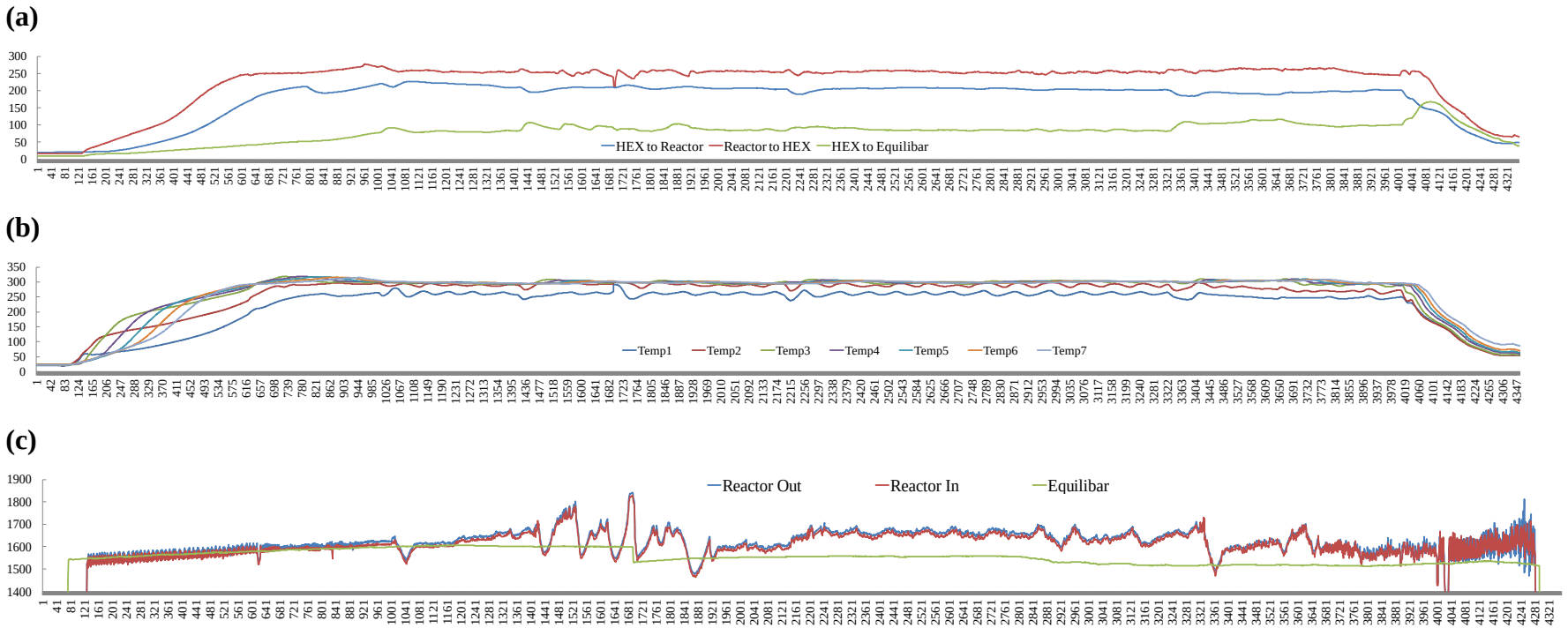


**Figure A-1. Temperature and pressure of a continuous HTL of swine manure at 280°C with a reaction time of 2h (x-axis: reaction time, y-axis: reaction temperature (°C) or pressure (psi)): (a) temperatures of heat exchangers (HEX) to reactors and reactor outlet (Equilibar); (b) temperature of different sections in the reactor vessel; and (c) pressure of different sections of reactors**

# APPENDIX B: TEMPERATURE PROFILE OF DISTILLATION

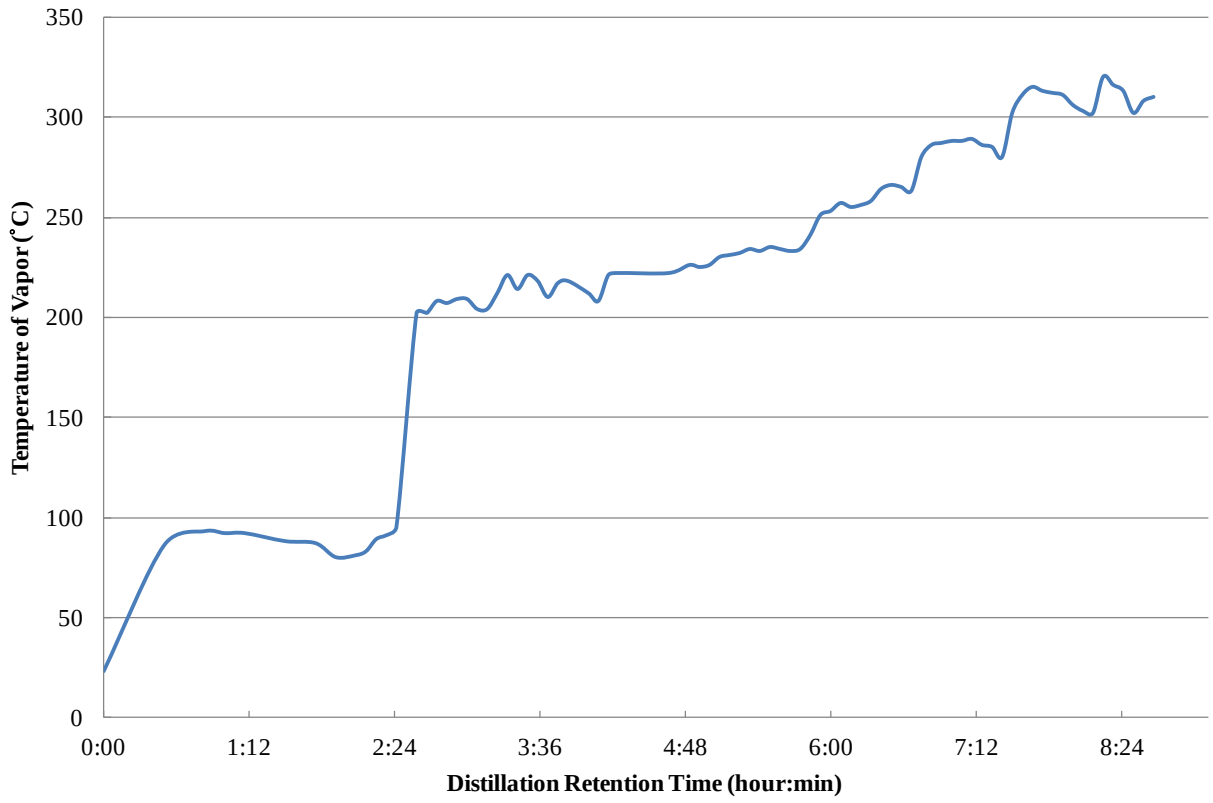


**Figure B-1. A typical temperature profile of distillation of biocrude oil converted from food processing waste via HTL at 260°C for 0.5 h**

# APPENDIX C: THERMOGRAVIMETRIC ANALYSIS OF DISTILLATES

(a)

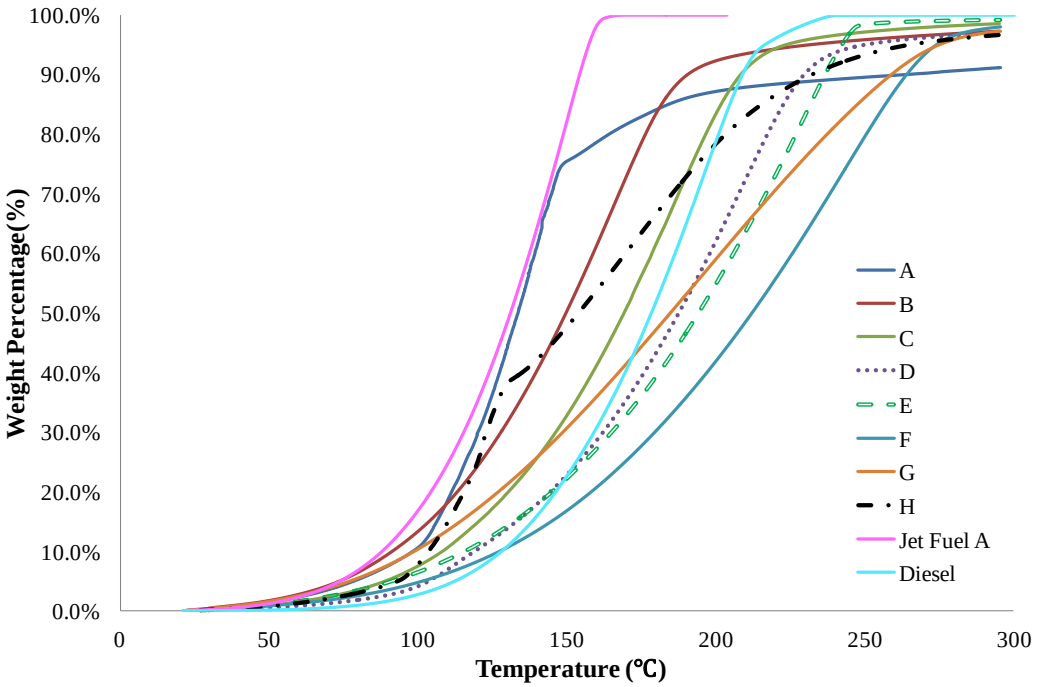


(b)

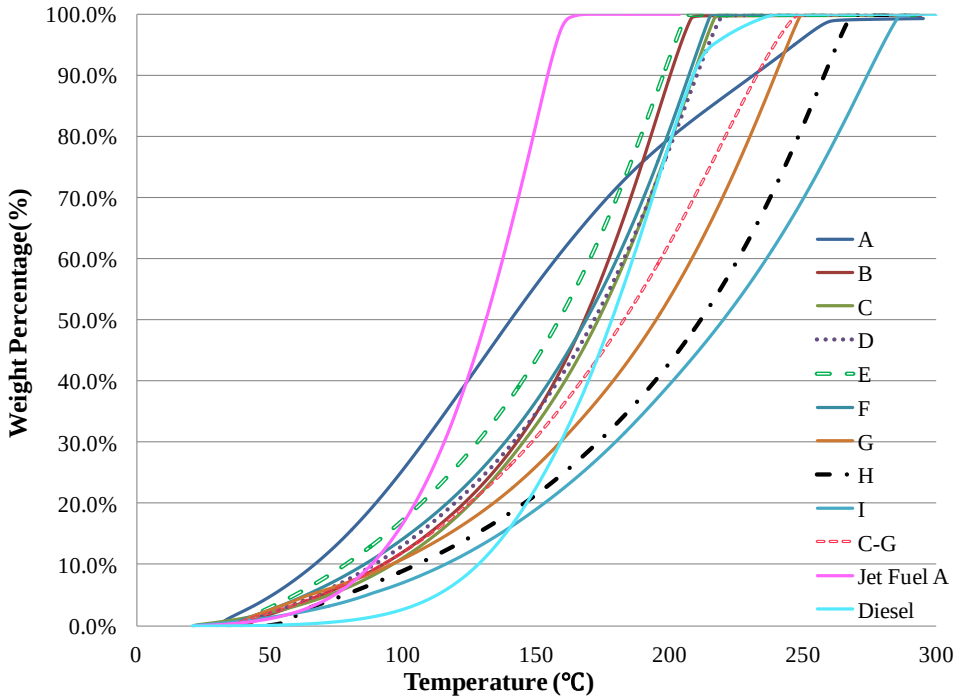


**Figure C-1. Thermogravimetric (TG) curves of different fractions of distillates from (a) swine manure (SW), and (b) food-processing waste (FPW)-derived biocrude**

In order to compare the boiling point distribution of the distillates and transportation fuels, the thermogravimetric analysis (TGA) was operated and the results were presented in Figure C-1. Figure C-1 shows that all the fractions can be distilled out before 300°C under TGA, indicating the distillation has effectively separated the biocrude. The fractions E-G of SW-derived biocrude present a slightly higher boiling point distribution than that of diesel and jet fuel. On the other hand, the fractions C-G of FPW-derived biocrude demonstrate a close boiling point distribution to that of diesel. Further molecular level analyses and fuel specification tests would be significantly needed to understand the feasibility of using the distillates as drop-in biofuels.

# APPENDIX D: CHEMICAL COMPOSITIONS IDENTIFIED IN THE AQUEOUS PHASE SEPARATED FROM DISTILLATES

**Table D-1. Normalized GC-MS signals of components identified in the aqueous phase separated from the distillates from SW-derived biocrude; "×" indicates the chemical was not detected**

| Compound Name | Normalized Signal (-) | |
|---|---|---|
| | D-AQ | E-AQ |
| **Phenols** | | |
| Phenol | 0.47 | 0.38 |
| Methyl phenol | 0.26 | 0.22 |
| Ethyl phenol | 0.03 | 0.10 |
| Ethyl-methoxy phenol | 0.06 | 0.06 |
| Methoxy phenol | 0.56 | 0.05 |
| **Nitrogen Heterocyclic Compounds** | | |
| Pyridines | 0.52 | 0.07 |
| Pyrazines | 0.90 | 0.23 |
| Pyridinols | 0.39 | 1.96 |
| Pyrroles | × | 1.18 |
| **Amino acids, Amines and Amides** | | |
| Dimethylaminoanisole | 0.02 | 0.27 |
| **Fatty Acids & Fatty Alcohols** | | |
| Benzoic acid | 0.03 | 1.33 |
| Benzenepropanoic acid | × | 1.26 |
| Acetic acid | 0.52 | 0.94 |
| Propanoic acid | 0.64 | 0.51 |
| Butanoic acid | 1.86 | × |
| Pentanoic acid | 0.78 | 1.17 |
| Hexanoic acid | 0.19 | 2.02 |
| Hexadecanoic acid | 0.03 | × |
| Octadecanoic acid | 0.01 | × |

# APPENDIX E: COMPONENTS IDENTIFIED IN THE DISTILLATES WITH DERIVATIVE TREATMENT

To further explore if these distillates may include other relatively polar compounds that cannot be observed under regular GC-MS, derivative GC-MS analysis were also performed with the distillates from SW-derived biocrude. Figure E-1 and Table E-1 show that fatty acids and amino acid derivatives are the major compounds found in the distillates from SW-derived biocrude under derivative GC-MS analysis. In addition, Figure E-1 and Table E-1 reveal that the aqueous-phase like products in the distillates from SW-derived biocrude mainly include phenols, acids (*e.g.*, oxalic acid and benzoic acids), nitrogen-heterocyclic ompounds and amino acid derivatives (*e.g.*, isocyanates). It may be worth to extract these compounds as a commodity for chemical application. For instance, phenols can be used as precursors for epoxies (Asada et al., 2015) while isocyanates are widely used to synthesize polyurethanes (Saunders, 1973).

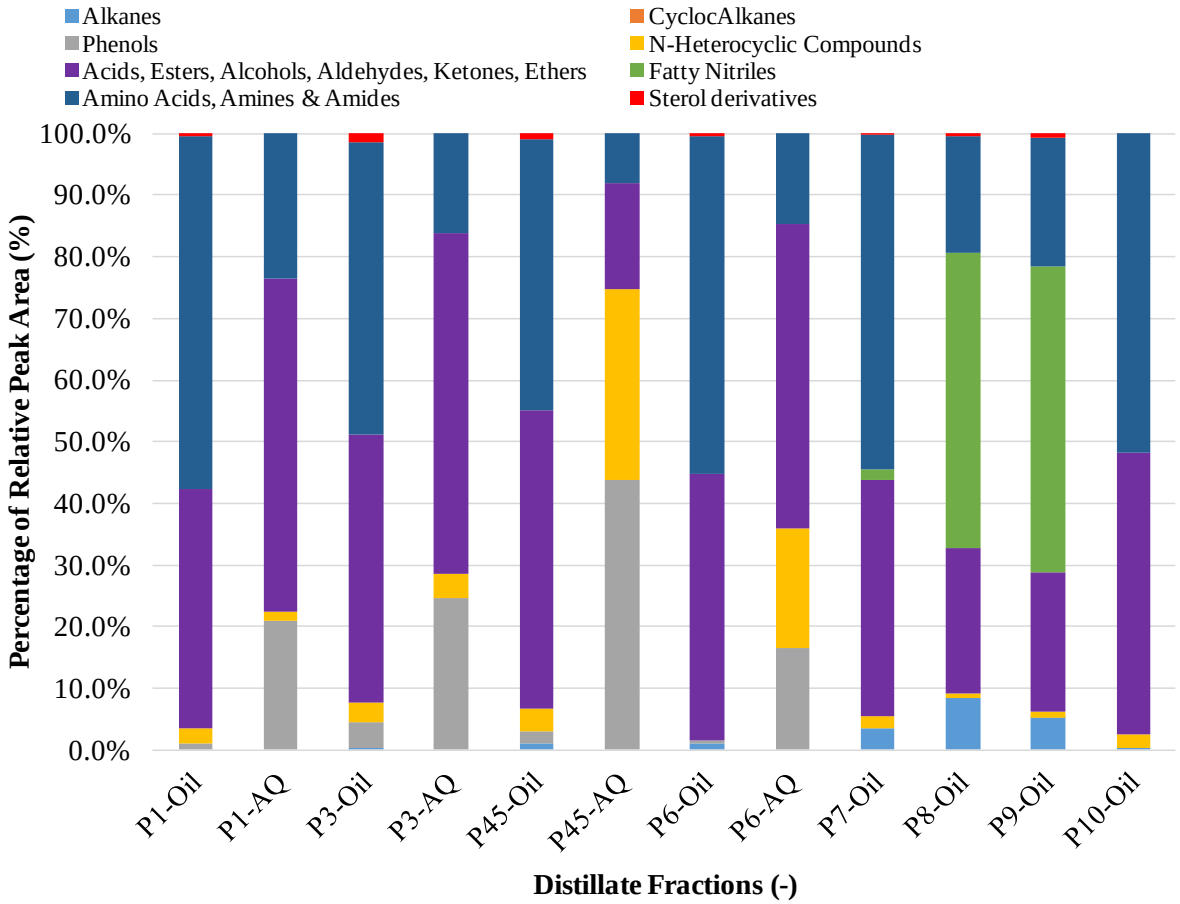


**Figure E-1. Percentage of the relative peak area of different chemical compositions obtained under GC-MS analysis with derivative treatment for the distillates from SW-derived biocrude oil**

**Table E-1. Normalized GC-MS signals of components identified in the distillates with derivative treatment, from SW-derived biocrude; "×" indicates the chemical was not detected**

| Compound Name | Normalized Signal (-) | | | | | | | | | | |
|---|---|---|---|---|---|---|---|---|---|---|---|
| | A-AQ | C-AQ | D-AQ | E-AQ | A-Oil | C-Oil | D-Oil | E-Oil | F-Oil | G-Oil | H-Oil |
| **Hydrocarbons** | | | | | | | | | | | |
| Eicosane | × | × | × | × | × | × | × | × | × | 0.21 | 0.03 |
| Henicosane | × | × | × | × | × | × | × | × | × | 0.12 | 0.03 |
| Docosane | × | × | × | × | × | × | × | × | × | 0.07 | 0.03 |
| Tricosane | × | × | × | × | × | × | × | × | × | 0.03 | 0.02 |
| **Phenols** | | | | | | | | | | | |
| Phenol | 0.02 | 0.02 | 0.61 | 0.36 | × | 0.001 | × | 0.002 | × | × | × |
| Methyl phenol | 0.04 | 0.06 | 1.1 | 0.13 | 0.75 | 0.01 | × | × | × | × | × |
| Ethyl phenol | 0.01 | 0.02 | 3.27 | 0.58 | 0.01 | 0.01 | 0.01 | × | × | × | 0.002 |
| Catechol | 0.03 | 0.13 | 1.65 | 1.55 | × | 0.001 | 0.004 | × | × | × | × |
| Methyl catechol | × | × | 1.19 | 0.24 | × | × | × | × | × | × | × |
| Vanillin | 0.12 | 0.08 | 0.22 | 0.11 | × | 0.01 | × | × | × | × | × |
| **Nitrogen Heterocyclic Compounds** | | | | | | | | | | | |
| Hydroxypyridine | 0.02 | 0.05 | 1.58 | 1.31 | 1.85 | 0.02 | 0.03 | × | 0.01 | 0.06 | 0.02 |
| Dimethyl carbazole | × | 0.003 | 0.65 | × | × | × | × | × | × | × | × |
| Hydroxy methylpyridine | × | 0.02 | 4.13 | 1.82 | × | × | × | × | × | × | × |
| **Fatty Nitriles** | | | | | | | | | | | |
| Hexadecane-nitrile | × | × | × | × | × | × | × | × | × | 1.92 | 0.19 |
| Octadecanenitrile | × | × | × | × | × | × | × | × | × | 1.42 | 0.57 |
| **Amino acids, Amines and Amides** | | | | | | | | | | | |
| Propylamine | 0.01 | 0.01 | 0.18 | 0.08 | 0.48 | 0.004 | 0.004 | 0.004 | 0.004 | 0.02 | 0.01 |
| Butylamine | 0.04 | 0.06 | 0.25 | 0.03 | 9.23 | 0.07 | × | 0.07 | 0.07 | 0.27 | 0.11 |
| Diethyl carbamate | 0.15 | 0.17 | 0.18 | 0.09 | 26.4 | 0.21 | 0.23 | 0.23 | 0.23 | 0.83 | 0.35 |
| Glyoxime | × | 0.003 | × | 1.42 | × | 0.01 | 0.01 | 0.01 | 0.01 | 0.02 | 0.01 |
| **Sterol Derivatives** | | | | | | | | | | | |
| Dehydroabietic acid | × | × | × | × | 0.33 | 0.01 | 0.01 | 0.003 | 0.002 | 0.01 | 0.01 |
| **Fatty Acids & Fatty Alcohols** | | | | | | | | | | | |
| Lactic acid | 0.03 | 0.02 | 0.04 | × | 2.09 | 0.01 | 0.01 | 0.03 | 0.01 | 0.12 | 0.06 |
| Glyoxalic hydrate | 0.08 | 0.10 | 0.15 | × | 15.7 | 0.14 | 0.15 | 0.15 | 0.14 | 0.51 | 0.21 |
| Glycerol | 0.01 | 0.003 | 0.01 | 0.004 | 0.49 | 0.003 | 0.002 | 0.004 | 0.003 | 0.03 | 0.01 |
| Propenylthio Acetic acid | × | 0.004 | × | × | 1.02 | × | × | × | × | × | × |
| Dodecanol | × | × | × | 0.11 | 4.42 | 0.03 | 0.04 | 0.03 | 0.03 | 0.25 | 0.09 |
| Hexanoic acid | 0.35 | 0.39 | 1.08 | 2.71 | 1.03 | 0.01 | 0.01 | 2.71 | × | 0.04 | 0.01 |
| Hexadecanoic acid | × | × | × | 0.003 | × | × | × | × | × | × | 0.01 |
| Octadecanoic acid | × | × | × | 0.003 | × | 0.01 | 0.004 | × | × | × | × |
| Propanoic acid thiobis dodecyl ester | × | × | × | × | 2.39 | 0.10 | 0.12 | 0.01 | 0.07 | 0.23 | 0.11 |
| Phosphate | 0.02 | 0.01 | 0.02 | 0.02 | 2.39 | 0.01 | 0.02 | × | 0.01 | 0.26 | 0.06 |
| Lauryl acrylate | × | × | × | × | × | 0.01 | × | × | × | × | 0.06 |

# APPENDIX F: FT-IR ANALYSIS OF DISTILLATES FROM HTL BIOCRUDE OIL

FT-IR analyses were also conducted to understand the chemical compositions in the distillates. The distillates were separated into one oil-like phase (floating on the top) and one aqueous-like phase (with transparent color settling in the bottom). Since only a fraction of the distillates is identifiable by GC-MS, due to the fact that the distillates may contain compounds with high molecular weights and chemicals that are not volitable (Gai et al., 2014a; Vardon et al., 2011; Yu, 2012), FT-IR analysis was carried out to investigate the functional groups in the distillates to compensate this limitation.

**Table F-1. Functional groups identified in the oil-phase products in the distillates from SW-derived biocrude**

| Functional Groups | A-Oil | C-Oil | D-Oil | E-Oil | F-Oil | G-Oil | H-Oil |
|---|---|---|---|---|---|---|---|
| Phenols | O | O | O | O | X | X | O |
| Aromatic Ethers | O | O | O | O | X | X | O |
| Aromatic Hydrocarbons | X | O | O | X | X | O | X |
| Aliphatic Amides | O | X | X | X | X | X | X |
| Aliphatic Amines | X | X | X | X | X | X | O |
| Aliphatic Hydrocarbons | O | O | O | O | O | O | O |
| Vinyl Olefins | X | X | X | X | X | O | X |
| Aliphatic Ketones | X | O | X | X | X | X | X |
| Aliphatic Carboxylic Acids | X | O | X | X | X | X | X |
| Aliphatic Alcohols | X | X | O | O | O | O | X |

**Table F-2. Function groups identified in the aqueous-phase products in the distillates from SW-derived biocrude**

| Functional Groups | A-AQ | B-AQ | C-AQ | D-AQ | E-AQ |
|---|---|---|---|---|---|
| Phenols | X | X | X | X | O |
| Aromatic Isothiocyanates | X | X | X | O | O |
| Aromatic Hydrocarbons | X | X | X | O | X |
| Aliphatic Amides | O | O | X | O | O |
| Aliphatic Hydrocarbons | X | X | X | X | O |
| Aliphatic Alcohols | X | X | O | X | O |

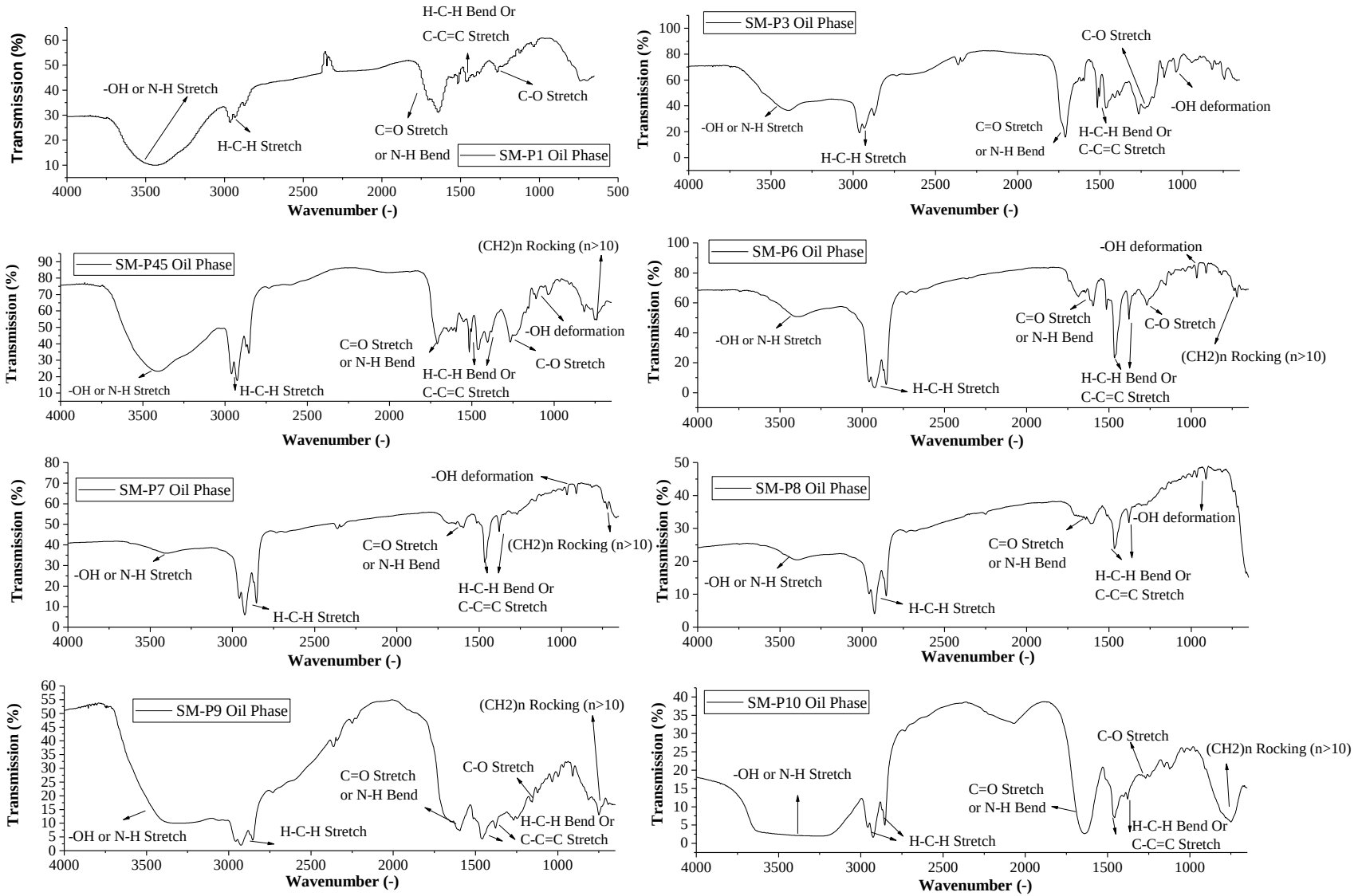


**Figure F-1. FT-IR spectra of the oil-phase product in the distillates from SW-derived biocrude**

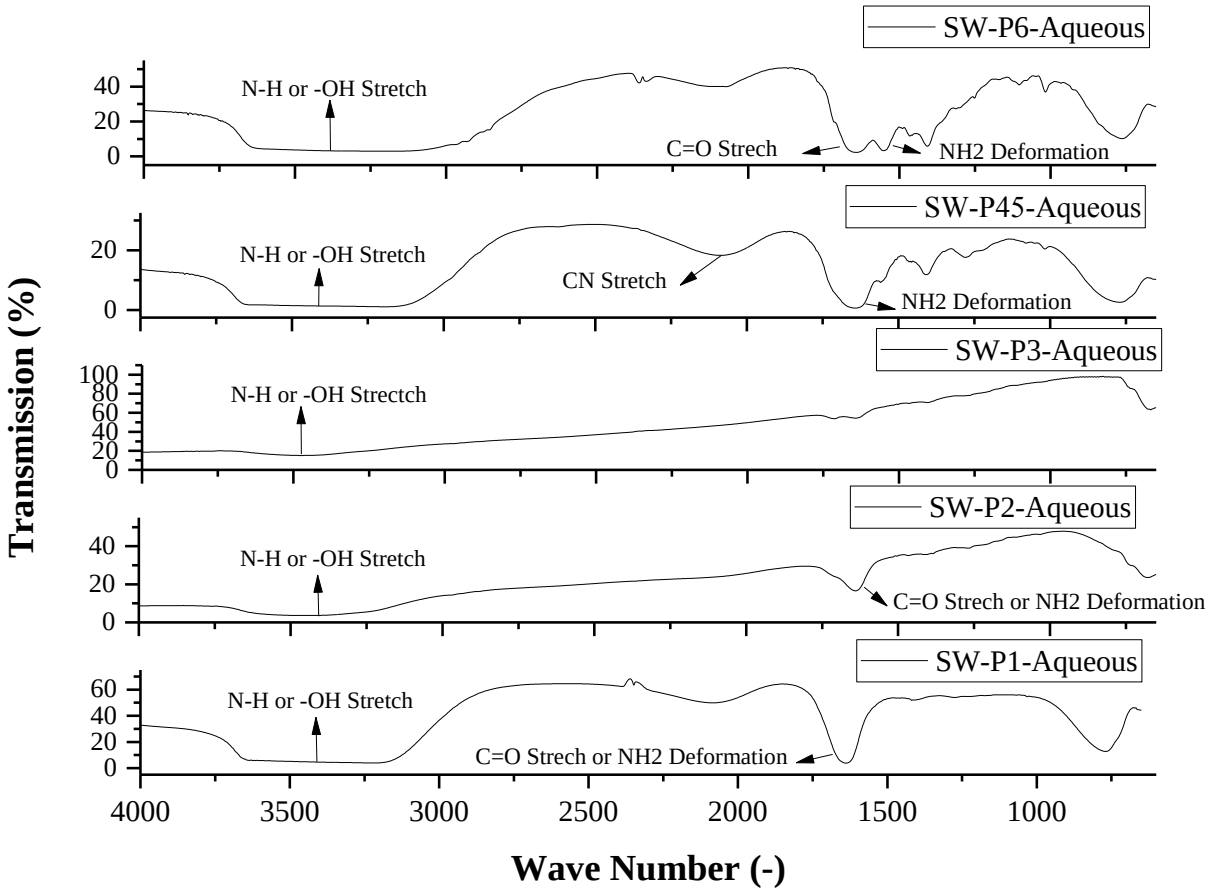


**Figure F-2. FT-IR spectra of the aqueous-phase product in the distillates from SW-derived biocrude**

FT-IR analyses were also subjected to the distillates from FPW-derived biocrude, which were separated into one oil-like phase (floating on the top) and one aqueous-like phase (with transparent color settling in the bottom) as well.

**Table F-3. Functional groups identified in the oil-phase products in the distillates from FPW-derived biocrude**

| Functional Groups | A-Oil | B-Oil | C-Oil | D-Oil | D-Oil | F-Oil | G-Oil | H-Oil |
|---|---|---|---|---|---|---|---|---|
| Aromatic Hydrocarbons | X | X | X | X | X | X | X | O |
| Amine Salts | X | X | X | O | X | X | X | X |
| Aliphatic Amines | X | X | X | X | X | X | X | X |
| Aliphatic Hydrocarbons | O | O | O | O | O | O | O | O |
| Vinyl Olefins | X | X | O | O | O | O | O | O |
| Aliphatic Ketones | X | O | O | O | O | O | O | O |
| Aliphatic Carboxylic Acids | O | O | X | X | X | O | X | X |
| Aliphatic Alcohols | X | X | X | O | X | X | O | X |

FT-IR analysis was also conducted on the aqueous-phase like products in the fractions A-D to further explore their chemical functionality (Table F-4). Table F-4 reveals that the aqueous-phase like products contain not only oxygenates, but also inorganic carbonates, nitrates, and phosphates. These organic and inorganic nutrients are essential for life. Therefore, it is suggested to recycling the aqueous-phase like products in the distillates from FPW-derived biocrude as a substrate to grow microorganisms (*e.g.*, algae and bacteria) (Tommaso et al., 2015; Zhou et al., 2013).

**Table F-4. Functional groups identified in the aqueous-phase products in the distillates from FPW-derived biocrude oil**

| Functional Groups | A-AQ | B-AQ | C-AQ | D-AQ |
|---|---|---|---|---|
| Inorganic Nitrates | O | X | X | X |
| Inorganic Carbonates | O | X | X | X |
| Aliphatic Phosphates | X | O | X | X |
| Aliphatic Amides | X | X | X | X |
| Aliphatic Hydrocarbons | O | O | O | O |
| Vinyl Olefins | X | X | O | O |
| Aliphatic Ketones | X | X | O | O |
| Aliphatic Carboxylic Acids | X | O | O | O |
| Aliphatic Alcohols | O | X | X | X |

# APPENDIX G: DROP-IN BIOFUEL SAMPLES

**Table G-1. Drop-in aviation biofuel samples prepared with 10 wt.% distillates from (a) FPW- and (b) SW-derived biocrude, and 90 wt.% jet fuel A**

| (a) Fractions C-G:JA=1:9 (FPW) | (b) Fraction F:JA=1:9 (SW) |
|---|---|
| 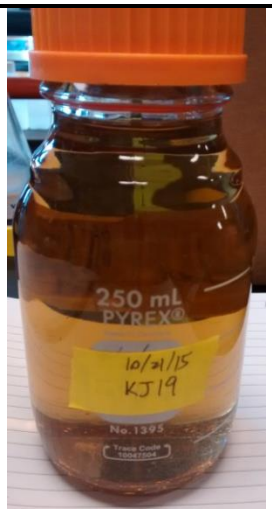  | 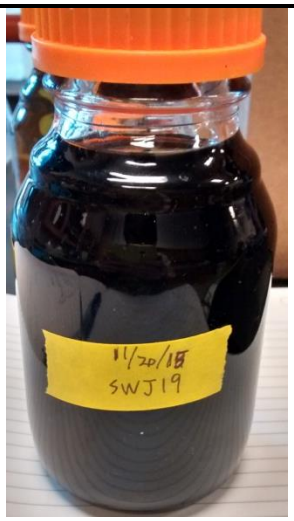  |

# APPENDIX H: FUEL SPECIFICATION OF DROP-IN AVIATION BIOFUEL

**Table H-1. Fuel specification analysis of drop-in aviation biofuel (10 wt.% distillates from HTL biocrude oil plus 90 wt.% jet fuel A)**

| Fuel Spec Property | C-G:JA=1:9 (FPW) | F:JA=1:9 (SW) | Jet Fuel (JA) |
|---|---|---|---|
| Density ($kg/m^3$)[a] | 805 | 810 | 805 |
| Viscosity @20°C ($mm^2/s$)[b] | 1.638 | 1.786 | 1.747 |
| Acidity (mg KOH/g)[c] | 4.28 | 0.29 | 0.10[e] |
| Flash Point (°C)[d] | 30 | 43.5 | 38>[e] |
| Copper Corrosion (-)[e] | 1A | 1A | No. 1[e] |
| Existent Gum (mg/100ml) | 328.8[f] | 724.6[g] | <7[e] |
| Net Heat of Combustion (MJ/kg)[e] | 45.4 | 45.8 | 46.0 |
| Total sulfur Content (%)[e] | 0.011% | 0.014% | <0.30%[e] |

[a]Measured by hydrometer (ASTM D7566-14a); [b]Measured by Cannon-Fenske Viscometer (ASTM D7566-14a); [c]Measured by ASTM D664; [d]Measured by ASTM D93; [e] According to ASTM D7566-14a; [f] Modified ASTM D381, put the sample on a hot plate to evaporate out the volatile fraction

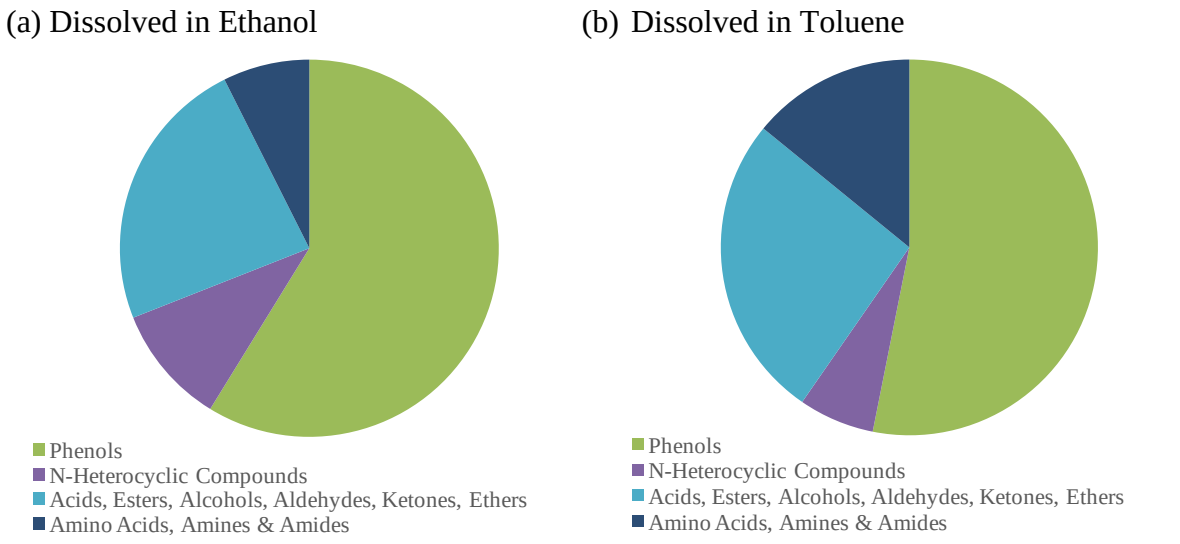


**Figure H-1. Chemical compositions of the insoluble fraction in drop-in aviation biofuel prepared with 10 wt.% distillates from SW-derived biocrude oil and 90 wt.% jet fuel A**

# APPENDIX I: DIRECTLY UPGRADING BIOCRUDE OIL CONVERTED FROM SWINE MANURE VIA HTL

A preliminary upgrading study has been conducted with the biocrude oil converted from swine manure via HTL at 300°C for 1h reaction time. The product yields and elemental compositions of the upgraded biocrude oil were given in Tables I-1 and I-2. Tables I-1 and I-2 show that upgrading methods such as thermal cracking, hydrotreating, and/or hydrocracking cannot improve the heating values (as well as flowability) of HTL biocrude oil.

**Table I-1. The effect of reaction temperature, reaction time, catalysts, and processing gas on product yields of upgraded biocrude converted from swine manure via HTL**

| Sample[a] | Oil (%) | Solid Residue (%) | Gas (%) | Aqueous Product (%) | Loss (%) |
|---|---|---|---|---|---|
| **With H2 (150 psi)** | | | | | |
| 45060HZSM5 | 43.7% | 39.5% | 10.0% | 0% | 6.80% |
| 40060R-Ni[b] | 73.8% | 20.8% | 20.8% | 1.91% | 3.52% |
| **With N2 (100 psi)** | | | | | |
| 40060R-Ni | 49.8% | 21.8% | 10.0% | 14.6% | 3.73% |
| 40030R-Ni | 44.9% | 32.6% | 0% | 4.35% | 18.1% |
| 40030HZSM5 | 25.4% | 20.7% | 0% | 0.22% | 53.8% |
| 35060HZSM5 | 48.4% | 16.8% | 0% | 3.35% | 31.5% |
| 40030 | 24.3% | 19.4% | 8.70% | 0% | 47.6% |
| **With Formic Acid (in-situ hydrogenation)** | | | | | |
| 450120N2Pt | 43.7% | 38.4% | N/A[c] | N/A[c] | N/A[c] |
| 40060N2R-Ni | 64.2% | 22.0% | N/A[c] | N/A[c] | N/A[c] |

[a]Sample was named as reaction temperature (°C);reaction time (minutes);catalyst type. For example, 40060R-Ni means the biocrude was upgraded at 400°C for 60 minutes reaction time with R-Ni as a catalyst.
[b]Raney®-Ni
[c] Not applied

Nevertheless, this preliminary analysis did reveal information for designating the experimental design for future upgradation on the distillates from SW- and FPW-derived biocrude. In order to achieve efficient hydrotreating, creating a highly reduced environment with high pressure of hydrogen seemed to be necessary. Table I-2 shows that the hydrogen content in HTL biocrude oil can only be increased when the upgradation took place with an initial hydrogen pressure of 150 psi. In addition, an excessively high reaction temperature (*e.g.*, 450°C) and reaction time (*e.g.*, 120 min) may lead to degradation of HTL biocrude and char formation. Moreover, thermal cracking appeared to effectively deoxygenate HTL biocrude, with and

without HZSM-5 as a catalyst. However, the nitrogen content also increased in the upgraded HTL biocrude oil. Further reaction mechanism studies may be needed to elucidate how (catalytic) thermal cracking may affect HTL biocrude oil. In contrast, in-situ hydrotreating with formic acid failed to increase the hydrogen content and improve the heating value of HTL biocrude oil. Hence, in-situ hydrotreating is not suggested for future upgradation tests on distillates from HTL biocrude.

**Table I-2. The effect of reaction temperature, reaction time, catalysts, and processing gas on elemental compositions of upgraded biocrude oil converted from swine manure via HTL**

| Samples | C (%) | H (%) | N (%) | O (%) | HHV (MJ/kg) | Energy Recovery (%) |
|---|---|---|---|---|---|---|
| **With H2 (150 psi)** | | | | | | |
| 45060HZSM5 | 74.7 | 6.56 | 6.12 | 12.6 | 32.4 | 35.0% |
| 40060R-Ni | 80.0 | 10.1 | 4.9 | 5.07 | 40.4 | 73.8% |
| **With N2 (100 psi)** | | | | | | |
| 40060R-Ni | 79.3 | 8.83 | 4.61 | 7.29 | 38.1 | 46.9% |
| 40030R-Ni | 79.1 | 9.63 | 5.18 | 6.07 | 39.4 | 43.7% |
| 40030HZSM5 | 79.7 | 10.3 | 4.85 | 5.16 | 40.6 | 25.5% |
| 35060HZSM5 | 78.7 | 9.76 | 4.95 | 6.55 | 39.4 | 47.1% |
| 40030 | 80.5 | 10.3 | 4.77 | 4.39 | 41.1 | 24.7% |
| **With Formic Acid** | | | | | | |
| 450120N2Pt | 79.4 | 7.77 | 6.72 | 6.14 | 36.8 | 30.6% |
| 40060N2R-Ni | 79.5 | 9.43 | 5.32 | 5.80 | 39.3 | 62.4% |
| **Biocrude Oil (Before Upgrading)** | 76.2 | 9.81 | 4.32 | 9.71 | 38.0 | 78.5% |

The distillates from SW-derived biocrude oil (fractions F-G) that have similar physicochemical properties to transportation fuels were also upgraded by catalytic hydrotreating under supercritical water. Since the major non-hydrocarbon compounds in the distillates from SW-derived biocrude oil are phenols and nitrogen-containing compounds (*e.g.*, indoles), catalysts such as Raney-Ni were selected to promote hydrodeoxygention and hydrodenitrogenation of the distillates based on multiple previous studies upgrading algal biocrude and heavy asphalt as well as the preliminary results listed in Tables I-1 and I-2 (Duan et al., 2013a; Duan & Savage, 2011a; Duan & Savage, 2011c; Zhao et al., 2012; Zhao et al., 2009). Furthermore, it was reported that supercritical water can prevent char formation during the upgrading processes. Thus, supercritical water is selected for further investigation (Duan et al.,

2013a). Preliminary results upgrading the distillates from SW-derived biocrude oil (fractions F-G) were reported in Tables A-14, A-15 and A-16.

As Tables I-3, I-4, and I-5 demonstrate, upgrading the distillates from SW-derived biocrude oil seems not promising. First, the upgraded oil yield is much lower than those obtained via neutralization. Moreover, the HHV of upgraded oil is even decreased after hydrotreating with Raney-Ni. Possible reasons of these preliminary results could be that partial compounds were gasified during the upgrading processes. Further, it has to point out that leaking happened when using the mini-reactor (20 ml) that was assembled with Swagelok fittings to upgrade the distillates. As a consequence, there were 20-60 wt.% of the distillates lost (Table I-3 and I-4). Future work should pay attention to how to properly address this leaking issue and effectively recover upgrade oil when using the mini-reactor.

**Table I-3. Preliminary results upgrading the distillates from SW-derived biocrude oil (fractions F-G) at 300°C for a 1h reaction time with Raney-Ni under 150 psi $H_2$ (n=1)**

| Samples | Upgraded Oil Yield (wt.%) | Solid Residue (wt.%) | Gas Products (wt.%) | Aqueous products and lost (wt.%) |
|---|---|---|---|---|
| With Supercritical $H_2O$ | 55.4 | 12.5 | 16.1 | 16 |
| Without $H_2O$ | 33.0 | 4.27 | 6.7 | 56 |
| Neutralized SW-Distillates F-G | 70-80 | N/A [a] | N/A [a] | 20-30 |
| SW-Distillates F-G (Before Upgrading) | N/A [a] | N/A [a] | N/A [a] | N/A [a] |

[a] Not applied

**Table I-4. Preliminary results upgrading the distillates from SW-derived biocrude oil (fractions F-G) at 350-375°C for a 1h reaction time with HZSM5 under 100 psi $N_2$ (n=1)**

| Samples | Upgraded Oil Yield (wt.%) | Solid Residue (wt.%) | Gas Products (wt.%) | Aqueous products and lost (wt.%) |
|---|---|---|---|---|
| With Supercritical $H_2O$ (375°C ) | 51.6 | 9.44 | 4.29 | 34.7 |
| Without $H_2O$ (350°C ) | 38.5 | 0 | 0 | 61.5 |
| Neutralized SW-Distillates F-G | 70-80 | N/A [a] | N/A [a] | 20-30 |
| SW-Distillates F-G (Before Upgrading) | N/A [a] | N/A [a] | N/A [a] | N/A [a] |

[a] Not applied

**Table I-5. Elemental composition of the distillates from SW-derived biocrude oil (fractions F-G) upgraded at 300 °C for a 1h reaction time with Raney-Ni under 150 psi $H_2$**

| Samples | C (%) | H (%) | N (%) | O (%) | HHV (MJ/kg) |
|---|---|---|---|---|---|
| With Supercritical $H_2O$ | 78.1 | 10.4 | 3.79 | 7.72 | 39.8 |
| Without $H_2O$ | 82.0 | 12.4 | 2.15 | 3.45 | 44.8 |
| SW-Distillates F-G (Before Upgrading) | 82.8 | 12.8 | 1.55 | 2.88 | 45.7 |

In addition, it is suggested to more thoroughly study reaction temperature and reaction time in terms of upgrading the distillates from HTL biocrude oil. Reaction temperature and reaction time were reported as significant parameters that may impact the upgrading processes of fatty acids (Vardon et al., 2014). An orthogonal study (Table I-6) is recommended to investigate the effect of (1) sub- and supercritical water density (0, 0.025, 0.1 g/cm3), (2) catalyst types (Raney-Ni, Pt/C, HZSM-5), (3) reaction temperatures (300°C, 350°C, 400°C), and (4) reaction time (1hr, 3hr, 6hr), with the initial hydrogen of 500 psi (can be adjusted later based on preliminary results). The upgrading experiments can be performed with a mini-reactor (20 ml) that was assembled with Swagelok fittings and described with details in previous studies (Breinl & Zhang, 2015; Duan & Savage, 2011c; Zhang et al., 2014). Since the purpose of the hydrotreating is to screen out the most effective catalyst, a 5 wt.% catalyst will be used and may be changed in future studies.

**Table I-6. Orthogonal experimental design of catalytic hydrotreating distillates from biocrude oil**

| Run # | Water Density | Reaction Temperature (°C) | Reaction Time (hr) | Catalysts (5 wt.%) |
|---|---|---|---|---|
| 1 | 0 | 300 | 1 | Raney-Ni |
| 2 | 0 | 350 | 3 | Pt/C |
| 3 | 0 | 400 | 6 | HZSM-5 |
| 4 | 0.025 | 300 | 3 | HZSM-5 |
| 5 | 0.025 | 350 | 6 | Raney-Ni |
| 6 | 0.025 | 400 | 1 | Pt/C |
| 7 | 0.1 | 300 | 6 | Pt/C |
| 8 | 0.1 | 350 | 1 | HZSM-5 |
| 9 | 0.1 | 400 | 3 | Raney-Ni |

The product yields, elemental (CHN contents) and GC-MS analysis will be evaluated on the upgraded distillates, solid char, aqueous and gas products. A potential reaction network will

be proposed based on the upgrading results. If needed, catalytic hydrotreating with model compounds will also be conducted to elucidate and validate the reaction pathways.

In order to investigate if the upgradation would make the distillates from HTL biocrude more stable towards transportation fuels, the fuel specification test will also be subjected to the drop-in aviation biofuels with the upgraded distillates. The related results will be compared to those with regular distillates.

# APPENDIX J: COMBUSTION PROFILES FROM DIESEL ENGINE TEST

(a)

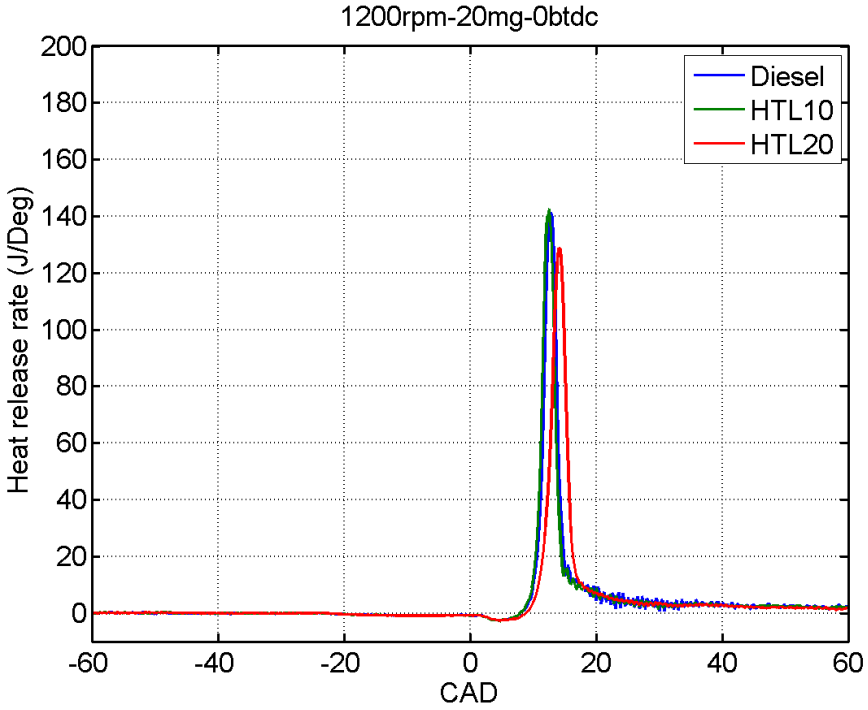


(b)

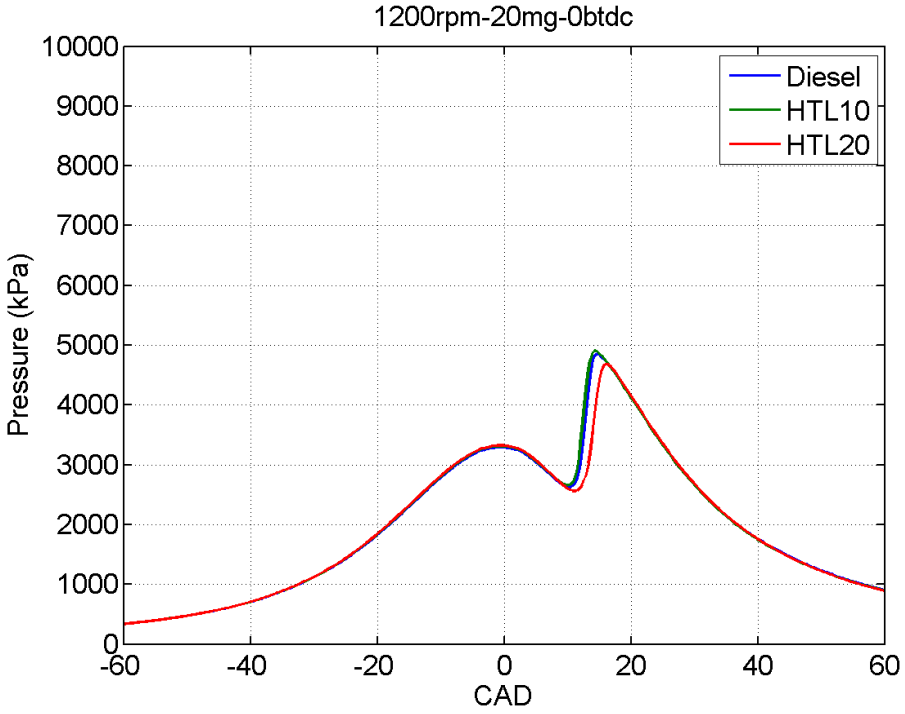


**Figure J-1. (a) Heat release rate and (b) Pressure of HTL10 and HTL20 at 1200 rpm with 20 mg fuel/stroke under 0 btdc under diesel engine test (this test is conducted by Prof. Chia-Fon lee's lab)**

(a)

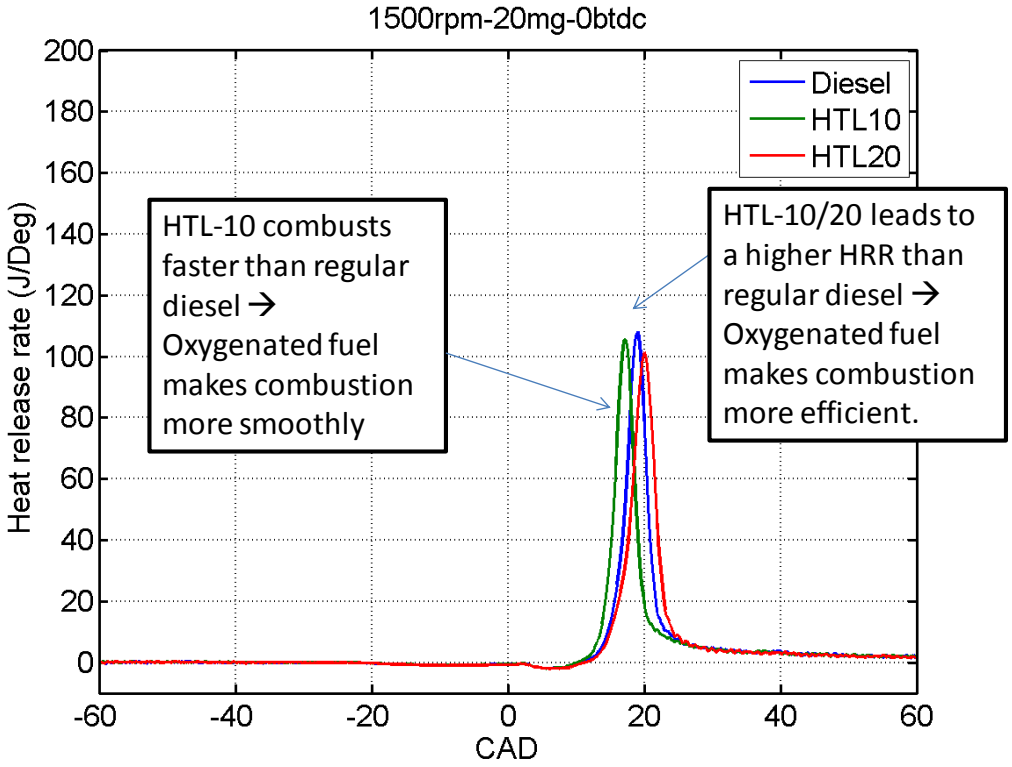


(b)

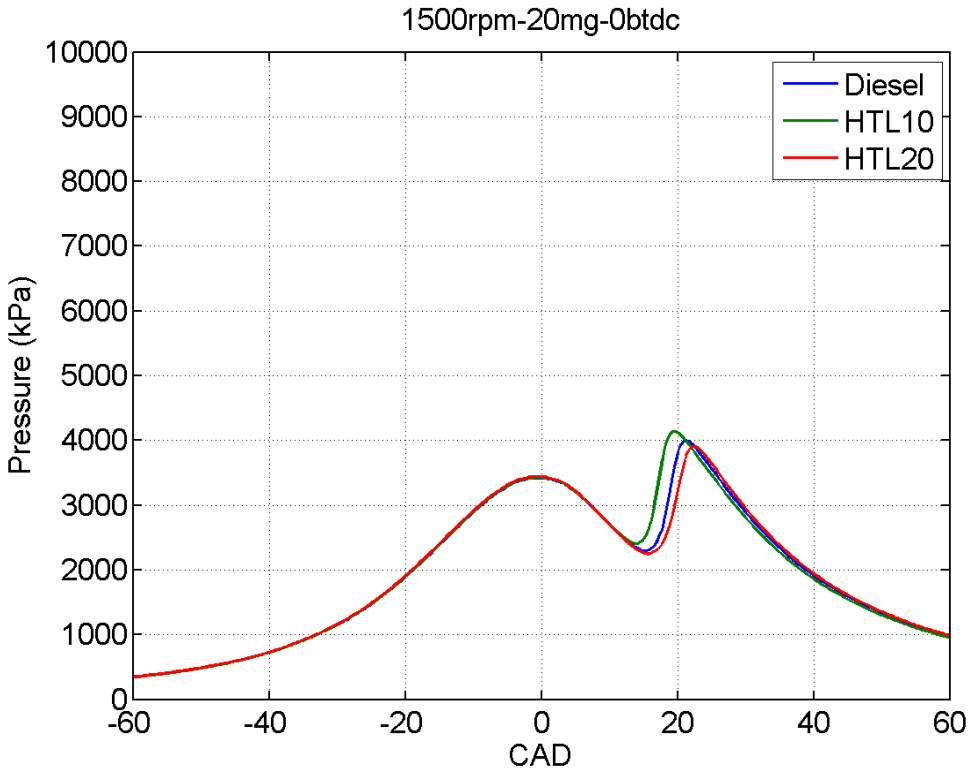


**Figure J-2. (a) Heat release rate and (b) Pressure of HTL10 and HTL 20 at 1500 rpm with 20 mg fuel/stroke under 0 btdc under diesel engine test (this test is conducted by Prof. Chia-Fon lee's lab)**

(a)

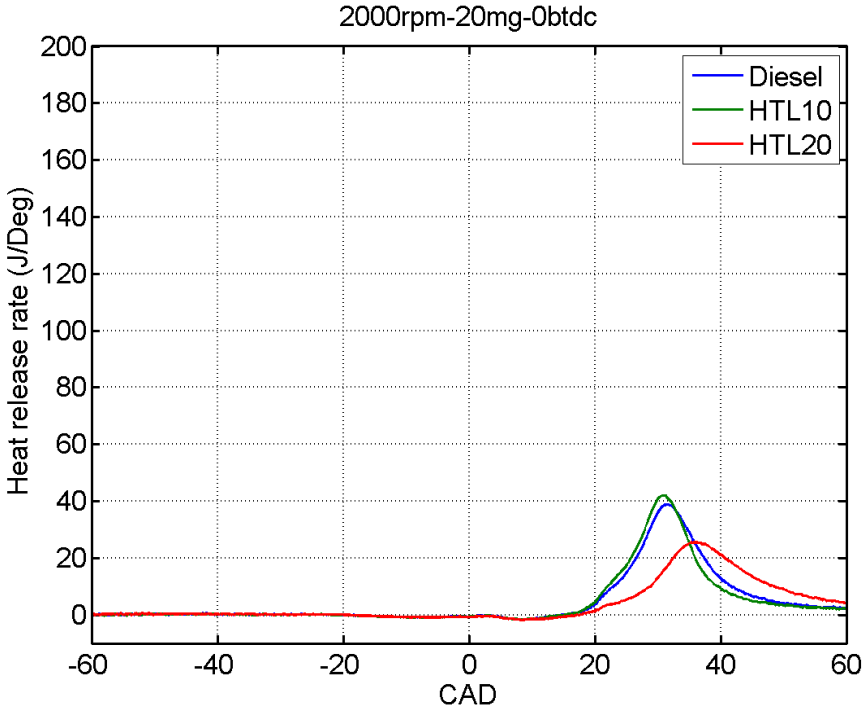


(b)

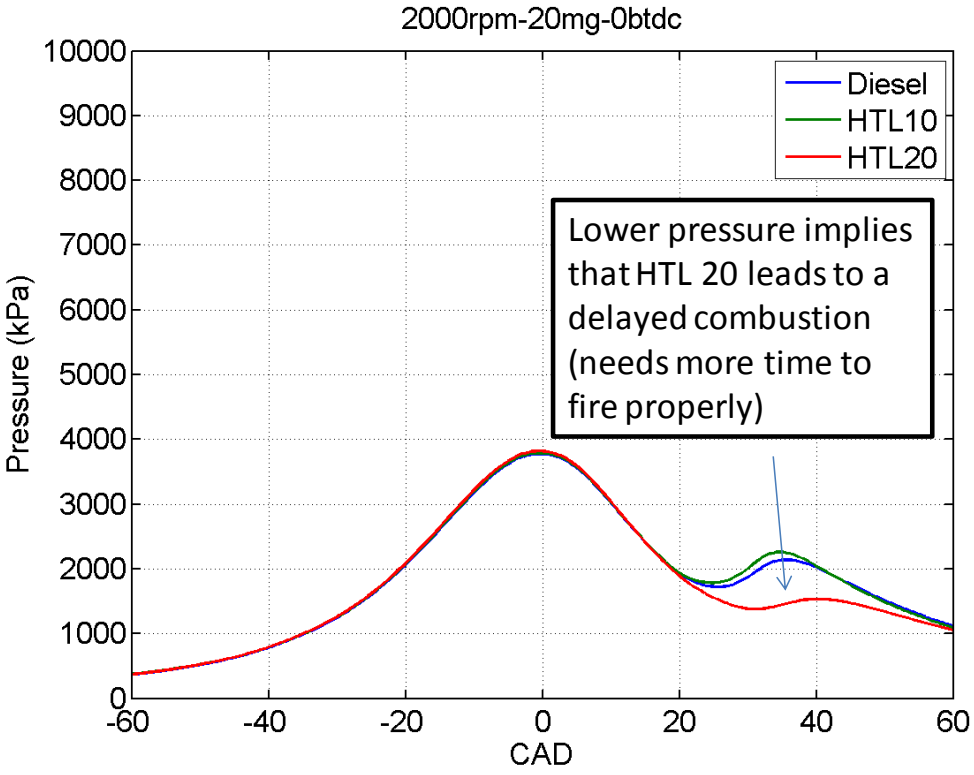


**Figure J-3. (a) Heat release rate and (b) Pressure of HTL10 and HTL 20 at 2000 rpm with 20 mg fuel/stroke under 0 btdc under diesel engine test (this test is conducted by Prof. Chia-Fon lee's lab)**

# APPENDIX K: POTENTIAL APPLICATION OF SOLID RESIDUAL FROM DISTILLATION

**Table K-1. Elemental composition and higher heating value of solid residue from distillation of SW-derived biocrude oil**

| Test | C (wt.%) | H (wt.%) | N (wt.%) | P (wt.%) | K (wt.%) | O[a] (wt.%) | HHV[b] (MJ/kg) |
|---|---|---|---|---|---|---|---|
| 1 | 58.0 ± 0.66 | 1.37 ± 0.66 | 6.00 ± 0.12 | 3.14 | 0.05 | 31.5 | 15.4 |
| 2 | 60.2 ± 0.28 | 1.48 ± 0.04 | 5.70 ± 0.08 | N/A[c] | N/A[c] | 30.6 | 17.7 |

[a]Calculated by difference; [b]based on Dulong Formula (HHV=0.3383*C+1.422*(H-O/8);
[c]Not Applied

**Table K-2. Surface area, pore volume, and pore size of commercial activated carbon and solid residue from distillation of SW-derived biocrude oil***

| Property | Distillate Residue from SW-derived Biocrude Oil | Commercial Activated Carbon |
|---|---|---|
| BET Surface Area ($m^2/g$) | 1.6209 | 1118.2921 |
| BJH Pore Volume ($cm^3/g$) | 0.001081 | 0.641290 |
| BJH Pore size (Å) | 10.507 | 12.597 |

*This test is conducted by Dr. Shihang Zhang at Dr. Yongqi Lu's lab in Illinois State Geological Survey in UIUC. Alternatively, it can be done in Prof. Suslick's lab at School of Chemical Science in UIUC.

**Table K-3. Elemental compositions and higher heating value of KOH-actived solid residue from distillation of SW-derived biocrude oil**

| C (wt.%) | H (wt.%) | N (wt.%) | O[a] (wt.%) | HHV[b] (MJ/kg) |
|---|---|---|---|---|
| 80.1 ± 1.07 | 2.66 ± 0.01 | 5.67 ± 0.12 | 10.8 | 29.2 |

[a]Calculated by difference; [b]based on Dulong Formula (HHV=0.3383*C+1.422*(H-O/8)

**Table K-4. Chemical functional groups of distillate solid residue from SW-derived biocrude oil**

| Functional Groups | Distillate Residue from SW-derived Biocrude Oil | Calcined distillate residue from SW-derived biocrude oil (550°C) | KOH activated distillate residue from SW-derived biocrude oil |
|---|---|---|---|
| Kaolin Clays/ Alumino Silicates | X | O | X |
| Aromatic Hydrocarbons | O | X | X |
| Aliphatic Amines | X | X | O |
| Aliphatic Hydrocarbons | X | X | O |
| Aliphatic Alcohols | O | X | X |

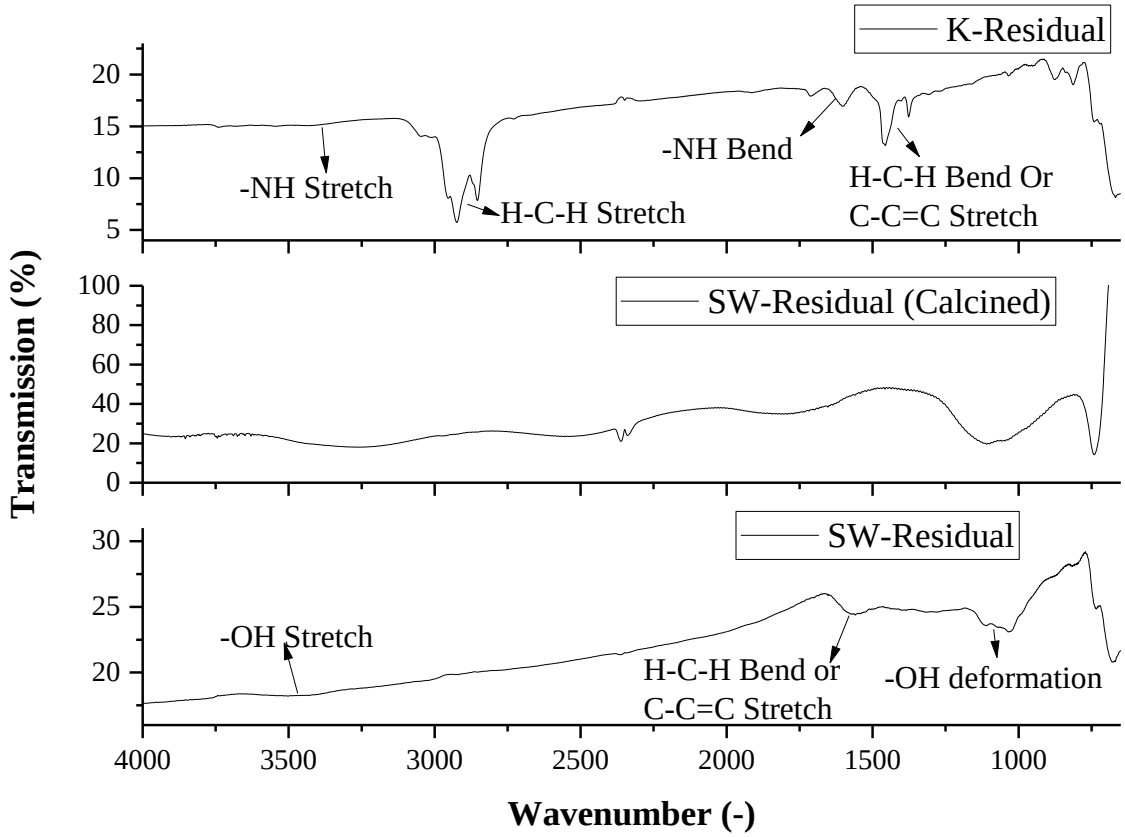


**Figure K-1. Preliminary FTIR spectrum of SW-derived biocrude oil (SW-Residual: without any treatment; SW-Residual (Calcined): burned at 550°C; K-Residual: KOH-activated)**

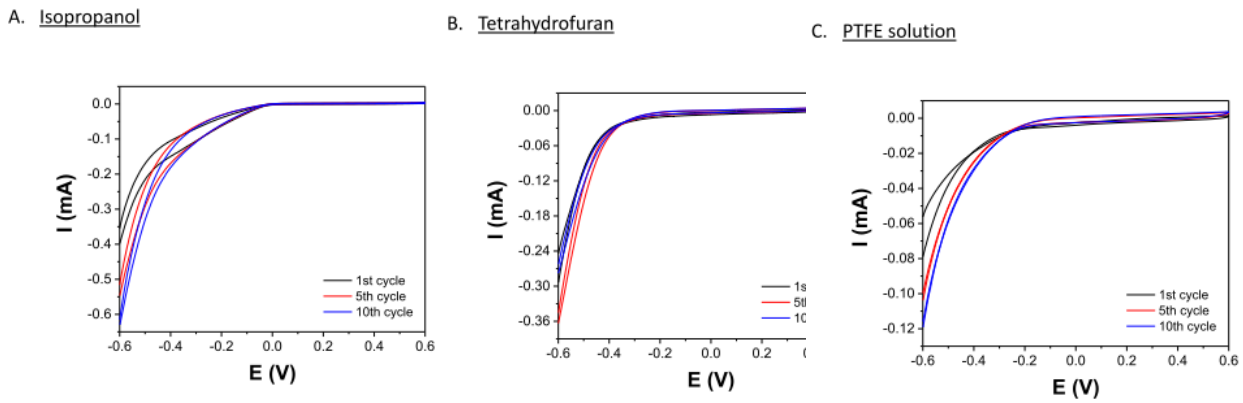


**Figure K-2. Preliminary electrochemical test of KOH-activated solid residue from SW-derived biocrude oil via cyclic voltammetry (CV test) dissolved in (a) isopropanol, (b) tetrahydrofurn, and (c) PTFE solution (this work is conducted by Prof. Hong Yang's lab)**

Notably, the catalyst (carbon material) cannot disperse well in any of these solvents, so it is hard to know the exact catalyst weight on the RDE. Simply put, the data shown below can only be used for qualitative study instead of quantitative study.

In the future, the non-volatile solid residual will be exposed to alkaline solutions (*e.g.*, KOH), acidic solutions (HCl), and thermal calcinations to potentially improve their electrochemical performance under CV test.

# APPENDIX L: PROTOCOL OF DISTILLATION OF BIOCRUDE OIL CONVERTED FROM WET BIOWASTE VIA HTL

## Introduction

Distillation has been conducted with two types of biocrude oil (swine manure and Kraft Salad Food Waste) in this project (2015.03-2017.05). It seems that the distillation operation would be different from feedstock to feedstock. For example, the swine manure-based biocrude oil is more viscous and thereby the up-scaled distillation was extremely challenging and dangerous (eruption happened for several times). On the other hand, the food waste-derived biocrude oil is more flowable and therefore the distillation appears to be more efficient. As a consequence, please keep in mind, the distillation operation of biocrude oil will be very different from feedstocks to feedstocks. The rule of thumb is that conducting the distillation with a small scale (*e.g.*, 300 ml system) first and then move forward to a middle scale (*e.g.*, 1000 ml system), and a up-scaled (*e.g.*, 2000 ml system) in this case.

(a)

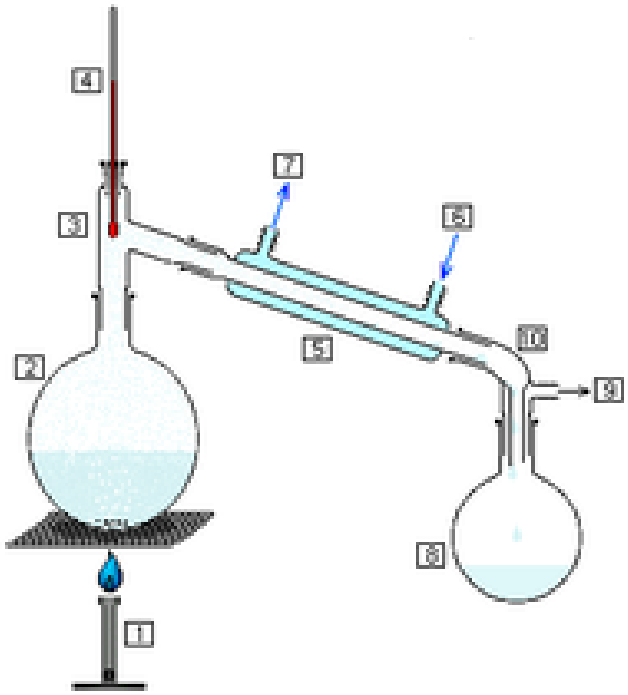


(b)

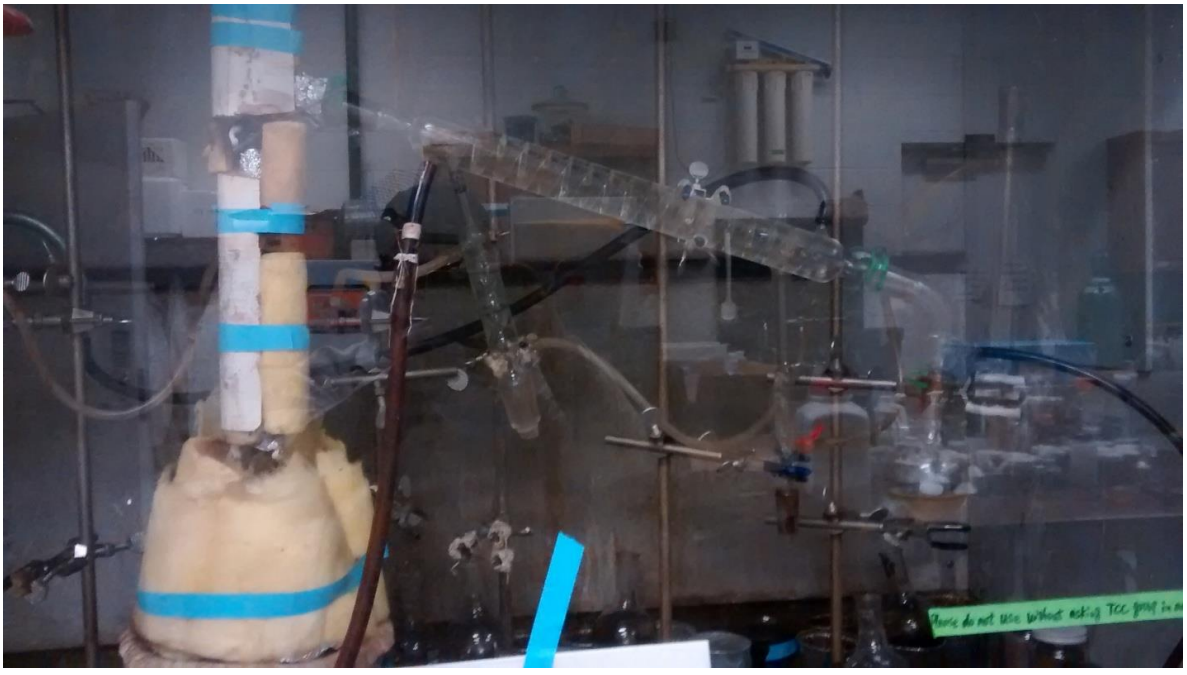

**Figure L-1. Basic set-up of a simple distillation system (a) cartoon illustration (b) actual set-up**

**(1) Kraft Salad Food Waste**

1. Wight the round flask. Add some glass beads (10-30g) in the round flask. Weight the glass beads.
2. Feed 2/3 volume of the biocrude oil in the round flask. Weight the biocrude oil.
3. Gently put the stir bar in the round flask and weight it. Be CAREFUL, the stir bar could break the glass round flask.
4. Set up the distillation system. Paste a little bit DOW Lubricant between the connection of each piece of glassware, making sure every connection do link well. Particularly, the connection between the thermocouple adaptor and condenser ([3] in Figure L-1) can tilt very easily. Also, check the highest temperature the lubricant (DOW lubricant is suggested) and plastic clamp can sustain. Metal (or at least PTFE) clamps are recommended.
5. For Kraft Salad Food Waste, please use the thermocouple rather than the thermometer (because of the limit of thermometer, which is 250°C). Apply 2-3 layers of Teflon tape to the thermocouple to avoid the leaking of gaseous products during the distillation. Change the Teflon tape for every distillation test.
6. Weight the collection flask. Use clamp to tight it well ([8] in Figure L-1). Connect the rubber tube to a water plate for observing how quickly the gaseous products coming out.
7. Turn on the cooling water.
8. Turn on the stir to knob 2.5-3.
9. Turn on the heating to KNOB 2.5 (about 150 degree C). Keep in mind that sometimes the AZZOTA heating mantle cannot heat until the KNOB is tuned to more than 2.5.
10. Wrap up the round flask, Synder column, and thermocouple adaptor with foil wrapping and glass fiber to achieve a better insulate. Figure L-1 is a good example.
11. After 1-1.5 hour heating, if the temperature is not increased you can tune heating KNOB to 3.
12. Record the temperature of steam every 5-15 minutes.
13. If the temperature of steam drops, now you can tune the heating KNOB to 3 1/3 and then to 3.5 and 3 2/3, so on and so on. BE CAREFUL, after KNOB 3, the temperature of the heating mantel will be changed more largely. The distillate will be more

sensitive to the change of the KNOB too. Tune the KNOB SLOWLY AND CATIOUSLY AT THIS STAGE.

14. After the distillation is finished, PLEASE WAIT FOR 1-2 hours until the whole system is cooled down. Use thermocouple to confirm if the system cools down or not. During the waiting period, please still keep a small amount of the cooling water on.
15. Remember to turn off the cooling water.
16. Carefully dissemble the distillation setup from [8]→ [9]→[10]→[5]→[4]→[3]→[2] (please see Figure L-1a).
17. When clean part [10] (Figure L-1a), wash it gently in case the thin collection glass tubing is broken. Use the soft brush to clean it.
18. If necessary, add 300-500 ml of ethanol (or toluene) and distill the whole system again for cleaning (Use the steam of ethanol or toluene to wash out those sticky products).

**(2) Swine Manure**

1. Basically, the protocol is very similar to the above steps for Kraft Salad Waste. However, due to the high viscosity of swine manure, there are some things that should be pointed out and needed high attention.
2. If there is any bumping/eruption happens, please DO NOT TOUCH THE SYSTEM until the whole system cools down. DO NOT OPEN THE HOOD RIGHT AWAY. WAIT until the heating was turned off, the cooling water is turned off and the whole system is cooling down.
3. Because the swine manure-derived biocrude oil is very viscous, please make sure there is stirring function of the heating mantle. DO STIR THE BIOCRUDE OIL ALL THE TIME.
4. Keep the chemical hood as clean as possible, in case the eruption happens. It could be very messy and dangerous when high temperature “lava” type of distillate erupts out.

**DURING THE DISTILLATION REACTION:**

5. WEAR THE RESPIRATION MASK, GOGGLE, insulation gloves (or at least 8mm or two layers of regular gloves), lab coat all the time when you need to touch the distillation system.
6. Do NOT OPEN THE HOOD ALL THE WAY. ALWAYS OPEN THE HOOD A LITTLE BIT BY ALITTLE BIT TO OBESEVE THE SYSTEM.

**Important Notes:**

**1.** Heavy duty round flask, especially for running an up-scaled system. The thick glass would make the heat distribution unevenly and cause a significant eruption/bumping of "hot" and "viscous" liquid. Please do keep the hood close most of the time. The picture below is an unforgettable example for bumping and eruption.

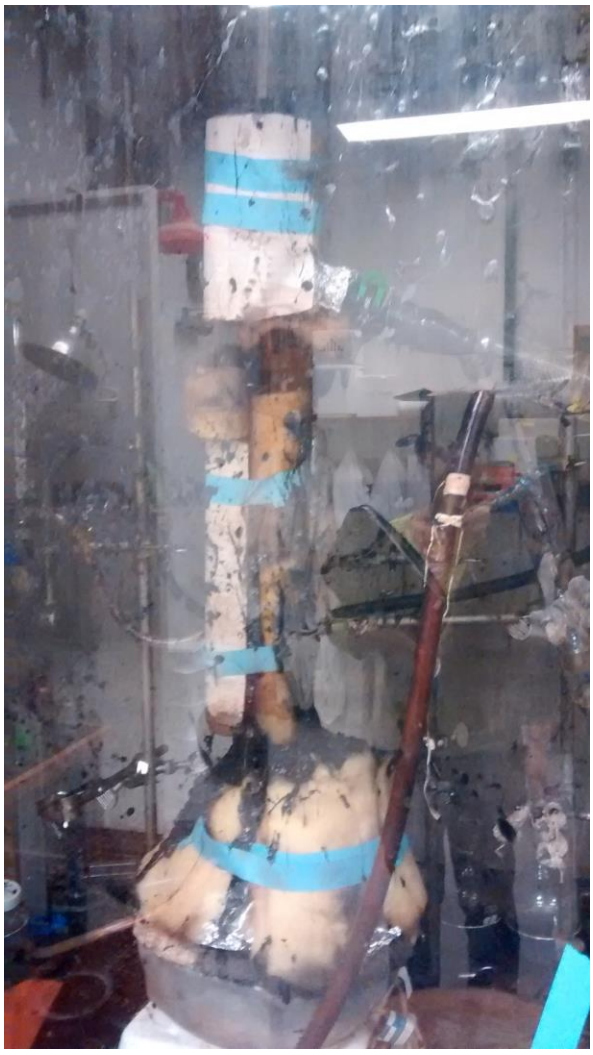

2. Try to choose a more robust heating mantle. Three of the heating mantles purchased from ChemGlass were broken in the bottom because the glass round flask would stick into the glass fiber after the high temperature reaction for such a long time (12-48 hours). If there is only the ChemGlass heating mantle can be used, please add some sand for sand bath heating to help distribute the heat more evenly. Following three pictures are good examples to be memorable!!!

3. Try to keep a short section in the Snyder column for observation. If the bumping seems to happen, turn off the heating right away and DO NOT TOUCH anything.
4. If there is fume coming up (usually due to the distillate coming out too quickly and making the connection not tight anymore), two strategies can be considered:
    1) If the heating is just at the beginning stage, please stop heating right away and check the whole system.
    2) If the heating is in the middle stage, try to avoid to moving the distillation system (it could potentially cause bumping). In a 1000-2000 ml system, please DO STOP HEATING. In a 300-500 ml system, it should be okay to let the distillation finish. However, if a great amount of fume arising, it means something WRONG. STOP HEATING.

**Additional Notes**

1. I would recommend to use a metal or Quartz round flask in the future for distillation (available from Fischer Scientific).
2. Actually, the cooling capacity of the condenser is not good enough, particularly for the 1000-2000 ml system. Later on, if there is any available grant, I would highly suggest to purchasing a recirculation cooling unit to achieve a well-controlled cooling. Plus, the cooling water can be recycled and avoid to wasting clean D.I. water. This kind of unit can be found on Chem Glass or Cole-Parmer. More can be found here.

# REFERENCES


The Engineering ToolBox, Vol. 2017.

2006. *The Merck Index: An Encyclopedia of Chemicals, Drugs, and Biologicals*. Wiley.

2012. *Sustainable Development of Algal Biofuels in the United States*. The National Academies Press.

Adams, T., Appel, B., Samson, P., Roberts, M. 2004. Converting turkey offal into bio-derived hydrocarbon oil with the CWT thermal process. *Power-Gen Renewable Energy Conference*.

Ahmad, A.L., Yasin, N.H.M., Derek, C.J.C., Lim, J.K. 2011. Microalgae as a sustainable energy source for biodiesel production: A review. *Renewable and Sustainable Energy Reviews*, **15**(1), 584-593.

Akhtar, J., Amin, N.A.S. 2011. A review on process conditions for optimum bio-oil yield in hydrothermal liquefaction of biomass. *Renewable and Sustainable Energy Reviews*, **15**(3), 1615-1624.

Albrecht, K.O., Zhu, Y., Schmidt, A.J., Billing, J.M., Hart, T.R., Jones, S.B., Maupin, G., Hallen, R., Ahrens, T., Anderson, D. 2016. Impact of heterotrophically stressed algae for biofuel production via hydrothermal liquefaction and catalytic hydrotreating in continuous-flow reactors. *Algal Research*, **14**, 17-27.

Allen, N.S. 1974. Endoplasmic filaments generate the motive force for rotational streaming in Nitella. *The Journal of cell biology*, **63**(1), 270-287.

Anastasakis, K., Ross, A.B. 2011. Hydrothermal liquefaction of the brown macro-alga Laminaria Saccharina: Effect of reaction conditions on product distribution and composition. *Bioresource Technology*, **102**(7), 4876-4883.

Appleford, J., Ocfemia, K., Zhang, Y., Christianson, L., Funk, T., Dong, R. 2005. Analysis and characterization of the product oil and other products of hydrothermal conversion of swine manure. *2005 ASAE Annual Meeting*. American Society of Agricultural and Biological Engineers. pp. 1.

Asada, C., Basnet, S., Otsuka, M., Sasaki, C., Nakamura, Y. 2015. Epoxy resin synthesis using low molecular weight lignin separated from various lignocellulosic materials. *International Journal of Biological Macromolecules*, **74**, 413-419.

ASTM. 2015a. ASTM D86-15, Standard Test Method for Distillation of Petroleum Products and Liquid Fuels at Atmospheric Pressure. *Annual Book of ASTM Standards*.

ASTM. 2004a. ASTM D95-99:Standard test method for water in petroleum products and bituminous materials by distillation. *Annual Book of ASTM Standards*.

ASTM. 2004b. ASTM D4072-98: Standard test method for toluene-insoluble (TI) content of tar and pitch. . *Annual Book of ASTM Standards*.

ASTM. 2015b. ASTM D7467: Standard Specification for Diesel Fuel Oil, Biodiesel Blend (B6 to B20), ASTM International.

ASTM. 2015c. ASTM D7566 Standard Specification for Aviation Turbine Fuel Containing Synthesized Hydrocarbons. *Annual Book of ASTM Standards*.

Atkins, P., Jones, L., Laverman, L. 2016. *Chemical Principles: The Quest for Insight*. W. H. Freeman.

Audo, M., Paraschiv, M., Queffélec, C.m., Louvet, I., Hémez, J., Fayon, F., Lépine, O., Legrand, J., Tazerout, M., Chailleux, E. 2015. Subcritical Hydrothermal Liquefaction of Microalgae Residues as a Green Route to Alternative Road Binders. *ACS Sustainable Chemistry & Engineering*, **3**(4), 583-590.

Bae, Y.J., Ryu, C., Jeon, J.-K., Park, J., Suh, D.J., Suh, Y.-W., Chang, D., Park, Y.-K. 2011. The characteristics of bio-oil produced from the pyrolysis of three marine macroalgae. *Bioresource Technology*, **102**(3), 3512-3520.

Balat, M. 2008. Mechanisms of thermochemical biomass conversion processes. Part 3: reactions of liquefaction. *Energy Sources, Part A*, **30**(7), 649-659.

Barreiro, D.L., Samorì, C., Terranella, G., Hornung, U., Kruse, A., Prins, W. 2014. Assessing microalgae biorefinery routes for the production of biofuels via hydrothermal liquefaction. *Bioresource technology*, **174**, 256-265.

Barreiro, D.L., Zamalloa, C., Boon, N., Vyverman, W., Ronsse, F., Brilman, W., Prins, W. 2013. Influence of strain-specific parameters on hydrothermal liquefaction of microalgae. *Bioresource technology*, **146**, 463-471.

Becker, E. 2007. Micro-algae as a source of protein. *Biotechnology advances*, **25**(2), 207-210.

Biddy, M., Davis, R., Jones, S., Zhu, Y. 2013. *Whole algae hydrothermal liquefaction technology pathway*. National Renewable Energy Laboratory Golden.

Biller, P., Friedman, C., Ross, A.B. 2013. Hydrothermal microwave processing of microalgae as a pre-treatment and extraction technique for bio-fuels and bio-products. *Bioresource technology*, **136**, 188-195.

Biller, P., Madsen, R.B., Klemmer, M., Becker, J., Iversen, B.B., Glasius, M. 2016. Effect of hydrothermal liquefaction aqueous phase recycling on bio-crude yields and composition. *Bioresource technology*, **220**, 190-199.

Biller, P., Riley, R., Ross, A. 2011. Catalytic hydrothermal processing of microalgae: decomposition and upgrading of lipids. *Bioresource technology*, **102**(7), 4841-4848.

Biller, P., Ross, A. 2011a. Potential yields and properties of oil from the hydrothermal liquefaction of microalgae with different biochemical content. *Bioresource Technology*, **102**(1), 215-225.

Biller, P., Ross, A.B. 2011b. Potential yields and properties of oil from the hydrothermal liquefaction of microalgae with different biochemical content. *Bioresource Technology*, **102**(1), 215-225.

Biller, P., Ross, A.B., Skill, S., Lea-Langton, A., Balasundaram, B., Hall, C., Riley, R., Llewellyn, C. 2012. Nutrient recycling of aqueous phase for microalgae cultivation from the hydrothermal liquefaction process. *Algal Research*, **1**(1), 70-76.

Biller, P., Sharma, B.K., Kunwar, B., Ross, A.B. 2015. Hydroprocessing of bio-crude from continuous hydrothermal liquefaction of microalgae. *Fuel*, **159**, 197-205.

Bolin, K. 2001. The SlurryCarb Process: Turning Municipal Wastewater Solids into a Profitable Renewable Fuel. *Proceedings of the Water Environment Federation*, **2001**(1), 1456-1470.

Breinl, J., Zhang, Y. 2015. Hydrothermal Gasification of HTL wastewater.

Brown, T.M., Duan, P., Savage, P.E. 2010. Hydrothermal Liquefaction and Gasification of Nannochloropsis sp. *Energy & Fuels*, **24**(6), 3639-3646.

Buyukkaya, E. 2010. Effects of biodiesel on a DI diesel engine performance, emission and combustion characteristics. *Fuel*, **89**(10), 3099-3105.

Buzby, J.C., Farah-Wells, H., Hyman, J. 2014. The estimated amount, value, and calories of postharvest food losses at the retail and consumer levels in the United States. *USDA-ERS Economic Information Bulletin*(121).

Calvo, L., Vallejo, D. 2002. Formation of organic acids during the hydrolysis and oxidation of several wastes in sub-and supercritical water. *Industrial & Engineering Chemistry Research*, **41**(25), 6503-6509.

Canakci, M., Van Gerpen, J. 2001. Biodiesel production from oils and fats with high free fatty acids. *Transactions of the ASAE*, **44**(6), 1429.

Cao, J.-P., Zhao, X.-Y., Morishita, K., Li, L.-Y., Xiao, X.-B., Obara, R., Wei, X.-Y., Takarada, T. 2010. Triacetonamine formation in a bio-oil from fast pyrolysis of sewage sludge using acetone as the absorption solvent. *Bioresource technology*, **101**(11), 4242-4245.

Chakraborty, M., McDonald, A.G., Nindo, C., Chen, S. 2013. An α-glucan isolated as a co-product of biofuel by hydrothermal liquefaction of Chlorella sorokiniana biomass. *Algal Research*, **2**(3), 230-236.

Chakraborty, M., Miao, C., McDonald, A., Chen, S. 2012. Concomitant extraction of bio-oil and value added polysaccharides from Chlorella sorokiniana using a unique sequential hydrothermal extraction technology. *Fuel*, **95**, 63-70.

Chen, H., Wan, J., Chen, K., Luo, G., Fan, J., Clark, J., Zhang, S. 2016a. Biogas production from hydrothermal liquefaction wastewater (HTLWW): Focusing on the microbial communities as revealed by high-throughput sequencing of full-length 16S rRNA genes. *Water research*.

Chen, J.-H., Huang, C.-E. 2007. Selective Separation of Cu and Zn in the Citric Acid Leachate of Industrial Printed Wiring Board Sludge by D2EHPA-Modified Amberlite XAD-4 Resin. *Industrial & Engineering Chemistry Research*, **46**(22), 7231-7238.

Chen, W.-T. 2013. Hydrothermal liquefaction of wastewater algae mixtures into bio-crude oil.

Chen, W.-T., Lin, C.-W., Shih, P.-K., Chang, W.-L. 2012. Adsorption of phosphate into waste oyster shell: thermodynamic parameters and reaction kinetics. *Desalination and Water Treatment*, **47**(1-3), 86-95.

Chen, W.-T., Ma, J., Zhang, Y., Gai, C., Qian, W. 2014a. Physical pretreatments of wastewater algae to reduce ash content and improve thermal decomposition characteristics. *Bioresource Technology*, **169**(0), 816-820.

Chen, W.-T., Tang, L., Qian, W., Scheppe, K., Nair, K., Wu, Z., Gai, C., Zhang, P., Zhang, Y. 2016b. Extract Nitrogen-Containing Compounds in Biocrude Oil Converted from Wet Biowaste via Hydrothermal Liquefaction. *ACS Sustainable Chemistry & Engineering*.

Chen, W.-T., Zhang, Y., Zhang, J., Schideman, L., Yu, G., Zhang, P., Minarick, M. 2014b. Co-liquefaction of swine manure and mixed-culture algal biomass from a wastewater treatment system to produce bio-crude oil. *Applied Energy*, **128**(0), 209-216.

Chen, W.-T., Zhang, Y., Zhang, J., Yu, G., Schideman, L.C., Zhang, P., Minarick, M. 2014c. Hydrothermal liquefaction of mixed-culture algal biomass from wastewater treatment system into bio-crude oil. *Bioresource Technology*, **152**(0), 130-139.

Chen, Y.-Q., Wang, N., Zhang, P., Zhou, H., Qu, L.-H. 2002. Molecular evidence identifies bloom-forming Phaeocystis (Prymnesiophyta) from coastal waters of southeast China as Phaeocystis globosa. *Biochemical Systematics and Ecology*, **30**(1), 15-22.

Cheng, D., Wang, L., Shahbazi, A., Xiu, S., Zhang, B. 2014a. Catalytic cracking of crude bio-oil from glycerol-assisted liquefaction of swine manure. *Energy Conversion and Management*, **87**(0), 378-384.

Cheng, D., Wang, L., Shahbazi, A., Xiu, S., Zhang, B. 2014b. Characterization of the physical and chemical properties of the distillate fractions of crude bio-oil produced by the glycerol-assisted liquefaction of swine manure. *Fuel*, **130**, 251-256.

Cheng, J., Huang, R., Yu, T., Li, T., Zhou, J., Cen, K. 2014c. Biodiesel production from lipids in wet microalgae with microwave irradiation and bio-crude production from algal residue through hydrothermal liquefaction. *Bioresource Technology*, **151**, 415-418.

Cherad, R., Onwudili, J., Biller, P., Williams, P., Ross, A. 2016. Hydrogen production from the catalytic supercritical water gasification of process water generated from hydrothermal liquefaction of microalgae. *Fuel*, **166**, 24-28.

Chiaberge, S., Leonardis, I., Fiorani, T., Cesti, P., Reale, S., Angelis, F.D. 2014. Bio-oil from waste: a comprehensive analytical study by soft-ionization FTICR mass spectrometry. *Energy & Fuels*, **28**(3), 2019-2026.

Chiaramonti, D., Bonini, M., Fratini, E., Tondi, G., Gartner, K., Bridgwater, A., Grimm, H., Soldaini, I., Webster, A., Baglioni, P. 2003a. Development of emulsions from biomass pyrolysis liquid and diesel and their use in engines—Part 1: emulsion production. *Biomass and Bioenergy*, **25**(1), 85-99.

Chiaramonti, D., Bonini, M., Fratini, E., Tondi, G., Gartner, K., Bridgwater, A., Grimm, H., Soldaini, I., Webster, A., Baglioni, P. 2003b. Development of emulsions from biomass pyrolysis liquid and diesel and their use in engines—Part 2: tests in diesel engines. *Biomass and Bioenergy*, **25**(1), 101-111.

Clarens, A.F., Resurreccion, E.P., White, M.A., Colosi, L.M. 2010. Environmental Life Cycle Comparison of Algae to Other Bioenergy Feedstocks. *Environmental Science & Technology*, **44**(5), 1813-1819.

Cole, A., Dinburg, Y., Haynes, B.S., He, Y., Herskowitz, M., Jazrawi, C., Landau, M., Liang, X., Magnusson, M., Maschmeyer, T. 2016. From macroalgae to liquid fuel via waste-water

remediation, hydrothermal upgrading, carbon dioxide hydrogenation and hydrotreating. *Energy & Environmental Science*, **9**(5), 1828-1840.
Colket, M., Edwards, T., Williams, S., Cernansky, N.P., Miller, D.L., Egolfopoulos, F., Lindstedt, P., Seshadri, K., Dryer, F.L., Law, C.K. 2007. Development of an experimental database and kinetic models for surrogate jet fuels. *45th AIAA Aerospace Sciences Meeting and Exhibit*. pp. 8-11.
Collins, C.D. 2007. Implementing phytoremediation of petroleum hydrocarbons. in: *Phytoremediation*, Springer, pp. 99-108.
Costanzo, W., Jena, U., Hilten, R., Das, K., Kastner, J.R. 2015. Low temperature hydrothermal pretreatment of algae to reduce nitrogen heteroatoms and generate nutrient recycle streams. *Algal Research*, **12**, 377-387.
Coulson, J.M., Richardson, J.F., Harker, J.H., Backhurst, J.R. 2002. *Chemical Engineering*. Butterworth-Heinemann.
Crampon, C., Boutin, O., Badens, E. 2011. Supercritical carbon dioxide extraction of molecules of interest from microalgae and seaweeds. *Industrial & Engineering Chemistry Research*, **50**(15), 8941-8953.
Cuéllar, A.D., Webber, M.E. 2010. Wasted Food, Wasted Energy: The Embedded Energy in Food Waste in the United States. *Environmental science & technology*, **44**(16), 6464-6469.
Demirbaş, A. 2000a. Effect of lignin content on aqueous liquefaction products of biomass. *Energy Conversion and Management*, **41**(15), 1601-1607.
Demirbaş, A. 2000b. Mechanisms of liquefaction and pyrolysis reactions of biomass. *Energy Conversion and Management*, **41**(6), 633-646.
Deniz, I., Ozen, M.O., Yesil-Celiktas, O. 2016. Supercritical fluid extraction of phycocyanin and investigation of cytotoxicity on human lung cancer cells. *The Journal of Supercritical Fluids*, **108**, 13-18.
Dhasmana, H., Ozer, H., Al-Qadi, I.L., Zhang, Y., Schideman, L., Sharma, B.K., Chen, W.-T., Minarick, M.J., Zhang, P. 2015. Rheological and Chemical Characterization of Biobinders from Different Biomass Resources. *Transportation Research Record: Journal of the Transportation Research Board*(2505), 121-129.
Dong, R. 2009. *Hydrothermal process for bioenergy production from corn fiber and swine manure*. ProQuest.
Dong, R., Zhang, Y., Christianson, L.L., Funk, T.L., Wang, X., Wang, Z., Minarick, M., Yu, G. 2009. Product Distribution and Implication of Hydrothermal Conversion of Swine Manure at Low Temperatures. *Transactions of the ASABE*, **52**(4), 1239-1248.
Dote, Y., Sawayama, S., Inoue, S., Minowa, T., Yokoyama, S.-y. 1994. Recovery of liquid fuel from hydrocarbon-rich microalgae by thermochemical liquefaction. *Fuel*, **73**(12), 1855-1857.
Duan, P., Bai, X., Xu, Y., Zhang, A., Wang, F., Zhang, L., Miao, J. 2013a. Catalytic upgrading of crude algal oil using platinum/gamma alumina in supercritical water. *Fuel*, **109**, 225-233.
Duan, P., Chang, Z., Xu, Y., Bai, X., Wang, F., Zhang, L. 2013b. Hydrothermal processing of duckweed: effect of reaction conditions on product distribution and composition. *Bioresource Technology*, **135**, 710-719.
Duan, P., Savage, P.E. 2011a. Catalytic hydrothermal hydrodenitrogenation of pyridine. *Applied Catalysis B: Environmental*, **108**, 54-60.
Duan, P., Savage, P.E. 2011b. Catalytic hydrothermal hydrodenitrogenation of pyridine. *Applied Catalysis B: Environmental*, **108–109**, 54-60.
Duan, P., Savage, P.E. 2011c. Catalytic treatment of crude algal bio-oil in supercritical water: optimization studies. *Energy & Environmental Science*, **4**(4), 1447-1456.
Duan, P., Savage, P.E. 2010. Hydrothermal Liquefaction of a Microalga with Heterogeneous Catalysts. *Industrial & Engineering Chemistry Research*, **50**(1), 52-61.
Eboibi, B., Lewis, D.M., Ashman, P.J., Chinnasamy, S. 2015. Influence of process conditions on pretreatment of microalgae for protein extraction and production of biocrude during hydrothermal liquefaction of pretreated Tetraselmis sp. *RSC Advances*, **5**(26), 20193-20207.

Eboibi, B.E.-O., Lewis, D.M., Ashman, P.J., Chinnasamy, S. 2014a. Hydrothermal liquefaction of microalgae for biocrude production: Improving the biocrude properties with vacuum distillation. *Bioresource technology*, **174**, 212-221.
Eboibi, B.E., Lewis, D.M., Ashman, P.J., Chinnasamy, S. 2014b. Effect of operating conditions on yield and quality of biocrude during hydrothermal liquefaction of halophytic microalga Tetraselmis sp. *Bioresource technology*, **170**, 20-29.
Elliott, D.C., Biller, P., Ross, A.B., Schmidt, A.J., Jones, S.B. 2015. Hydrothermal liquefaction of biomass: developments from batch to continuous process. *Bioresource technology*, **178**, 147-156.
Elliott, D.C., Hart, T.R., Neuenschwander, G.G., Rotness, L.J., Roesijadi, G., Zacher, A.H., Magnuson, J.K. 2014. Hydrothermal Processing of Macroalgal Feedstocks in Continuous-Flow Reactors. *ACS Sustainable Chemistry & Engineering*, **2**(2), 207-215.
Elliott, D.C., Hart, T.R., Schmidt, A.J., Neuenschwander, G.G., Rotness, L.J., Olarte, M.V., Zacher, A.H., Albrecht, K.O., Hallen, R.T., Holladay, J.E. 2013. Process development for hydrothermal liquefaction of algae feedstocks in a continuous-flow reactor. *Algal Research*, **2**(4), 445-454.
Faeth, J.L., Savage, P.E., Jarvis, J.M., McKenna, A.M. 2016. Characterization of products from fast and isothermal hydrothermal liquefaction of microalgae. *AIChE Journal*, **62**(3), 815-828.
Faeth, J.L., Valdez, P.J., Savage, P.E. 2013. Fast hydrothermal liquefaction of Nannochloropsis sp. to produce biocrude. *Energy & Fuels*, **27**(3), 1391-1398.
Fernandez, L.P., Hepler, L.G. 1959. Heats and Entropies of Ionization of Phenol and Some Substituted Phenols. *Journal of the American Chemical Society*, **81**(8), 1783-1786.
Fogler, H.S. 2016. *Elements of Chemical Reaction Engineering*. Pearson Education.
Fu, J., Lu, X., Savage, P.E. 2010. Catalytic hydrothermal deoxygenation of palmitic acid. *Energy & Environmental Science*, **3**(3), 311-317.
Furimsky, E., Massoth, F.E. 2005. Hydrodenitrogenation of petroleum. *Catalysis Reviews*, **47**(3), 297-489.
Gai, C., Zhang, Y., Chen, W.-T., Zhang, P., Dong, Y. 2014a. Energy and nutrient recovery efficiencies in biocrude oil produced via hydrothermal liquefaction of Chlorella pyrenoidosa. *RSC Advances*, **4**(33), 16958-16967.
Gai, C., Zhang, Y., Chen, W.-T., Zhang, P., Dong, Y. 2015. An investigation of reaction pathways of hydrothermal liquefaction using Chlorella pyrenoidosa and Spirulina platensis. *Energy Conversion and Management*, **96**, 330-339.
Gai, C., Zhang, Y., Chen, W.-T., Zhang, P., Dong, Y. 2013. Thermogravimetric and kinetic analysis of thermal decomposition characteristics of low-lipid microalgae. *Bioresource Technology*.
Gai, C., Zhang, Y., Chen, W.-T., Zhou, Y., Schideman, L., Zhang, P., Tommaso, G., Kuo, C.-T., Dong, Y. 2014b. Characterization of aqueous phase from the hydrothermal liquefaction of< i> Chlorella Pyrenoidosa</i>. *Bioresource Technology*.
Garcia Alba, L., Torri, C., Samorì, C., van der Spek, J., Fabbri, D., Kersten, S.R., Brilman, D.W. 2011. Hydrothermal treatment (HTT) of microalgae: evaluation of the process as conversion method in an algae biorefinery concept. *Energy & Fuels*, **26**(1), 642-657.
Ghadge, S.V., Raheman, H. 2005. Biodiesel production from mahua (Madhuca indica) oil having high free fatty acids. *Biomass and Bioenergy*, **28**(6), 601-605.
Ghatak, H.R. 2011. Biorefineries from the perspective of sustainability: Feedstocks, products, and processes. *Renewable and Sustainable Energy Reviews*, **15**(8), 4042-4052.
Gouveia, L., Oliveira, A.C. 2009. Microalgae as a raw material for biofuels production. *Journal of industrial microbiology & biotechnology*, **36**(2), 269-74.
Guo, B., Zhang, Y., Ha, S.-J., Jin, Y.-S., Morgenroth, E. 2012. Combined biomimetic and inorganic acids hydrolysis of hemicellulose in< i> Miscanthus</i> for bioethanol production. *Bioresource Technology*, **110**, 278-287.
Guo, B., Zhang, Y., Yu, G., Lee, W.-H., Jin, Y.-S., Morgenroth, E. 2013. Two-Stage Acidic–Alkaline Hydrothermal Pretreatment of Lignocellulose for the High Recovery of Cellulose and Hemicellulose Sugars. *Applied Biochemistry and Biotechnology*, **169**(4), 1069-1087.

Guo, Y., Yeh, T., Song, W., Xu, D., Wang, S. 2015. A review of bio-oil production from hydrothermal liquefaction of algae. *Renewable and Sustainable Energy Reviews*, **48**, 776-790.
Han, J., Elgowainy, A., Cai, H., Wang, M.Q. 2013. Life-cycle analysis of bio-based aviation fuels. *Bioresource technology*, **150**, 447-456.
Havre, T.E. 2002. Formation of calcium naphthenate in water/oil systems, naphthenic acid chemistry and emulsion stability.
Haynes, W.M. 2016. *CRC Handbook of Chemistry and Physics, 97th Edition*. CRC Press.
He, B., Zhang, Y., Funk, T.L., Riskowski, G.L., Yin, Y. 2000a. Thermochemical conversion of swine manure: An alternative process for waste treatment and renewable energy production. *Transactions of the ASAE*, **43**(6), 1827-1833.
He, B., Zhang, Y., Yin, Y., Funk, T.L., Riskowski, G.L. 2001a. Effects of alternative process gases on the thermochemical conversion process of swine manure. *Transactions of the ASAE*, **44**(6), 1873-1880.
He, B., Zhang, Y., Yin, Y., Funk, T.L., Riskowski, G.L. 2001b. Effects of feedstock pH, initial CO addition, and total solids content on the thermochemical conversion process of swine manure. *Transactions of the ASAE*, **44**(3), 697-704.
He, B., Zhang, Y., Yin, Y., Funk, T.L., Riskowski, G.L. 2000b. Operating temperature and retention time effects on the thermochemical conversion process of swine manure. *Transactions of the ASAE*, **43**(6), 1821-1825.
He, Y., Liang, X., Jazrawi, C., Montoya, A., Yuen, A., Cole, A.J., Neveux, N., Paul, N.A., de Nys, R., Maschmeyer, T. 2016. Continuous hydrothermal liquefaction of macroalgae in the presence of organic co-solvents. *Algal Research*, **17**, 185-195.
Heywood, J. 1988. *Internal Combustion Engine Fundamentals*. McGraw-Hill Education.
Hilten, R.N., Bibens, B.P., Kastner, J.R., Das, K.C. 2010. In-Line Esterification of Pyrolysis Vapor with Ethanol Improves Bio-oil Quality. *Energy & Fuels*, **24**(1), 673-682.
Hoekman, S.K. 2009. Biofuels in the US–challenges and opportunities. *Renewable Energy*, **34**(1), 14-22.
Hoffmann, J., Jensen, C.U., Rosendahl, L.A. 2016a. Co-processing potential of HTL bio-crude at petroleum refineries–Part 1: Fractional distillation and characterization. *Fuel*, **165**, 526-535.
Hoffmann, J., Jensen, C.U., Rosendahl, L.A. 2016b. Co-processing potential of HTL bio-crude at petroleum refineries – Part 1: Fractional distillation and characterization. *Fuel*, **165**, 526-535.
Huber, G.W., Iborra, S., Corma, A. 2006a. Synthesis of transportation fuels from biomass: chemistry, catalysts, and engineering. *Chemical reviews*, **106**(9), 4044-4098.
Huber, G.W., Iborra, S., Corma, A. 2006b. Synthesis of Transportation Fuels from Biomass: Chemistry, Catalysts, and Engineering. *Chemical Reviews*, **106**(9), 4044-4098.
Hunton, P. 2005. Research on eggshell structure and quality: an historical overview. *Revista Brasileira de Ciência Avícola*, **7**(2), 67-71.
Incropera, F.P. 2007. *Fundamentals of heat and mass transfer*. John Wiley.
Information, N.C.f.B. 2016. PubChem Compound Database, Vol. 2016.
Jaber, J., Probert, S. 2000. Non-isothermal thermogravimetry and decomposition kinetics of two Jordanian oil shales under different processing conditions. *Fuel Processing Technology*, **63**(1), 57-70.
Jazrawi, C., Biller, P., He, Y., Montoya, A., Ross, A.B., Maschmeyer, T., Haynes, B.S. 2015. Two-stage hydrothermal liquefaction of a high-protein microalga. *Algal Research*, **8**, 15-22.
Jazrawi, C., Biller, P., Ross, A.B., Montoya, A., Maschmeyer, T., Haynes, B.S. 2013. Pilot plant testing of continuous hydrothermal liquefaction of microalgae. *Algal Research*, **2**(3), 268-277.
Jena, U., Das, K. 2011. Comparative evaluation of thermochemical liquefaction and pyrolysis for bio-oil production from microalgae. *Energy & Fuels*, **25**(11), 5472-5482.
Jena, U., Das, K., Kastner, J. 2011a. Effect of operating conditions of thermochemical liquefaction on biocrude production from Spirulina platensis. *Bioresource Technology*, **102**(10), 6221-6229.

Jena, U., McCurdy, A.T., Warren, A., Summers, H., Ledbetter, R.N., Hoekman, S.K., Seefeldt, L.C., Quinn, J.C. 2015. Oleaginous yeast platform for producing biofuels via co-solvent hydrothermal liquefaction. *Biotechnology for biofuels*, **8**(1), 1.

Jena, U., Vaidyanathan, N., Chinnasamy, S., Das, K. 2011b. Evaluation of microalgae cultivation using recovered aqueous co-product from thermochemical liquefaction of algal biomass. *Bioresource technology*, **102**(3), 3380-3387.

Jones, S., Zhu, Y., Anderson, D., Hallen, R.T., Elliott, D.C., Schmidt, A., Albrecht, K., Hart, T., Butcher, M., Drennan, C. 2014. Process design and economics for the conversion of algal biomass to hydrocarbons: whole algae hydrothermal liquefaction and upgrading. *Pacific Northwest National Laboratory*.

Kabyemela, B.M., Adschiri, T., Malaluan, R.M., Arai, K. 1999. Glucose and fructose decomposition in subcritical and supercritical water: detailed reaction pathway, mechanisms, and kinetics. *Industrial & Engineering Chemistry Research*, **38**(8), 2888-2895.

Karagöz, S., Bhaskar, T., Muto, A., Sakata, Y., Oshiki, T., Kishimoto, T. 2005. Low-temperature catalytic hydrothermal treatment of wood biomass: analysis of liquid products. *Chemical Engineering Journal*, **108**(1–2), 127-137.

Kaushik, R., Parshetti, G.K., Liu, Z., Balasubramanian, R. 2014. Enzyme-assisted hydrothermal treatment of food waste for co-production of hydrochar and bio-oil. *Bioresource technology*, **168**, 267-274.

Knothe, G., Steidley, K.R. 2005. Kinematic viscosity of biodiesel fuel components and related compounds. Influence of compound structure and comparison to petrodiesel fuel components. *Fuel*, **84**(9), 1059-1065.

Kruse, A., Funke, A., Titirici, M.-M. 2013. Hydrothermal conversion of biomass to fuels and energetic materials. *Current Opinion in Chemical Biology*, **17**(3), 515-521.

Kumar, N. 2017. Oxidative stability of biodiesel: Causes, effects and prevention. *Fuel*, **190**, 328-350.

Kumar, S., Hablot, E., Moscoso, J.L.G., Obeid, W., Hatcher, P.G., DuQuette, B.M., Graiver, D., Narayan, R., Balan, V. 2014. Polyurethanes preparation using proteins obtained from microalgae. *Journal of Materials Science*, **49**(22), 7824-7833.

Lavanya, M.R., Meenakshisundaram, A., Renganathan, S., Chinnasamy, S., Lewis, D.M., Nallasivam, J., Bhaskar, S. 2015. Hydrothermal liquefaction of freshwater and marine algal biomass: A novel approach to produce distillate fuel fractions through blending and co-processing of biocrude with petrocrude. *Bioresource technology*.

Leal, J.P., de Matos, A.P., Simões, J.A.M. 1991. Standard enthalpies of formation of sodium alkoxides. *Journal of Organometallic Chemistry*, **403**(1), 1-10.

Lee, T.H., Lin, Y., Meng, X., Li, Y., Nithyanandan, K. 2016. Combustion Characteristics of Acetone, Butanol, and Ethanol (ABE) Blended with Diesel in a Compression-Ignition Engine, SAE International.

Leema, J.M., Kirubagaran, R., Vinithkumar, N., Dheenan, P., Karthikayulu, S. 2010. High value pigment production from Arthrospira (Spirulina) platensis cultured in seawater. *Bioresource technology*, **101**(23), 9221-9227.

Leng, L., Yuan, X., Chen, X., Huang, H., Wang, H., Li, H., Zhu, R., Li, S., Zeng, G. 2015. Characterization of liquefaction bio-oil from sewage sludge and its solubilization in diesel microemulsion. *Energy*, **82**, 218-228.

Leng, L., Yuan, X., Shao, J., Huang, H., Wang, H., Li, H., Chen, X., Zeng, G. 2016. Study on demetalization of sewage sludge by sequential extraction before liquefaction for the production of cleaner bio-oil and bio-char. *Bioresource technology*, **200**, 320-327.

Leonardis, I., Chiaberge, S., Fiorani, T., Spera, S., Battistel, E., Bosetti, A., Cesti, P., Reale, S., De Angelis, F. 2013. Characterization of Bio-oil from Hydrothermal Liquefaction of Organic Waste by NMR Spectroscopy and FTICR Mass Spectrometry. *ChemSusChem*, **6**(1), 160-167.

Leung, D.Y., Wu, X., Leung, M. 2010. A review on biodiesel production using catalyzed transesterification. *Applied Energy*, **87**(4), 1083-1095.

Li, D., Chen, L., Xu, D., Zhang, X., Ye, N., Chen, F., Chen, S. 2012. Preparation and characteristics of bio-oil from the marine brown alga Sargassum patens C. Agardh. *Bioresource Technology*, **104**(0), 737-742.
Li, H., Liu, Z., Zhang, Y., Li, B., Lu, H., Duan, N., Liu, M., Zhu, Z., Si, B. 2014. Conversion efficiency and oil quality of low-lipid high-protein and high-lipid low-protein microalgae via hydrothermal liquefaction. *Bioresource technology*, **154**, 322-329.
Li, H., Yuan, X., Zeng, G., Huang, D., Huang, H., Tong, J., You, Q., Zhang, J., Zhou, M. 2010a. The formation of bio-oil from sludge by deoxy-liquefaction in supercritical ethanol. *Bioresource technology*, **101**(8), 2860-2866.
Li, R., Zhang, B., Xiu, S., Wang, H., Wang, L., Shahbazi, A. 2015. Characterization of solid residues obtained from supercritical ethanol liquefaction of swine manure. *American Journal of Engineering and Applied Sciences*, **8**(4), 465.
Li, W., Pan, C., Zhang, Q., Liu, Z., Peng, J., Chen, P., Lou, H., Zheng, X. 2011. Upgrading of low-boiling fraction of bio-oil in supercritical methanol and reaction network. *Bioresource technology*, **102**(7), 4884-4889.
Li, Y., Wang, T., Liang, W., Wu, C., Ma, L., Zhang, Q., Zhang, X., Jiang, T. 2010b. Ultrasonic preparation of emulsions derived from aqueous bio-oil fraction and 0# diesel and combustion characteristics in diesel generator. *Energy & Fuels*, **24**(3), 1987-1995.
Li, Z., Savage, P.E. 2013. Feedstocks for fuels and chemicals from algae: treatment of crude bio-oil over HZSM-5. *Algal Research*, **2**(2), 154-163.
Lide, D.R. 2004. *CRC Handbook of Chemistry and Physics, 85th Edition*. Taylor & Francis.
Lin, C.-Y., Lin, H.-A. 2006. Diesel engine performance and emission characteristics of biodiesel produced by the peroxidation process. *Fuel*, **85**(3), 298-305.
Liu, H.-M., Li, M.-F., Yang, S., Sun, R.-C. 2013. Understanding the mechanism of cypress liquefaction in hot-compressed water through characterization of solid residues. *Energies*, **6**(3), 1590-1603.
Liu, H., Lee, C.-f.F., Huo, M., Yao, M. 2011. Combustion Characteristics and Soot Distributions of Neat Butanol and Neat Soybean Biodiesel. *Energy & Fuels*, **25**(7), 3192-3203.
López Barreiro, D., Beck, M., Hornung, U., Ronsse, F., Kruse, A., Prins, W. 2015. Suitability of hydrothermal liquefaction as a conversion route to produce biofuels from macroalgae. *Algal Research*, **11**, 234-241.
Lu, Q., Li, W.-Z., Zhu, X.-F. 2009. Overview of fuel properties of biomass fast pyrolysis oils. *Energy conversion and management*, **50**(5), 1376-1383.
Luo, J., Fang, Z., Smith Jr, R.L. 2013. Ultrasound-enhanced conversion of biomass to biofuels. *Progress in Energy and Combustion Science*.
Luo, L., Sheehan, J.D., Dai, L., Savage, P.E. 2016. Products and Kinetics for Isothermal Hydrothermal Liquefaction of Soy Protein Concentrate. *ACS Sustainable Chemistry & Engineering*, **4**(5), 2725-2733.
Masjuki, H., Abdulmuin, M.Z., Sii, H.S. 1997. Indirect injection diesel engine operation on palm oil methyl esters and its emulsions. *Proceedings of the Institution of Mechanical Engineers, Part D: Journal of Automobile Engineering*, **211**(4), 291-299.
Matsui, T.-o., Nishihara, A., Ueda, C., Ohtsuki, M., Ikenaga, N.-o., Suzuki, T. 1997. Liquefaction of micro-algae with iron catalyst. *Fuel*, **76**(11), 1043-1048.
Miao, C., Chakraborty, M., Chen, S. 2012. Impact of reaction conditions on the simultaneous production of polysaccharides and bio-oil from heterotrophically grown Chlorella sorokiniana by a unique sequential hydrothermal liquefaction process. *Bioresource technology*, **110**, 617-627.
Miao, C., Chakraborty, M., Dong, T., Yu, X., Chi, Z., Chen, S. 2014. Sequential hydrothermal fractionation of yeast Cryptococcus curvatus biomass. *Bioresource technology*, **164**, 106-112.
Minarick, M., Zhang, Y., Schideman, L., Wang, Z., Yu, G., Funk, T., Barker, D. 2011. Product and Economic Analysis of Direct Liquefaction of Swine Manure. *BioEnergy Research*, **4**(4), 324-333.
Mingxia Zheng, L.C.S., Giovana Tommaso, Wan-Ting Chen, Yan Zhou, Ken Nair, Wanyi Qian, Yuanhui Zhang, Kaijun Wang. 2016. Anaerobic Digestion of Wastewater Generated from the

Hydrothermal Liquefaction of Spirulina: Toxicity Assessment and Minimization. *Energy conversion and management*, (accepted).
Mishima, S., Maeta, S., Tatsuoka, T., Koga, N., Furukawa, Y. 2009. Thermochemical Approaches to Neutralization Reaction between Weak Acid and Strong Base. *Chem. Educ. J.(Web)*, **13**(1), 13-4.
Mortensen, P.M., Grunwaldt, J.-D., Jensen, P.A., Knudsen, K., Jensen, A.D. 2011. A review of catalytic upgrading of bio-oil to engine fuels. *Applied Catalysis A: General*, **407**(1), 1-19.
Mullen, C.A., Boateng, A.A., Reichenbach, S.E. 2013. Hydrotreating of fast pyrolysis oils from protein-rich pennycress seed presscake. *Fuel*, **111**, 797-804.
Naik, M., Meher, L., Naik, S., Das, L. 2008. Production of biodiesel from high free fatty acid Karanja (Pongamia pinnata) oil. *Biomass and Bioenergy*, **32**(4), 354-357.
Narayan, S., Muldoon, J., Finn, M., Fokin, V.V., Kolb, H.C., Sharpless, K.B. 2005. "On water": Unique reactivity of organic compounds in aqueous suspension. *Angewandte Chemie International Edition*, **44**(21), 3275-3279.
Nazari, L., Yuan, Z., Souzanchi, S., Ray, M.B., Xu, C.C. 2015. Hydrothermal liquefaction of woody biomass in hot-compressed water: Catalyst screening and comprehensive characterization of bio-crude oils. *Fuel*, **162**, 74-83.
NIST. NIST Chemistry WebBook.
Normah, O., Nazarifah, I. 2003. Production of semi-refined carrageenan from locally available red seaweed, Eucheuma cottonii on a laboratory scale. *JOURNAL OF TROPICAL AGRICULTURE AND FOOD SCIENCE*, **31**(2), 207.
Noureddini, H., Teoh, B., Clements, L.D. 1992. Densities of vegetable oils and fatty acids. *Journal of the American Oil Chemists Society*, **69**(12), 1184-1188.
Oasmaa, A., Kuoppala, E., Selin, J.-F., Gust, S., Solantausta, Y. 2004. Fast Pyrolysis of Forestry Residue and Pine. 4. Improvement of the Product Quality by Solvent Addition. *Energy & Fuels*, **18**(5), 1578-1583.
Ocfemia, K., Zhang, Y., Funk, T. 2006a. Hydrothermal processing of swine manure into oil using a continuous reactor system: Development and testing. *Transactions of the ASAE*, **49**(2), 533.
Ocfemia, K., Zhang, Y., Funk, T. 2006b. Hydrothermal processing of swine manure to oil using a continuous reactor system: Effects of operating parameters on oil yield and quality. *Trans. ASABE*, **49**(6), 1897-1904.
Ong, M. 2013. Evaluation of anaerobic membrane bioreactors and hydrothermal catalytic gasification for enhanced conversion of organic wastes to renewable fuels, University of Illinois at Urbana-Champaign.
Ortiz-Toral, P.J. 2008. Steam reforming of bio-oil: Effect of bio-oil composition and stability.
Ott, L.S., Smith, B.L., Bruno, T.J. 2008. Advanced distillation curve measurement: Application to a bio-derived crude oil prepared from swine manure. *Fuel*, **87**(15), 3379-3387.
Patel, B., Hellgardt, K. 2013. Hydrothermal upgrading of algae paste: Application of 31P-NMR. *Environmental Progress & Sustainable Energy*, **32**(4), 1002-1012.
Pavlovič, I., Knez, Z.e., Škerget, M. 2013. Hydrothermal reactions of agricultural and food processing wastes in sub-and supercritical water: a review of fundamentals, mechanisms, and state of research. *Journal of agricultural and food chemistry*, **61**(34), 8003-8025.
Pei, Y., Wang, J., Wu, K., Xuan, X., Lu, X. 2009. Ionic liquid-based aqueous two-phase extraction of selected proteins. *Separation and Purification Technology*, **64**(3), 288-295.
Peterson, A.A., Vogel, F., Lachance, R.P., Fröling, M., Antal Jr, M.J., Tester, J.W. 2008. Thermochemical biofuel production in hydrothermal media: a review of sub-and supercritical water technologies. *Energy & Environmental Science*, **1**(1), 32-65.
Pham, M., Schideman, L., Scott, J., Rajagopalan, N., Plewa, M.J. 2013a. Chemical and biological characterization of wastewater generated from hydrothermal liquefaction of Spirulina. *Environmental science & technology*, **47**(4), 2131-2138.

Pham, M., Schideman, L., Sharma, B.K., Zhang, Y., Chen, W.T. 2013b. Effects of hydrothermal liquefaction on the fate of bioactive contaminants in manure and algal feedstocks. *Bioresource technology*, **149**, 126-135.
Pratas, M.J., Freitas, S., Oliveira, M.B., Monteiro, S.C., Lima, A.S., Coutinho, J.A.P. 2010. Densities and Viscosities of Fatty Acid Methyl and Ethyl Esters. *Journal of Chemical & Engineering Data*, **55**(9), 3983-3990.
Quitain, A.T., Sato, N., Daimon, H., Fujie, K. 2001. Production of valuable materials by hydrothermal treatment of shrimp shells. *Industrial & Engineering Chemistry Research*, **40**(25), 5885-5888.
Ramos-Tercero, E.A., Bertucco, A., Brilman, D. 2015. Process water recycle in hydrothermal liquefaction of microalgae to enhance bio-oil yield. *Energy & Fuels*, **29**(4), 2422-2430.
Reiter, A.J., Kong, S.-C. 2011. Combustion and emissions characteristics of compression-ignition engine using dual ammonia-diesel fuel. *Fuel*, **90**(1), 87-97.
Reyes, F.A., Mendiola, J.A., Ibanez, E., del Valle, J.M. 2014. Astaxanthin extraction from Haematococcus pluvialis using CO 2-expanded ethanol. *The Journal of Supercritical Fluids*, **92**, 75-83.
Roberts, G.W., Fortier, M.-O.P., Sturm, B.S.M., Stagg-Williams, S.M. 2013. Promising pathway for algal biofuels through wastewater cultivation and hydrothermal conversion. *Energy & Fuels*, **27**(2), 857-867.
Rogalinski, T., Herrmann, S., Brunner, G. 2005. Production of amino acids from bovine serum albumin by continuous sub-critical water hydrolysis. *The Journal of Supercritical Fluids*, **36**(1), 49-58.
Rojas-Pérez, A., Diaz-Diestra, D., Frias-Flores, C.B., Beltran-Huarac, J., Das, K., Weiner, B.R., Morell, G., Díaz-Vázquez, L.M. 2015. Catalytic effect of ultrananocrystalline Fe 3 O 4 on algal bio-crude production via HTL process. *Nanoscale*, **7**(42), 17664-17671.
Roussis, S.G., Cranford, R., Sytkovetskiy, N. 2012. Thermal Treatment of Crude Algae Oils Prepared Under Hydrothermal Extraction Conditions. *Energy & Fuels*, **26**(8), 5294-5299.
Saber, M., Nakhshiniev, B., Yoshikawa, K. 2016. A review of production and upgrading of algal bio-oil. *Renewable and Sustainable Energy Reviews*, **58**, 918-930.
Saunders, K. 1973. *Polyurethanes*. Springer.
Savage, P.E. 2009. A perspective on catalysis in sub-and supercritical water. *The Journal of Supercritical Fluids*, **47**(3), 407-414.
Schramm, W., Yang, D., Haemmerich, D. 2006. Contribution of direct heating, thermal conduction and perfusion during radiofrequency and microwave ablation. *Engineering in Medicine and Biology Society, 2006. EMBS'06. 28th Annual International Conference of the IEEE*. IEEE. pp. 5013-5016.
Sheehan, J., Dunahay, T., Benemann, J., Roessler, P. 1998. A Look Back at the US Department of Energy's Aquatic Species Program: Biodiesel from Algae; Close-Out Report.
Sheehan, J.D., Savage, P.E. 2016. Products, Pathways, and Kinetics for the Fast Hydrothermal Liquefaction of Soy Protein Isolate. *ACS Sustainable Chemistry & Engineering*.
Shi, W., Gao, Y., Yang, G., Zhao, Y. 2013a. Conversion of Cornstalk to Bio-oil in Hot-Compressed Water: Effects of Ultrasonic Pretreatment on the Yield and Chemical Composition of Bio-oil, Carbon Balance, and Energy Recovery. *Journal of agricultural and food chemistry*, **61**(31), 7574-7582.
Shi, W., Jia, J., Gao, Y., Zhao, Y. 2013b. Influence of ultrasonic pretreatment on the yield of bio-oil prepared by thermo-chemical conversion of rice husk in hot-compressed water. *Bioresource technology*, **146**, 355-362.
Shi, W., Li, S., Jia, J., Zhao, Y. 2012. Highly Efficient Conversion of Cellulose to Bio-Oil in Hot-Compressed Water with Ultrasonic Pretreatment. *Industrial & Engineering Chemistry Research*, **52**(2), 586-593.
Shin, Y.H., Schideman, L. 2015. Characterizing the fate and transport of Chemicals of Emerging Concerns (CECs) from integrated bioenergy and manure management system. *2015 ASABE Annual International Meeting*. American Society of Agricultural and Biological Engineers. pp. 1.

Shuping, Z., Yulong, W., Mingde, Y., Kaleem, I., Chun, L., Tong, J. 2010. Production and characterization of bio-oil from hydrothermal liquefaction of microalgae Dunaliella tertiolecta cake. *Energy*, **35**(12), 5406-5411.
Sınağ, A., Kruse, A., Rathert, J. 2004. Influence of the Heating Rate and the Type of Catalyst on the Formation of Key Intermediates and on the Generation of Gases During Hydropyrolysis of Glucose in Supercritical Water in a Batch Reactor. *Industrial & Engineering Chemistry Research*, **43**(2), 502-508.
Sinag, A., Kruse, A., Schwarzkopf, V. 2003. Key compounds of the hydropyrolysis of glucose in supercritical water in the presence of K2CO3. *Industrial & Engineering Chemistry Research*, **42**(15), 3516-3521.
Singh. 1995. *Bioseparation Processes in Food*. Taylor & Francis.
Singh, R., Balagurumurthy, B., Bhaskar, T. 2015. Hydrothermal liquefaction of macro algae: effect of feedstock composition. *Fuel*, **146**, 69-74.
Soh, L., Zimmerman, J. 2011. Biodiesel production: the potential of algal lipids extracted with supercritical carbon dioxide. *Green Chemistry*, **13**(6), 1422-1429.
Speight, J.G., Speight, J. 2002. *Handbook of Petroleum Product Analysis*. Wiley-Interscience Hoboken,NJ.
Spolaore, P., Joannis-Cassan, C., Duran, E., Isambert, A. 2006. Commercial applications of microalgae. *Journal of bioscience and bioengineering*, **101**(2), 87-96.
Sprynskyy, M. 2009. Solid–liquid–solid extraction of heavy metals (Cr, Cu, Cd, Ni and Pb) in aqueous systems of zeolite–sewage sludge. *Journal of Hazardous Materials*, **161**(2–3), 1377-1383.
Takanabe, K., Aika, K.-i., Inazu, K., Baba, T., Seshan, K., Lefferts, L. 2006. Steam reforming of acetic acid as a biomass derived oxygenate: Bifunctional pathway for hydrogen formation over Pt/ZrO2 catalysts. *Journal of Catalysis*, **243**(2), 263-269.
Tekin, K. 2015. Hydrothermal conversion of russian olive seeds into crude bio-oil using a CaO catalyst derived from waste mussel shells. *Energy & Fuels*, **29**(7), 4382-4392.
Theegala, C.S., Midgett, J.S. 2012. Hydrothermal liquefaction of separated dairy manure for production of bio-oils with simultaneous waste treatment. *Bioresource Technology*, **107**(0), 456-463.
Tian, C., Li, B., Liu, Z., Zhang, Y., Lu, H. 2014. Hydrothermal liquefaction for algal biorefinery: a critical review. *Renewable and Sustainable Energy Reviews*, **38**, 933-950.
Tian, C., Liu, Z., Zhang, Y., Li, B., Cao, W., Lu, H., Duan, N., Zhang, L., Zhang, T. 2015. Hydrothermal liquefaction of harvested high-ash low-lipid algal biomass from Dianchi Lake: effects of operational parameters and relations of products. *Bioresource technology*, **184**, 336-343.
Tommaso, G., Chen, W.-T., Li, P., Schideman, L., Zhang, Y. 2015. Chemical Characterization and Anaerobic Biodegradability of Hydrothermal Liquefaction Aqueous Products from Mixed-culture Wastewater Algae. *Bioresource Technology*, **178**, 139-146.
ToolBox, E. Liquids and Fluids - Specific Heats.
Toor, S.S., Rosendahl, L., Rudolf, A. 2011. Hydrothermal liquefaction of biomass: A review of subcritical water technologies. *Energy*, **36**(5), 2328-2342.
Torri, C., Fabbri, D., Garcia-Alba, L., Brilman, D.W.F. 2013. Upgrading of oils derived from hydrothermal treatment of microalgae by catalytic cracking over H-ZSM-5: a comparative Py-GC-MS study. *Journal of Analytical and Applied Pyrolysis*.
Trane-Restrup, R., Jensen, A.D. 2015. Steam reforming of cyclic model compounds of bio-oil over Ni-based catalysts: Product distribution and carbon formation. *Applied Catalysis B: Environmental*, **165**, 117-127.
Tsukahara, K., Sawayama, S. 2005. Liquid fuel production using microalgae. *J Jpn Pet Inst*, **48**(5), 251.
United States. Environmental Protection Agency. Office of Policy, P., Evaluation. 2017. *Inventory of U.S. greenhouse gas emissions and sinks, 1990-2015*. U.S. Environmental Protection Agency, Office of Policy, Planning, and Evaluation.
USEIA (United States. Energy Information Administration). Diesel Fuel.

Vagia, E.C., Lemonidou, A.A. 2008. Hydrogen production via steam reforming of bio-oil components over calcium aluminate supported nickel and noble metal catalysts. *Applied Catalysis A: General*, **351**(1), 111-121.

Valdez, P.J., Dickinson, J.G., Savage, P.E. 2011. Characterization of Product Fractions from Hydrothermal Liquefaction of Nannochloropsis sp. and the Influence of Solvents. *Energy & Fuels*, **25**(7), 3235-3243.

Valdez, P.J., Nelson, M.C., Wang, H.Y., Lin, X.N., Savage, P.E. 2012. Hydrothermal liquefaction of Nannochloropsis sp.: Systematic study of process variables and analysis of the product fractions. *Biomass and Bioenergy*, **46**(0), 317-331.

Valdez, P.J., Savage, P.E. 2013. A reaction network for the hydrothermal liquefaction of Nannochloropsis sp. *Algal Research*, **2**(4), 416-425.

Valdez, P.J., Tocco, V.J., Savage, P.E. 2014. A general kinetic model for the hydrothermal liquefaction of microalgae. *Bioresource technology*, **163**, 123-127.

Vardon, D.R., Sharma, B.K., Blazina, G.V., Rajagopalan, K., Strathmann, T.J. 2012. Thermochemical conversion of raw and defatted algal biomass via hydrothermal liquefaction and slow pyrolysis. *Bioresource Technology*, **109**(0), 178-187.

Vardon, D.R., Sharma, B.K., Jaramillo, H., Kim, D., Choe, J.K., Ciesielski, P.N., Strathmann, T.J. 2014. Hydrothermal catalytic processing of saturated and unsaturated fatty acids to hydrocarbons with glycerol for in situ hydrogen production. *Green Chemistry*, **16**(3), 1507-1520.

Vardon, D.R., Sharma, B.K., Scott, J., Yu, G., Wang, Z., Schideman, L., Zhang, Y., Strathmann, T.J. 2011. Chemical properties of biocrude oil from the hydrothermal liquefaction of Spirulina algae, swine manure, and digested anaerobic sludge. *Bioresource Technology*, **102**(17), 8295-8303.

Vasudevan, V., Stratton, R.W., Pearlson, M.N., Jersey, G.R., Beyene, A.G., Weissman, J.C., Rubino, M., Hileman, J.I. 2012. Environmental performance of algal biofuel technology options. *Environmental science & technology*, **46**(4), 2451-9.

Wang, Y., Wang, H., Lin, H., Zheng, Y., Zhao, J., Pelletier, A., Li, K. 2013. Effects of solvents and catalysts in liquefaction of pinewood sawdust for the production of bio-oils. *Biomass and Bioenergy*, **59**, 158-167.

Wang, Z. 2011a. REACTION MECHANISMS OF HYDROTHERMAL LIQUEFACTION OF MODEL COMPOUNDS AND BIOWASTE FEEDSTOCKS in: *Agricultrual and BIological Engineering*, Vol. PhD, University of Illinois at Urbana-Champaign. Urbana, Illinois.

Wang, Z. 2011b. Reaction mechanisms of hydrothermal liquefaction of model compounds and biowaste feedstocks, PhD Dissertation. in: *Agricultrual and BIological Engineering*, Vol. PhD, University of Illinois at Urbana-Champaign. Urbana, IL.

Warneck, P. 1999. *Chemistry of the Natural Atmosphere*. Elsevier Science.

Watanabe, M., Iida, T., Inomata, H. 2006. Decomposition of a long chain saturated fatty acid with some additives in hot compressed water. *Energy Conversion and Management*, **47**(18), 3344-3350.

White, J.E., Catallo, W.J., Legendre, B.L. 2011. Biomass pyrolysis kinetics: a comparative critical review with relevant agricultural residue case studies. *Journal of Analytical and Applied Pyrolysis*, **91**(1), 1-33.

Xiong, W.-M., Zhu, M.-Z., Deng, L., Fu, Y., Guo, Q.-X. 2009. Esterification of Organic Acid in Bio-Oil using Acidic Ionic Liquid Catalysts. *Energy & Fuels*, **23**(4), 2278-2283.

Xiu, S., Shahbazi, A. 2012. Bio-oil production and upgrading research: A review. *Renewable and Sustainable Energy Reviews*, **16**(7), 4406-4414.

Xiu, S., Shahbazi, A., Shirley, V., Cheng, D. 2010. Hydrothermal pyrolysis of swine manure to bio-oil: effects of operating parameters on products yield and characterization of bio-oil. *Journal of Analytical and Applied Pyrolysis*, **88**(1), 73-79.

Xiu, S., Shahbazi, A., Shirley, V.B., Wang, L. 2011a. Swine manure/crude glycerol co-liquefaction: physical properties and chemical analysis of bio-oil product. *Bioresource Technology*, **102**(2), 1928-1932.

Xiu, S., Shahbazi, A., Wallace, C.W., Wang, L., Cheng, D. 2011b. Enhanced bio-oil production from swine manure co-liquefaction with crude glycerol. *Energy Conversion and Management*, **52**(2), 1004-1009.
Xu, D., Savage, P.E. 2015. Effect of reaction time and algae loading on water-soluble and insoluble biocrude fractions from hydrothermal liquefaction of algae. *Algal Research*, **12**, 60-67.
Xu, J., Jiang, J., Dai, W., Zhang, T., Xu, Y. 2011. Bio-Oil Upgrading by Means of Ozone Oxidation and Esterification to Remove Water and to Improve Fuel Characteristics. *Energy & Fuels*, **25**(4), 1798-1801.
Xu, Q., Lan, P., Zhang, B., Ren, Z., Yan, Y. 2010. Hydrogen production via catalytic steam reforming of fast pyrolysis bio-oil in a fluidized-bed reactor. *Energy & Fuels*, **24**(12), 6456-6462.
Xu, X., Zhang, C., Zhai, Y., Liu, Y., Zhang, R., Tang, X. 2014. Upgrading of Bio-Oil Using Supercritical 1-Butanol over a Ru/C Heterogeneous Catalyst: Role of the Solvent. *Energy & Fuels*, **28**(7), 4611-4621.
Xue, J., Grift, T.E., Hansen, A.C. 2011. Effect of biodiesel on engine performances and emissions. *Renewable and Sustainable Energy Reviews*, **15**(2), 1098-1116.
Yang, C., Jia, L., Chen, C., Liu, G., Fang, W. 2011. Bio-oil from hydro-liquefaction of Dunaliella salina over Ni/REHY catalyst. *Bioresource technology*, **102**(6), 4580-4584.
Yen, H.W., Hu, I.C., Chen, C.Y., Ho, S.H., Lee, D.J., Chang, J.S. 2013. Microalgae-based biorefinery--from biofuels to natural products. *Bioresource technology*, **135**, 166-74.
Yin, S.D., Dolan, R., Harris, M., Tan, Z.C. 2010. Subcritical hydrothermal liquefaction of cattle manure to bio-oil: Effects of conversion parameters on bio-oil yield and characterization of bio-oil. *Bioresource Technology*, **101**(10), 3657-3664.
Yoshida, H., Terashima, M., Takahashi, Y. 1999. Production of Organic Acids and Amino Acids from Fish Meat by Sub-Critical Water Hydrolysis. *Biotechnology progress*, **15**(6), 1090-1094.
Yu, G. 2012. Hydrothermal liquefaction of low-lipid microalgae to produce bio-crude oil, PhD Dissertation. in: *Agricultrual and BIological Engineering*, Vol. PhD, University of Illinois at Urbana-Champaign. Urbana, IL.
Yu, G., Zhang, Y., Guo, B., Funk, T., Schideman, L. 2014. Nutrient Flows and Quality of Bio-crude Oil Produced via Catalytic Hydrothermal Liquefaction of Low-Lipid Microalgae. *BioEnergy Research*, 1-12.
Yu, G., Zhang, Y., Schideman, L., Funk, T.L., Wang, Z. 2011a. Hydrothermal liquefaction of low lipid content microalgae into bio-crude oil. *Transactions of the ASABE*, **54**(1), 239-246.
Yu, G., Zhang, Y.H., Schideman, L., Funk, T., Wang, Z.C. 2011b. Distributions of carbon and nitrogen in the products from hydrothermal liquefaction of low-lipid microalgae. *Energy & Environmental Science*, **4**(11), 4587-4595.
Zacher, A.H., Olarte, M.V., Santosa, D.M., Elliott, D.C., Jones, S.B. 2014. A review and perspective of recent bio-oil hydrotreating research. *Green Chemistry*, **16**(2), 491-515.
Zapp, K.-H., Wostbrock, K.-H., Schäfer, M., Sato, K., Seiter, H., Zwick, W., Creutziger, R., Leiter, H. 2000. Ammonium Compounds. in: *Ullmann's Encyclopedia of Industrial Chemistry*, Wiley-VCH Verlag GmbH & Co. KGaA.
Zhang, B., von Keitz, M., Valentas, K. 2009. Thermochemical liquefaction of high-diversity grassland perennials. *Journal of Analytical and Applied Pyrolysis*, **84**(1), 18-24.
Zhang, C., Duan, P., Xu, Y., Wang, B., Wang, F., Zhang, L. 2014. Catalytic upgrading of duckweed biocrude in subcritical water. *Bioresource Technology*, **166**, 37-44.
Zhang, C., Tang, X., Sheng, L., Yang, X. 2016a. Enhancing the performance of Co-hydrothermal liquefaction for mixed algae strains by the Maillard reaction. *Green Chemistry*, **18**(8), 2542-2553.
Zhang, J., Chen, W.-T., Zhang, P., Luo, Z., Zhang, Y. 2013a. Hydrothermal liquefaction of Chlorella pyrenoidosa in sub- and supercritical ethanol with heterogeneous catalysts. *Bioresource Technology*, **133**(0), 389-397.
Zhang, J., Luo, Z., Zhang, Y. 2013b. Hydrothermal liquefaction of Chlorella pyrenoidosa in water and ethanol. *Transactions of the ASABE*, **56**(1), 253-259.

Zhang, J., Nithyanandan, K., Li, Y., Lee, C.-F., Huang, Z. 2015. Comparative Study of High-Alcohol-Content Gasoline Blends in an SI Engine, SAE International.
Zhang, L., Champagne, P., Xu, C. 2011. Bio-crude production from secondary pulp/paper-mill sludge and waste newspaper via co-liquefaction in hot-compressed water. *Energy*, **36**(4), 2142-2150.
Zhang, L., Lu, H., Zhang, Y., Li, B., Liu, Z., Duan, N., Liu, M. 2016b. Nutrient recovery and biomass production by cultivating Chlorella vulgaris 1067 from four types of post-hydrothermal liquefaction wastewater. *Journal of Applied Phycology*, **28**(2), 1031-1039.
Zhang, P. 2014. Characterization of biofuel from diatoms via hydrothermal liquefaction. in: *Agricultural & Biological Engineering*, Vol. Master of Science, University of Illinois at Urbana-Champaign. Urbana.
Zhang, Y. 2010. Hydrothermal liquefaction to convert biomass into crude oil. in: *Biofuels from Agricultural Wastes and Byproducts*, Wiley-Blackwell. Hoboken, NJ, pp. 201-232.
Zhao, C., Camaioni, D.M., Lercher, J.A. 2012. Selective catalytic hydroalkylation and deoxygenation of substituted phenols to bicycloalkanes. *Journal of Catalysis*, **288**, 92-103.
Zhao, C., Kou, Y., Lemonidou, A.A., Li, X., Lercher, J.A. 2009. Highly Selective Catalytic Conversion of Phenolic Bio-Oil to Alkanes. *Angewandte Chemie*, **121**(22), 4047-4050.
Zhao, P., Shen, Y., Ge, S., Chen, Z., Yoshikawa, K. 2014. Clean solid biofuel production from high moisture content waste biomass employing hydrothermal treatment. *Applied Energy*, **131**, 345-367.
Zheng, J.-L., Zhu, M.-Q., Wu, H.-t. 2015. Alkaline hydrothermal liquefaction of swine carcasses to bio-oil. *Waste Management*, **43**, 230-238.
Zheng, M., Schideman, L.C., Tommaso, G., Chen, W.-T., Zhou, Y., Nair, K., Qian, W., Zhang, Y., Wang, K. 2016. Anaerobic digestion of wastewater generated from the hydrothermal liquefaction of Spirulina: Toxicity assessment and minimization. *Energy Conversion and Management*.
Zhong, C., Wei, X. 2004. A comparative experimental study on the liquefaction of wood. *Energy*, **29**(11), 1731-1741.
Zhou, D., Zhang, L., Zhang, S., Fu, H., Chen, J. 2010. Hydrothermal liquefaction of macroalgae Enteromorpha prolifera to bio-oil. *Energy & Fuels*, **24**(7), 4054-4061.
Zhou, D., Zhang, S., Fu, H., Chen, J. 2012. Liquefaction of macroalgae Enteromorpha prolifera in sub-/supercritical alcohols: direct production of ester compounds. *Energy & Fuels*, **26**(4), 2342-2351.
Zhou, N., Huo, M., Wu, H., Nithyanandan, K., Chia-fon, F.L., Wang, Q. 2014. Low temperature spray combustion of acetone–butanol–ethanol (ABE) and diesel blends. *Applied Energy*, **117**, 104-115.
Zhou, Y. 2015a. Improving integrated systems for algal biofuels and wastewater treatment. in: *Agricultural and Biological Engineering*, University of Illinois at Urbana-Champaign. Urbana.
Zhou, Y. 2015b. Improving integrated systems for algal biofuels and wastewater treatment, University of Illinois at Urbana-Champaign.
Zhou, Y., Schideman, L., Yu, G., Zhang, Y. 2013. A synergistic combination of algal wastewater treatment and hydrothermal biofuel production maximized by nutrient and carbon recycling. *Energy & Environmental Science*, **6**(12), 3765-3779.
Zhou, Y., Schideman, L., Zheng, M., Martin-Ryals, A., Li, P., Tommaso, G., Zhang, Y. 2015. Anaerobic digestion of post-hydrothermal liquefaction wastewater for improved energy efficiency of hydrothermal bioenergy processes. *Water science and technology*, **72**(12), 2139-2147.
Zhu, Y., Albrecht, K.O., Elliott, D.C., Hallen, R.T., Jones, S.B. 2013. Development of hydrothermal liquefaction and upgrading technologies for lipid-extracted algae conversion to liquid fuels. *Algal Research*, **2**(4), 455-464.
Zhu, Z., Rosendahl, L., Toor, S.S., Yu, D., Chen, G. 2015. Hydrothermal liquefaction of barley straw to bio-crude oil: Effects of reaction temperature and aqueous phase recirculation. *Applied Energy*, **137**, 183-192.
Zou, S., Wu, Y., Yang, M., Li, C., Tong, J. 2010. Bio-oil production from sub-and supercritical water liquefaction of microalgae Dunaliella tertiolecta and related properties. *Energy & Environmental Science*, **3**(8), 1073-1078.